

Paul Lowman

Exploring Space Exploring Earth

New Understanding of the
Earth from Space Research

Foreward by **Neil Armstrong**



CAMBRIDGE

CAMBRIDGE

more information - www.cambridge.org/9780521661256

This page intentionally left blank

Exploring Space, Exploring Earth

Paul Lowman, a NASA scientist for over 40 years, describes the impact of space flight on geology and geophysics. A foreword by Neil Armstrong emphasizes that the exploration of space has led us to a far deeper understanding of our own planet. Direct results from Earth-orbital missions include studies of Earth's gravity and magnetic fields. In contrast, the recognition of the economic and biological significance of impact craters on Earth is an indirect consequence of the study of the geology of other planets. The final chapter presents a new theory for the tectonic evolution of the Earth based on comparative planetology and the Gaia concept. Extensive illustrations, a glossary of technical terms, and a comprehensive bibliography provide geologists and geophysicists with a valuable summary of research. The book will also serve as a supplementary text for students of tectonics, remote sensing and planetary science.

PAUL LOWMAN has been involved in a wide range of space research programs at the Goddard Space Flight Center. In 1963–4 he took part in planning for the *Apollo* missions. He was Principal Investigator for Synoptic Terrain Photography on the *Mercury*, *Gemini*, and *Apollo* Earth-orbital missions, an experiment that laid the foundation for *Landsat*. Between 1965 and 1970 he taught lunar geology at the University of California, Catholic University of America, and the Air Force Institute of Technology. Dr Lowman was also involved with the *Mariner 9* Mars mission, the *Apollo* X-ray fluorescence experiment and *Apollo 11* and *12* sample analysis among others. His main research interest was and still is the origin of the continental crust, as approached through comparative planetology.

In 1974, Dr Lowman received the Lindsay Award from the Goddard Space Flight Center. He was elected a Fellow of the Geological Society of America in 1975, and of the Geological Society of Canada in 1988. Drawing on his dual career in terrestrial and lunar geology, he authored *Space Panorama* (1968), *Lunar Panorama* (1970), and *The Third Planet* (1972). He also contributed to *Mission to Earth* (1976), the first NASA compilation of *Landsat* pictures, edited by N. M. Short.

Exploring Space, Exploring Earth

New Understanding of the Earth from
Space Research

Paul D. Lowman Jr.
Goddard Space Flight Center

Foreword by Neil A. Armstrong



CAMBRIDGE
UNIVERSITY PRESS

CAMBRIDGE UNIVERSITY PRESS

Cambridge, New York, Melbourne, Madrid, Cape Town, Singapore, São Paulo

Cambridge University Press

The Edinburgh Building, Cambridge CB2 2RU, United Kingdom

Published in the United States by Cambridge University Press, New York

www.cambridge.org

Information on this title: www.cambridge.org/9780521661256

© NASA 2002

This book is in copyright. Subject to statutory exception and to the provision of relevant collective licensing agreements, no reproduction of any part may take place without the written permission of Cambridge University Press.

First published in print format 2002

ISBN-13 978-0-521-66125-6 hardback

ISBN-10 0-521-66125-0 hardback

ISBN-13 978-0-521-89062-5 paperback

ISBN-10 0-521-89062-4 paperback

Cambridge University Press has no responsibility for the persistence or accuracy of URLs for external or third-party internet websites referred to in this book, and does not guarantee that any content on such websites is, or will remain, accurate or appropriate.

Exploring Space, Exploring Earth constitutes a Work of the United States Government for which no copyright coverage shall exist in the United States 2002

To John A. O'Keefe
Founder of Space Geodesy

CONTENTS

<i>Foreword by Neil A. Armstrong</i>	x ⁱ
<i>Preface</i>	x ⁱⁱⁱ
<i>Acknowledgements</i>	xvii
1 Preview of the orbital perspective: the million-year day	1
1.1 Introduction	1
1.2 A digital tectonic activity map of the Earth	1
1.3 Sea-surface satellite altimetry	5
1.4 Satellite measurement of plate motion and deformation	7
1.5 Satellite remote sensing	7
1.6 Satellite magnetic surveys	10
1.7 Origin and significance of the digital tectonic activity map	12
2 Space geodesy	16
2.1 Introduction	16
2.2 Space geodesy methods	17
2.3 Shape of the Earth	33
2.4 Gravity anomalies and global tectonics	37
2.5 Marine gravity and ocean-floor topography	39
2.6 Plate motion and deformation	45
2.7 Plate tectonics and continental drift	51
2.8 GPS measurements of crustal deformation	56
2.9 Earth rotation and expansion tectonics	67
2.10 Extraterrestrial gravity fields	71
2.10.1 Gravity field of the Moon	71
2.10.2 Gravity field of Mars	76
2.10.3 Gravity field of Venus	79
2.11 Summary	82
3 Satellite studies of geomagnetism	83
3.1 Introduction	83
3.2 Satellite investigations of the Earth's magnetic field	91
3.3 The main field	92
3.4 The crustal field	94
3.5 Extraterrestrial magnetic fields	112
3.6 Summary	120

CONTENTS

4 Remote sensing: the view from space	123
4.1 Introduction	123
4.2 Orbital remote sensing in geology: a brief history	126
4.3 Tectonics and structural geology	129
4.3.1 Global tectonic activity map	129
4.3.2 Tectonics of southern Asia	131
4.3.3 Elsinore Fault	136
4.3.4 Lineament tectonics	141
4.4 Exploration geology	153
4.4.1 Petroleum exploration	153
4.4.2 Mineral exploration	162
4.5 Environmental geology	167
4.5.1 Active volcanism	167
4.5.2 Glacial geology	178
4.5.3 Aeolian geology and desertification	183
4.6 Summary	190
5 Impact cratering and terrestrial geology	191
5.1 Introduction	191
5.2 Hypervelocity impact	193
5.3 Impact craters	196
5.4 Cratering studies and the space age	203
5.5 Origin of continents	207
5.6 Origin of ocean basins	209
5.7 Economic importance of terrestrial impact structures	210
5.8 Origin of the Sudbury Structure	214
5.9 Impacts and basaltic magmatism	220
5.10 Impacts and mass extinctions	221
5.11 Summary	223
6 Comparative planetology and the origin of continental crust	227
6.1 Introduction	227
6.2 Origin of the continental crust	229
6.3 Previous studies	230
6.3.1 Crustal province boundaries: are they sutures?	232
6.3.2 Ensilic greenstone belts	237
6.3.3 Terrane accretion vs. reworking	239
6.4 Thermal histories of planets	242
6.5 Crustal evolution in silicate planets	244
6.5.1 First differentiation	245

6.5.2	Late heavy bombardment	253
6.5.3	Second differentiation	253
6.5.4	Summary	254
6.6	A model of continental crust	255
6.7	Evolution of the continental crust	259
6.7.1	Stage I: first differentiation	261
6.7.2	Stage II: second differentiation	265
6.8	Petrologic evolution of the Earth	269
7	Geology and biology: the influence of life on terrestrial geology	272
7.1	Introduction	272
7.2	Gaia	273
7.3	The geologic role of water	276
7.4	Gaia and geology	278
7.5	A biogenic theory of tectonic evolution	278
7.6	Summary	279
	<i>Afterword</i>	282
	<i>Appendix A</i> Essentials of physical geology	288
	<i>Appendix B</i> Lunar missions, 1958 to 1994	290
	<i>Appendix C</i> Planetary missions, 1961 to 1992	297
	<i>Glossary of geologic terms</i>	305
	<i>Selected bibliography</i> (by chapter)	309
	<i>Index</i>	358
Color plates		between pages 204 and 205

FOREWORD

In the works of Homer, the Earth was portrayed as a circular disc floating on a vast sea and covered with a sky built from a hemispherical bowl. Critics soon noticed a flaw in this concept: the visible star field varied from place to place. From Greece, the Big Dipper was visible throughout its circle around the North Star, but southward along the Nile, it dipped below the horizon. Clearly, the surface of the Earth was somehow curved. Some thought the Earth was like the surface of a cylinder, curving to the north and south, but stretching in a straight line to the east and west. A student of Socrates, Parmenides, reasoned that the Earth must be a sphere, because any other shape would fall inward on itself. Plato also concluded that the Earth must be a sphere because a sphere was the most perfect shape for a solid body. Whether persuaded by the logic of Parmenides, or by loyalty to Plato, the Greeks came to accept a spherical Earth. A final argument, the most persuasive, was recorded by Aristotle. He noted that during an eclipse of the Moon, when the Earth's shadow fell on the surface of the Moon, the shadow was curved. The shape of the Earth would not be truly known, however, until the philosophers were replaced by the measurers.

In that category, one name stands above all others: Eratosthenes of Cyrene. To characterize him simply as a “measurer” would not do him justice; Eratosthenes was a Renaissance man long before the Renaissance. But we focus on his measuring. He determined the inclination of the ecliptic with an error of only one-half a degree. His most memorable measurement was the difference in latitude from Syene to Alexandria. By comparing the shadow lengths at noon on the summer solstice for the two locations, he calculated that they were separated by 7.5 degrees. Knowing the distance between the two cities, he calculated the circumference of the Earth to an accuracy of 99%. Eratosthenes further collected the observations of travelers, explorers, and sailors from throughout the known world –

FOREWORD

a very small world by today's standards – and integrated that knowledge in his *Geographica*.

Understanding of the Earth grew slowly after this Golden Age. It was not until the invention of the caravel in the 15th century, and John Harrison's chronometer in the 18th century, that man's understanding of his planet began again to grow. With ships capable of long ocean voyages, precisely navigated in latitude and longitude, maps of the oceans, continents, and islands became increasingly comprehensive and reliable.

Despite this great increase in knowledge, our planet remained in many ways almost as mysterious as it had been in Homer's time. The forces causing volcanic eruptions, earthquakes, and hurricanes remained enigmatic. The interior of the Earth, the topography of the ocean floor, and the dynamic nature of the atmosphere, the ocean currents, and the global magnetic field eluded understanding well into the 20th century. Two world wars stimulated impressive improvements in instruments and methods.

The late 20th century also brought new caravels, ships that could sail the oceans of space. The fortuitous development of the liquid-fueled rocket and, at about the same time, the digital computer made flight through space a reality. Space was the new high ground, the place for a new perspective, from which the "measurers" could acquire information never before available. In just a few decades, knowledge of the Earth's secrets has increased beyond imagining.

Exploring Space, Exploring Earth describes this increase in knowledge of the solid earth – geology and geophysics. Paul Lowman is a geologist who has been involved in space research since 1959 at Goddard Space Flight Center, which has taken a leading part in space geodesy, remote sensing, lunar geology, and satellite meteorology and oceanography. He is thus one of the new "measurers" and summarizes their accomplishments since the launch of *Sputnik 1* in 1957. The book is dedicated to John O'Keefe, who in the tradition of Parmenides and Eratosthenes made a fundamental discovery about the shape of the Earth from the orbit of only the second American satellite launched, *Vanguard 1*, in 1959.

The 20th century brought remarkable changes in our understanding of the Earth, the Moon, and the universe. Let us hope that the present century is equally productive.

Neil A. Armstrong

PREFACE

Mine was the first generation in humanity's million-year history to have seen the Earth as a globe, hanging in the blackness of space.

When the spacecraft *Eagle* landed on Mare Tranquillitatis in 1969, there were still people alive who had seen the Wright brothers flying. A century of progress has permitted us to see almost the entire surface of the Earth, even the ocean floor thanks to satellite altimetry. It has also given us the first opportunity to compare the Earth with other planets, starting with the Moon (geologically a "planet").

My purpose in this book is to explore the impact of space flight on geology and its subsurface counterpart, geophysics, an impact largely unappreciated in the earth science community. We geologists tend to be conservative, perhaps more so than other scientists. One reason for this may be the nature of our subject: the solid earth, ideally the part of it we can see, feel, and hammer. Another may be the nature of our work, often involving field work in harsh and remote terrains. Whatever the cause, geologists are demonstrably conservative, which is basically why this book is needed.

Geology at the end of the 20th century had reached what appears to be a certain maturity, as I described in a 1996 review, whose abstract is reproduced here. It seems true that we really have settled some questions that in 1900 were not only unanswered but even unasked. The age of the Earth is no longer debated, except in the third significant figure. The mechanism responsible for most earthquakes is now well understood, to the point that seismologists can often tell us which fault slipped, in what direction, and by how much. The origin of granite, intensely controversial as late as 1960, is, in general, understood for most granites – caveats inserted because nature has fooled us before.

It was a magnificent century for science in general, and for the

Twelve Key 20th-Century Discoveries in the Geosciences

Paul D. Lowman Jr.
Goddard Space Flight Center, Code 921
Greenbelt, Maryland 20771

ABSTRACT

This paper reviews 12 major discoveries in geology and geophysics during the 20th century, reasonably mature and discrete with respect to subject, time, or discoverer. The *Textbook of Geology* (Geikie, 1903) and *Understanding the Earth* (Brown and others, 1992) are used as benchmarks, supplemented by Yoder's 0007-1992 "Timetable of Petrology" (1993). The discovery of the radioactive decay law by Rutherford and Soddy was fundamental, bearing on the age of the Earth, internal energy, nature of the crust, and a quantitative geologic time scale. Discoveries of the internal structure of the Earth, investigated seismically, included definition of the core boundary (Gutenberg and Weichert), the inner core (Lehmann), the mantle/crust boundary (Mohorovic), the lithosphere, and the asthenosphere. Deep structure of the continental crust, revealed since 1975 by reflection profiling and study of exposed sections, has been found to be drastically different from previous concepts. The magnetic reversal time scale was developed by correlating reversed magnetization in terrestrial and marine rocks with radiometric and stratigraphic data, interpreted in light of sea-floor spreading. Sea-floor spreading, the key element of plate-tectonic theory, discovered by several independent lines of inquiry, has been directly confirmed by space-geodesy measurements of plate motion and intraplate rigidity in the Pacific Basin. Elastic rebound, the cause of shallow-focus earthquakes, was proposed after the 1906 California earthquake by Reid, using geodetic evidence; deep-focus events are still not understood. The mechanism of overthrust faulting, a major problem as late as the 1950s, was discovered by Hubbert and Rubey, who demonstrated that high fluid pressure could reduce normal stress to the point that gravity sliding would be effective. X-ray diffraction by the crystal lattice was discovered in 1912, and its applications revolutionized mineralogy, confirming solid solution and clarifying many crystallographic phenomena. The origins of basaltic and granitic magmas, completely unknown in 1900, were definitively explained for basalts by Bowen as partial melting of a peridotitic mantle, and for most granitic magmas as partial melting of crustal rocks by Tuttle and Bowen. Space exploration has revealed common patterns of planetary differentiation, including a first (or ielsic) differentiation forming global primitive crusts, followed by a second (or basaltic) differentiation, including continued basaltic magmatism. Another major result of space exploration and related research has been discovery of the importance of impact cratering, proposed as being responsible for formation of continental nuclei, the first ocean basins, and many mass extinctions in the geologic record. The most important scientific achievement of the 20th century is suggested to be the discovery of the DNA structure, revealing not only the molecular basis for all life on Earth but a critical line of investigation, formation of RNA, for study of the origin of life.

Keywords: Extraterrestrial geology; geochemistry; geochronology; geology – general; geophysics – general; history of geology; history of science; mineralogy and crystallography; petrology – general; plate tectonics; reviews – articles; structural geology; volcanoes and volcanism.

Introduction

The 20th century opened with a surge of technological progress never equaled before or since. A mere two decades, from 1890 to 1910, saw the development of radio, aviation, electronics, the automobile industry, the steel-frame skyscraper, the Diesel engine, the steam turbine, and many other features of today's world existing, if at all, only in rudimentary form in 1890. In combination with the well known revolution in physics, these developments laid the infrastructure for a century of extraordinary scientific progress. The purpose of this review is to focus on advances in the solid-earth sciences, geology and geophysics, during the 20th century.

The approach will be to outline 12 discrete and reasonably mature discoveries of features or phenomena, and their consequences. Stress will be on the discoveries rather than on the people who made them, primarily to keep the paper within practical length. Two textbooks provide excellent benchmarks of progress since 1900: Geikie's (1903) *Textbook of Geology* and *Understanding the Earth* (Brown and others, 1992). Sullivan's (1991) *Continents in Motion*, though focussed on plate tectonics, is a well documented history of the earth sciences in general from the mid-19th century on. Yoder's (1993) "Timetable of Petrology" lists and documents specific developments from 0007 to 1992. Citations given will be largely of original sources.

solid-earth sciences. However, the “certain maturity” just described may be instead a certain stagnation, a feeling that the big problems in geology have now been solved. Most scientists will recognize this situation; it describes the prevailing view in physics around 1890.

I think that geology is on the verge of a major paradigm shift, to use the fashionable term, comparable to that in physics between 1895 and 1905. Geologists today subscribe almost unanimously to what W. K. Hamblin has called a “master plan,” the theory of plate tectonics. The three essential mechanisms of plate tectonics – sea-floor spreading, subduction, and transform faulting – have in fact been confirmed by so many independent lines of evidence that we can consider them observed phenomena, at least in and around the ocean basins. Plate tectonic theory is called upon to explain, directly or indirectly, almost all aspects of terrestrial geology above the level of the crystal lattice. Even metamorphic petrology, in particular the new field of ultra-high pressure metamorphism, invokes phenomena such as continental collision to explain how rocks recrystallized 150 kilometers down are brought to the surface.

I think this is a mistake. We now know, from space exploration, that bodies essentially similar to the Earth in composition and structure have developed differentiated crusts, mountain belts, rift valleys, and volcanoes without plate tectonics, in fact without plates. Furthermore, we now know, thanks partly to remote sensing from space, that the Earth’s crust can not realistically be considered a mosaic of 12 discrete rigid plates. For these and other reasons, I disagree with certain aspects of plate tectonic theory, as will be explained in the text.

Is the Earth fundamentally unique? Most geologists think it is, and consider the discoveries of space exploration to be interesting but irrelevant to terrestrial geology. The basic objective of this book is to show the contrary: that **the exploration of space has also been the exploration of the Earth**, and that real understanding of its geology is just beginning now that we can see our own planet in almost its entirety, and can compare it with others.

Exploring Space, Exploring Earth is aimed primarily at geologists and geophysicists. However, it has been written to be understood even by readers without a single geology course. Such readers may in fact have the advantage of freedom from preconceived notions. Jargon is unavoidable, but has been kept to the minimum possible. Technical terms are explained either in context or in the glossary. Petrologic topics are presented without the use of phase diagrams, with one exception. The book is quantitative but non-mathematical, without a single equation. Readers who may be

uneasy about this are invited to read the appropriate references, where they will find equations reaching to the horizon.

A serious word about mathematics: students should not be misled by the absence of equations in this book. Most of the topics covered here, in particular space geodesy and geomagnetism, involve enormous amounts of mathematical analysis and computer data handling. Any student considering a career in geophysics or geology in the 21st century must have a fundamental grasp of higher mathematics, such as algebra, calculus, and numerical analysis, and computer science (such as programming).

A minor stylistic point: the expressions “manned space flight” and “manned missions” will be used without apology in this book. Women have for years flown on space missions, manned warships, piloted eight-engined bombers. They no longer need condescending euphemisms.

A suggestion to the reader: geology is very much a visual science. If you have never had a geology course, I urge you to buy one of the many popular geology guides, get out of town, and *look* at your local geology. (If you live in San Francisco, you don’t have to leave town.) Once you have learned even the most elementary facts about geology, you will be amazed at what you can see – and understand – in even a road cut. When you travel by air, especially over the western US, try to get a window seat (on the shady side: left going east, right going west), ignore the movie, and enjoy the panorama from 35,000 feet. The strangest planet in the solar system is our own; explore it yourself.

Space exploration begins on the ground. If you have never had an astronomy course, I suggest that you buy a \$40 pair of binoculars (not a telescope), and *look* at the sky, in particular the Moon. Even 7×50 binoculars reveal a surprising amount of detail along the terminator, and may show the Galilean satellites of Jupiter, which were invisible until the invention of the telescope. Even without binoculars, simply learning your way around the night sky with a cardboard star finder will be fun. The constellations are a compass, a map, a clock, and a calendar; learn why.

Paul D. Lowman Jr.

ACKNOWLEDGEMENTS

This book summarizes the efforts of thousands of people, and the reference list is implicitly a partial acknowledgement of their contribution. I am particularly indebted to my colleagues at Goddard Space Flight Center, far too many after 41 years to name individually, with a few outstanding exceptions.

The first of these is the late John A. O'Keefe, without whom this book would never have been written. He and Robert Jastrow, in 1959 head of the Theoretical Division, took a chance on me when I was a graduate student on the "Korean G.I. Bill," with no academic credentials beyond a B.S. from a state university. I owe my career to them. However, beyond that, John O'Keefe was the founder of space geodesy, as the dedication indicates. The late Eugene Shoemaker also credited him with being "the godfather of astrogeology." He was instrumental in bringing the US Geological Survey into NASA programs in 1960, and helped draw up the first scientific plans for the *Apollo* landings. His tektite field work took him to North Africa, Australia, and many parts of North America. He also played a little-known but critical role in the *Landsat* program, by getting terrain photography onto the experiment list for the later *Mercury* flights, as documented in the remote sensing chapter. John O'Keefe was, in summary, one of the great figures of the heroic age of space exploration, ranking with Goddard, von Braun, Shoemaker, Van Allen, and von Karman. He died in September 2000, but I am gratified that he saw the manuscript of the book and its dedication well before his death.

I was originally invited to write this book in 1993 by Dr Catherine Flack, then with Cambridge University Press. I accepted the invitation at once, one reason being that Neil Armstrong and I had co-authored a paper "New Knowledge of the Earth from Space Exploration" in 1984, which Neil presented at the Royal Academy of Sciences in Morocco. We covered the same major topics presented in this book, now supplemented by 15 years of progress.

ACKNOWLEDGEMENTS

Exploring Space, Exploring Earth was written with the encouragement and support of the Goddard Space Flight Center management. However, I wish to specifically acknowledge the support of two Director's Discretionary Fund (DDF) grants. The first of these, from Tom Young in 1983, was for a lineament study by Nick Short and me on the Canadian Shield. It led to a successful *Shuttle Imaging Radar* experiment and gave me access to both the geology and the geologic community of Canada, a world leader in the field. The second DDF grant, from Joe Rothenberg in 1997, provided support for the Digital Tectonic Activity Map that opens the book.

In a long career I have had several branch chiefs, all of whom were friends as well as supervisors. I must specifically acknowledge the decision of the late Lou Walter, first chief of the Planetology Branch, to transfer me to the Geophysics Branch during a major reorganization in 1973. By forcing me to broaden my scientific scope, Lou helped lay the foundation for this book. My present branch chief, Herb Frey, has given me continual encouragement and support through the years the book has been in preparation. Herb's own scientific work on the tectonic effects of large impacts, and on crustal magnetism, cited in the text, has been important in my studies of crustal evolution.

I wish to thank the many Canadian geologists who have helped me, often by vigorous arguments, in particular Lorne Ayres, Hayden Butler, Ken Card, Tony Davidson, Mike Dence, Dave Graham, Jeff Harris, Paul Hoffman, Darrel Long, Wooil Moon, John Murray, John Percival, Walter Peredery, Don Rousell, Vern Singhroy, John Spray, Hank Williams, and Susan Yatabe. My wife, Karen, has accompanied me on many Canadian trips, making them much broader experiences by persuading me to look at something beside outcrops.

The late Eugene Shoemaker was both a friend and a continual inspiration as a pioneer in comparative planetology. His sudden death in a 1997 auto accident in the Australian outback was felt by thousands of geologists, as a personal and professional loss.

The Library of Congress Geography and Map Division has been an invaluable resource in writing this book. Ruth Freitag and Barbara Christy in particular have been generous with critical reviews, and in providing information for compilation of the tectonic activity maps. At Goddard Space Flight Center, the staff of the Homer E. Newell Library has been continually cooperative and helpful for many years.

Technical reviews of specific chapters have been provided by Barbara Christy, Steve Cohen, John O'Keefe, Mike Purucker, Tikku

Ravat, Dave Rubincam, Terry Sabaka, Pat Taylor, and Jacob Yates, to whom I am indebted.

An eminent French scientist, commenting on the value of the *International Space Station*, said, in 1998, that he was unaware of any scientific discovery made by an astronaut. Taking a narrow view, neither am I, but this book would not have been possible without the enormous accomplishments of the American manned space flight program.

Since 1962 I have worked frequently in Houston with the staff of Johnson Space Center, originally the Manned Spacecraft Center, and thank them collectively for their invaluable support in efforts ranging from terrain photography to analysis of lunar samples.

A specific acknowledgement, also collective, is to the astronauts of the *Mercury*, *Gemini*, *Apollo*, and *Skylab* programs for their outstanding accomplishments in hand-held terrain photography. It is not generally realized that the *Landsat* program was originally stimulated by the spectacular 70 mm color pictures they returned. I had the privilege of working with these men – the best of the best – and have tried to document their fundamental contributions in the remote sensing chapter and in the referenced article on the *Apollo* program.

This book is in a sense the final report on two radar experiments carried on the 41-G *Shuttle* mission of 1984, focussed on the origin of the Grenville and Nelson Fronts, east and west boundaries respectively of the Superior Province of the Canadian Shield. I thank the crew of the 41-G mission for their performance in overcoming in-flight problems, my co-investigators in the US and Canada for their contributions, and Dr R. E. Murphy for his support of the 41-G investigation.

The contribution of astronauts to space research, returning to the comment cited above, is not generally appreciated. The crew of HMS Beagle made no scientific discoveries. But their passenger did; he was Charles Darwin. My final acknowledgement is therefore to those whose day-to-day work laid the foundation for *Exploring Space*, *Exploring Earth*: astronauts, of course; deck hands on oceanographic expeditions; field geologists the world over; jug-hustlers in seismic reflection profiling; darkroom technicians; computer programmers; motor pool dispatchers; librarians; secretaries; and many more, too many to thank specifically. This is their book.

Paul D. Lowman Jr.

CHAPTER 1

Preview of the orbital perspective: the million-year day

1.1 Introduction

“The present is the key to the past.” This axiom is familiar to all geologists, expressing the belief that the Earth has evolved over billions of years by processes still going on today. In recent years there has been something of a revival in catastrophism, with the realization that rare events such as meteoritic impacts and sudden glacial floods do occasionally happen. These events – and better known sporadic ones, such as volcanic eruptions and great earthquakes – require us to reconsider our concept of the geologic “present.” How long must we watch the Earth to get a realistic picture – a day in the life of the Earth, so to speak – of geologic processes?

The geologic events of a month or even a decade clearly do not represent the full spectrum of geologic activity. The map (see Fig. 1.1) that opens this book, derived largely from space-acquired data, was designed to illustrate the tectonic and volcanic activity of the last one million years – a “million-year day.” Mathematically-inclined readers may think of it as a first derivative – the instantaneous rate of change – of a conventional tectonic map. The tectonic activity map and related ones are presented at this point as a preview, to demonstrate at once the fundamental impact of orbital data on geology and geophysics.

1.2 A digital tectonic activity map of the Earth

It is only in the last 40 years, since about 1965, that we have finally arrived at something like a true understanding of “the way the Earth works” in the title of Wyllie’s (1976) geology text. As late as 1962, for example, it could still be reasonably proposed in a leading journal (Chenoweth, 1962) that the deep ocean floor, if uncovered, would be a primordial cratered surface resembling the face of the Moon. As it happened, the same year saw the publication of Hess’s (1962) classic “essay in geopolity” (his words), which laid the foundation

1 PREVIEW OF THE ORBITAL PERSPECTIVE: THE MILLION-YEAR DAY

for the new global tectonics, soon to be termed “plate tectonics,” showing that the oceanic crust is geologically young and mobile.

Plate tectonic theory holds that roughly two-thirds of the Earth’s crust, the ocean basins, is both active and, in a geologic sense, ephemeral. Oceanic crust, chiefly basaltic, or “mafic,” is continually generated by volcanic eruptions along features known but little understood for years: the mid-ocean ridges such as that bisecting the Atlantic Ocean. Its Pacific counterpart is the East Pacific Rise. These ridges are seismically active, an expression of processes in the deep interior generating basaltic magma that is erupted along the ridges (generally under water with the notable exception of Iceland, sitting astride the Mid-Atlantic Ridge). This newly generated crust moves away from the ridges at a few centimeters a year in the now-familiar process of “sea-floor spreading,” a term coined by Dietz (1961), who credited Hess with the concept although an earlier version had been proposed by Arthur Holmes (1931).

The Earth is tectonically a closed system, and newly generated crust in most areas is eventually destroyed by “subduction,” in zones several hundred kilometers deep in which the oceanic crust descends, to be re-absorbed in the mantle by processes still not fully understood. (Most active volcanos, notably those of the Pacific rim, occur over these subduction zones.) These phenomena collectively account for the term “ephemeral” used to describe oceanic crust, in that sea-floor spreading and subduction recycle this crust in a few hundred million years. Far from being primordial as suggested by Chenoweth, very little of the basaltic ocean crust is more than about 200 million years old. The continental crust in contrast is at least four billion years old and as will be argued later – from comparative planetology – may be fundamentally “primordial.”

Since the emergence of the theory just outlined, many global tectonic maps have been published. However, regardless of the validity of plate tectonic theory itself, these maps have all been unconstrained by time limits, showing all mappable features of whatever age. The word “features” is critical to understanding the map presented here, which is focussed on phenomena rather than features, the phenomena being tectonic and volcanic activity of the “million-year day.”

Two versions of the digital tectonic activity map (DTAM henceforth) are presented. The first (Fig. 1.1) is a composite of shaded relief with superimposed tectonic and volcanic features; the second (Fig. 1.2) is a schematic map showing the same features in purely symbolic form, with the addition of continental/oceanic crust boundaries. The following discussion of the DTAM will be focussed

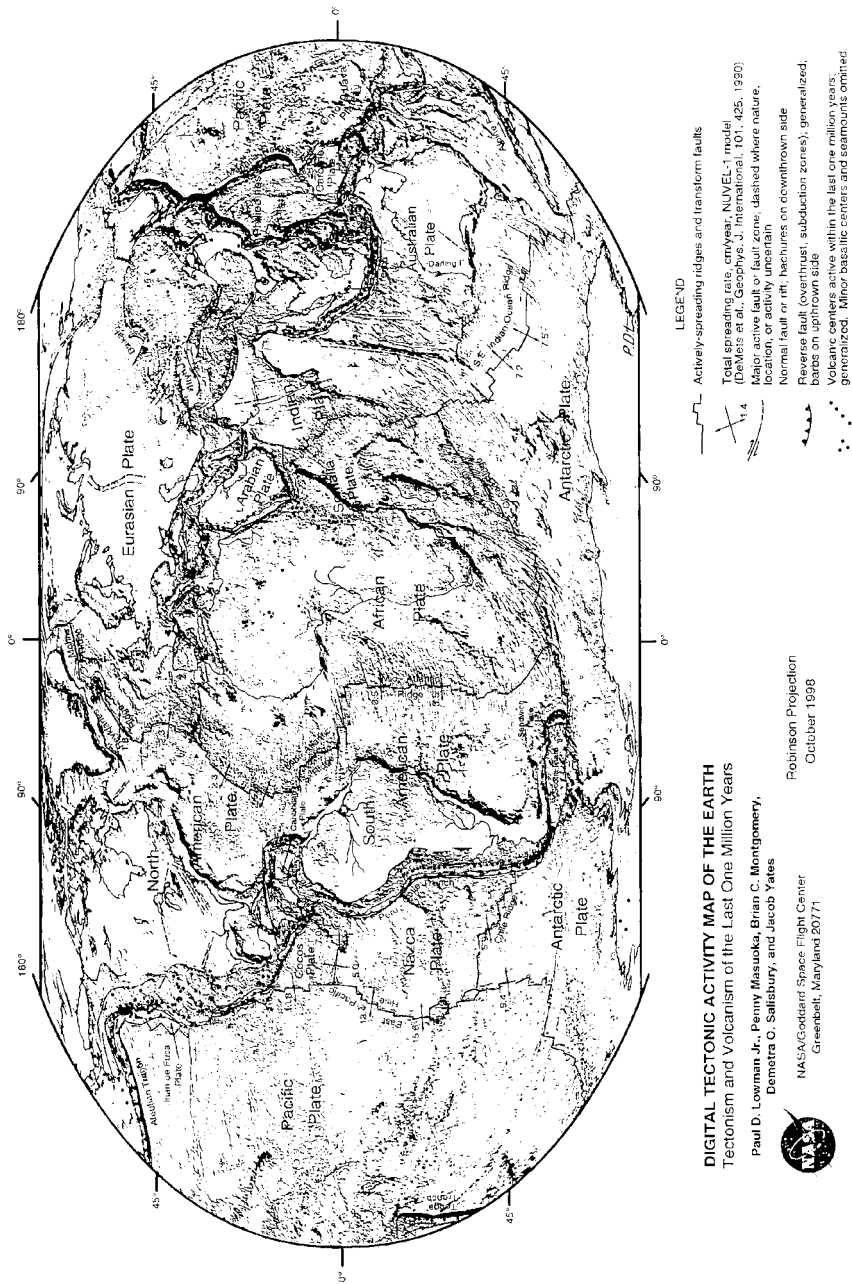


Fig. 1.1 (See also Plate I) Digital tectonic activity map (DTAM) of the Earth, based on shaded relief map largely generated from satellite altimetry.

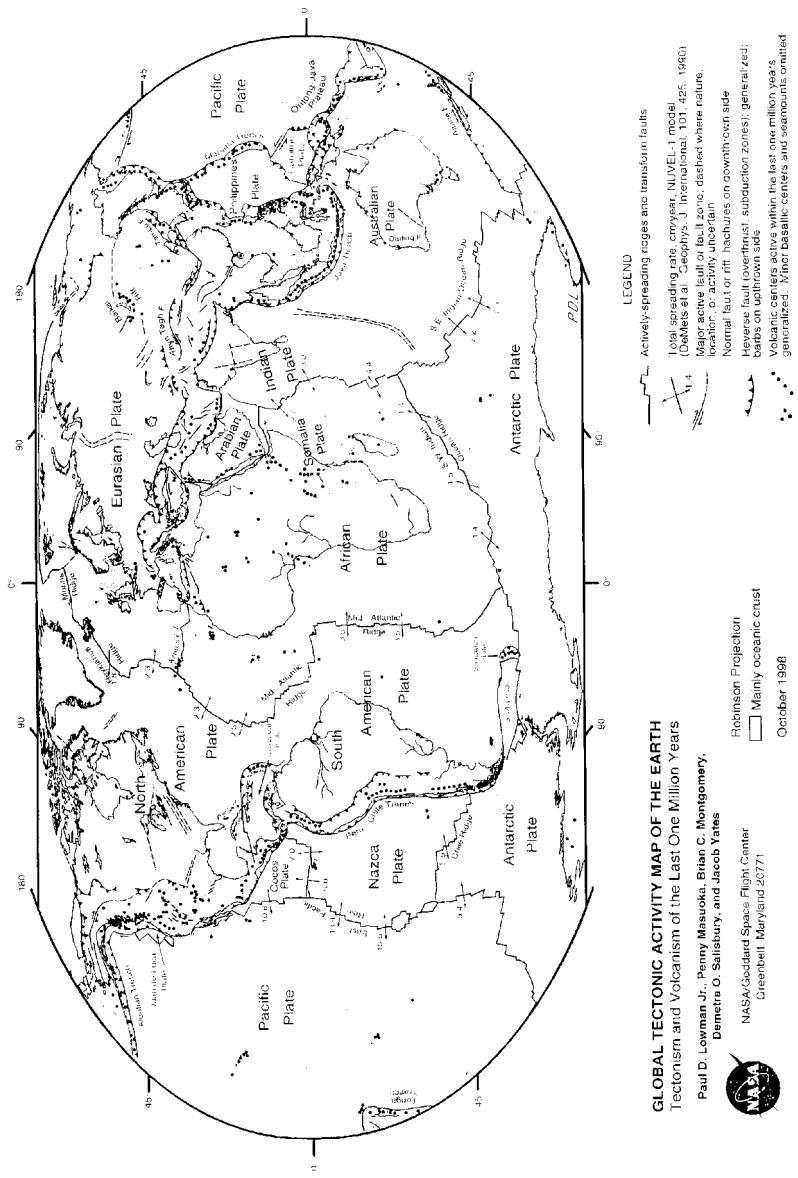


Fig. 1.2 (See also Plate II) Schematic global tectonic activity map (GTAM), from Fig. 1.

primarily on the relief version, with the objective of summarizing the contributions of space data to its compilation. A series of seismicity maps, computer-drawn with the same scale and projection, was essential for the DTAM and one is accordingly included (Fig. 1.3). Software and major data sources are given by Lowman *et al.* (1999) and Yates *et al.* (1999).

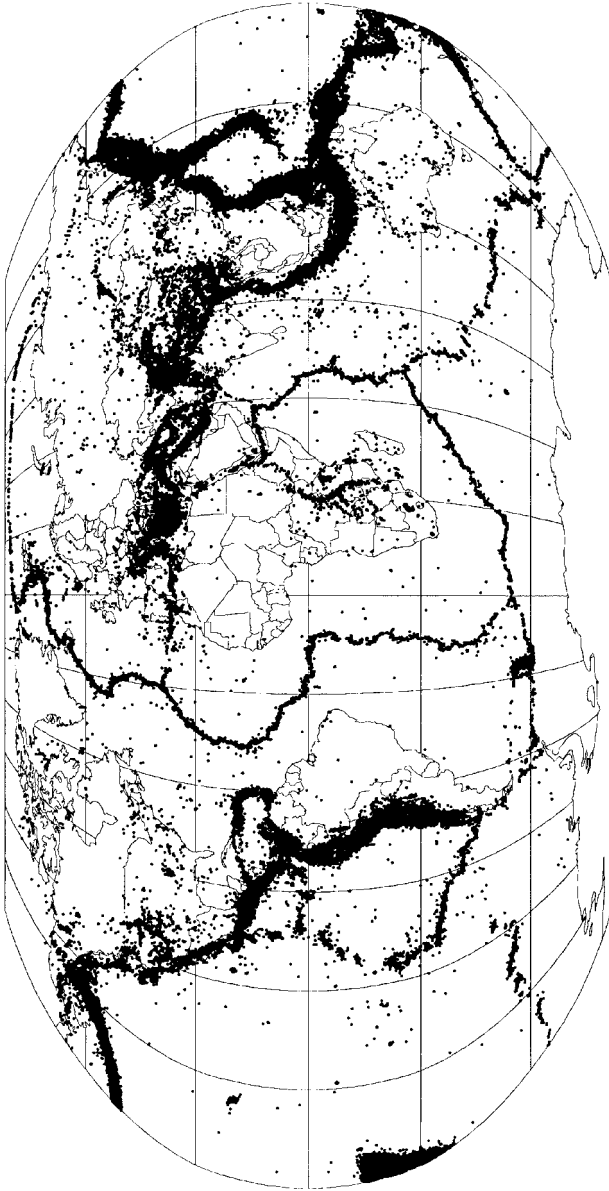
1.3 Sea-surface satellite altimetry

The DTAM is derived from an enormous data base of surface and space-related surveys and studies. The contribution of space data begins with the delineation of the topography of the ocean basins (that is, bathymetry) by satellite altimetry. Comparable maps became available in the 1960s with publication of the now-classic hand-drawn maps of Bruce Heezen and Marie Tharp, for several decades familiar features of most introductory geology books. The Heezen–Tharp maps were based on conventional marine surveys, chiefly echo-sounding. But, since such surveys produced depth data along single survey lines they could not begin to show the topography of large uninterrupted areas of the ocean basins. Consequently, many features had to be drawn by extrapolation in unsurveyed areas.

This situation has now been remedied by sea-surface satellite altimetry (Sandwell, 1991; Smith and Sandwell, 1997). This method (discussed in detail in Chapter 2) depends on the fact, first demonstrated in 1973 by a radar altimeter carried on *Skylab*, that the mean sea surface (after correction for tides, currents, and the like) forms a very subdued replica of the underlying ocean-floor topography. The effect is suggestive of snow-covered ground. It is caused by the lateral gravitational attraction of ocean-floor relief features. A submerged volcano, for example, will pull the surrounding ocean toward itself, forming a very slight hump (generally a few meters at most) on the overlying ocean. The ocean floor adjacent to a trench will similarly pull the water very slightly away from the trench, which will thus be mirrored in the overlying sea surface.

In the decades since the phenomenon was first demonstrated, satellite altimetry has become an essential tool for mapping the ocean floor. Hundreds of thousands of satellite altimetry passes have been combined to produce a digital elevation model, available from the National Geophysical Data Center, of almost the entire ocean floor. It is that model on which the computer-drawn shaded relief map of Fig. 1.1 is based. The software used for its construction exaggerates the relief, emphasizing it with pseudo-illumination from the northwest. However, this map is fundamentally different

Preliminary Determination of Epicenters 200,855 Events, 1963 - 1998



Paul D. Lowman, Jr.
NASA
Goddard Space Flight Center
Greenbelt, MD 20771
USA

Data Source:
Seismicity Catalogs
Volume 2 Global and Regional, 2150 B. C. - 1996 A. D.
The National Geophysical Data Center and
The National Earthquake Information Center

Map prepared in Robinson Projection
with magnitudes greater than 3.5.
August 12, 1998

Fig. 1.3 Earthquake epicenter map, used to delineate zones of tectonic activity.

from previous maps in being an objective one, not an artist's rendition. Subject to scale and resolution limits, satellite altimetry has given us a view of some $\frac{2}{3}$ of the Earth's surface that was until recently much more poorly mapped than the near side of the Moon. The active tectonic features shown in the schematic DTAM (Fig. 1.2) are thus offered as reasonably objective representations.

1.4 Satellite measurement of plate motion and deformation

The digital tectonic activity map shows recent estimates of total sea-floor spreading rates from the mid-ocean ridges. These estimates owe nothing to space techniques, being based on the distances of dated magnetic anomalies from spreading centers, as will be explained in Chapter 3. However, space geodetic techniques (Robbins *et al.*, 1993), specifically satellite laser ranging (SLR) and very long baseline interferometry (VLBI) have made it possible to measure intercontinental distances with precisions on the order of one centimeter. The *Global Positioning System* (GPS) is now filling in areas with denser measurement nets. It is hardly necessary to point out that such an achievement was unimaginable before satellite methods and radio astronomy were available.

The contribution of satellite distance measurements to the DTAM lies in the direct demonstration (Fig. 1.4) independently by SLR and VLBI, that several islands in the Pacific Ocean, such as Kauai, are moving northwest toward Japan at rates of roughly 6–7 centimeters per year. These rates are very close to those implied by the NUVEL-1 sea-floor spreading estimates, which are averages for about the last 3 million years. To extrapolate these spreading rates to the motion of entire plates of course requires the assumption that the plates are internally rigid. But here SLR and VLBI are again useful, by showing that the inter-island distances are essentially constant, that the Pacific Plate is indeed rigid to a close approximation.

In summary, the dynamic behavior of the oceanic crust as outlined by plate tectonic theory has been directly observed by space geodetic methods, confirming estimates made by totally independent measurements along the mid-ocean ridges.

1.5 Satellite remote sensing

The tectonic activity of large areas, especially in southern Asia, as shown on the DTAM is derived to a major degree from satellite remote sensing data, especially *Landsat* imagery. As will be

1 PREVIEW OF THE ORBITAL PERSPECTIVE: THE MILLION-YEAR DAY

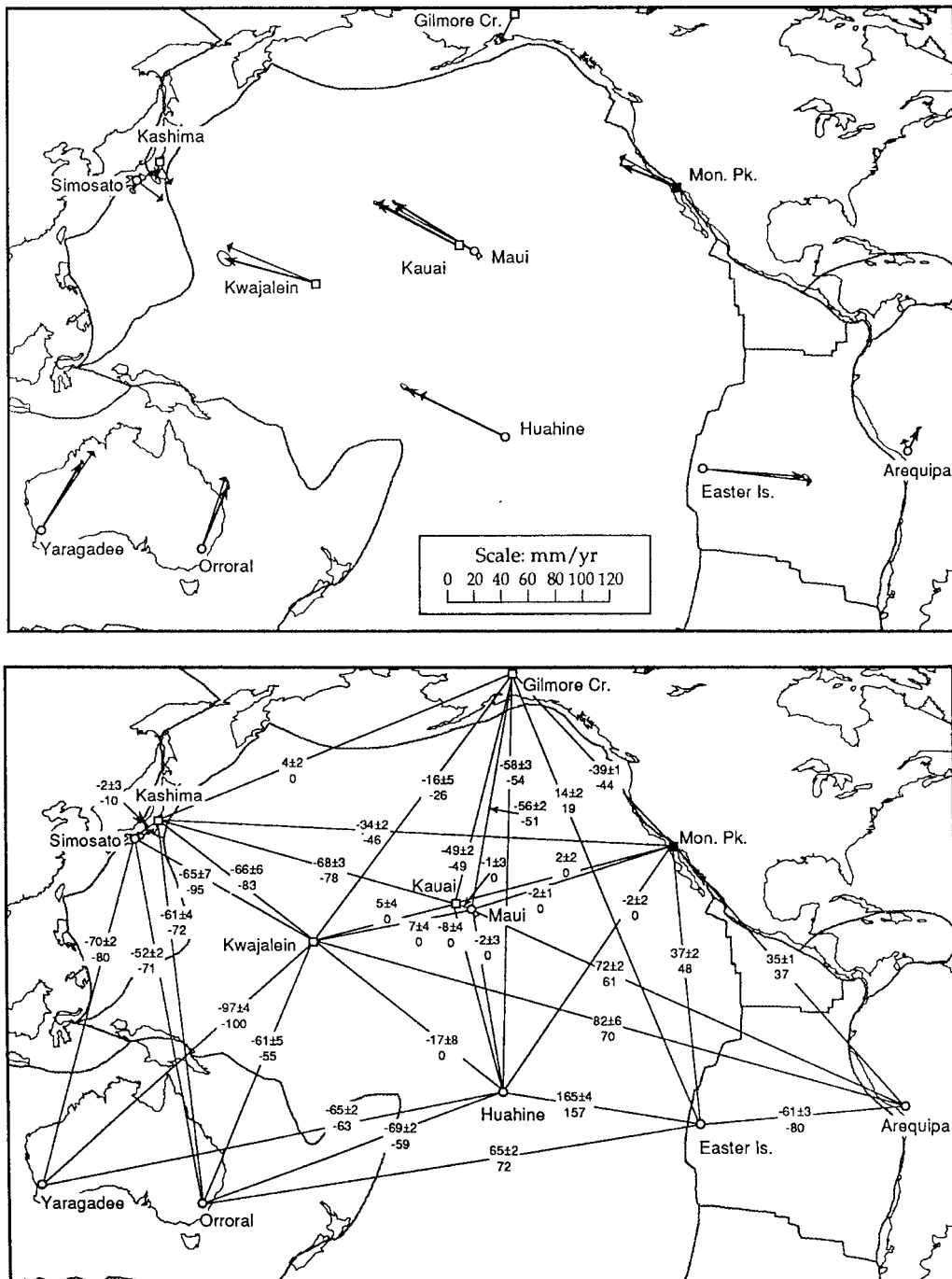




Fig. 1.5 (See also Plate III) Gemini 12 photograph S66-63082; view to east over the Zagros Mountains (left), Strait of Hormuz, and Makran Range. Width of view 600 km. From Lowman (1999).

described in Chapter 4, the tectonic structure of Asia, especially north of the Himalayas, was almost completely unknown until the availability of satellite imagery, starting with hand-held 70 mm photographs (Fig. 1.5) taken by *Mercury* and *Gemini* astronauts (Lowman, 1999). The Tibetan Plateau, for example, was essentially inaccessible for many years because of its remoteness and, after World War II, political barriers. Satellites surmounted these barriers, providing superb synoptic views of hundreds of thousands of square kilometers. *Landsat* images were first used to produce tectonic maps of Tibet. Chinese geologists were among the first to use *Landsat* for similar maps, and in the years since, satellite imagery has become widely used to map the tectonic structure of not only southern Asia but other parts of the Alpine fold belt and even supposedly well-mapped areas such as northern Norway.

Satellite imagery not only reveals the existence of large faults in remote areas, but often gives a good idea of their current activity by

showing features such as fault scarps and offset streams. This is only the beginning of a rapidly expanding field, since satellite radar interferometry and space geodesy by means of the *Global Positioning System*, to be described in Chapter 2, are rapidly complementing satellite imagery.

The DTAM is explicitly a very generalized map, especially in its representation of continental volcanism. The contribution of space data here also comes from satellite imagery. As will be described, many previously-unmapped volcanos have been found with *Landsat* imagery and astronaut 70 mm photography starting with the *Gemini* missions of the mid-1960s. However, the real value of satellite imagery for showing volcanism is simply in making the map's compiler aware of geomorphically fresh, and hence young, volcanos and lava flows in previously-mapped but remote areas. The best available compilations of active volcanos are restricted to historical records, covering the last 10,000 years. By revealing many other young but historically inactive volcanos and lava flows, satellite imagery has made it possible to produce the first global representation of volcanic activity extending back about one million years.

1.6 Satellite magnetic surveys

The existence of the Earth's magnetic field has been known for centuries, and scientific study goes back to the time of Queen Elizabeth I, as we will see in Chapter 3. However, it has been an extremely difficult feature to study. To begin with, it is highly variable, from minute to minute during solar storms, or over hundreds of thousands of years during reversals of the Earth's main magnetic field. Additionally, the magnetic poles are constantly moving. A recent Canadian geophysical expedition on Ellesmere Island found that the north magnetic pole actually passed under them while they were at one camp site. (Canada has been a traditional leader in geomagnetic studies; it may help to own one of the magnetic poles.) Moreover, magnetism in general was not understood until the 19th century, in particular until the work of James Clerk Maxwell.

Study of the Earth's crustal magnetism was given a jump start, so to speak, during World War II, when greatly improved magnetometers for submarine detection were developed. Aeromagnetic studies in the early post-war years discovered many valuable ore deposits, in Canada and elsewhere. However, such studies are time-consuming and expensive. Mapping of crustal magnetism in the oceans is even more time-consuming when done by ships. The next big step forward in the study of geomagnetism came with the launching of artificial satellites.

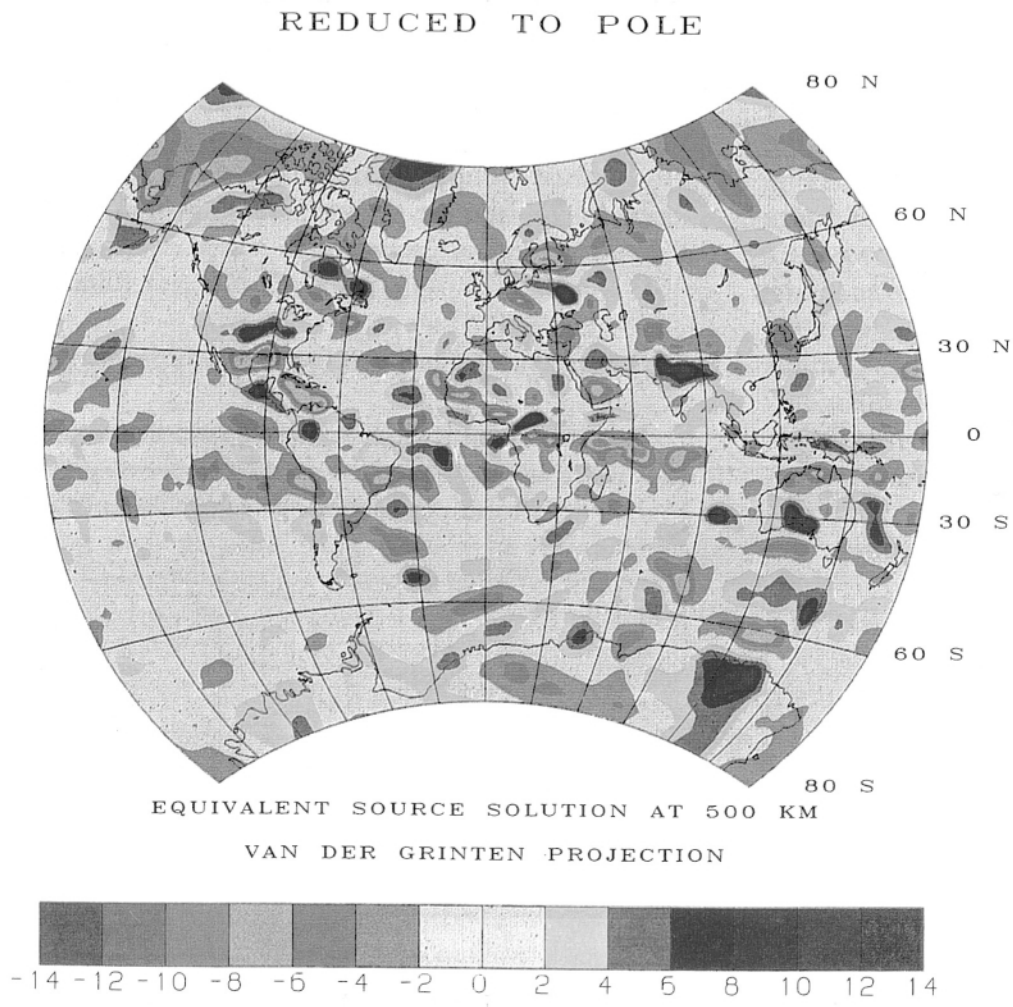


Fig. 1.6 (See also Plate IV) Scalar (non-directional) magnetic anomaly map from *POGO* data, equivalent sources at 500 km altitude, reduced to pole. Values in nanoteslas (nT). From Langel (1990).

A major contribution of satellite data has come from measurements of crustal magnetism by satellites, notably the *Polar Orbiting Geophysical Observatory* series (*POGO*) and *Magsat*. They are illustrated (Fig. 1.6) by an early map from *POGO* data, compiled by the late R. A. Langel (1990), *Magsat* Project Scientist and a pioneer in the use of satellite magnetic data. Principles and details of such maps will be covered in Chapter 3. At this point, it will just be mentioned that this *POGO* map, actually using data from three different

satellites, illustrates the promise of satellite data as well as the difficulties in using them.

The “promise” is demonstrated simply by the global coverage of this map (accompanied by polar projections, not reproduced here). Entire ocean basins, and large unsurveyed continental areas, are shown, admittedly in relatively little detail. One previously unknown feature, the Bangui anomaly in central Africa, was essentially discovered in satellite data, as will be discussed in Chapter 3. However, the compiler of this map had to allow for different satellite altitudes, geomagnetic latitudes, and short-term variations in the magnetic field caused by external influences. The term “reduced to pole” refers to the problem of the inclination of the Earth’s main magnetic field, assumed to produce the observed features by induction. If one were at the north magnetic pole, the field would be pointing essentially straight down, in contrast to the magnetic equator, where it would be horizontal. In this map, Langel reduced all data to a common inclination, vertical, as if the features were at the north magnetic pole.

This and other magnetism maps typify the advantages of satellites for earth observations: global coverage, rapid and systematic repetition of coverage, and broad field of view. These advantages can be discussed further by returning to the digital tectonic activity map.

1.7 Origin and significance of the digital tectonic activity map

The post-*Apollo* realignment of NASA roles and missions, in the early-1970s, led to increased emphasis at Goddard Space Flight Center on solid-earth geophysics and space geodesy. Focussed on the Earth, these fields required realistic global maps of tectonic activity. However, it was found that even the best small-scale tectonic maps were highly interpretive representations intended to illustrate plate tectonic theory. Furthermore, they were generally not time-constrained, illustrating many features as old as Mesozoic (some 200 million years ago).

Fortunately, in 1975 the National Geographic Society published “The Physical World,” a hand-drawn Van der Grinten projection color representation of the Earth. Far outclassing all previous maps of this type, the National Geographic map was used (Lowman, 1982) to compile “Global Tectonic and Volcanic Activity of the Last One Million Years,” (an updated version of which appears elsewhere in Chapter 4). This global tectonic activity map has proven useful in many applications. It served as the base map for laying out baselines

for SLR and VLBI measurements in the NASA Crustal Dynamics Program, and was used for interpretation of satellite gravity and magnetic measurements as illustrated in Chapters 2 and 3. However, its widest application was in geologic education, appearing in more than a dozen textbooks and many general articles.

The flood of new information about the Earth's topography, from satellite remote sensing and sea-surface altimetry among other things, combined with new computer-based cartographic techniques, made a modernized version of the 1982 tectonic activity map desirable and possible. The DTAM (Lowman *et al.*, 1999) was the result. The point of this historical account is that the very origin of the DTAM can be directly traced to space research, which provided not only the means to compile the DTAM but the necessity to produce it and its predecessor.

This chapter is essentially an illustrated essay, leaving out most references and postponing detailed discussion of the DTAM to later chapters. However, a few of the most fundamental implications of this map should be briefly mentioned.

The most significant aspect of the DTAM concerns the question: *How well does plate tectonic theory describe and explain the structure and activity of the solid earth?* The theory has been eloquently described by Hamblin (1978) as “a master plan into which everything we know about the Earth seems to fit.” A more recent text (Press and Siever, 2001) describes it as an “all-encompassing theory,” treating most physical geology topics in a plate tectonic context. Plate maps are familiar features of every geology text and most popular articles about geology, and any good student can point out the major plates. However, the DTAM shows that such maps, and the theory they illustrate, are at best oversimplifications of a complex and active planet. For example, the Eurasian Plate is shown on most “plate maps” as including the entire area from Iceland to Indonesia. If a plate is defined, loosely, as a torsionally rigid segment of lithosphere bounded by some combination of ridges, trenches, and transform faults, the artificiality of an Iceland–Indonesia “plate” is obvious.

The California part of the boundary between the North American and Pacific Plates is generally shown, and described, as the San Andreas fault, whereas the DTAM shows tectonic activity reaching to at least the Wasatch Mountains and probably beyond. (As described in Chapter 2, space geodesy has verified this.) The boundary between the African and Eurasian Plates is not a line but a broad zone including the intensely active Mediterranean Sea and the Alpine fold belt. It is clear that there are large areas of the Earth’s

surface, notably on the continents, that simply can not be assigned to any particular plate. A frequent approach to this problem is to postulate “microplates.” However, as discussed by Thatcher (1995), the crust in many areas seems to behave as a continuum. Which description – continuum or microplate – is correct remains to be seen. This problem will be discussed in more detail in Chapter 2. At this point, it will simply be suggested that plate tectonic theory is at best an incomplete description of the Earth.

A related aspect of plate tectonic theory is its explanation of the Earth’s geologic behavior, i.e., its tectonic and volcanic activity. The theory as commonly presented in today’s textbooks often explains features such as folded mountain belts as the result of “continental collisions,” or more accurately “plate convergence.” The DTAM and its associated seismicity map (Fig. 1.3) should raise questions at once about this facile explanation. For example, the western part of the Alpine fold belt, from Pakistan to the Atlantic Ocean, is intensely active. Can this activity be explained by continental collisions, or plate convergence? Plate tectonic models, such as the one (NUVEL-1) used for the DTAM spreading rates, all show even the schematic Eurasian and African Plates as moving extremely slowly. Two leading proponents of plate tectonic theory, K. C. Burke and J. T. Wilson (1972) have pointed out that the absence of age-progressive volcano chains on Africa (“hot-spot trails” in plate tectonic terms) indicates in fact that Africa has been *stationary* with respect to the mantle for at least 25 million years (Burke, 1996). The DTAM thus brings out the paradox that some of the most intense tectonic activity on Earth occurs in a broad zone between two plates that hardly appear to be moving at all.

Perhaps the most controversial and speculative question raised by the DTAM is whether plates actually carry continental crust along with them, as implied by the common phrase “plate tectonics and continental drift.” Here it will simply be pointed out, with reference to Fig. 1.2, that movement of the Eurasian Plate involves the rotation of a block of lithosphere extending from Iceland to Siberia. Can such a block behave as a rigid unit? The tectonic activity of western Europe, and even of the Urals (commonly thought to have been formed in the late-Paleozoic), throws strong doubt on the rigidity of this “plate.” Furthermore, the DTAM illustrates a problem brought out by the author, discussed in Chapter 3: the driving force for such a plate. Can sea-floor spreading, or ridge push, in the North Atlantic actually move a segment of lithosphere covering some 120 degrees in longitude? The answer will at this point be left as an exercise for the reader. (The author’s views are given in Skinner and

Porter, 1995.) But it can be suggested that among the most important implications of the digital tectonic activity map are the uncertainties, anomalies, and questions it illustrates in the supposed “master plan,” plate tectonic theory. Science progresses by recognition of such anomalies: the supposedly unsuccessful Michelson–Morley experiment, Fleming’s spoiled Petri-dish culture, Plunkett’s clogged Freon cylinder being just three examples. Consensus is satisfying, comfortable, and easy to teach, but it can turn into stagnation. The DTAM, and the findings of space research in general, may help prevent such stagnation.

CHAPTER 2

Space geodesy

2.1 Introduction

Space geodesy is a new term for a new science, one in which satellite tracking and related techniques are used to study the shape, deformation, and motions of the Earth. However, this “new” science has a history going back millennia. As Neil Armstrong’s Foreword makes clear, scientists of today using satellites and radio telescopes are continuing the work begun by Eratosthenes, whose value for the circumference of the Earth was within 1% of the true value. Even the very first artificial satellites produced new knowledge of the Earth’s size and shape. Four decades of successive satellite and manned spacecraft missions have added enormously to this knowledge, and the field of space geodesy has turned out to have great scientific and applied value, value only now beginning to be realized.

The first formal proposal to use satellites for what is now called space geodesy was by J. A. O’Keefe (1955), as part of a proposal to the National Science Foundation for “an artificial unmanned earth satellite” (Haley and Rosen, 1955). O’Keefe proposed a reflective inflated satellite, to be illuminated by searchlights or radar. Tracking of such a satellite would permit (1) precise measurement of intercontinental distances, (2) mapping of absolute gravity values, and (3) calculation of the Earth’s semimajor axis. This was the first and for several years the only forecast of the applications of satellites to the solid-earth sciences. O’Keefe’s proposal was actually carried out in 1966 when the *PAGEOS* (*P*Assive *GEO*tic *Satellite*) was launched (Newell, 1980), although by that time space geodesy was well under way with other satellites and techniques, as we shall see.

Space geodesy is the application of various space-related techniques to the problems of what can be called *geophysical* (or *physical*) *geodesy* and *geometrical geodesy*. Geophysical geodesy is the study of the interior of the Earth, by precise measurement of features such as the gravity field. An alternative and equally valid use of “geophysical geodesy” is the study of the “slow deformations of

the Earth" (Lambeck, 1988). This usage reflects the fact that the apparently solid crust and mantle are in fact dynamic features, as demonstrated by earthquakes, volcanic eruptions, and tilting of the land such as that which is slowly lowering London below sea level. Geometrical geodesy is closer to the traditional definition, being concerned with the precise measurement of positions on the surface of the Earth. The term "precise" has taken on new meaning with the advent of space geodesy, with trans-oceanic distances now being measured routinely with a precision close to the length of a well-trimmed fingernail. "Geometrical geodesy" now includes topographic mapping from space by means of satellite altimetry of the mean sea surface and of land elevations. A third subdivision of space geodesy is becoming distinctive enough to merit a new name, *earth dynamics*, referring to variations in the Earth's rotation rate, its orientation in space, and similar phenomena.

Space geodesy is a difficult subject to treat concisely and clearly, for several reasons. The field is a large and rapidly growing one. Geophysical and geometrical geodesy and earth dynamics are closely interrelated, divisions among them being somewhat artificial. Data from any one technique, such as satellite laser ranging, can be applied to the study of a wide range of geophysical parameters, from sea-floor topography to rotation of the Earth. Furthermore, interpretation of geophysical data in general is beset by inherent ambiguities. Regional gravity anomalies, for example, can be interpreted in terms of variations in rock type, thickness of the crust, temperature of the lithosphere, or convection in the upper mantle. A final difficulty is the rapid pace of space geodesy technique development, a topic already filling books by itself. This new field has involved remarkable technological and mathematical progress in areas far removed from satellite launching. It is safe to say that had an artificial satellite been launched in 1940, only the most elementary geometric use could have been made of it, lacking laser and microwave techniques and especially today's massive computing capability (Cohen and Smith, 1985). However, let us begin with a brief summary of the main techniques used in space geodesy.

2.2 Space geodesy methods

The oldest technique of space geodesy is satellite tracking, i.e., precise monitoring of a satellite's orbit. The satellite need not be artificial, for "tracking" of the Moon by astronomers long before *Sputnik* provided fundamental, if imprecise, information on the Earth's rotation and structure (O'Keefe, 1972; Rubincam, 1975).

This technique was in effect modernized when laser retroreflectors were put on the lunar surface. However, most space geodesy involves tracking of artificial satellites in low earth orbit, “low” meaning subsynchronous ($< 36,000$ km) altitudes. Good historical summaries of satellite-tracking techniques have been presented by O’Keefe (1958), Murray (1961), and King-Hele (1983, 1992).

Optical tracking is in principle the simplest method, requiring nothing from the satellite but its visibility. Instruments used profitably can be as simple as binoculars and stopwatch. Early satellites were tracked by the “Moonwatch” program organized by F. L. Whipple, in which arrays of ground observers with simple home-built telescopes set up optical fences for satellite observation. Most professional satellite tracking is done with wide-angle telescopes, such as the Baker–Nunn cameras operated in the early years by the Smithsonian Astrophysical Observatory, or with their modern electronic equivalents using charge-coupled device (CCD) arrays. The first American satellite launched for geodetic purposes, *ANNA 1-B*, carried a flashing light; simultaneous photographs from several ground stations permitted precise triangulation among the stations (Schmid, 1974). Optical tracking is still producing useful data, as shown by King-Hele (1983, 1992), and though being superseded by other geodetic techniques, is still needed for study of atmospheric density at orbital altitudes because this changes with solar cycle and other phenomena.

Radio tracking has also been widely used since the first satellites were orbited. The two main methods are Doppler tracking and interferometry. Doppler tracking depends on the frequency shift of an orbiting transmitter as it approaches and then recedes from the tracking antenna. Usually the antenna is on the Earth, but the new French system, DORIS, (Cazenave *et al.*, 1993) uses a network of radio beacons on the ground whose signals are received by suitable receivers on satellites. Satellites can track other satellites using the Doppler technique. Satellite-to-satellite tracking, as described by Kahn and Bryan (1972), has the advantage of permitting continuous tracking throughout an entire revolution, hard to achieve with ground stations for low satellites because of the number of stations required. Satellite-to-satellite tracking data are becoming widely used (Lemoine *et al.*, 1998b), involving the *Global Positioning System (GPS, to be described)* and the *Tracking and Data Relay System Satellites (TDRSS)*.

Interferometry uses arrays of orthogonally oriented antennas and measurement of the phase difference of the satellite signals received by each antenna; a good description can be found in

Glasstone (1965). The NASA Minitrack system (now part of the Space Tracking and Data Acquisition Network) uses interferometry, especially for low earth orbit satellites.

Radar tracking is an active technique, in contrast to the optical and radio methods just described. Its big advantage is independence of satellite visibility and weather. Radar space tracking installations are of course much more expensive to operate than those using passive methods, and they are less accurate than optical methods because of the longer wavelengths used (generally in the centimeter range). Radar and interferometry are combined in the US *Navy Naval Space Surveillance* system, using an array of six interferometer stations extending from Georgia to California in an east–west direction.

The most accurate tracking method of all uses satellite laser ranging (SLR), in effect an optical radar, now capable of range accuracies of 1–3 millimeters (Degnan, 1993). First used in the 1960s for precise orbit determination, SLR has become a primary geodetic tool. The technique uses lasers mounted in combination with telescopes, sending pulses every few seconds to cube corner reflectors mounted on satellites. Cube corners have the property of reflecting incoming radiation back in the same direction it came, and are widely used for SLR. The main disadvantage of lasers for satellite tracking is the narrowness of the beam; the satellite orbit must be determined precisely so that the laser beam will hit the satellite. In addition, the technique depends on good weather. More than a dozen reflector-carrying satellites have been launched at this writing, the flagships being *Starlette* (France), *LAGEOS I* (US), and *LAGEOS II* (Italy) (Fig. 2.1). These are high-density satellites in very stable, high-altitude orbits, planned so as to minimize the effects of atmospheric drag (Marsh *et al.* 1985; Christodoulidis *et al.* 1985; Tapley *et al.*, 1993) and the high-frequency harmonics of the gravitational field, i.e., the smaller irregularities. International efforts in both earth satellite ranging and lunar laser ranging, to be discussed, are coordinated through the International Laser Ranging Service.

There are two general types of techniques for using satellite-tracking data (Smith *et al.*, 1991): dynamic and geometric. The simplest method is geometric geodesy, in which the satellite is observed simultaneously from more than one ground station and the observations then used for triangulation or trilateration. This is essentially the method originally proposed by O'Keefe (1955), in which the satellite serves as a passive target, whose orbit must be known only well enough to find it. The method is limited by several factors, such as the location of ground stations, weather conditions for all ground

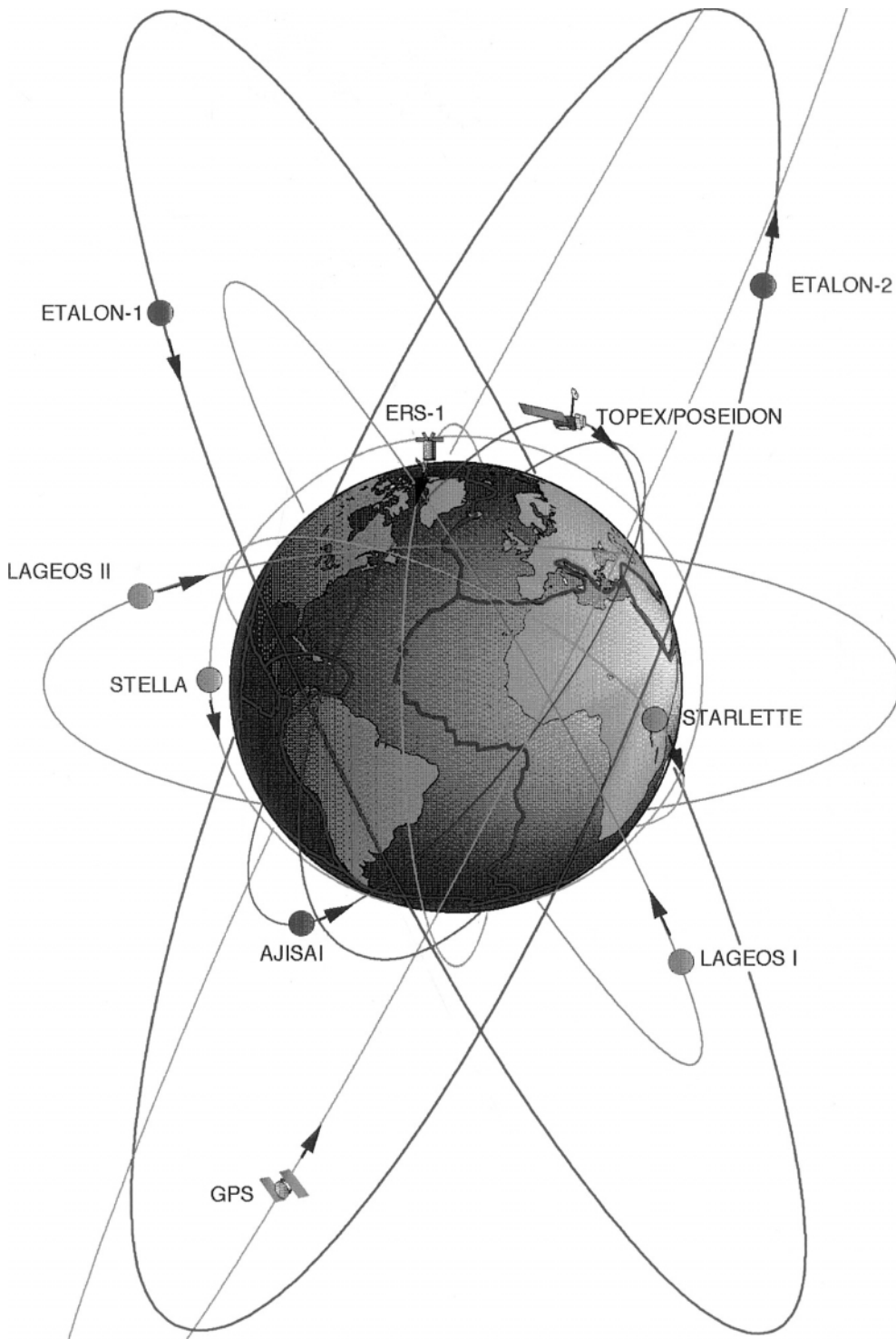


Fig. 2.1 (See also Plate V) Satellites used for laser ranging.

stations at any given time, and the accuracy of data from each station. Consequently, the increased number of retroreflector-bearing satellites (Tapley *et al.*, 1993) has greatly improved the effectiveness of geometric space geodesy. Dynamic satellite geodesy, in contrast, uses the satellite in effect as a sensor passing through the Earth's gravity field. It is far more complicated, requiring accurate modeling of the satellite orbits and great computing power. In addition to the gravitational forces, the main factor controlling the orbits, a wide range of other disturbing forces such as atmospheric drag, solar radiation, and terrestrial radiation must be allowed for. For meaningful geodetic use of the tracking data, the motions of the ground stations, such as earth tides, must be known. Tectonic setting and local ground conditions must also be considered (Allenby, 1983). However, if all these complexities can be overcome, dynamic satellite geodesy as carried out with *LAGEOS* can produce valuable data in addition to the precise distance between ground stations: the broad features of the gravity field (i.e., the low harmonics), polar motion, earth rotation, and earth tides. Frequent intercomparison among SLR, VLBI, and terrestrial geodesy show that the dynamic approach has been highly successful (Sauber, 1986; Ryan *et al.*, 1993). To show the wide range of data types used in mapping the global gravity field, a table of satellites used for earlier models, from Lemoine *et al.* (1998b), is presented (Table 2.1).

The general process of geodetic satellite tracking is an iterative one, so to speak, in that tracking data can be repeatedly fed back into the determination of satellite orbits, increasing the accuracy of the final result. This is especially important for the *Global Positioning System*, as will be discussed below.

The ultimate SLR experiment uses earth-based lasers and cube corner reflector arrays on the surface of the Moon (Fig. 2.2) (Bender *et al.*, 1973; Williams, *et al.*, 1993). A diffuse laser return had been received in 1962 from the surface by L. D. Smullin and G. Fiocco (Lambeck, 1988), but could not be used for precise ranging. However, beginning with *Apollo 11*, three retroreflector arrays were emplaced by *Apollo* astronauts, and two French arrays were carried on the Soviet *Lunokhod* remotely-driven vehicles. The simplicity of the technique may obscure the tremendous technological difficulty of lunar ranging. Despite their coherence, laser beams obey the inverse square law (both ways, so that the beam loses strength in proportion to the fourth power of the Earth–Moon distance). The telescopes that detect reflections from the lunar arrays are sometimes detecting only one photon of the 10^{18} transmitted by each pulse. Laser-ranging measurements with a precision of a few centimeters

Table 2.1 *Satellites and orbital characteristics used for JGM-1 and -2 (Joint Gravity Models, also in honor of late James G. Marsh, GSFC). From Lemoine et al. (1998b).*

Satellite	<i>a</i> (km)	<i>e</i>	Inclination (°)	Perigee height (km)	Mean motion (rev/d)	Primary resonant period (d)	Data type
ATS-6	41867	0.0010	0.9	35781	1.01	92.8	SST
Peole	7006	0.0162	15.0	515	14.82	2.1	L
Courier-1B	7469	0.0174	28.3	989	13.46	3.8	O
Vanguard-2	8298	0.1648	32.9	562	11.49	2.7	O
Vanguard-2RB	8496	0.1832	32.9	562	11.09	294.3	O
DI-D	7622	0.0842	39.5	589	13.05	8.4	O,L
DI-C	7341	0.0526	40.0	587	13.81	2.5	O,L
BE-C	7507	0.0252	41.2	902	13.35	5.6	O,L
Telstar-1	9669	0.2421	44.8	951	9.13	14.9	O
Echo-1RB	9766	0.0121	47.2	1501	12.21	11.9	O
Starlette	7331	0.0200	49.8	785	13.83	2.8	L
Ajisai	7870	0.0010	50.0	1487	12.43	3.2	L
Ana-1B	7501	0.0070	51.5	1076	13.37	4.8	O
GEOS-1	8075	0.0725	59.3	1108	11.96	7.0	O,L
ETALON-1	2550	0.0007	64.9	19121	2.13	7.9	L
TOPEX/POSEIDON	7716	0.0004	66.0	1342	12.80	3.2	L,D
Transit-4A	7322	0.0079	66.8	806	13.85	3.5	O
Injun-1	7316	0.0076	66.8	895	13.87	3.8	O
Secor-5	8151	0.0801	69.2	1140	11.79	3.4	O
BE-B	7354	0.0143	79.7	902	13.76	3.0	O
OGO-2	7341	0.0739	87.4	425	13.79	3.8	O
OSCAR-14	7448	0.0030	89.2	1042	13.50	2.2	Dp
OSCAR-7	7411	0.0242	89.7	848	13.60	3.2	Dp
5BN-2	7462	0.0058	90.0	1063	13.46	2.4	O
NOVA	7559	0.0010	90.0	1123	13.20	6.3	Dp
Midas-4	9995	0.0121	95.8	1505	8.69	3.0	O
SPOT-2	7208	0.0015	98.7	840	14.17	6.2	Dp
GEOS-2	7711	0.0308	105.8	1114	12.82	5.7	O,L
Seasat	7171	0.0010	108.0	812	14.29	3.1	O,L,R,A
Geosat	7169	0.0010	108.0	754	14.30	3.0	Dp,A
LAGEOS	12273	0.0010	109.9	5827	6.39	2.7	L
GEOS-3	7226	0.0010	114.9	841	14.13	4.5	L,A,SST
OVI-2	8317	0.1835	144.3	415	11.45	2.2	O

Key: L = Laser, Dp = TRANET/OPNET Doppler, O = Optical, D = DORIS, R = Radar,
 A = Altimetry, SST = sat.-to-sat. range rate

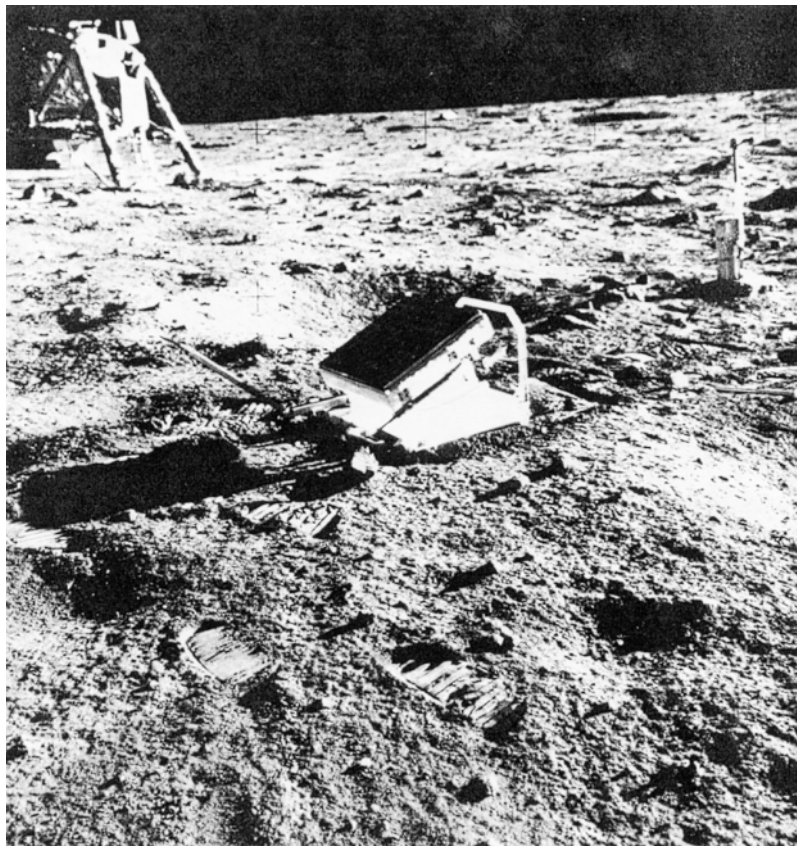


Fig. 2.2 Laser retroreflector placed on the Moon during *Apollo 11* mission to Mare Tranquillitatis. Photograph by N. A. Armstrong.

to these arrays are being carried out by two observatories at this writing (in the US and France), and continue to produce useful data. (The fact that these unprotected optical surfaces continue to reflect normally more than twenty-five years after emplacement is an important demonstration that the lunar surface would be suitable for emplacement of astronomical instruments (Lowman, 1996).)

Some of the most productive space geodesy techniques have been termed “satellite positioning.” These invert the procedure described for satellite tracking, in that the satellites are used to, in effect, track points on the surface of the Earth. Early navigation satellites, such as the US *Transit* system, transmitted radio signals which, when received on the surface, could locate the receiver to within roughly a kilometer by the Doppler frequency shift. Since then, there have been enormous increases in accuracy and coverage of navigation satellites, with the 24-satellite American *Global*

Positioning System (GPS) (Hager *et al.*, 1991) and a corresponding Soviet one, the *GLONASS* system (Daly, 1993). The *GPS* was started by the Department of Defense in 1978, but by the early-1990s, as the constellation was completed, it became very widely used for geodesy in addition to its primary function of real-time navigation. Accordingly, it will be described in some detail.

The *GPS* uses a constellation of 24 active *NAVSTAR* satellites (including spares) in 20,000-km high 12-hour orbits, arranged so that at least four satellites are visible to ground receivers at any one time (UNAVCO, 1998). The satellites, whose orbits are continually updated, transmit coded radio signals giving their positions and the time of transmission (Yunck *et al.*, 1985). Ground receivers compute the transit time, thus finding the range to each satellite. Ranges from three satellites gives the position of two points (intersection of three spheres), one of which is known to be on the surface of the Earth. Range to a fourth satellite allows correction for clock errors. The *GPS* is intended to give real-time absolute locations to within 10 m accuracy, which it does very well. However, it was found rapidly that relative locations, horizontal and vertical, could be measured to accuracies of a few centimeters despite the necessary security measures (e.g., selective availability) necessary for this military system. Differential *GPS*, using fixed reference receivers in combination with mobile ones, is coming into very wide use for precision location. Small hand-held units can achieve accuracies of 2–10 meters, and survey-grade ones better than 1 meter (UNAVCO, 1998). The *GPS* has opened a “new era” (Hager *et al.*, 1991) for the study of tectonic activity and many other scientific applications, as will be described later in this chapter. An interesting synergism is between geodetic satellites carrying laser retroreflectors and *GPS*, in that new satellites are equipped with *GPS* receivers.

Most satellite geodesy techniques might have been understood by Eratosthenes, but one of the most productive – satellite radar altimetry – is genuinely novel. Radar altimetry from satellites measures the instantaneous distance above the ocean surface (Kahn *et al.*, 1979). This technique was originally intended to monitor the oceans themselves – currents, eddies, and fronts. However, as shown when first tried from *Skylab*, radar altimetry also reveals the topography of the ocean floor, i.e., the bathymetry. Depressions such as trenches produce geometrically-similar depressions in the mean sea surface; elevations, such as seamounts, produce slight elevations of the sea surface. The principle behind this is roughly that positive topography tends to pull the ocean horizontally toward it; for depressions, the surrounding higher topography pulls the ocean away. A useful

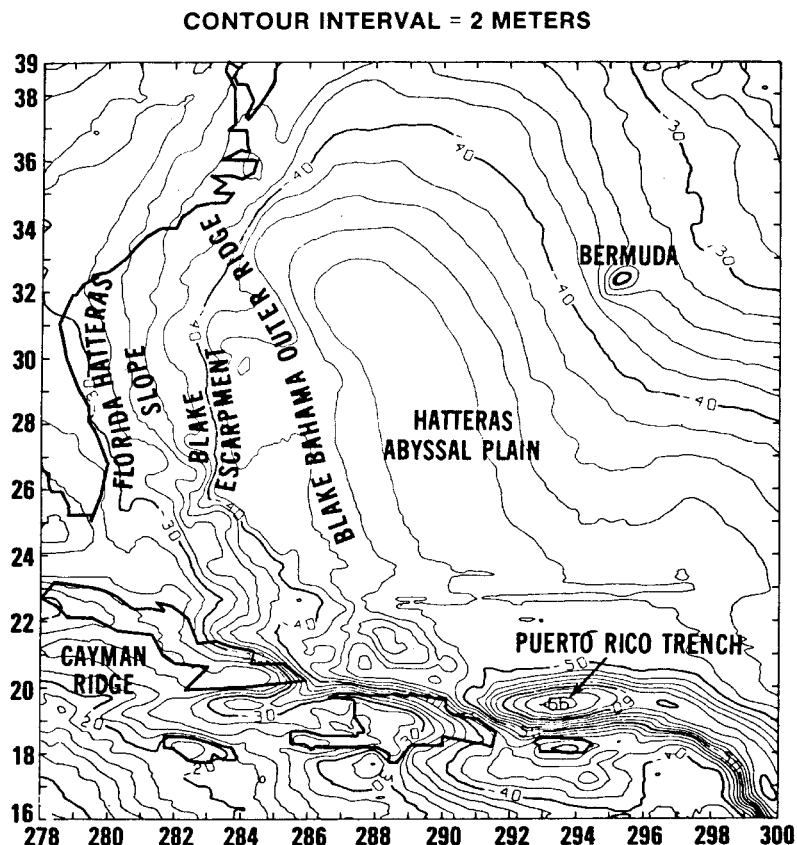


Fig. 2.3 Map of marine geoid north of Puerto Rico, from *GEOS-C* radar altimetry. From Marsh and Chang (1985).

example is from an early study by Marsh and Chang (1985), using *GEOS-C* altimeter data over the Atlantic Ocean (Fig. 2.3). The effects on the mean sea surface are surprisingly great. Bermuda, for example, has pulled the surrounding ocean up roughly 3 meters; the Puerto Rico Trench is reflected in a 22 meter depression relative to the coast.

The ratio between the sea-surface deflection and the underlying topography, termed the “admittance” by Cazenave and Dominh (1987), is generally a few meters per kilometer, and is by itself a potentially valuable indicator of crust and mantle conditions, such as the isostatic compensation mechanism (Rapp, 1989). Satellite altimetry, although originally intended to monitor oceanographic conditions, has proven a remarkably effective way to map the ocean-floor topography (Sandwell, 1991; Smith and Sandwell, 1997). The

base map for the digital tectonic activity map (see Fig. 1.1) is the latest version of a series of such maps, earlier versions of which have been produced by Haxby (1987) and others. A popular account of Haxby's work has been published by Hall (1992).

The map based on the Sandwell and Smith data is presented here (Fig. 2.4), this time without tectonic features overlaid, to illustrate the resolution of their techniques, combining surface and space data. Their map is properly termed a gravity map, but because of the effects just described is also a bathymetric map. The great advantage of satellite altimetry over satellite tracking is that because of the much smaller footprint of the radar (usually around 10 km), the spatial resolution is far better than that of purely orbital methods, as shown by the shaded relief map.

The most comprehensive map of the Earth's gravity field at this writing is the Earth Gravitational Model 1996 (EGM96) (Lemoine *et al.*, 1998a, b). To illustrate both the techniques used and their relative precisions, a table of data types is presented (Table 2.2) To show two ways in which the gravity field can be represented, earlier maps by Marsh (1979), based on satellite tracking, are presented. The free-air gravity anomaly map (Fig. 2.5) shows the Earth's gravity field, in milligals. This is primarily the Earth's topography, since a free-air gravity anomaly is that remaining after correction for height (but not intervening crust) has been made. The gravimetric geoid map (Fig. 2.6) shows the broad features of the equipotential surface, equivalent to an undisturbed global ocean. The geoid expresses deeper features, chiefly in the mantle. A tectonic and volcanic activity map (Fig. 2.7), similar to that in Fig. 1.2 but with the same projection as the gravity maps, is presented for comparison with them.

Another important technique, Very Long Baseline Interferometry (VLBI), can be considered either not true space geodesy or the ultimate space geodesy, since it depends on ground-based radio telescope interferometry of the radiation emitted by quasars several billion light-years distant (Fig. 2.8). The technique uses fixed or portable radio telescopes that can be separated by any distance up to the diameter of the Earth. (The technique could be used for telescopes on the Earth and Moon, the Ultra Long Baseline Interferometry proposed by J. O. Burns, 1988.) Originally developed as an astronomical technique to produce very high resolution radio images of distant objects, it was found that the distance between widely separated radio telescopes could be determined to precisions of a few centimeters. VLBI has developed more or less in parallel with SLR, permitting frequent intercomparison of the results from each method (Kolenkiewicz *et al.*, 1985).



Fig. 2.4 Shaded relief map of global topography, based on digital elevation data from National Geophysical Data Center; marine gravity from Smith and Sandwell (1997). Robinson Projection; prepared by Penny M. Masuoka, GSFC.

Table 2.2 Satellite-tracking methods. From Lemoine et al. (1998b).

Technology	Configurations	Precision	Typical orbit fit	Strengths	Weakness	Period of use
Camera: Baker– Nunn MOTS SPEOPT	satellite image against stars, right ascension and declination; passive and/or active (i.e., spaceborne flashing lamp)	1–2 arcsec arcsec (10–20 m)	1–2 arcsec	first precision tracking systems	atmospheric shimmer star catalog errors passive data tracking limited to dawn/dusk geometry	1960–1974
Satellite laser ranging	2-way range, use restricted to satellites carrying retroreflectors	0.5 cm	2 cm (LAGEOS) 5 cm (Starlette)	most precise absolute range unbiased excellent optical refraction modeling	clouds obstruct observations only 40–60% of passes acquired	1968+
Radiometric ground- based	2-way range 2-way range-rate S band-> NASA-> active C-band-> DoD-> passive	1 m 0.3 cm/s	5 m 1 cm/s	first all-weather precision tracking system	early network limited in distribution	1972+
TDRSS (NASA)	1-/2-way ground–TDRSS–sat. range/range-rate single-frequency S and K band links	1 m 0.4 mm/s	1.5 m 0.8 mm/s	excellent global coverage of user sat.s.	single-frequency transponder delay (range biases) TDRSS orbit errors	1983+

OPNET/ TRANET (USN)	1-way sat.-ground range-rate dual frequency (150 and 400 MHz)	0.2 cm/s	0.7 cm/s	good global network distribution	poor clocks large third-order ionospheric refraction errors 40% of data rejected	1965–1995, TRANET phasing out
DORIS (CNES)	1-way ground-sat. range-rate dual frequency (401.25 and 2036.25 MHz)	0.4 mm/s	0.5 mm/s	high-precision, all weather excellent global coverage	sat. tracks only one ground station at a time Note: the new DORIS system envisioned for the JASON mission will track two stations simultaneously. Additionally, the noise floor should be reduced to 0.1 mm/s	1992+
GPS (DoD)	pseudo-range/carrier phase (sat.-to-sat.)/(sat.-to-ground)	1–2 cm	1–2 cm	3-D navigation of low satellites unparalleled coverage	controlled by DoD some on-orbit receivers cannot cope with antispooing future receivers will use codeless technology and track 12+ sats.	1992+
Altimetry	2-way range (sat.–ocean) both single- and dual-freq. altimeters flown	1–2 cm	7 cm	precise range to directly map ocean-surface topography	limited by modeling of complex ocean-surface signals	1975

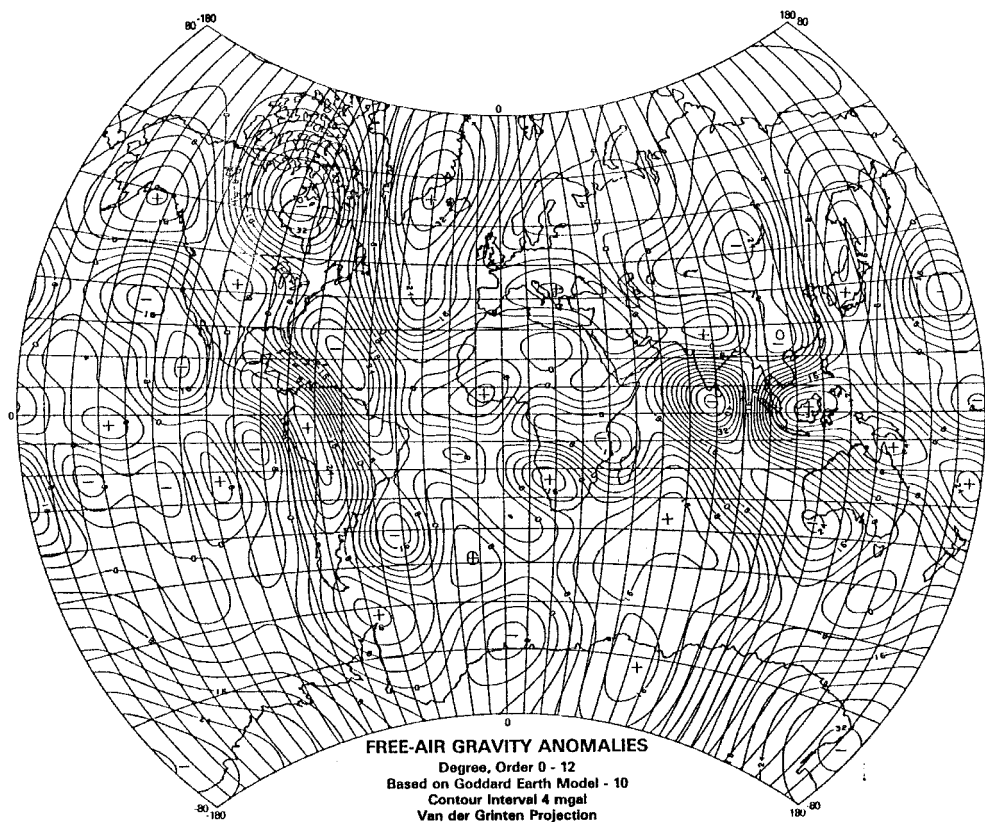


Fig. 2.5 Free-air gravity anomalies. From Marsh (1979).

In addition to its use as a terrestrial survey device, VLBI permits measurement of the Earth's rotation rate with unprecedented accuracy (Carter and Robertson, 1986; Dickey and Eubanks, 1985). The rotation rate of the Earth, or more properly changes in this rate, has been a long-standing issue, the problem being to explain the various changes in length of day (LOD). This topic clearly belongs in the "earth dynamics" category, but full understanding of changes in LOD bears on many problems in solid-earth geophysics, oceanography, and even meteorology.

Before moving on to the results of the techniques now in use, it should be pointed out that serendipity or "spinoff," chiefly in the form of unexpected uses for military technology, has played a continuing role in their geodetic application. J. A. O'Keefe's original proposal for a geodetic satellite was stimulated by his World War II experiences with mis-matched and inaccurate topographic maps,

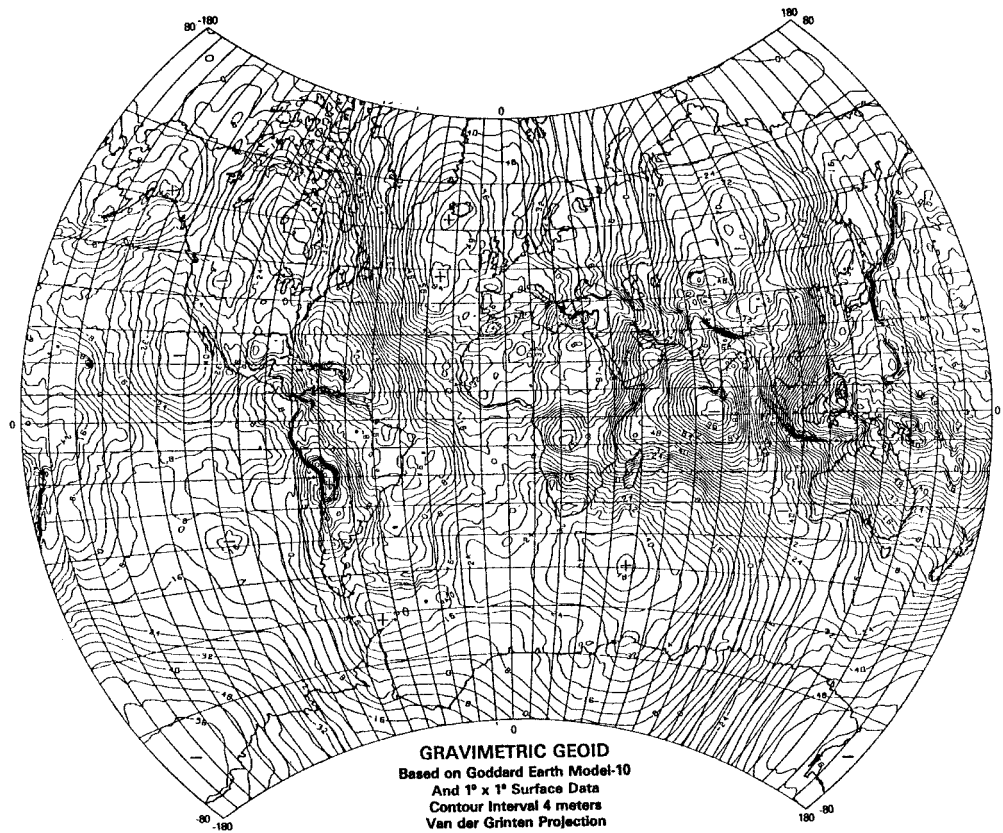


Fig. 2.6 Gravimetric geoid, from satellite and surface data. From Marsh (1979).

problems that had “serious effects” on the later conduct of the war in Europe (O’Keefe, 1966; this paper is highly recommended as an inside look at geodesists at work). Accurate global knowledge of the Earth’s gravity field is a military necessity (Newell, 1980) for accurate control of navigation and photographic satellites, as well as for aiming long-range ballistic missiles. Radar altimetry was originally developed for the US Navy, for monitoring the condition of the ocean surface. The *Global Positioning System* was developed by the US Department of Defense as a military navigation tool. Satellite laser ranging was intended primarily for satellite tracking, and very long baseline interferometry was intended as an astronomical technique. The “spinoff” argument is often criticized by saying that we could get the same results by a direct approach. But the history of satellite geodesy shows that we often do not know what the direct approach should be. Furthermore, military requirements can

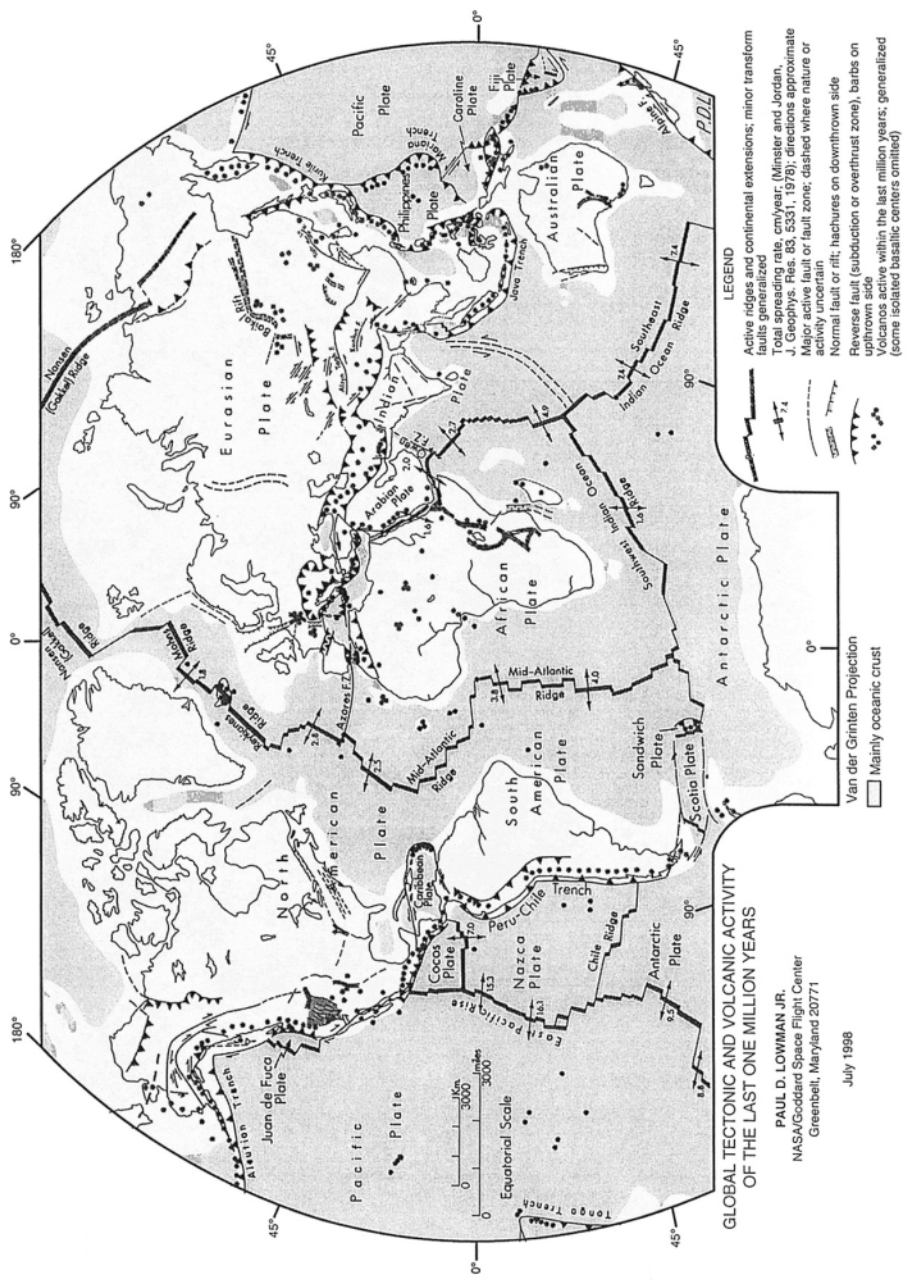


Fig. 2.7 Tectonic and volcanic activity map. See Chapter 1, this book.

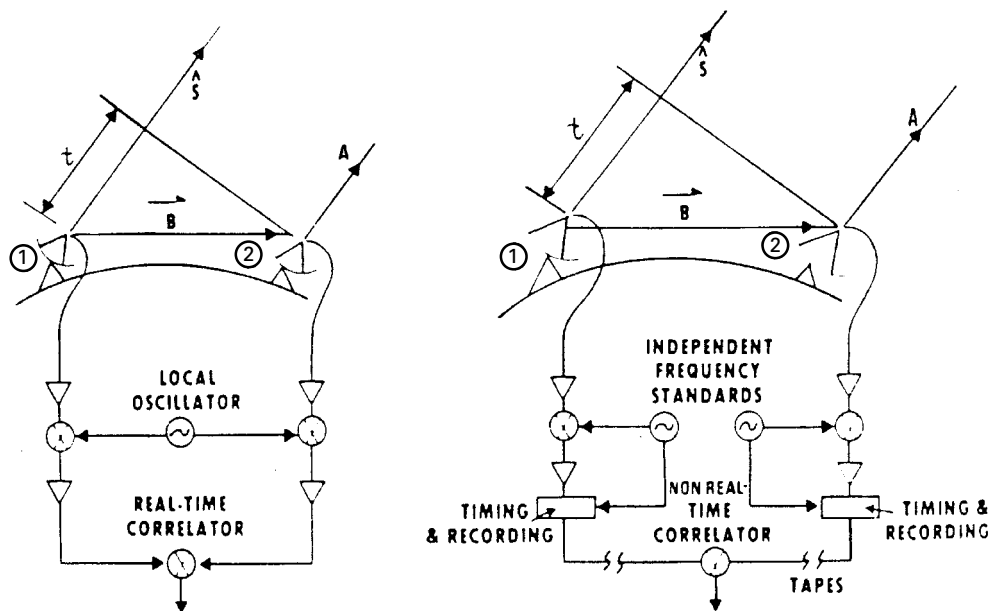


Fig. 2.8 Principles of radio telescope interferometry, for cable-connected instruments (left) and independent instruments (right). Phase differences measured on radio signals from extremely distant sources, so that wave front is effectively a plane, permit precise determination of straight-line distance B between instruments.

understandably command far bigger budgets than science. Proposed civilian space geodesy programs, such as the *Geopotential Research Mission* (two satellites), have in recent years been routinely turned down on grounds of cost. No one can seriously imagine NASA getting \$10.5 billion for a constellation of 24 large active satellites, i.e., the *Global Positioning System*.

Turning from these bleak reflections, let us examine the more general scientific results of space geodesy, treating its major fields of application in very rough historical order. For background, publications by NASA (1983, 1988) and the National Research Council (1987) will be helpful.

2.3 Shape of the Earth

The first scientific discoveries of the Space Age included new knowledge of the Earth's gravity field, and from that its shape and internal structure. The very first satellite, *Sputnik 1*, caught the western world by surprise on October 4, 1957, although the Soviet Union had announced its intentions several months earlier. However, as

described by Massey and Boyd (1958), *Sputnik 1* was successfully tracked by radio and radar in Britain, producing new values for the atmospheric density about 10 times higher than the then standard USAF model. *Sputnik 1* and its final rocket stage (which is what most people actually saw) produced little information beyond this but, in addition to galvanizing the United States into action, it also gave western satellite trackers valuable practice that was applied to *Sputnik 2*, launched a month later.

A minor non-technical comment may not be out of order at this point. The many failures and misdeeds of the Soviet Union are now well known, and few people inside or outside the former USSR would wish to re-establish it. But any impartial historian must agree that the Soviet Union was in its day a true leader in space flight, regardless of its motives. Beside launching the first satellite, the Soviets for decades pursued an ambitious program of space exploration, often in the face of repeated failures. Space flight has long since become truly international, and the “Space Race” in its original sense is over. But Russia, Ukraine, and other former members of the Soviet Union can be justly proud of their role in a competition in which all sides were the ultimate winners.

Returning to space geodesy: *Sputnik 2* was much bigger than *Sputnik 1* and stayed in orbit much longer. Accordingly, it was observed many more times than its predecessor; observations bearing on the shape of the Earth, that mark the true beginning of space geodesy. As used in this context, “shape of the Earth” means the geoid, essentially the undisturbed sea-level surface if the Earth were completely covered with water (King-Hele, 1976). It is an equi-potential surface, to which the acceleration of gravity is everywhere perpendicular. If the Earth were internally homogeneous, spherically symmetrical, non-rotating, and alone in the universe, the geoid would be a sphere. None of these conditions prevail, in particular the absence of rotation, and it was recognized by Isaac Newton that the Earth would be slightly flattened by its rotation. The degree of flattening he calculated, assuming a homogenous interior, was 1/230, a fraction expressing the difference between equatorial and polar diameters. (A concise mathematical treatment of this subject has been presented by Kaula, 1968.)

This value is important for regional surveys, and efforts were made to improve Newton’s estimate by, for example, measuring the width of a degree of latitude in South America and then in Scandinavia. After centuries of effort, by 1957 a figure of 1/297.1 had been agreed upon (O’Keefe, 1966).

It was at this point that astronautics began to influence geophys-

ics, for orbital observations of *Sputnik 2* were immediately used to calculate the flattening value by application of Clairaut's Theorem relating gravity to the geoid (Garland, 1965). The first value, obtained by Buchar (1958), was 1/297.4, not far from the accepted one. However, Merson and King-Hele (1958), using many additional observations, soon calculated a value of 1/298.1 (the presently-accepted value is 1/298.3). This may seem a trivial improvement, but as King-Hele (1983) has pointed out, it was not trivial for geodetic surveying. Geodesists had been working to an accuracy of 10 meters for long baselines, and the new value for flattening meant the assumed size for the Earth was 170 meters off. Thus the very shape and size of our planet were re-measured, in a few months, by the second satellite ever launched.

Further improvement in our knowledge of the Earth's shape followed rapidly, from radio tracking of *Vanguard 1* in 1958 (Siry, 1959). It had been shown earlier by O'Keefe and Batchlor (1957) how the ellipticity of the Earth might be derived from motion of the node (equator crossing point of the orbit) of a close satellite. Using this method, O'Keefe, Eckels, and Squires (1959) discovered the third zonal (latitudinal) harmonic of the gravity field, expressing the "pear-shaped" component of the geoid. The formal publication of this discovery is so short, and so elegantly written, that it will be reproduced in full here (Fig. 2.9).

The "pear-shaped Earth," as it was labeled in headlines the world over, was fascinating by itself (Fig. 2.10). But it also had major implications for the internal structure of the Earth, typifying "geophysical geodesy." A widely-accepted concept of the Earth's internal structure at the time held it to be close to that of a fluid in equilibrium, the "basic hypothesis of geodesy" of Heiskanen and Vening Meinesz (1958). Opposed to this was the view of Jeffreys (1962), that the Earth could support substantial stress differences. Discovery of the third harmonic showed that Jeffreys was more nearly correct, and that either mechanical strength or large-scale convection currents in the mantle must be supporting stress differences of the magnitude he had estimated (O'Keefe, 1959). Gravity interpretations are inherently non-unique by themselves, since any given value is the expression of mass *and* distance. Runcorn (1967) and many others have shown that the satellite data can be interpreted in terms of mantle convection. The weight of other evidence, such as glacial rebound and sea-floor spreading, has led most geophysicists to accept mantle convection as the cause of the broadest features of the gravity field. A comprehensive (and highly mathematical) discussion has been presented by Peltier (1985).

Vanguard Measurements Give Pear-Shaped Component of Earth's Figure

The determination of the orbit of the Vanguard satellite, 1958 β_2 , has revealed the existence of periodic variations in the eccentricity of that satellite (1). Our calculations indicate that the periodic changes in eccentricity can be explained by the presence of a third zonal harmonic in the earth's gravitational field. The third zonal harmonic modifies the geoid toward the shape of a pear. In the present case, the stem of the pear is up—that is, at the North Pole. According to our analysis, the amplitude of the third zonal harmonic is 0.0047 cm/sec² in the surface acceleration of gravity, or 15 meters of undulation in the geoid.

Figure 1 shows the observed variation in eccentricity. The period of the variation in eccentricity is 80 days, approximately equal to the period of revolution of the lines of apsides. The eccentricity is a maximum when the perigee is in the Northern Hemisphere. The amplitude of the variation is 0.00042 ± 0.00003 . Similar perturbations may exist in the angle of inclination of the orbit, although the data for them are much less accurate. No perturbations of this magnitude appear to exist in the semimajor axis.

In principle, the perturbation might be caused by both odd and even harmonics. However, the even harmonics can be excluded because the observed effect has opposite signs in the Northern and Southern hemispheres. Furthermore, we can also exclude tesseral harmonics (those which depend on longitude as well as latitude) because these also are the same in the Northern and Southern hemispheres, apart from a shift in longitude. We are left with the zonal harmonics (those which depend only on latitude) of odd degree.

Of the odd zonal harmonics, the first degree is forbidden; and those of higher degree are unlikely to have a large effect because they die out inversely as the $(n+1)$ power of the distance. The effect is therefore due mostly to the third zonal harmonic, with a possible contribution from the fifth.

Accordingly, a calculation was made of

the effect of the third zonal harmonic on the orbit elements of 1958 β_2 , by methods developed by O'Keefe and Batchlor (2). In the resultant expression for the eccentricity, the dominant terms were those whose argument was the mean motion of perigee. These were larger than the others by a factor of 10^3 . Keeping only the large terms, we find

$$e = e_0 + \frac{3}{2} A_{3,0} \frac{(1-e_0^2)^{1/2}}{na'} \frac{1}{n} \times \sin i \left(1 - \frac{5}{4} \sin^2 i \right) \sin \omega \quad (1)$$

where $A_{3,0}$ represents the coefficient of the third zonal harmonic in the notation of Jeffreys (3), n is the orbital mean motion and n' is the mean motion of the perigee, e is the eccentricity and e_0 the mean eccentricity, i is the angle of inclination, ω is the argument of perigee, and a is the semimajor axis.

Setting in the constants of the orbit and the observed amplitude of e , we find

$$A_{3,0} = (2.5 \pm 0.2) \times 10^{-9} \quad (2a)$$

in meter-second units. Utilizing the relation given by Jeffreys,

$$A_{n,s} = \frac{c^{n+2}}{n-1} g_{n,s}$$

(where $A_{n,s}$ is the coefficient of the disturbing potential, $g_{n,s}$ is the acceleration of gravity at the surface of the earth, and c is the earth's equatorial radius), we find that the third zonal harmonic of gravity at the earth's surface, in milligals, is

$$g_{3,0} = 4.7 \pm 0.4 \quad (2b)$$

Equation 2 is relevant to what Vening Meinesz (4) and Heiskanen call the "basic hypothesis of geodesy." These au-

thors assume that the earth's gravitational field is very nearly that of a fluid in equilibrium. They consider that the deviations from such an ellipsoid, in any given area, do not exceed about 30 milligal-megameter units—that is, they assume that one will not find deviations of more than 30 milligals over an area of 1000 kilometers on a side, or deviations of more than 3 milligals in an area 3000 kilometers on a side.

Our determination of the third-degree zonal harmonic shows that the hypothesis of Vening Meinesz and Heiskanen is not justified; for example, each of the polar areas has a value of about 120 milligal-megameters, and each of the equatorial belts a value more than twice as great.

The presence of a third harmonic of the amplitude (2) indicates a very substantial load on the surface of the earth. Following the arguments of Jeffreys, we may calculate the values of this load and the minimum stress required in the interior to support it. We find a crustal load of 2×10^7 dy/cm². We can choose between assuming that stresses of approximately this order of magnitude exist down to the core of the earth, or that stresses of about 4 times that amount exist in the uppermost 700 kilometers only (3, p. 199). These stresses must be supported either by a mechanical strength larger than that usually assumed for the interior of the earth or by large-scale convection currents in the mantle (5).

J. A. O'KEEFE
ANN ECKELS
R. K. SQUIRES

Theoretical Division, National Aeronautics and Space Administration, Washington, D.C.

References and Notes

1. J. W. Siry, distribution to orbit-computing centers, 1958.
2. J. A. O'Keefe and C. D. Batchlor, *Astron. J.* 62, 183 (1957).
3. H. Jeffreys, *The Earth* (Cambridge Univ. Press, Cambridge, 1952).
4. W. A. Heiskanen and F. A. Vening Meinesz, *The Earth and Its Gravity Field* (McGraw-Hill, New York, 1958), pp. 72, 73.
5. We would like to thank the Vanguard Minitrack Branch, the IBM Vanguard Computing Center, and Dr. Paul Herget, whose work in obtaining and processing the data made this study possible.

27 January 1959

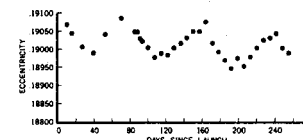


Fig. 1. Eccentricity of satellite 1958 β_2 (Vanguard).

Fig. 2.9 Complete report of discovery of "pear-shaped Earth." From O'Keefe, Eckels, and Squires (1959).

Further refinements of the gravity field followed rapidly. Following in Newton's tradition, British scientists took a leading role in this area. By 1961 the second-, fourth-, and sixth-degree harmonics had been obtained from satellite tracking (Smith, 1961). The areal extent of these "harmonics" decreases with increasing degree. For zonal, or latitudinal harmonics, their width is very roughly the circumference of the globe divided by the degree; the sixth harmonic

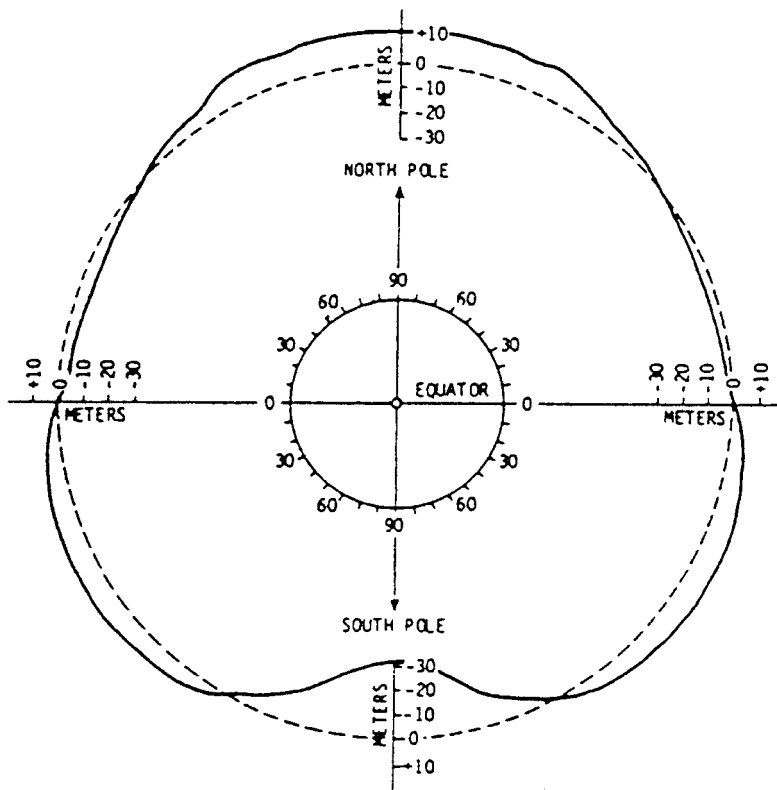


Fig. 2.10 Pear-shaped component of the Earth's shape, shown in section through poles; deviation in meters.

thus corresponds to a wavelength of between six and seven thousand kilometers. Lemoine *et al.* (1998a, b) define resolution as one-half the wavelength, or 20,000 km divided by the degree of the harmonic. The increasing lateral resolution of these findings permitted more specific correlations with crustal features, warranting separate discussion in the following section.

2.4 Gravity anomalies and global tectonics

Before discussing the application of satellite geodesy to tectonics, it should be stressed again that interpretation of gravity data is inherently ambiguous. As put concisely by Rubincam (1982), “. . . there is an infinite number of density distributions which can generate the observed gravity field.” Gravity data by themselves are of little value for geophysics and geology, but must be interpreted in combination with information from as many other sources as possible. Gravity data put constraints on interpretations, as well as suggesting

interpretations impossible from exposed geology. Gravity data are difficult to use, but not using them will lead to even more difficulties.

The very first gravity anomalies studied from satellites, those of the third harmonic, led to the discovery, as we have seen, of correspondingly large features: the “pear-shaped” bulge circling the Earth in the southern hemisphere. By 1971, Gaposchkin and Lambeck (1971) were able to construct a global gravity map from satellite data through the sixteenth harmonic, corresponding to a spatial resolution of about 1200 km. This map was used by Kaula (1972) to study the relationship between gravity and global tectonics. Kaula’s interpretations have been largely supported by later studies (Lambeck, 1988). The major relationships noted by these authors can be best summarized with use of newer gravity and tectonic maps (Lowman and Frey, 1979).

The gravity map presented as Fig. 2.5 shows low-degree (i.e., very broad) free-air anomalies, i.e., anomalies calculated with corrections only for altitude, as explained in Section 2.2. (Good elementary accounts of gravity anomalies can be found in Garland, 1965, and Wyllie, 1971.) Another map (see Fig. 2.6) shows the geoid corresponding to the gravity anomaly map. The most obvious positive correlation is between gravity values and topography, as over the Andes, North American Cordillera, and the Tibetan Plateau (see Fig. 2.7). We encounter at once one of the main complications in gravity interpretations, the degree to which the topography is isostatically compensated. It has been known for more than two centuries that mountains are not simply additional mass on the crust, but features in which the apparent excess mass is compensated by a deficiency of mass below them. This compensation may result from variations in crustal thickness (Airy compensation) or lateral variations in crustal density (Pratt compensation). Other types of compensation have been proposed, and it is generally agreed that for any large area, several mechanisms may interact (Lambeck, 1988).

Passing over these complications, we see that the main positive anomalies appear to correlate with areas of what are, in plate tectonic theory, zones of crustal convergence (see Fig. 2.7). The Andes, for example, owe their elevation (and their correspondingly deep roots) to the convergence of the Nazca with the South American Plate. The Tibetan Plateau is thought by many to result from the convergence of Peninsular India with Asia. A similar positive correlation (Kaula, 1972) is between positive gravity anomalies and Quaternary volcanism, as in the Andes, Aleutian Islands, and Indonesia. Plate tectonic theory provides a consistent interpretation of this correlation as well, in that these volcanic areas can also be explained as resulting from plate convergence.

There are obvious exceptions to this correlation that readers can verify for themselves by reference to the maps. For example, the gravity map shows no correlation in sign or direction with the volcanic fields of the East African Rift Valleys (see Fig. 2.7). Kaula noted the absence of correlation between gravity and “temperature indicators” such as high heat flow, inferring that horizontal variations in rock type were important. The Rift Valleys are evidently zones of incipient plate divergence, as are the mid-ocean ridges, which over large areas also show little relation to the gravity.

Analyses such as that just discussed have in effect been summarized by Kaula (1989) in a classification of the sources of the Earth’s gravity field, with six categories: **deep heterogeneities (mantle)**, 50%; **plate tectonics**, 20%; **thermal isostasy**, 10%; **crustal isostasy**, 5%; **lithospheric strength**, 5%; and **surface loads**, 5%.

Such relationships can be interpreted, very broadly, in terms of mantle convection (Peltier, 1985; Lambeck, 1988). The reality of mantle convection is essentially unquestioned, but its nature – whole mantle vs. two layer, boundary layer vs. penetrative – is still not known. The study by Silver *et al.* (1988) shows how geoid models can serve as a constraint on seismic and geochemical data. The complexities of such interpretations are formidable and can not be pursued further here. The difficulty of interpreting the satellite gravity data will almost certainly lead to a better understanding of mantle dynamics and crustal movements. We will turn now to this subject as approached by a higher-resolution satellite gravity technique, radar altimetry.

2.5 Marine gravity and ocean-floor topography

One of the most unexpected results of space flight has been the ability to map the floors of the oceans from space, by satellite radar altimetry. This technique was first demonstrated from *Skylab* in 1973. This date is somewhat ironic, for in the same year the plans for the US Geodynamics Program were announced, including all known methods for study of the solid earth but omitting satellite altimetry.

As previously discussed (see Fig. 2.4), the mean sea surface is a subdued replica of the ocean-floor topography. The geoid as mapped from satellite tracking has already been illustrated; it shows only the very broad features, i.e., the low harmonics. Satellite sea-surface altimetry gives us a much higher resolution look at the geoid, showing far more detail than does satellite tracking.

A global satellite altimetry survey was carried out by *Seasat*, and the data used by Marsh *et al.* (1985) to map the physical geoid and hence the main bathymetric features of the world's oceans. Since then, radar altimetry has been carried out by other satellites. The US Navy *Geosat* mission, launched in 1985, generated nearly 5 years of coverage, launching what Douglas and Cheney (1990) termed "a new era in satellite oceanography." The data from the first 18 months, with ground track spacing averaging 4 km, were necessarily classified. However, after this period, the satellite was put in a 17-day exact repeat orbit for oceanographic research, and the data from this part of the mission have been made freely available (Sandwell, 1991). Satellite altimetry from this and other missions has proven remarkably valuable for mapping the ocean floor and in fact oceanic crustal structure, as already demonstrated. The following summary will include only a few additional examples of these applications, both scientific and economic (Bostrom, 1989).

A survey of marine geology using *Seasat* altimetry was carried out by Craig and Sandwell (1988), using along-track profiles. They found that seamounts – inactive underwater volcanoes – could be detected from the slight elevation of the overlying sea surface, but in addition their size could be estimated. A total of 8556 seamounts were mapped, about a quarter of them previously unknown. The map (Figs. 2.11, 2.12) produced in this way is thus an essentially new look at the major expression of intraplate volcanism, which must be understood for studies of plate tectonics, mantle chemistry, and the terrestrial geothermal flux. Craig and Sandwell point out several of the most interesting features of this map: the scarcity of seamounts in the Atlantic, the generally small size of those in the Indian Ocean, and the prominent linear trends in Pacific seamounts. The map stimulates obvious speculative questions. For example, the line of seamounts northeast of New Zealand, the Louisville Ridge, appear clearly related to the Eltanin Fracture zone on this map (and on that of Haxby, 1987), yet detailed surveys and dating of the volcanoes along the Ridge indicate no direct connection for at least the newer part of the chain. The complexities of this problem are reviewed by Gordon (1991).

Marine volcanoes are often interpreted as hot-spot trails, but satellite altimetry has found at least one area where this does not seem likely. Filmer and McNutt (1989), using conventional bathymetry in combination with geoid heights from *Seasat* and *GEOS-3*, have studied the Canary Islands. The smooth progression of ages of volcanic rocks in this group strongly suggests a hot-spot trail, presumably with a mantle plume under one end. However, after making

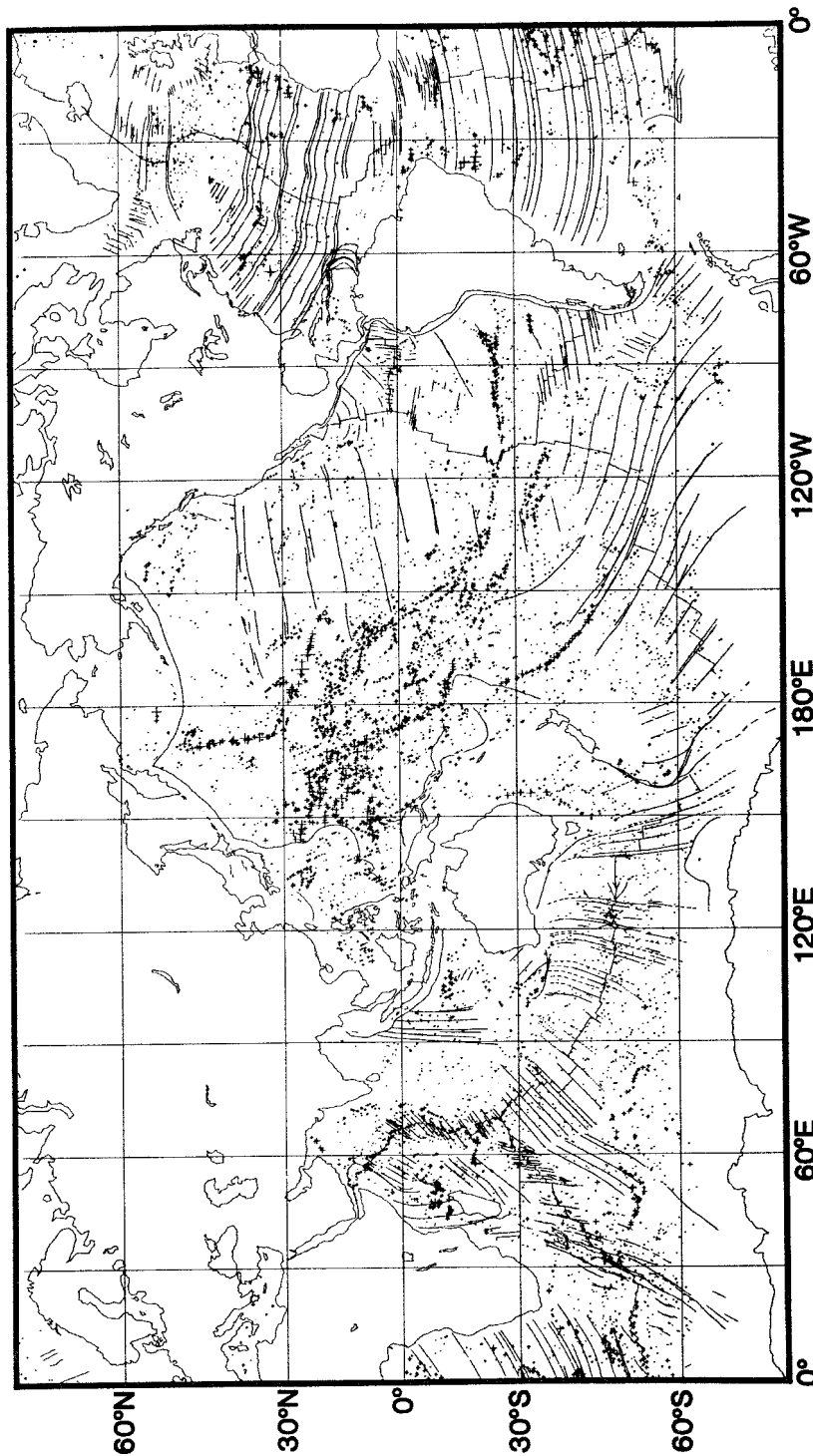


Fig. 2.11 Global map of all seamounts identified from *Seasat* altimetry data; symbol size proportional to signal amplitude (i.e., deflection from vertical). From Craig and Sandwell (1988).

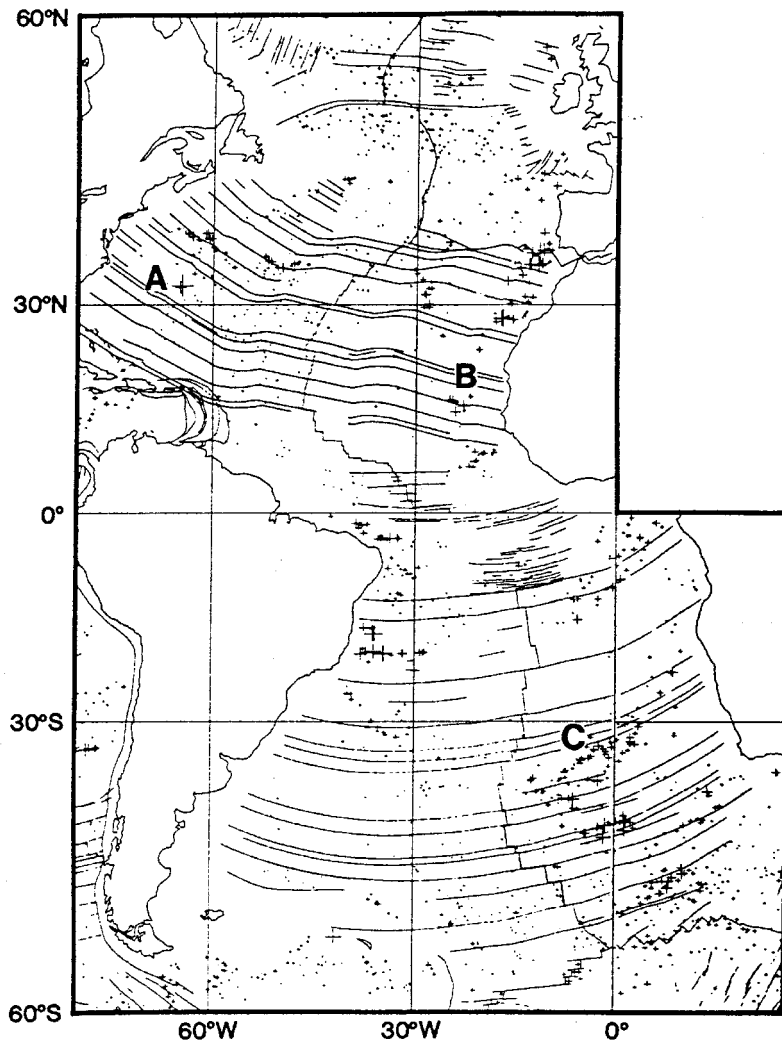


Fig. 2.12 Seamounts identified from *Seasat* altimetry in Atlantic Ocean; symbol size proportional to signal amplitude. A: Bermuda Rise; B: Cape Verde Islands; C: Walvis Ridge. From Craig and Sandwell (1988).

various corrections, Filmer and McNutt found no evidence of a swell expressing a plume or any thermal disturbance of the lithosphere, concluding that if the Canary Islands are a hot-spot trail, they represent a very different expression of a mantle plume from any other well-known hot spot. This anomaly is of some interest in view of the arguments by Lowman (1985a, b) that there are no valid hot-spot trails on continents; the Canary Islands example may represent control by crustal structure rather than crustal motion.

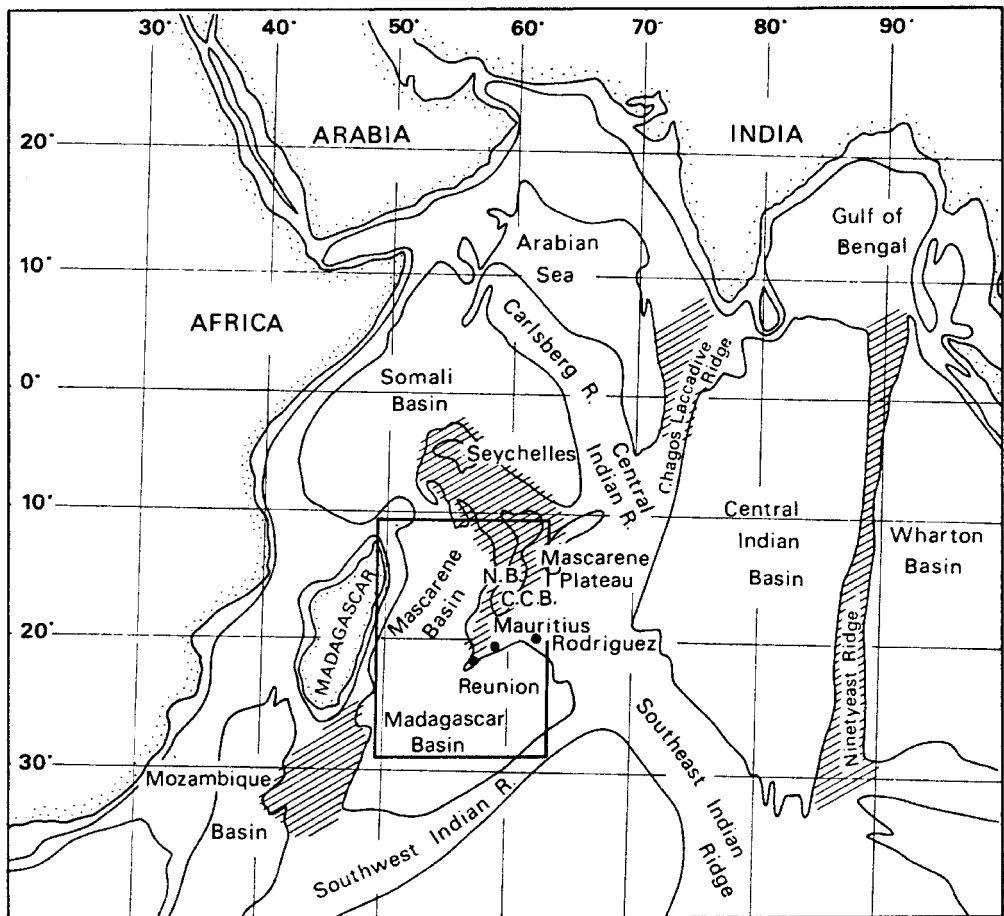


Fig. 2.13 Structural sketch map of Indian Ocean; study area in rectangle.

N.B.: Nazareth Bank; C.C.B.: Cargados-Carajos Banks.

From Bonneville *et al.* (1988).

A somewhat similar study using *Seasat* and *GEOS-3* altimetry was done by Bonneville *et al.* (1988) for the Indian Ocean. The origin of the Mascarene Plateau (Fig. 2.13) is not understood, although it appears continuous with the continental composition Seychelles Bank (see the Digital Tectonic Activity Map, Fig. 1.2). Bonneville *et al.* used the radar altimetry to compile a geoid map (Fig. 2.14) of the area, removing long-wavelength anomalies with the aid of other satellite data. They then calculated crustal rigidity for the area, finding the increasing rigidity to the south consistent with a hot spot or mantle plume origin for the southern Mascarene Plateau and the Mascarene Islands.

In addition to studies of ocean-floor topography, there are even

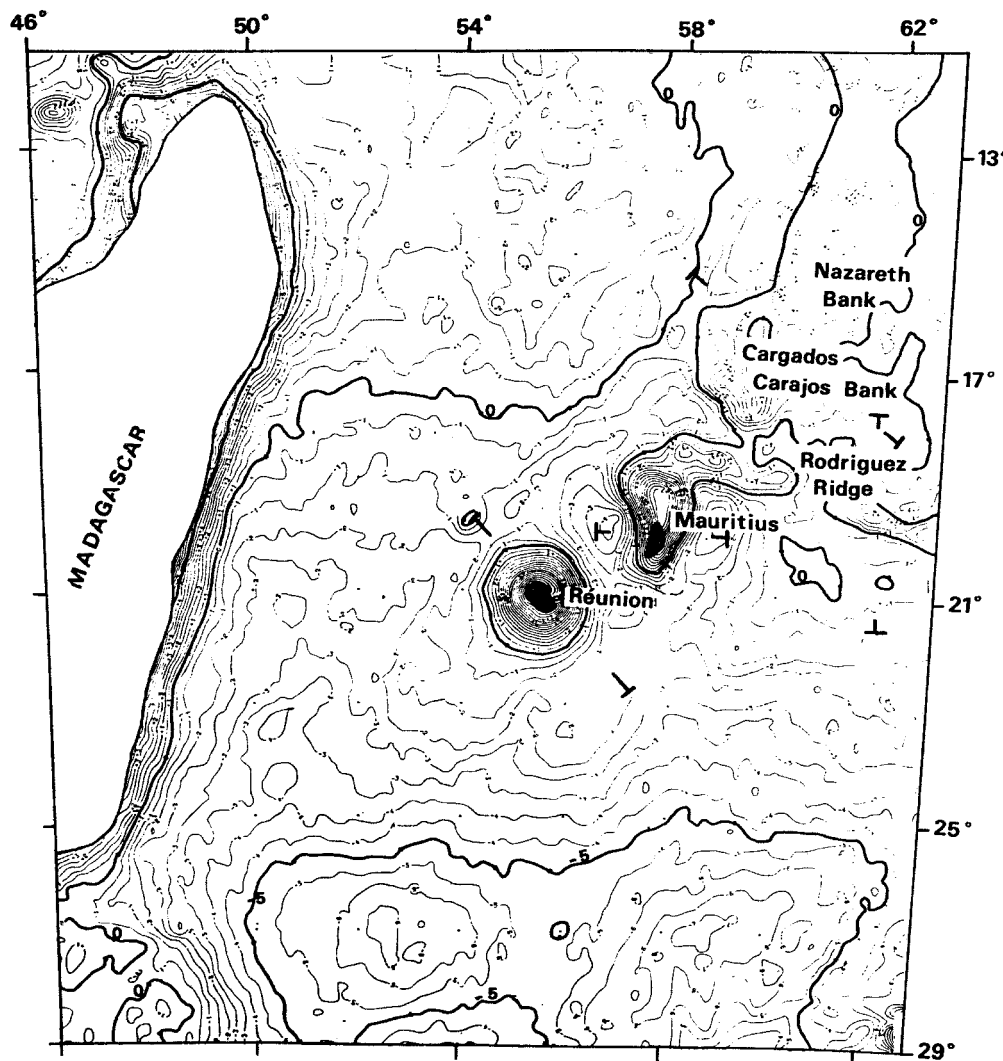


Fig. 2.14 Geoid level, 0.5 m contour interval. Long-wavelength anomalies (>3000 m) removed using GRIM3B model. From Bonneville *et al.* (1988).

now dozens of papers using satellite altimetry to study the upper mantle as expressed in the marine geoid (Sandwell, 1991), and in particular short-wavelength mantle convection. Only a few of these will be mentioned as examples. Haxby and Weissel (1986) reported evidence for small-scale mantle convection from *Seasat* data over the Pacific. Sandwell and Renkin (1988) in contrast found “no direct evidence” in the altimetry for mantle convection. McNutt and Judge (1990) noted the anomalous situation over the “superswell” around

French Polynesia, which is strongly negative gravitationally; high heat flow and a thinned lithosphere may contribute to this situation but the relationships are unclear. It is obvious that by itself satellite altimetry will not settle any of these problems, but it will obviously contribute to their solution in combination with data from seismology, marine magnetic surveys, and other investigations.

2.6 Plate motion and deformation

One of the most dramatic accomplishments of space geodesy has been the direct confirmation of oceanic crustal motions predicted by plate tectonic theory as the sea-floor spreading concept. As shown on the tectonic activity map (see Fig. 2.7), these motions are thought to be a few centimeters per year, roughly the rate at which fingernails grow. Direct measurement of such motions, over continental and especially oceanic distances, was utterly impossible before the development of space geodesy techniques. As pointed out by Flinn (1981), the cumulative errors of trilateration in land surveys introduce prohibitive errors into land surveys for distances over 100 km, and trilateration over large oceans is impossible. Wegener (1966) claimed direct measurement of continental drift by trans-Atlantic longitude measurements using radio time signals, but as his reported Greenland–Europe rate – 36 *meters* per year – suggests, this method was far too inaccurate to succeed. Even the monumental study by Proverbio and Quesada (1974), using several decades worth of data from the International Latitude Service, was not decisive (Lowman, 1985a, b). However, Wegener’s objective has been partially achieved in that the rate and direction of plate movements in and bordering the Pacific Ocean have now been measured by satellite laser ranging (SLR) and very long baseline interferometry (VLBI).

As previously discussed in Chapter 1, plate tectonic theory can be reduced to three essential elements: **ridges**, or spreading centers, where new crust is created; **trenches**, or subduction zones, where crust is destroyed or recycled by return to the mantle; and **transform faults**, fractures with dominantly horizontal movement connecting ridges or trenches. These elements bound **plates**, relatively rigid segments of the Earth’s lithosphere (which includes the crust and upper mantle above the asthenosphere). Plates may include oceanic and continental crust; the Eurasian Plate, for example, includes all crust between the Verkhoyansk Range of Siberia and the Mid-Atlantic Ridge in the North Atlantic Ocean; Fig. 2.15 from Stein (1993) shows the 12 main plates conventionally recognized and used for plate motion models. Plate movement of several centimeters per

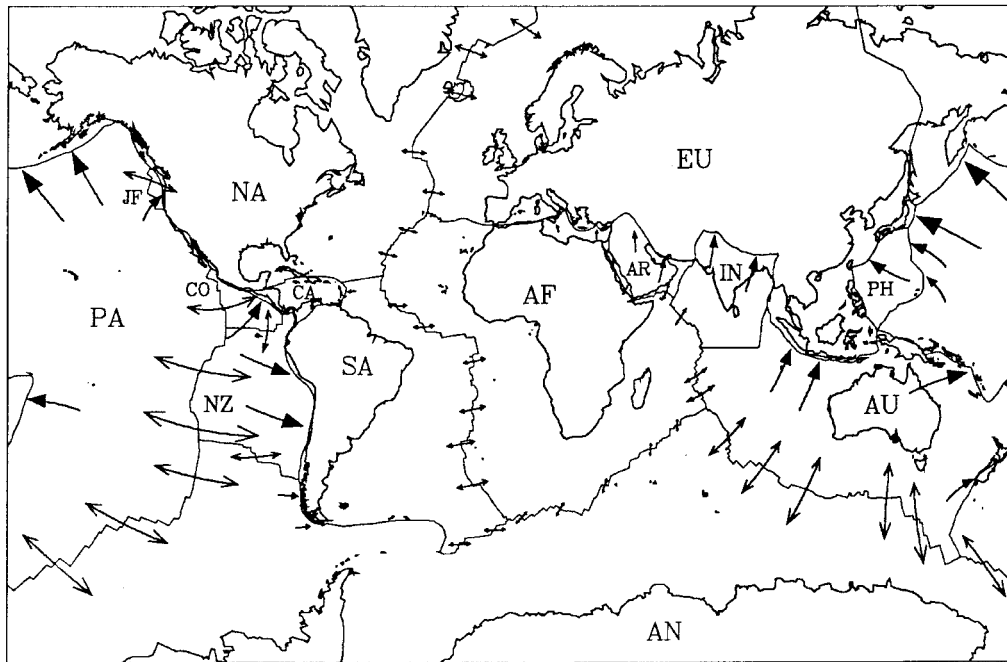


Fig. 2.15 Standard plates used for NUVEL-1 model. Relative plate velocities shown by arrows, length proportional to displacement if plates were to maintain their present angular velocities for 25 million years. Plate convergence with single solid arrow-head shows zones where convergence is asymmetric and polarity known. From Stein (1993).

year and continental drift are central to plate tectonic theory. All plate movements, taking place on a sphere, can be described as rotations (Dewey, 1975).

To demonstrate plate movement geodetically, three requirements must be met. First, the plates in question must be proven *rigid enough* to ensure that apparent baseline changes are not the result of local movements, crustal deformation in diffuse plate boundaries, or intraplate deformation in general. Sato (1993) has published a penetrating discussion of this problem, with reference to Japan and the western U.S., where non-rigid behaviour is well demonstrated. Second, the baseline changes, obviously vector rather than scalar quantities, must agree in *magnitude* with those predicted by plate tectonic theory, chiefly estimated from spacing of dated marine magnetic anomalies. Third, the apparent plate motions must agree in *direction* with those predicted by plate theory, generally normal to the magnetic anomalies and parallel to transform fault azimuths. The baselines and sites initially proposed for the NASA Crustal

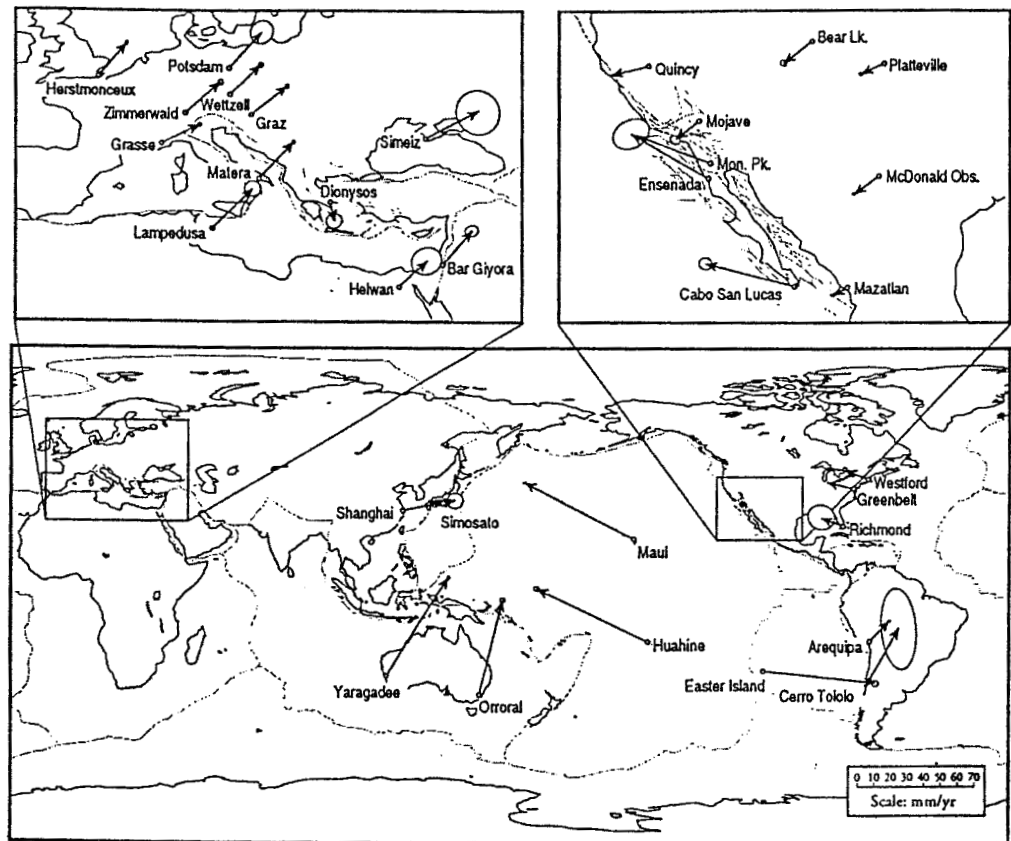


Fig. 2.16 Horizontal vector motion of SLR tracking sites; inset maps to same scale as main map. From Smith *et al.* (1994).

Dynamics Project (Lowman *et al.*, 1979; Allenby, 1983) were planned to meet these requirements. Measurements have been carried out now across many plate boundaries, and it appears that plate movements have now been successfully measured, independently by SLR and VLBI, in and around the Pacific Basin (Fig. 2.16). Detailed tabulations of these measurements have been presented by Robbins *et al.* (1993) (*LAGEOS*), Ma *et al.* (1992) (VLBI), and Ryan *et al.* (1993) (VLBI). Useful summaries and discussions of the results have been published by Sato (1993) and Smith *et al.* (1990).

The rigidity of the Pacific Plate has been demonstrated by the Maui–Huahine baseline (Fig. 2.17), showing no significant changes. A similar result is shown for the baselines from these islands to Monument Peak, California, showing very small changes. Since Monument Peak is just west of the active San Andreas fault system,

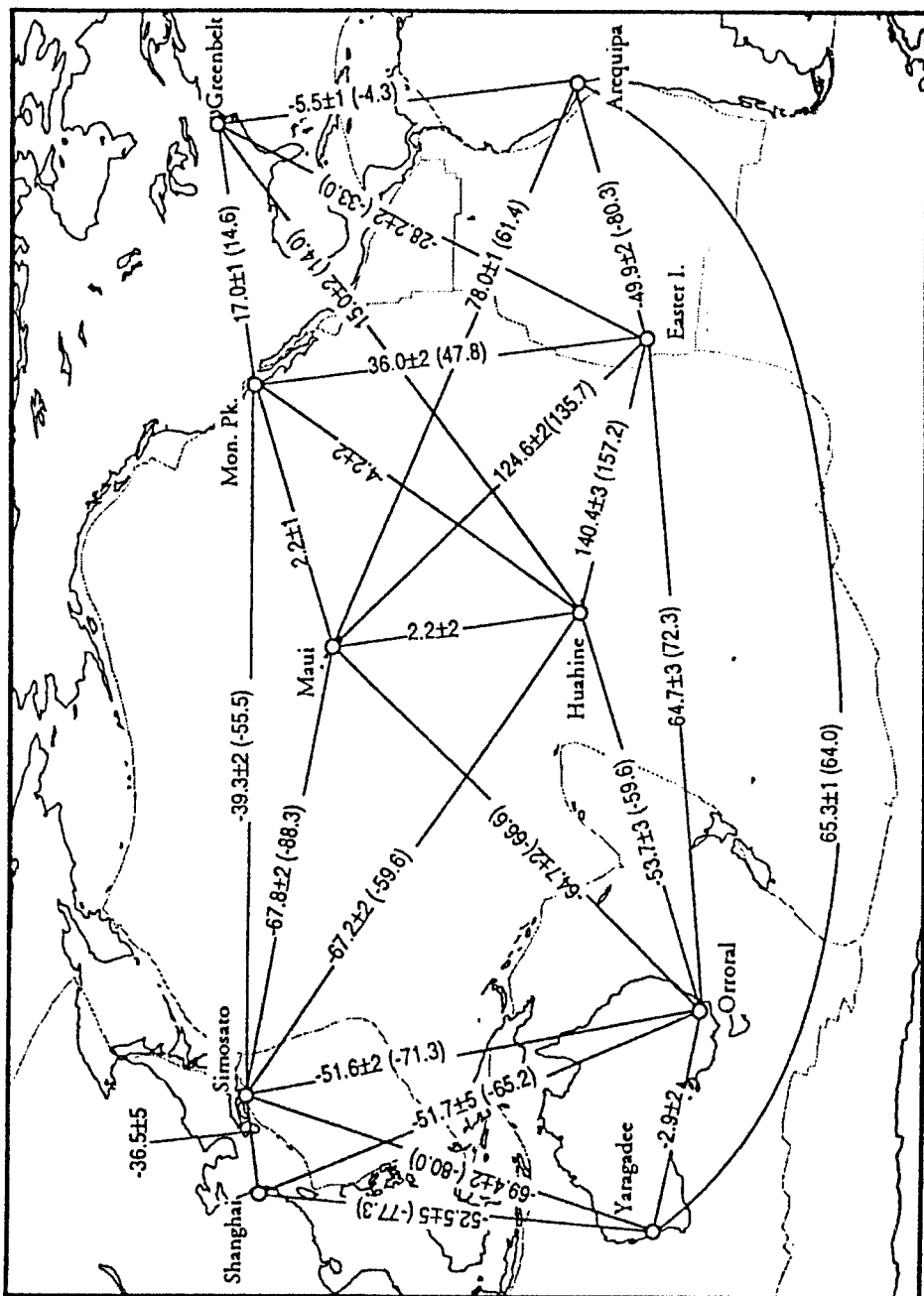


Fig. 2.17 Satellite laser ranging results (*LAGEOS*, 1993 spherical rates, mm/yr. Figures in parentheses are rates predicted by NUVEL-1. From Smith *et al.* (1994).

this result might surprise us, but in fact these three stations are all on the same (Pacific) plate. Distribution of shear between the Pacific and North American Plates, a long-standing problem, has been treated by Feigl *et al.* (1993).

Rigidity of intracontinental baselines has been demonstrated to date for North America (Jordan and Minster, 1988; Argus and Gordon, 1996), even though they cross areas of known activity. However, much remains to be done in this category, as will be discussed later in this chapter, especially for the Eurasian Plate.

Movement of the Pacific and Nazca Plates has been demonstrated: Kauai, for example, has been shown to be moving toward Japan at 8.7 cm/yr, compared with the predicted rate of 9.9 cm/yr; Maui is moving away from Arequipa. The apparent movement here is significantly greater than that calculated on the basis of rigid plates, the difference probably resulting from deformation of the South American Plate over the Peru–Chile Trench subduction zone (Robbins *et al.*, 1993). Similar effects have been seen in Alaska, a tectonically analogous area, over the subduction zone. Sato (1993) has shown that the Japanese station, Kashima, is moving to the northwest at about 2 cm/yr, a significant difference from rigid-plate behaviour. Collectively, however, the space geodesy measurements obtained by two independent methods – SLR and VLBI – appear to confirm the plate rigidity, movement direction, and rate required by plate tectonic theory.

The movement of a small continent, Australia, also appears to have been demonstrated although, as the geodetic results cited by Lambeck (1988) indicate, several more intracontinental baselines and several years of measurement are needed to demonstrate that the continent is in fact moving as a unit. Baja California is also demonstrably moving, as has been known from conventional geodesy for some time, although one would hardly characterize this small slice of crust as a “continent.”

Right lateral regional shear along the east margin of the Pacific Plate, in North America, has been measured by SLR and VLBI, in addition to conventional surveys, since the early-1970s (e.g., Sauber *et al.*, 1986). There is general agreement that the regional shear movement is several centimeters per year, but the way it is distributed is not yet clear. Contrary to popular belief, the San Andreas fault is not “the” plate boundary, but only one of many active faults along which the shear is distributed (Sauber *et al.*, 1994). There are also aspects not understood, such as the degree of vertical movement as demonstrated by the Loma Prieta earthquake of 1989. It has been argued by Martin (1992) that vertical movements may

dominate over geologic time, despite the horizontal movement demonstrably occurring now. However, the general pattern of contemporary plate motion seems well demonstrated by space geodetic techniques.

The precision of these results is, even to those familiar with the techniques, nothing less than astonishing: orders of magnitude greater than expected from satellite methods as late as the early-1960s. But beyond their precision, the results are also astonishing in that they agree with plate motions inferred from totally independent lines of evidence. Several numerical models of global plate motion, such as those of Minster and Jordan (1978), Chase (1978), and DeMets *et al.* (1990) have been based solidly on plate tectonic theory. The NUVEL-1 model of DeMets *et al.* illustrates the general procedures used. Plate directions for twelve assumed-rigid plates have been inferred from transform fault azimuths and earthquake slip vectors, and plate rates have been determined from the ridge spreading rates as measured from dated magnetic lineations. The spreading rates are particularly important in this context, for the lineations generally used cover about three million years and hence should give only average rates for this time. But as we have seen, the rates directly measured over only a decade or so are remarkably close to those estimated from the ridge spreading rates (Carter and Robertson, 1986; Gordon and Stein, 1992). Given the many problems in dating marine magnetic anomalies (Agocs *et al.*, 1992), this agreement must be considered strong support if not confirmation of sea-floor spreading. There are of course some glaring exceptions to simple sea-floor spreading from contemporary spreading centers, as in the north Pacific. The dated magnetic anomalies become younger as they approach the coast of Alaska and British Columbia, generally agreed to be a subduction zone where the oldest oceanic crust should be descending into the mantle. However, even this anomaly was ingeniously explained by Atwater (1970) as resulting from subduction of the spreading centers themselves.

In summary, the basic mechanisms of plate tectonics – sea-floor spreading and transform faulting, operating on rigid oceanic crust – appear to have been confirmed beyond reasonable doubt by space geodesy. However, we must consider the universally used term “plate tectonics and continental drift,” and ask if the new geodetic methods have confirmed continental drift as well. The classic evidence for drift, such as similar fossils on now-separated continents, has been repeatedly challenged by many geologists, such as Simpson (1947), Cloud (1968), Meyerhoff and Meyerhoff (1972), and Lowman (1995), and will not be further covered here.

2.7 Plate tectonics and continental drift

Continental drift is in plate tectonic theory considered simply as a corollary of plate movement (Hallam, 1983), and it is widely believed that continental drift has finally been confirmed by space geodesy. A *Science* headline “Continental drift nearing certain detection” (Kerr, 1985) gives the flavor of this belief. “Opening of the Atlantic” is referred to in effect as an observed event.

This judgement appears premature, at least for the classic continental drift cited by Wegener (1929), the separation of the Americas from Africa and Eurasia. One problem stems from the fundamental nature of continental crust as contrasted to oceanic crust. As discussed by McKenzie (1969), Molnar (1988), England and Jackson (1989), and Thatcher (1995), continental crust is inherently much more deformable than that of the ocean basins, as demonstrated by the broad areas of tectonic activity found in intracontinental plate boundaries shown on the tectonic activity map (see Fig. 2.7). The difficulty for space geodesy is that intraplate rigidity on these supposedly moving continents has not been demonstrated in several areas. For North America, the baselines across areas of known activity, such as the Basin and Range Province and the New Madrid seismic zone, appear stable within the measurement period (Jordan and Minster, 1988; Argus and Gordon, 1996). However, the problem is still unsolved in Eurasia, treated as a single plate in all plate-motion models cited (see Fig. 2.15). Taken at face value, continental drift as a result of plate movement implies that the crust between the Mid-Atlantic Ridge and Siberia is rotating as a unit in a counter-clockwise sense away from the Ridge. The apparent increase in space geodesy baselines between North America and western Europe (Smith *et al.*, 1994), for example, suggests such movement, to be discussed below. However, the original intracontinental baselines proposed for the Crustal Dynamics Project to demonstrate plate rigidity (Lowman *et al.*, 1979) have not yet been established although *GPS* nets are beginning to fill this need.

As shown on the tectonic activity maps, and the seismicity map in Chapter 1, there are sizable zones of major activity between the European geodetic sites and the interior of Eurasia. The catastrophic Rumanian earthquake of 1977, for example, was in plate theory the result of plate convergence. The occasional earthquakes of the Rhine Graben, some strong enough to be damaging, similarly must express crustal divergence. In plate tectonic theory, such orogeny, seismicity, and volcanic activity are the result of horizontal crustal movement. There is thus *a priori* evidence that apparent

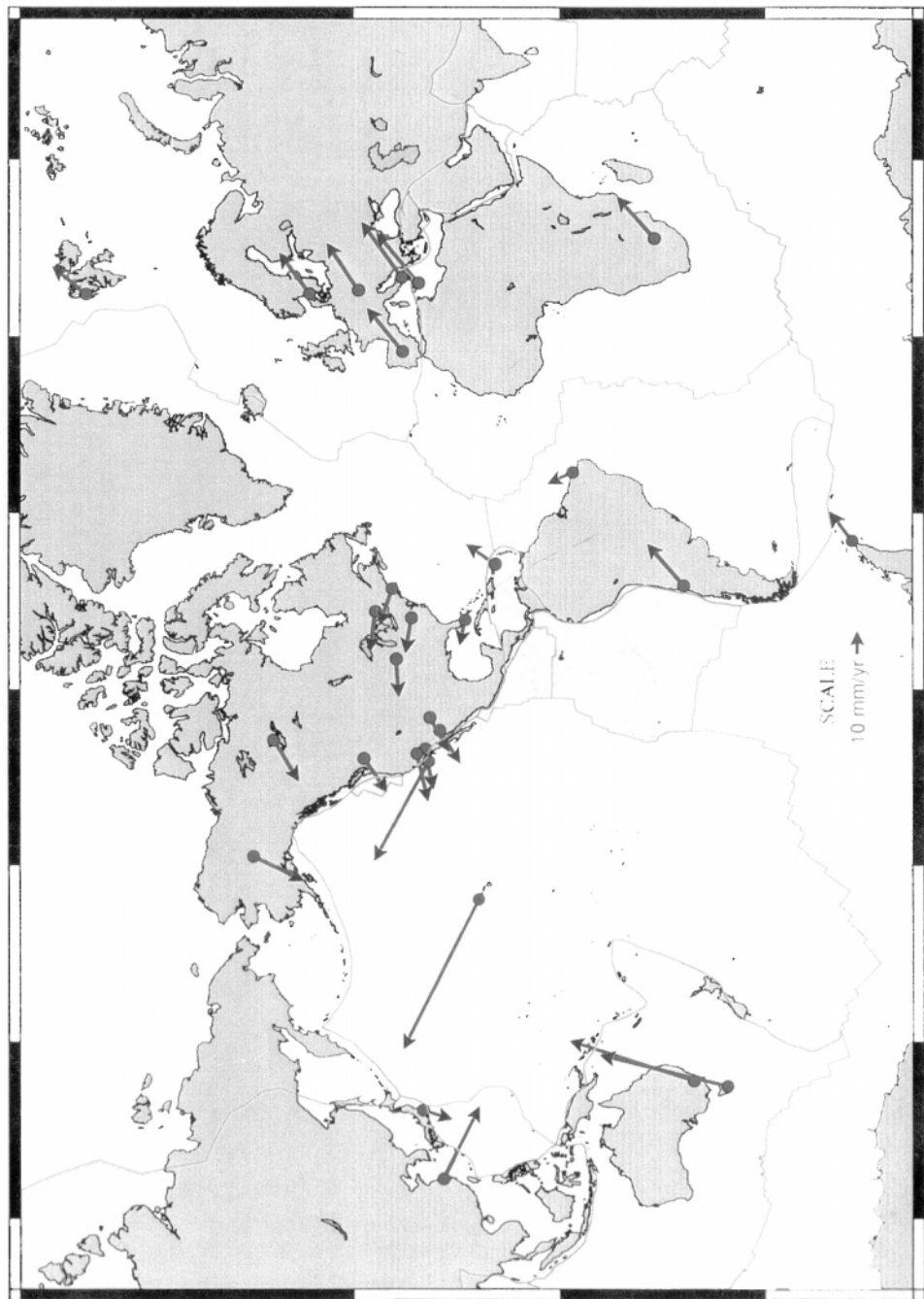


Fig. 2.18 (See also Plate VI) VLBI station velocities, NUVEL 1A-NNR reference frame. Computed by Space Geodesy Branch, Goddard Space Flight Center, 1998. Note similar azimuths of all European stations.

horizontal movements in western Europe do not necessarily reflect movement of the Eurasian Plate as a whole.

It is generally assumed that space geodesy measurements show plate movement over the mantle. This is clearly true for the Pacific Plate (see Fig. 2.16). However, as discussed by Lowman (2000), there is an apparent contradiction in western Europe between space geodesy results (Fig. 2.18) and the *World Stress Map* (Zoback, 1992), a simplified version of which is presented in Fig. 2.19. (A similar pattern for western Europe was found by Bird and Li, 1996.) Tectonism and seismicity in this area, as along the Rhine Graben, are considered to be caused by ridge push from the Mid-Atlantic Ridge, since the maximum horizontal stresses are generally parallel to the plate velocity trajectories implied by the AM-2 model of Minster and Jordan (1978). The problem is that space geodesy stations appear to be moving at almost right angles, to the northeast (Fig. 2.18), to the movement implied by the *World Stress Map*, to the southeast. A later investigation of global plate velocities using *GPS* data and the NUVEL-1A model by Larson *et al.* (1997) found similar velocities and directions.

There are several possible explanations for this contradiction. One is that the AM-2 model, based on movement over assumed-fixed mantle hot spots, is not applicable to Europe, in contrast to the Pacific Plate where it is successful. A more fundamental one may be that the assumption of fixed hot spots on which the AM-2 model is based is incorrect, as suggested by Molnar and Atwater (1973). The most obvious explanation is that the motions calculated for Fig. 2.18 – which are similar to those shown on other maps, including those based on *GPS* measurements – are dependent on choice of terrestrial reference frames. When motions of European sites are plotted (Ryan *et al.*, 1993) using NUVEL-1 but with the North American Plate held stationary, the site motions are to the southeast, in the direction implied by the stress directions. The geodetic sites are, in other words, being pushed to the southeast by the Mid-Atlantic Ridge, as one would expect both from the *World Stress Map* and the tectonic activity map. The anomalous results shown in Fig. 2.18 apparently result from use of NUVEL-1 but with the Pacific Plate held stationary. The implication of this anomaly is that numerical plate-motion models must be interpreted with caution, and that they are highly dependent on choice of terrestrial reference frames as discussed by Ma *et al.* (1992).

Another problem is new evidence that Europe is not the “passive margin” it appears to be. It has been suggested (Lowman, 1991) that western Europe is undergoing slow subduction, along the eastward

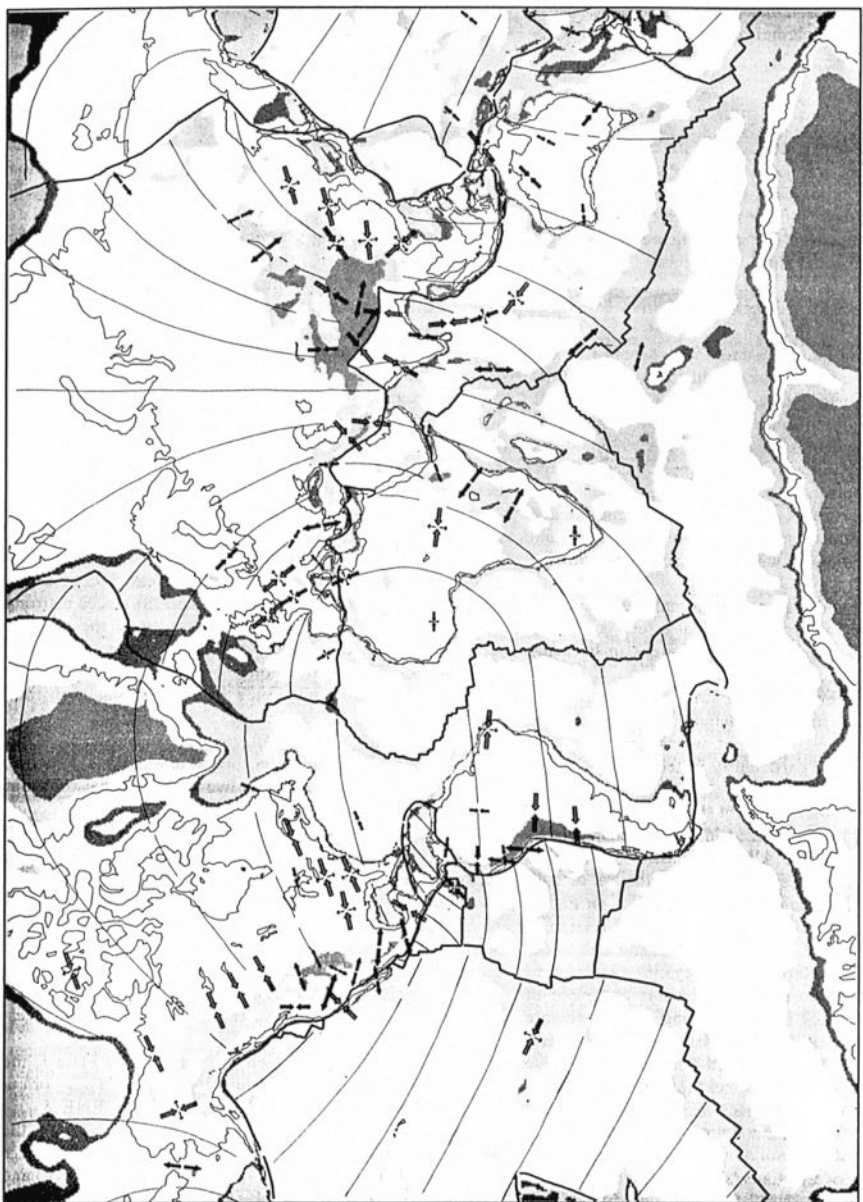


Fig. 2.19 Generalized version of *World Stress Map*, from Zoback (1992). Values shown in shading are topographic elevations or depressions in meters above or below sea level, respectively. Refer to original paper for details.

dipping Flannan Reflector under Scotland (Flack and Warner, 1990). The apparent drift of Europe may express a diffuse plate boundary analogous to that of southern Alaska where VLBI measurements have detected movement well north of the subduction zone (Ma *et al.*, 1990). It has been shown by Smith *et al.* (1990), from *LAGEOS* data, that underthrusting in subduction zones can produce regional deformation several hundred kilometers from the associated trenches. However, this speculation is also contradicted by the horizontal stress directions shown by the *World Stress Map*; as just discussed, motion caused by passive margin subduction should produce site motions to the southeast, not the northeast.

Another space geodesy measurement is at least suggestive of intracontinental deformation across the Eurasian Plate. Three baselines (Smith *et al.*, 1994) between western Europe and Shanghai for several years indicate consistent decreases of about one centimeter per year, despite the eastward movement of China implied by the “escape tectonics” theory of Molnar and Tapponier (1975). There is no obvious way, in the absence of a much denser geodetic net, to tell which station is actually moving, but a one centimeter annual rate for the European stations would account for most of the apparent trans-Atlantic increase. It must be pointed out that even if the western European stations are eventually shown to be moving eastward with the rest of the Eurasian Plate, this will produce a major problem for plate tectonic theory in that the European tectonic activity just cited could hardly be the direct result of horizontal plate movement. It would then be necessary to reassess the possible roles of vertical movement and magmatism in orogeny, as in the “surge tectonics” hypothesis of Meyerhoff *et al.* (1992).

To these problems must be added others inherent in plate tectonic theory. For trans-Atlantic drift, the chief difficulty is a driving force for the North American and Eurasian Plates (Lowman, 1985b). Purely oceanic plates can be driven by the well-understood slab pull: subduction of oceanic crust under the influence of increasing lithospheric density and the basalt–eclogite transition in subduction zones. Neither phenomenon can apply to plates whose leading edges are continental crust, and the edges of North America and Eurasia are obviously not being subducted. Added to the other evidence cited elsewhere (Lowman, 1985a) indicating that the trans-Atlantic continents are fixed above the mantle, and that there is no low-velocity zone under cratons (Knopoff, 1983), these problems must be considered major obstacles to confirmation of continental drift in the classic region where it must occur if it occurs at all.

It is suggested, in summary, that space geodesy can in principle

provide a decisive test of continental drift in a plate tectonics context, but that it has not yet done so. The establishment of much more extensive nets will be necessary to demonstrate that the continents in question are as rigid as plate theory requires. It should be remembered that although Einstein's theory of general relativity, published in 1916, was verified within three years by Eddington's 1919 eclipse observations, relativity is still tested at every opportunity many decades later. Plate tectonics and continental drift deserve similar testing.

2.8 GPS measurements of crustal deformation

The *Global Positioning System* is rapidly beginning to dominate space geodesy for distances of several hundred kilometers and even more. Applications of *GPS* have in fact become a sizable industry by themselves, with many compact receivers on the market. Hundreds of papers have been presented at scientific meetings, far too many to summarize here. Useful reviews have been presented by Lisowski (1991), Colombo and Watkins (1991), and for California, Feigl *et al.* (1993). A few examples will give some idea of the value of this system.

Perhaps the most general problem that has been approached with *GPS* is one discussed briefly in Chapter 1, that of how deformation of continental crust is best described: as collections of microplates, or by a continuum model. The discussion of Thatcher (1995) will again be cited, starting with an instructive diagram (Fig. 2.20) of the differences between these two kinematic models. Two further diagrams (Figs. 2.21, 2.22) show deformation patterns in two seismically active areas, the southwest US and the Middle East. As shown in a global context on the tectonic activity map (see Fig. 2.7), these areas are broad and irregular; they could, in principle, be explained by either continuum or microplate models. Thatcher's excellent discussion, which can not be reproduced here, brings out difficulties in each one, specifically calling for future *GPS* surveys to help settle the problem.

The study by Le Pichon *et al.* (1995) is focussed on the problem discussed by Thatcher, in this case the crustal deformation of Greece, Turkey, and the Aegean Sea. This area is intensely active seismically and volcanically, and has been interpreted as an example of extrusion tectonics by McKenzie (1972), the concept being that the Anatolian block is being squeezed westward by the northward movement of Africa and the Arabian Peninsula. However, given the density of faulting and seismicity, it is valid to interpret this as continuum deforma-

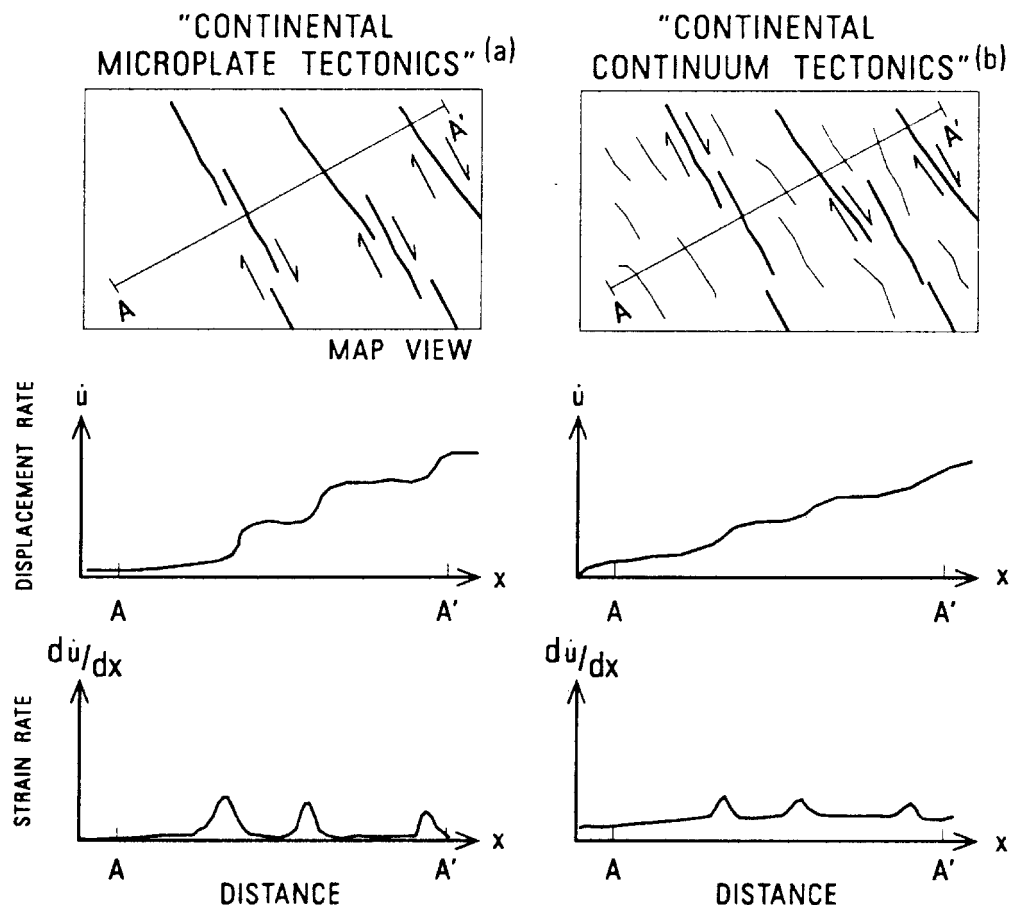


Fig. 2.20 Kinematic models of continental microplate tectonics vs. continuum tectonics. Fault motion assumed similar in both. From Thatcher (1995).

tion (Dewey and Sengor, 1979). Le Pichon *et al.* used both SLR (ranging to *LAGEOS 1*) and *GPS* methods to compile a map of the velocity field of Anatolia–Aegea relative to Europe (Fig. 2.23). As shown, the motion can be “approximated” by rigid rotation around a pole near the Nile delta, although the authors point out that the movement might have been started by phenomena such as gravitational collapse and trench retreat. The important point in the context of this chapter is simply that this study provides an excellent example of how space geodesy can be applied to the details of tectonic movements.

The *Global Positioning System* can also measure vertical movements precisely, as the following example will show.

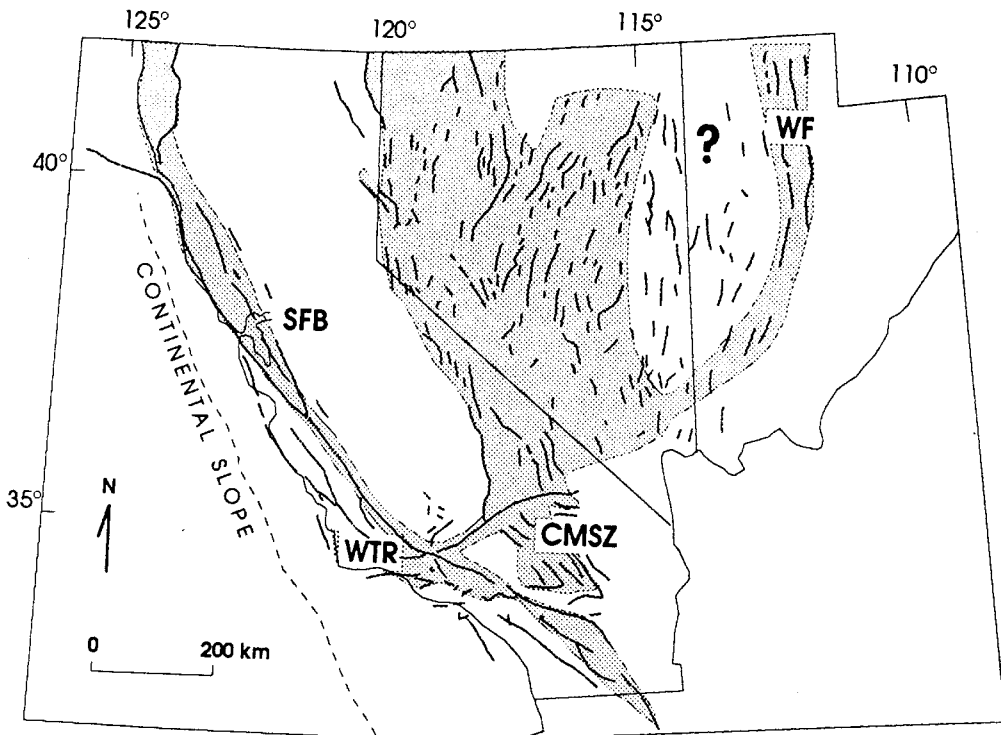


Fig. 2.21 Active faults and inferred deformation in western US.
WF: Wasatch fault; CMSZ: Central Mojave Shear Zone; WTR: western Transverse Ranges; SFB: San Francisco Bay. From Thatcher (1995).

The general mechanism of earthquakes of the Pacific Ocean subduction zones, such as southern Alaska and the Aleutian Islands, is now well established as sudden slippage along dipping faults. However, the deformation during and after such earthquakes is too complex to be explained by simple rigid-plate models. A *GPS* study of the Kenai Peninsula, Alaska, by Cohen *et al.* (1995) shows how this technique can throw light on the nature of this deformation (Fig. 2.24). The area was hit by the 1964 Prince William Sound earthquake, which with a moment magnitude, M_w , of 9.3, was the largest event in North America in historic times. The Kenai Peninsula subsided as much as 2 meters during the earthquake, and has been rising since. Cohen *et al.* used *GPS* receivers to measure the post-seismic uplift for the 1964–1993 period, comparing the *GPS* measurement with those of previous surveys. They found that the post-seismic uplift was decelerating, and deduced the probable post-seismic slip along the subduction zone. This turned out to be

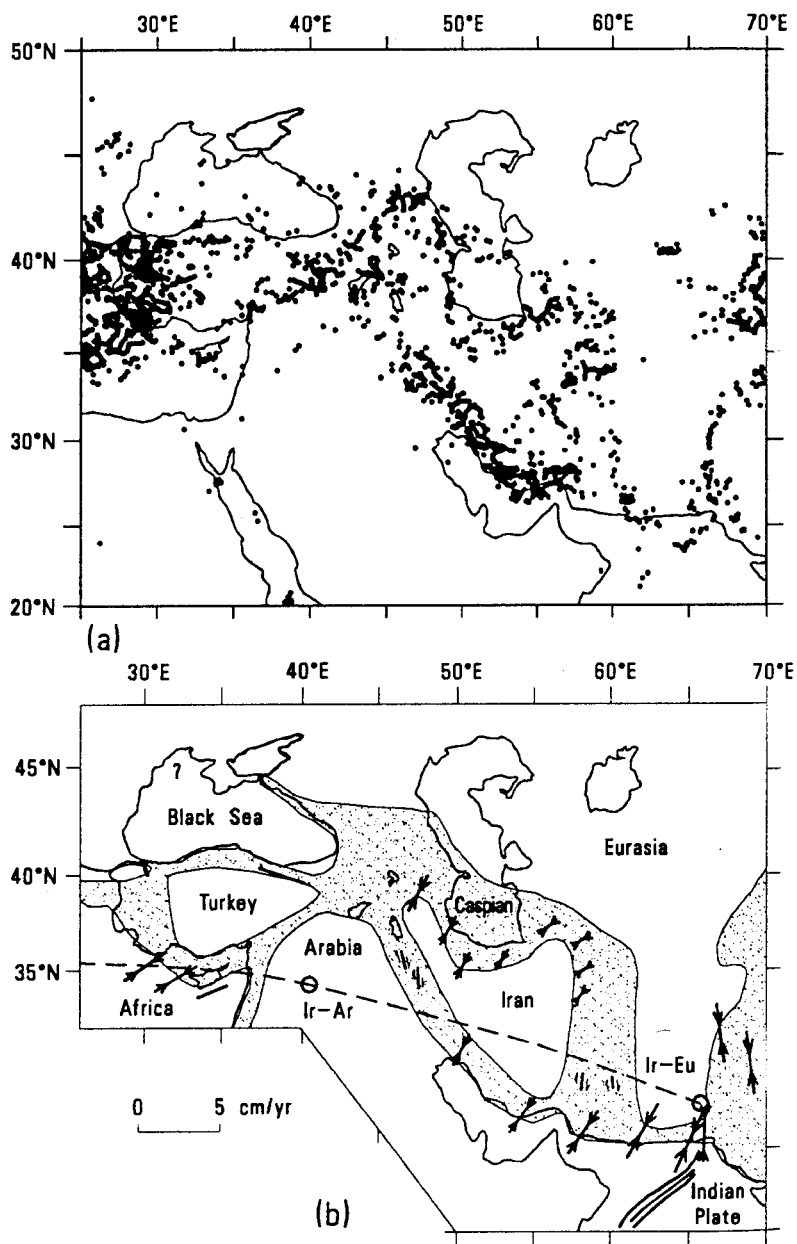


Fig. 2.22 Contemporary deformation patterns in Middle East; most intense deformation stippled. Dots: shallow earthquake epicenters, 1961–1980. Slip vectors show relative plate motion; circles are rotation poles. From Thatcher (1995).

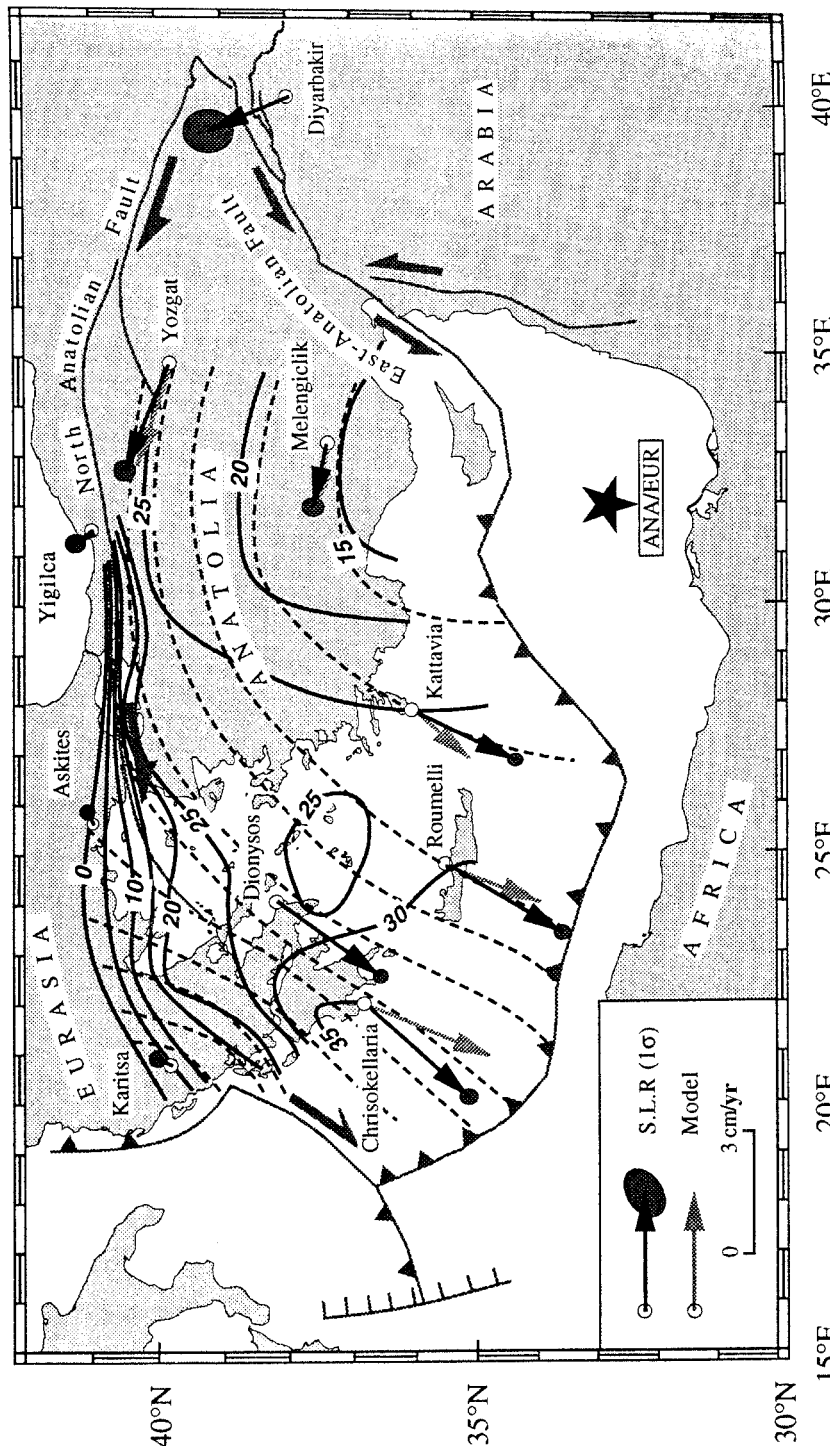


Fig. 2.23 Velocity field of Anatolia-Aegea with respect to Europe. Solid lines are equal velocity contours (5 mm/yr interval); dashed lines are flow lines. From Le Pichon *et al.* (1995).

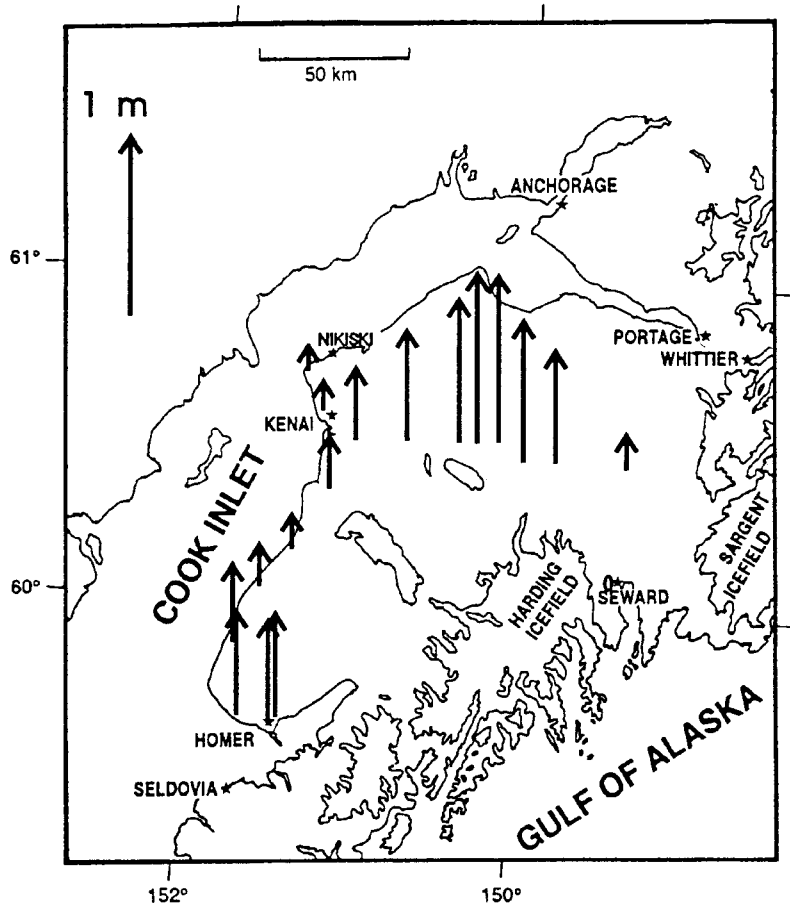


Fig. 2.24 Cumulative post-seismic uplift between 1964 and 1995, Kenai Peninsula. From Cohen and Freymueller (1997).

(Cohen, 1996) considerably greater than the 1.4 meters expected from rigid-plate motion of the Pacific Plate. The study provides a good example of how *GPS* measurements of vertical motion can in principle clarify the mechanism of plate motions.

Southern Alaska was also studied with *GPS*, this time concentrating on horizontal motions, by Sauber *et al.* (1997). This study carried out *GPS* measurements in 1993 and 1995 between the coast and the Denali fault. The area is extremely complex because it represents the transition between subduction under the Aleutian Islands and strike slip on major faults parallel to the coast, as shown in a generalized way on the tectonic activity map (see Fig. 1.1). The results are too complex to be reported here; the study is cited as an example of how space geodesy can be applied to the problem of

dangerous earthquakes, by clarifying the location and amount of strain accumulation.

Of immediate interest for the active and dangerous tectonism of the Pacific coast of North America were the many *GPS* studies of faulting and crustal deformation in California. There is ample geodetic evidence, going back several decades, that California is undergoing regional right lateral shear of several centimeters per year, as mentioned previously. However, the detailed pattern of strain accumulation and strain release, and its variation with time, is extremely complicated (Hager *et al.*, 1991). Some typical studies of this problem follow; the most general is that of Feigl *et al.* (1993).

A program of *GPS* measurements by Donellan *et al.* (1993) across the Ventura Basin found, in a 2.7-year period, shortening across the Basin of about 7 mm/yr. The authors suggested that this strain is occasionally released by earthquakes along the faults bounding the basin. Burgmann *et al.* (1992) carried out a *GPS* program across the San Andreas fault near the center of the 1989 Loma Prieta earthquake, finding very rapid aseismic slip on a nearby fault that might be precursory to a rupture. Similar *GPS* measurements were done by King *et al.* (1992) across the Hayward Fault, detecting within one year variations in horizontal slip rate and an anomalously high rate of vertical movement. Vertical movements are much more important than they might seem, for it has been realized since the Whittier Narrows earthquake of 1987 that much strain release may be along unexposed thrusts.

These studies illustrate the great advantage of *GPS* for dense nets of precise geodesy that can be established quickly, as they were after the 1989 Loma Prieta Ms 7.1 earthquake on the San Andreas fault. Such a program was carried out by Arnadottir and Segall (1994), as shown in Figs. 2.25 and 2.26. Apart from the substantial damage on the San Francisco peninsula, the Loma Prieta earthquake was scientifically interesting because there was little surface rupture, unlike the classic 1906 San Andreas event. Arnadottir and Segall combined geodetic data from several techniques including *GPS* and VLBI, inverting them to determine the actual nature of movement along the fault plane. They found the slip direction to be surprisingly complex, varying from right-lateral to oblique right-reverse at different locations. Such studies should eventually bring about a big improvement in our understanding of earthquake mechanisms, with obvious importance for geologic hazard mitigation.

The previous examples of *GPS* use in California have been essentially scientific. However, another example demonstrates the close connection between tectonics and everyday life. Southern

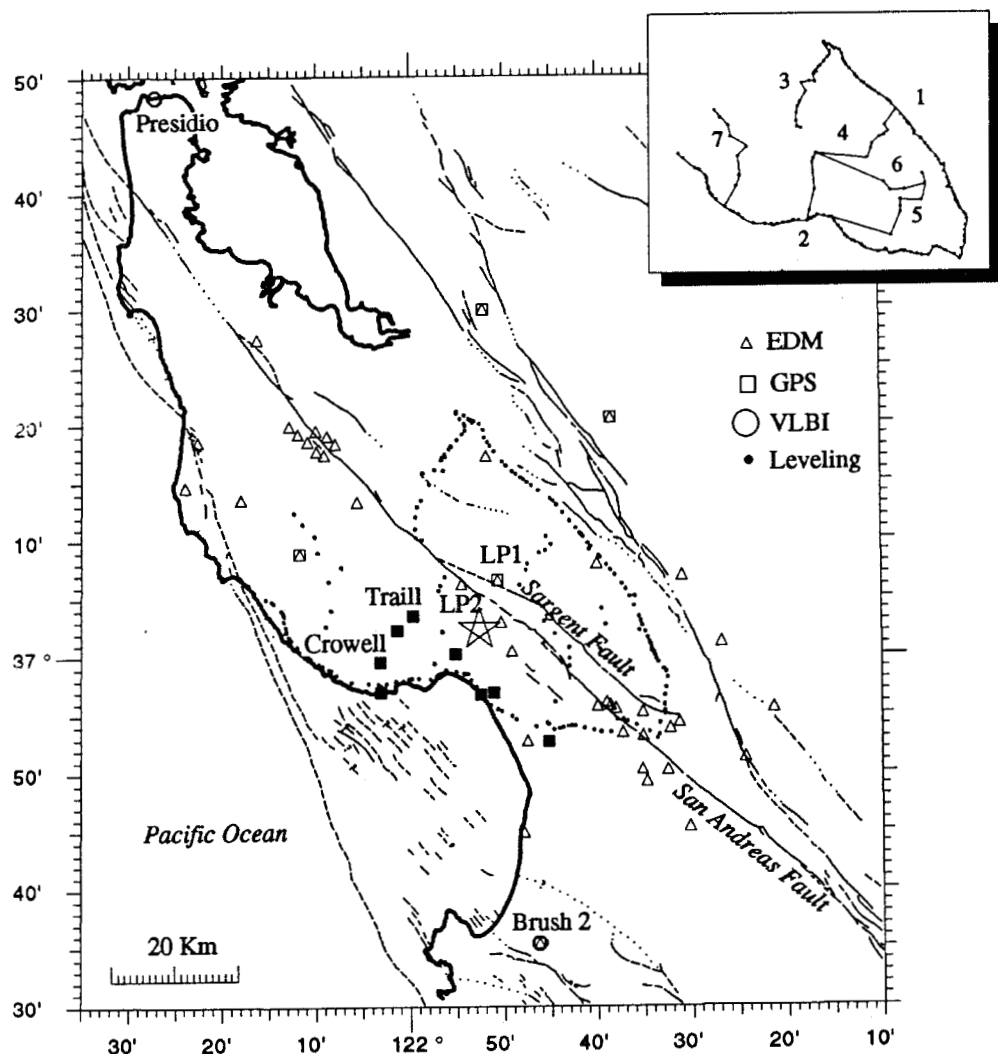


Fig. 2.25 Major faults of San Francisco Bay area, with locations of sites occupied for EDM, GPS, VLBI, and leveling. Insert shows leveling line. Star shows epicenter of main shock of Loma Prieta earthquake of 1989. From Arnadottir and Segall (1994).

California is a thicket of faults, most of them active or potentially so (Figs. 2.27, 2.28). This creates very real problems for surveyors and civil engineers, for the continual regional interplate shear, about 4 cm/yr, is literally bending geodetic nets, roads, pipelines, aqueducts, and railroads out of shape. Some of this motion, occurring during earthquakes, is sporadic, the rest secular. Satalich (1993) has described a large *GPS* program of precision surveying being carried

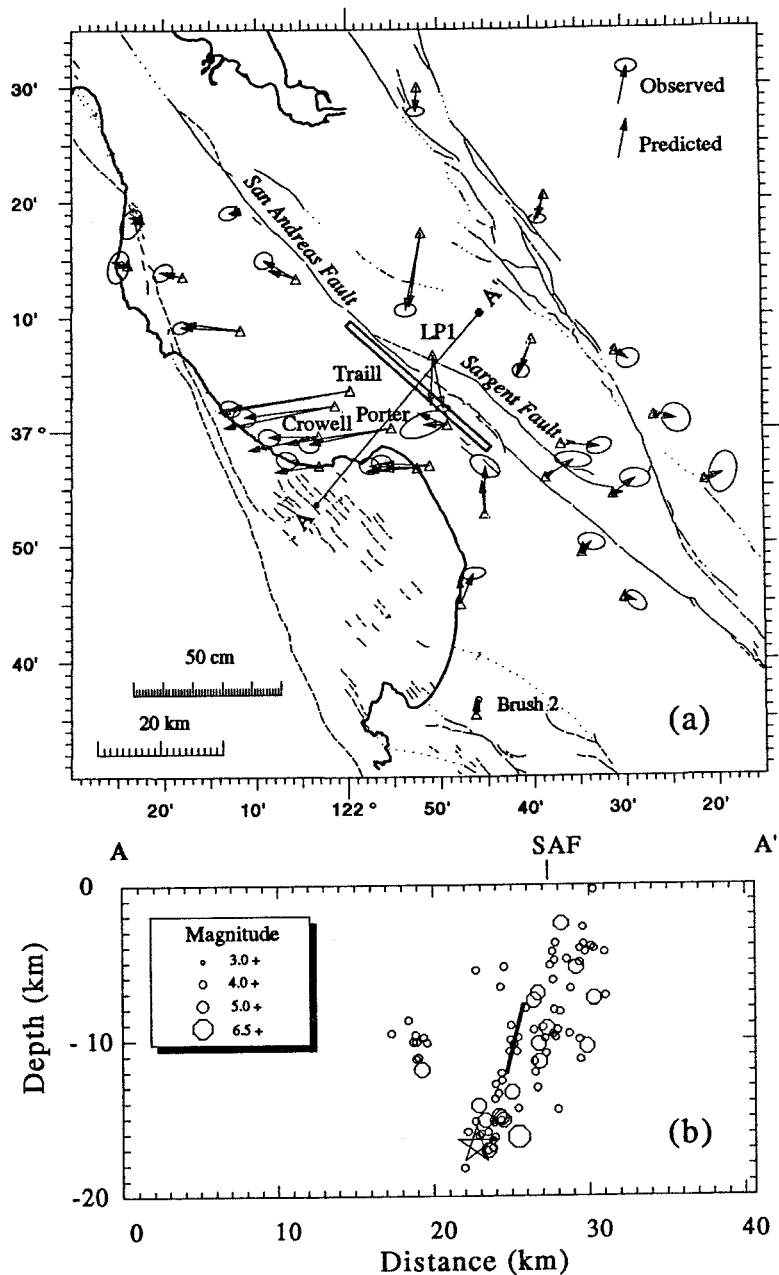
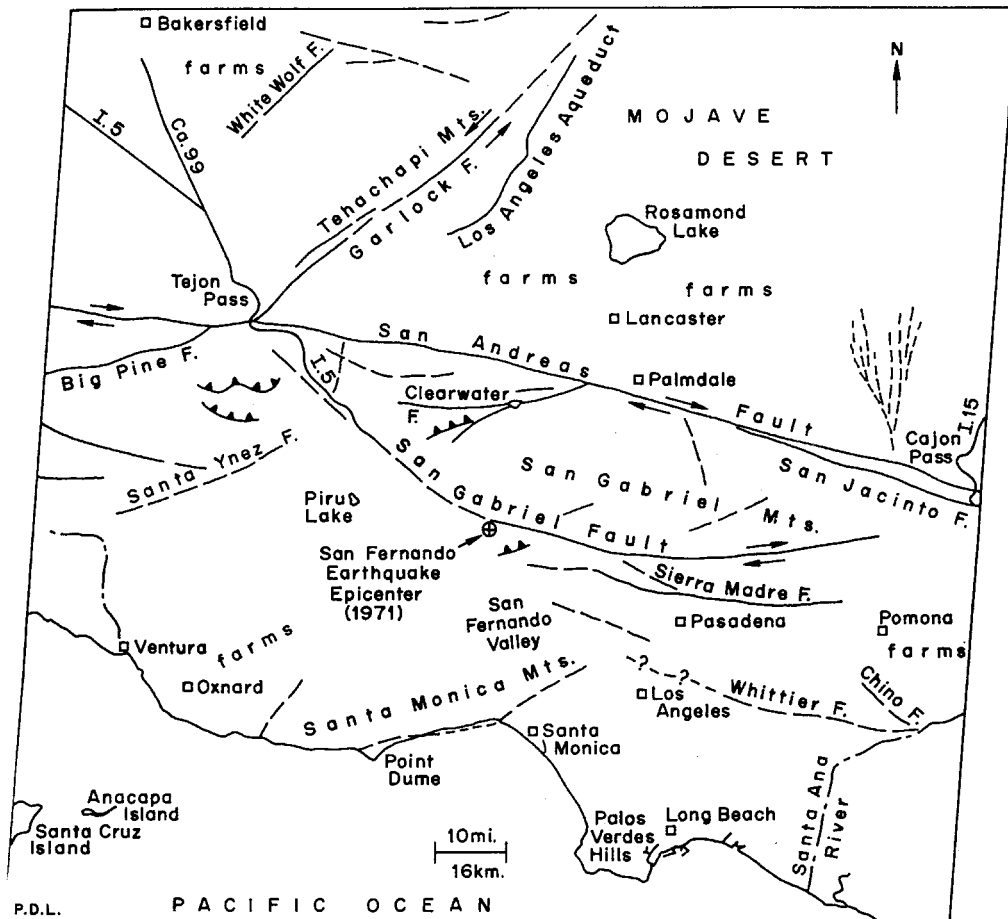


Fig. 2.26 (a) Observed and predicted horizontal displacements from the best uniform slip dislocation model. Rectangle shows surface projection of fault model. (b) Location of dislocation in cross section AA'. Main shock epicenter shown with star; hexagons are aftershocks from 18–31 October 1989. From Arnadottir and Segall (1994).



Fig. 2.27 Landsat 1 Band 6 image of Los Angeles; 1972. For scale, see Fig. 2.28.

out by the California Department of Transportation (Caltrans). Impelled by a series of bond issues intended to modernize California's transportation systems, Caltrans established a 90-station *GPS* control net. The objectives were to unify the regional control nets and to update them continually to allow for tectonic movement. Particular attention was paid to known active faults, and the effort coordinated with various agencies conducting *GPS* tectonic research, as described previously. Vertical as well as horizontal measurements were made, since in Los Angeles and Ventura Counties there is not only tectonic movement but elevation changes caused by oil or water withdrawal, water re-injection, and similar



GEOLOGIC SKETCH MAP
TRANSVERSE RANGES, CALIFORNIA
FROM LANDSAT-1 IMAGE 1090-18012

LEGEND:

-  FAULT (STRIKE-SLIP IF SHOWN WITH ARROWS)
-  THRUST FAULT (BARBS ON UPPER PLATE)

Fig. 2.28 Geologic sketch map of Fig. 2.27.

phenomena. Vertical movements are especially important for new rail lines. Collectively, the Caltrans project provides a dramatic demonstration of the dollar-value of space geodesy.

The *Global Positioning System* is a military system, whose full power can not always be utilized because of necessary security

restrictions, such as selective availability. However, it is clear that even with these restrictions *GPS* is now playing a major role in space geodesy. It has proven particularly useful for attacking the problem of diffuse plate boundaries and intracontinental deformation with which existing VLBI and SLR nets are beset. The tests of plate rigidity discussed before, necessary before continental drift can be directly demonstrated, are an obvious application of *GPS*.

2.9 Earth rotation and expansion tectonics

Space geodesy has implicitly provided a rigorous test of Earth expansion as a mechanism for tectonic activity, “expansion tectonics” henceforth. This theory, in brief, holds that the Earth has expanded greatly – by a large fraction of its initial radius – over geologic time, and is doing so today, accounting for sea-floor spreading, the distribution of continents, and other major features of terrestrial geology. Expansion tectonics is very much a minority view, but one held by many highly-qualified geologists and geophysicists. A leader in the field is S. W. Carey (1976, 1981a), who has compiled several well-documented lines of evidence supporting the “necessity” for Earth expansion. H. G. Owen (1981) has presented detailed plate reconstructions pointing in his view to expansion as a mechanism for “ocean-floor spreading.” Schmidt and Embleton (1979) found common apparent polar wander paths for several continents during the Precambrian, concluding that an increase of 45% for the Earth’s radius during the time involved was implied.

An important point in favor of expansion tectonics, whatever else can be said, is that it leads to testable predictions (Runcorn, 1981). One prediction implicit in a theory of major and continuing expansion is an increase in the length of day (LOD) because of the absolute necessity to conserve angular momentum. The principle is illustrated in elementary physics books by the familiar pirouetting skater, whose spin rate increases as she folds her arms, thus conserving angular momentum. As applied to the Earth, it means that the rotation rate must decrease if the solid part of the planet expands. (An elementary mathematical summary has been presented by Stewart, 1981.) The consequence of this is that LOD must increase if the Earth expands.

The constraints of angular momentum conservation are fundamental (Carey, 1981b), and they lead to several tests of expansion tectonics to which space geodesy can be applied. An obvious one, already discussed, is increasing baseline lengths among various space geodesy stations – among all of them, in principle. Expansion

has failed this test so far in that the changing baseline lengths generally fit the NUVEL-1 model, with serious but explainable exceptions as discussed previously, in which the radius of the Earth is implicitly constant.

The most definitive test would be a continuing increase in LOD. It must be pointed out here that scientists who have concentrated on the problem of Earth rotation, of which LOD is a major component, do not even mention the Earth-expansion hypothesis (e.g., Munk and MacDonald, 1960; Lambeck, 1980). This is probably because they consider the evidence for both paleorotation and present rotation rates to conclusively rule out major expansion.

As mentioned previously, space geodesy provides several ways to measure LOD with precision on the order of a few milliseconds (Dickey *et al.*, 1993). The literature on this is large and can not be even summarized here, but a tabulation by Chao (1994) (Table 2.3) shows that the precision now attained is good enough to detect mass redistributions as small as those caused by reservoir filling and emptying. Measurements of LOD have been going on for several decades by precise astronomical techniques, and in recent years by gravity-independent methods involving atomic clocks. Viewed together with the space geodesy results, they have essentially disproven major earth expansion by default: there is simply no sign of a steady trend in LOD pointing to such expansion.

A possible cause for Earth expansion suggested by several scientists, including Dirac, Jordan, Dicke, and Holmes, is secular decrease in the universal gravitational constant G . In principle, such a fundamental assumption would permit expansion, possibly to a very slight degree. However, space geodesy again appears to rule out this proposal. The value for G is fundamental to interpretation of, for example, *LAGEOS* orbits (Tapley, 1993). But the entire mathematical infrastructure of space geodesy is a rigid one. If fundamental quantities such as G were changing significantly now – as implied by expansion tectonics – such changes would show up within a few years at most. They have not.

Expansion tectonics is advocated by many scientists, who repeatedly demonstrate serious anomalies in conventional tectonic theory, many of which deserve intensive study. It was commented by one of Einstein's collaborators, Leopold Infeld, concerning the later-retracted “cosmological constant,” that an incorrect solution of an important problem can be more valuable than a correct solution of a trivial problem. Expanding-Earth advocates have made a real contribution to tectonics, but the hypothesis appears to have been conclusively disproven by space geodesy.

Table 2.3 *Geophysical causes of variation in length of day (LOD). From Chao (1994).*

Geophysical source	Temporal signal	$\Delta J_2 (\times 10^{-10})$	Amplitude (peak-to-peak)		
			$\Delta J_3 (\times 10^{-10})$	$ \Psi (\text{mas})^a$	$\Delta \text{LOD} (\text{ms})$
<i>Tidal deformation</i>					
Solid earth	Long-period	Up to 20	?	0	Up to 0.8
	Diurnal	0	0	Up to 4 (in $ m $)	0
	Semi-diurnal	0	0	0	0
Oceans	All tidal period	Up to 4		Up to 1 (in $ m $)	0.08
<i>Atmosphere</i>					
IB ^b	Days–Seasonal–Interannual	8 (peak) 3 (annual) 1 (interannual)	10 (peak) 5 (annual) 1 (interannual)	100 (peak) 55 (annual) <5 (interannual)	0.15 (peak) 0.05 (annual) 0.02 (interannual)
Non-IB	Days–Seasonal–Interannual	15 (peak) 5 (annual) 2 (interannual)	20 (peak) 6 (annual) 2 (interannual)	200 (peak) 82 (annual) <10 (interannual)	0.3 (peak) 0.1 (annual) 0.03 (interannual)
<i>Continental water</i>					
Snow	Seasonal–Interannual	2 (annual)	1 (annual)	20 (annual)	0.04 (annual)
Rain	Seasonal–Interannual	1 (annual)	1.7 (annual)	16 (annual)	0.02 (annual)
Glaciers	Secular	0.02 per year	0.01 per year	0.04 per year	4×10^{-4} per year
Reservoirs	Cumulative since 1950	-0.4	0.3	10	-0.006
Ice sheet	Secular	?	?	?	?
Groundwater	Seasonal–Secular	?	?	?	?

Table 2.3 (cont.)

Geophysical source	Temporal signal	$\Delta J_2 (\times 10^{-10})$	Amplitude (peak-to-peak)		
			$\Delta J_3 (\times 10^{-10})$	$ \Psi (\text{mas})^a$	$\Delta \text{LOD} (\text{ms})$
<i>Ocean</i>					
Sea level	Secular	0.03 per year	-0.02 per year	0.05 per year	5×10^{-4} per year
Circulation	Seasonal-Interannual	?	?	?	?
<i>Earthquake</i>					
	Episodic:	0.5 (2)	0.3 (1)	23 (1)	-0.008 (1)
	(1) 1960 Chile				
	(2) 1964 Alaska				
	Cumulative secular (1977-90)	-0.002 per year	0.008 (peak)	0.03 per year	- 10^{-4} per year
<i>Post-glacial reb.^c</i>					
	Secular	-0.3 per year	?	3 per year	?
	Secular	-0.005 per year	0	0	- 10^{-4} per year
<i>Tidal braking</i>					
<i>Manile convection/</i>					
<i>Tectonic movement</i>					
	Secular	?	?	?	?
<i>Core activity</i>					
	Secular	?	?	?	?

Note:^a mas = milliarcseconds; ^b IB = inverted barometer correction; ^c reb. = isostatic rebound.

2.10 Extraterrestrial gravity fields

The ability to cross space has given us the first opportunity to study in detail the gravity fields of other planets. At this writing, every planet but Pluto has been visited by spacecraft, in addition to many satellites. It will be instructive to compare the gravity fields of those bodies most similar to the Earth – the Moon, Mars, and Venus – with that of the Earth. Several useful reviews have been published on this and related subjects. The most comprehensive modern paper is by Phillips and Lambeck (1980), covering the gravity fields and tectonics of the terrestrial planets. However, the now-outdated paper by MacDonald (1963), essentially the last astronomical treatment of planetary geophysics, is still a valuable introduction to the principles and the first-order problems.

2.10.1 Gravity field of the Moon

As one would expect, we know far more about the lunar gravity field than any other, except that of the Earth itself. Reviewed by Kaula (1975) and Ferrari and Bills (1979), measurements related to lunar gravity come chiefly from Doppler tracking of spacecraft in lunar orbit, but also from laser ranging to the retroreflectors on the surface, laser altimetry from *Apollo* spacecraft, and instruments landed on the surface during the *Apollo* expeditions. There is consequently a very large literature on this subject, and one which is growing as new data are acquired from new lunar missions, *Clementine* (1994) and *Lunar Prospector* (1998) in particular. Accordingly, only the main findings from these sources will be summarized here, more or less in historic order.

As we have seen, the gravity field of a planet is closely related to the planet's shape. We should therefore begin by mentioning the pre-spacecraft discovery by ground-based astronomers (Baldwin, 1963; Kopal, 1971) that the Moon is a triaxial ellipsoid, roughly pear-shaped with the small end pointed away from the Earth. This shape is far too irregular to express hydrostatic equilibrium, and Urey (1952) cited it as evidence that the Moon must be cool and rigid throughout at present. The opposite view, that the Moon's shape represented mantle convection, was presented by Runcorn (1967), but this was before new information became available from Moon-orbiting satellites. The opposing views were somewhat analogous to those about the Earth's shape and gravity field, which as we have seen were not resolved until satellite tracking was possible.

The series of five *Lunar Orbiter* missions at different altitudes

and inclinations revolutionized our knowledge of the Moon's gravity (as well as its geology). The most immediate discovery from Doppler tracking of the *Lunar Orbiters* was a new value for the mass of the Moon and a map of its gravity field to degree and order 13 (Michael and Blackshear, 1972). However, the most surprising subsequent discovery from the tracking data, by Muller and Sjogren (1968), was of large positive gravity anomalies over the circular maria. They termed these "mascons," since they were clearly mass concentrations. Muller and Sjogren suggested that these features were the buried iron bodies that had formed the mare basins, but this suggestion was immediately challenged by several authors all of whom acknowledged the great achievement of discovering the mascons. An issue of *Science* published shortly after included several of these discussions; the most useful is that of O'Keefe (1968). O'Keefe pointed out that Muller and Sjogren's "astonishing" feat actually demonstrated that the Moon, in particular the lunar highlands, was roughly in isostatic equilibrium and, by implication, was probably differentiated, an interpretation confirmed after the *Apollo* landings began. A more general treatment of the mascon interpretation was published by Kaula (1969), discussing several issues such as the nature of the basin-forming impacts. The proposal that the mascons were caused by buried impacting bodies was generally rejected, one reason being the knowledge that such bodies are almost always destroyed and largely ejected from the crater.

Wise and Yates (1970) proposed the explanation that is still widely accepted, although modifications seem called for since the new data from *Clementine* and *Lunar Prospector*. The mascons are actually Bouguer anomalies, caused by unusually dense material. Wise and Yates suggested that after the basin-forming impacts, a plug of lunar mantle material was pushed upward to occupy the initial crater, approaching isostasy. At some later time, the basins were flooded by the mare basalts, which as added mass to the lunar crust produced the positive gravity anomalies. Later studies by various workers, taking into account mare structure and other geologic factors, has led to much more detailed reconstructions of the history of the lunar maria (Melosh, 1978; Solomon and Head, 1980; Bratt *et al.*, 1985).

The resumption of lunar exploration, unfortunately unmanned, in the 1990s has generated new models of the lunar gravity field. The *Clementine* mission of 1994 (Nozette *et al.*, 1994) provided more than 2 months of tracking and laser altimetry from a nearly circular low orbit, excellent for mapping. As reported by Zuber *et al.* (1994), *Clementine* confirmed O'Keefe's (1968) conclusion, from the

Muller–Sjogren analyses, that the highlands were isostatically compensated. However, the mare basins show a much more complicated behavior in this respect. The classic mascon basins, the near-side circular maria, are uncompensated, consistent with the interpretation of Solomon and Head (1979) that topography is supported by the strength of the cold and rigid lithosphere. An interesting early study of the lunar Apennines (Fig. 2.29), the rim of the Imbrium Basin, by Ferrari *et al.* (1978) concluded that these mountains were similarly supported, and were not in isostatic equilibrium. This points up one of the many differences between the Moon and the Earth, where major mountain ranges are in isostasy.

Using the *Clementine* tracking and laser altimetry data, Zuber *et al.* (1994) constructed a series of geophysical maps of the entire Moon. Another finding from the *Clementine* laser altimetry (Spudis *et al.*, 1994) was confirmation of several extremely old multi-ring basins and discovery of possible new ones. Of particular interest is the South Pole–Aitken Basin, 2500 km wide and hence the largest known impact basin in the solar system.

The *Clementine* data have been used by Wieczorek and Phillips (1997) to study the structure and composition of the lunar highland crust. Their work provides an excellent example of how geophysical and geochemical data can be combined. A detailed summary of their results is not possible here, except to note that they found Airy compensation to be dominant, and interpretable in terms of a stratified highland crust.

The *Lunar Prospector* mission (Binder, 1998) has been even more successful than *Clementine* in a geophysical sense because of its low-altitude (ca. 100 km high) circular near-polar orbit. Doppler tracking data have permitted construction of a greatly improved 75th degree lunar gravity model (Fig. 2.30) (Konopliv *et al.*, 1998), when combined with data from *Lunar Orbiter*, *Apollo*, and *Clementine*. The structure of the mascons, now seen with gravity data having a spatial resolution of 75 km, seems now to be more complex and less easily interpreted than previously thought, a conclusion reached earlier by Zuber *et al.* (1994). Seven new mascons have been discovered, some of which have little or no mare basalt fill. This implies that the mantle plug hypothesized by Wise and Yates (1970) may be more important for such features. The new data have generated new controversy on the degree and mechanisms of isostatic compensation in the Moon, a refreshing development. Further discussion of these would be out of place in a book about the Earth, except for mention of the mascon basin study by Golombek (1979).

After a perceptive discussion of faulting, Golombek analyzed

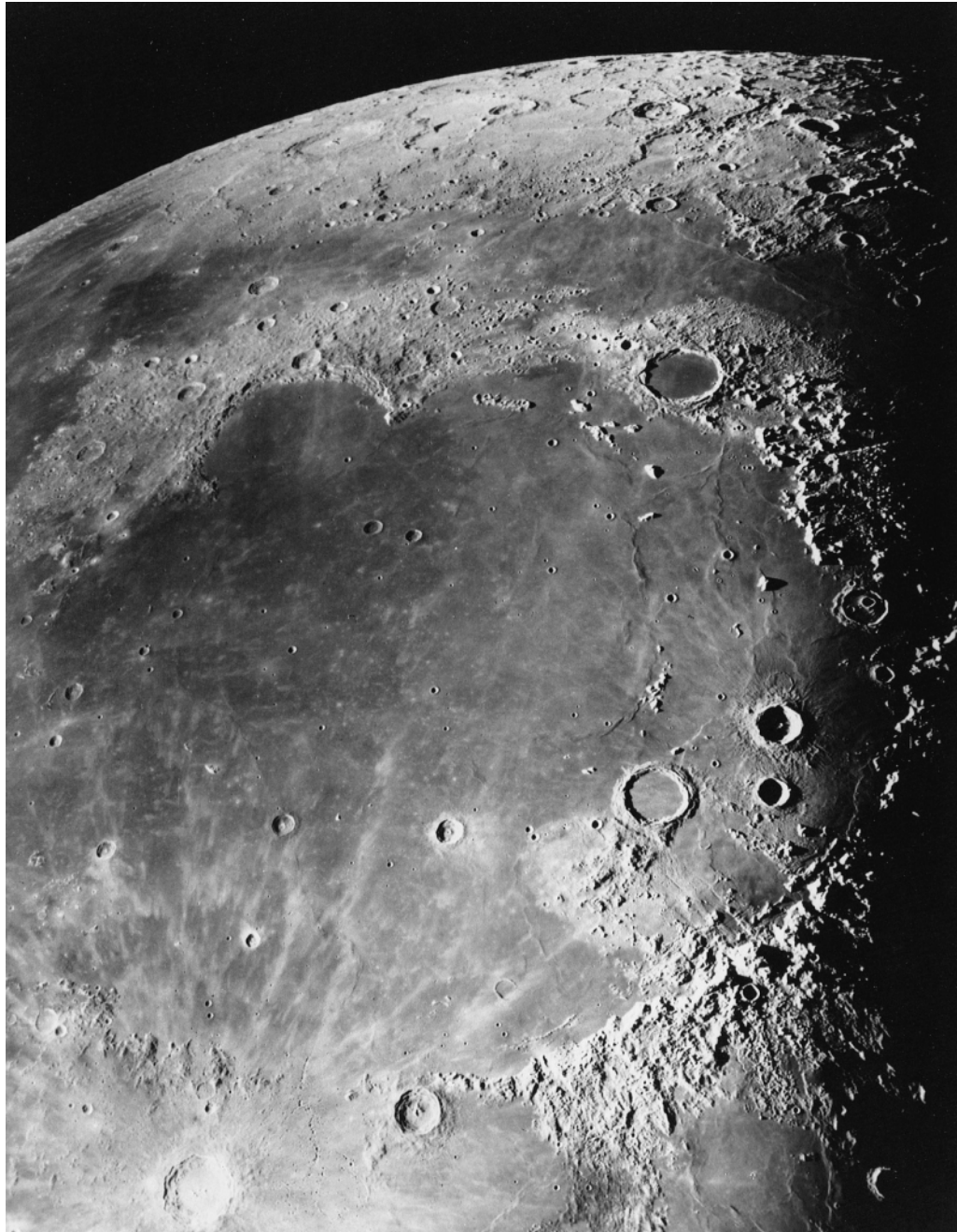


Fig. 2.29 Mount Wilson 100 inch (2.5 m) telescope view of the 1300-km-wide Mare Imbrium; north at top. Apennines at lower right.

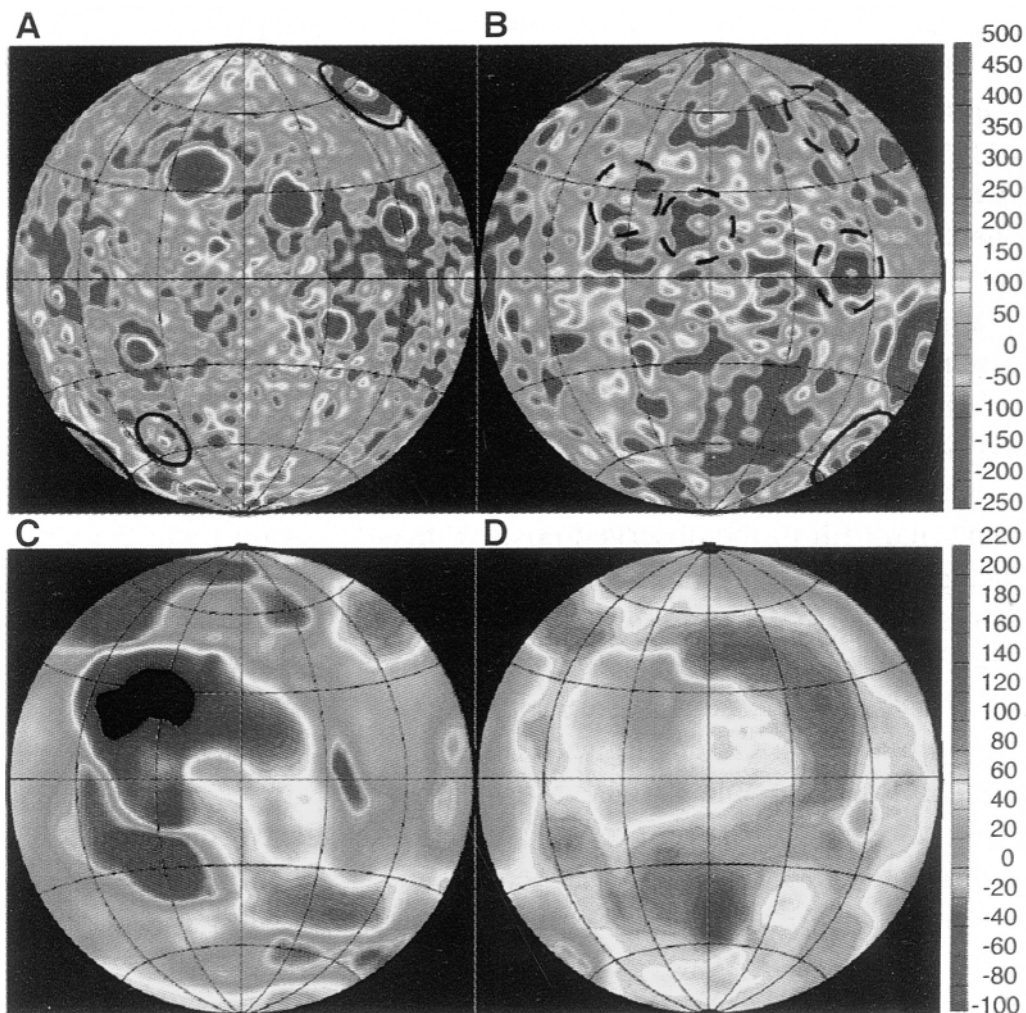


Fig. 2.30 (See also Plate VII) *Lunar Prospector* gravity and crustal thickness maps (Konopliv, *et al.*, 1998), Lambert equal-area projection. A, C: near side; B, D: far side. *Top:* Vertical gravity anomalies, in milligals. Newly-discovered near-side mascons shown with solid circles, far-side ones with dashed circles. *Bottom:* Crustal thickness in kilometers, calculated with an Airy compensation model (constant density) without principal mascons.

the structure of mascon basins. Among his conclusions relevant to terrestrial geology is the inference that fractures propagate upward, and that stresses can not be correctly calculated from the surface expression of fractures. He further explained the scarcity of strike-slip faults on extraterrestrial surfaces as resulting from fracture formation at depth, where maximum compressive stresses are vertical.

As discussed in Chapter 4, the nature and origin of crustal fracture patterns – lineaments – is still poorly understood. Golombek’s analysis, based originally on lunar gravity data, is a good example of how extraterrestrial geology can have implications for the geology of the Earth.

Even more fundamental inferences about the Moon have been made by Konopliv *et al.* (1998) from the new tracking data. These data have permitted calculation of a new value for the polar moment of inertia, close to a previous estimate by Hood and Jones. These values imply that the Moon may have a core, presumably of iron, as large as 900 km in diameter. If confirmed, this would put constraints on theories of the Moon’s origin, in particular the giant-impact model in which the Moon formed from debris ejected from the Earth by collision with a Mars-sized object. However, the latest version of the giant-impact theory (Cameron, 1997) has the impact happening in the late stages of accretion of the Earth.

In summary, the gravity field of the Moon has proved to be inherently interesting, by itself and by comparison with that of the Earth. The Moon’s geologic evolution has been shown to be much simpler than terrestrial geology, the basic reason being that the Moon ran out of internal energy at an early stage. Its crust accordingly has not undergone the repeated re-working experienced by the terrestrial crust. The Moon’s role as a fossil planet is discussed in Chapter 6. At this point it can simply be noted that its “fossil” nature has helped interpret the gravity data, in that structures produced billions of years ago have been essentially frozen in. Finally, the application of gravity methods to lunar exploration typifies their strengths and weaknesses: indecisive by themselves, but highly useful when interpreted in the context of other data.

2.10.2 Gravity field of Mars

Most of our knowledge of the gravity field of Mars comes from satellite tracking, which began in 1895 when Struve (1895) used the 30 inch (0.8 m) refractor at Pulkowa Observatory to monitor the orbits of Phobos and Deimos. He applied Clairaut’s Theorem, still the standard approach, to obtain a value of 5.210×10^3 for the flattening of Mars. This is essentially the modern value, from Doppler tracking of spacecraft (e.g., 5.216×10^3 , Reasenberg *et al.*, 1975).

Since the 1960s, several spacecraft have been put in orbit around Mars; the two *Viking Orbiters*, operating for about 4 years, were unusually valuable for Doppler tracking. The *Mars Global Surveyor (MGS)* was put into orbit around Mars in 1997, operating for more

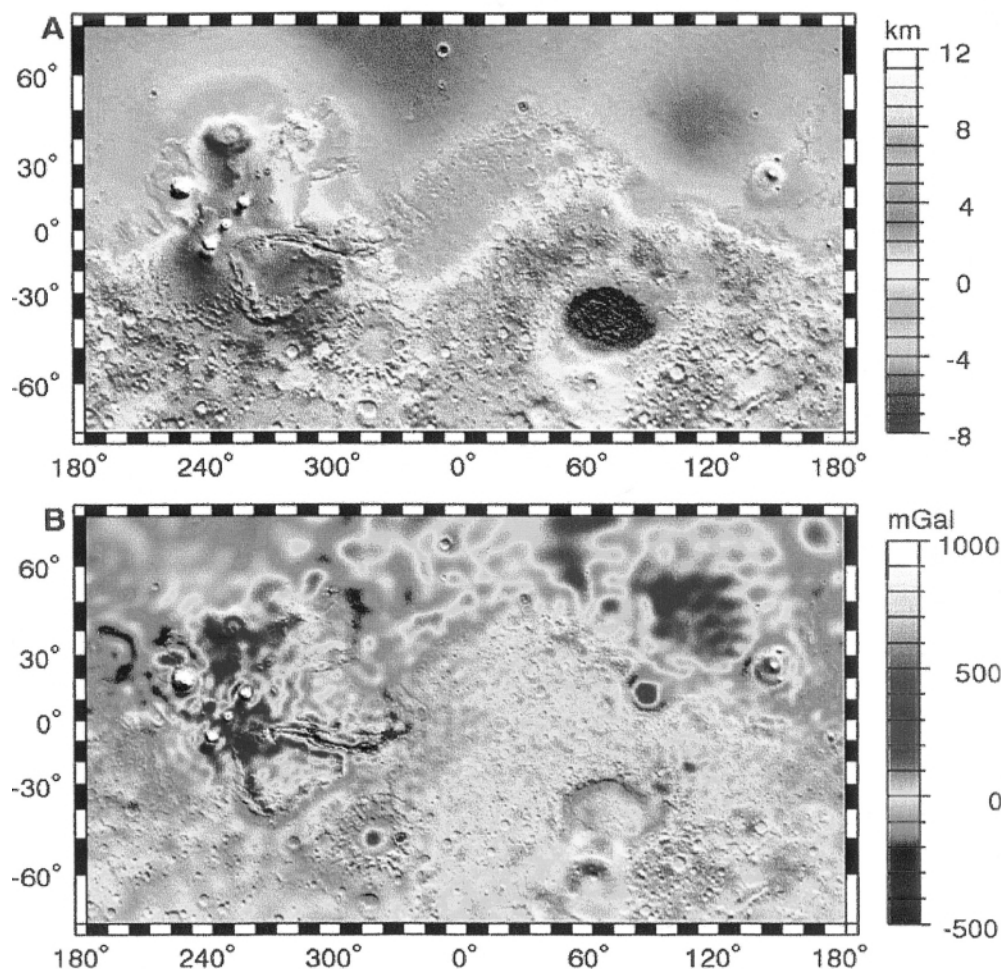


Fig. 2.31 (See also Plate VIII) Mars Global Surveyor maps (Zuber *et al.*, 2000) of topography (*top*) and free-air gravity values (*bottom*). Tharsis area near the equator between 220 and 300 deg. E.; Hellas Basin: 45 deg. S, 70 deg. E.; Utopia: 45 deg. N, 110 deg. E.

than 4 years. Tracking data and altimetry from the *MGS* Mars Observer Laser Altimeter (MOLA) have been extremely valuable (Zuber *et al.*, 1998), permitting compilation of detailed topographic, free-air gravity, and crustal thickness maps (Fig. 2.31) (Zuber *et al.*, 2000). Before discussing these, a few major characteristics of martian geology should be noted.

The most important factor is that Mars is much more evolved geologically, and more internally active now, than the Moon, as will be discussed in Chapter 6. Generally speaking, Mars can be

considered geologically intermediate between the Moon and the Earth. The present surface environment of Mars is physiologically that of space, with surface pressures of about 6 millibars. However, it is clear that Mars has retained considerable water, since recent fluvial erosion and deposition, stratification, and mass wasting are widespread. Consequently, the physiography of Mars is a complex palimpsest of impact craters, tectonic features, fluvial channels and deposits, volcanic rocks, and wind-deposited material. However, Mars has evidently not reached the stage of plate tectonics, and has occasionally been called a “one-plate planet.” Comprehensive treatments of the planet have been published by Carr (1982) and Kieffer *et al.* (1992).

Most discussions of the gravity field of Mars center on the Tharsis Uplift, a volcano-capped plateau several thousand kilometers wide that dominates the topography of the planet. Bills and Ferrari (1978) showed that with reasonable assumed values for crustal density, a negative Bouguer gravity anomaly can be mapped over Tharsis (and other volcanic areas). The latest maps from *MGS* (Fig. 2.31) have confirmed and refined early interpretations, providing a spatial resolution of about 178 km (from maps of degree and order 60). The main conclusions by Zuber *et al.* (2000) can be briefly summarized as follows.

The crust of Mars has been estimated to have an average thickness of 50 km, assuming a uniform density of 2900 kg/m^3 (somewhat denser than the average continental crust of the Earth, $2700\text{--}2800 \text{ kg/m}^3$ (Lodders and Fegley, 1998). However, there is a marked thinning from the southern highlands to the northern plains, with the exception of the crust under the Tharsis volcanos, which is estimated to be around 80 km thick. The boundary of the crustal dichotomy between south and north does not in general correspond to the crustal thickness change, and Zuber *et al.* concluded that this implies an essentially tectonic origin (Sleep, 1994) for the northern plains as opposed to an impact origin (Frey and Schultz, 1988). However, there is no agreement on this problem, many subtle impact craters having since been found by Mars Observer Laser Altimeter data (Frey *et al.*, 2000). High-resolution gravity maps (not shown) suggest that the northern plains are underlain by buried outflow channels. This would imply that the unusually flat plains (Smith *et al.*, 1998) are blanketed by a thick sediment layer, supporting views that Mars has had large amounts of water, perhaps even an ocean (Head *et al.*, 2000), at some time in its history.

Mars has several large impact basins, notably Hellas (Fig. 2.31), that display mascons similar to those found under the circular lunar

maria. Zuber *et al.* consider these to have formed by a Moon-like mechanism, post-impact isostatic adjustment followed by infilling.

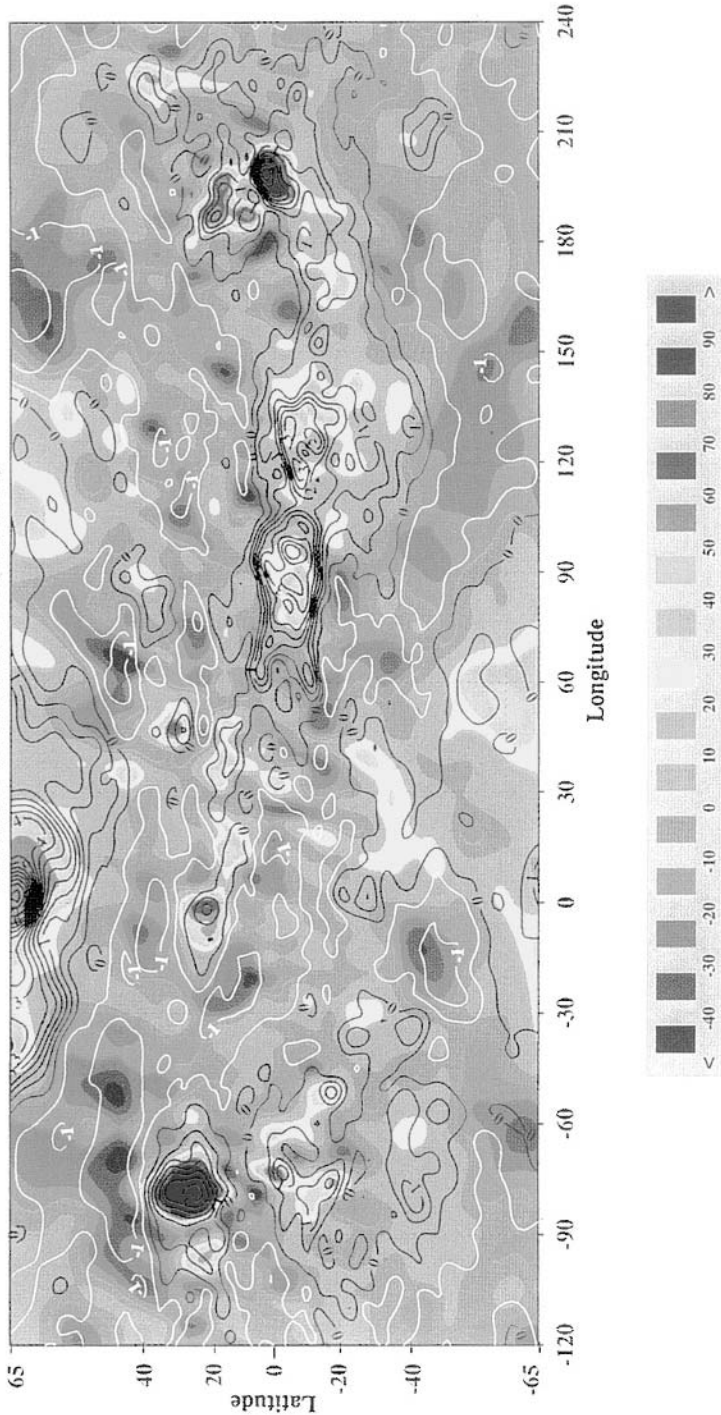
2.10.3 Gravity field of Venus

Because of its thick opaque atmosphere, very little was known about the geology of Venus until radar investigations – from Earth and from orbiting spacecraft – were possible. Since the mid-1980s, two Soviet missions and one American mission have finally given us a good look at the physiography of Venus, as will be discussed in Chapter 6. For the study of its gravity field, the best available data at this writing are Doppler tracking of the *Pioneer Venus Orbiter* (*PVO*) (Bills *et al.*, 1987), which transmitted radar altimetry and other data from orbit for over a decade until it entered the Venus atmosphere in 1993.

Because of its Earth-like size and density, Venus is an unusually valuable comparison planet for geophysical and geological studies. Consequently, much effort has gone into analyses of the *PVO* tracking data and geophysical interpretations. The availability of accurate topographic maps from the *PVO* altimeter, and high-resolution radar imagery from the *Magellan* mission, has made the *PVO* data even more valuable. An important finding from the altimetry is that the gross topography of Venus is unimodal, i.e., most features are at the same elevation relative to a reference spheroid (Masursky *et al.*, 1980). The Earth, in contrast, has bimodal topography, the two peaks corresponding to continents and the ocean floors. Gravity maps similar to those for the Moon and Mars have been compiled from the *PVO* data, complete to degree and order 50 (Fig. 2.32) (Nerem *et al.*, 1993).

The most important characteristic of the Venus gravity anomaly maps is that unlike the Earth, where large (long-wavelength) anomalies show relatively little correlation with topography (Phillips and Malin, 1984), the gravity anomalies of Venus do show such correlation. All the main high regions, such as Aphrodite Terra, are closely mirrored by positive free-air gravity anomalies. This at once raises the question of how these areas are supported, roughly analogous to the same question for the Earth's third harmonic. Given the mass of Venus, its lack of water, and the permanently high surface temperatures, a relatively thin (<20 km) lithosphere is inferred (Phillips and Malin, 1984). Isostatic compensation would have to be very deep, where the mantle has little strength, and isostatic support is thus “implausible” (Bills *et al.*, 1987). The general view (Kiefer *et al.*, 1986; Herrick and Phillips,

The Gravity Field of Venus
Goddard Venus Model-1 (GVM-1)



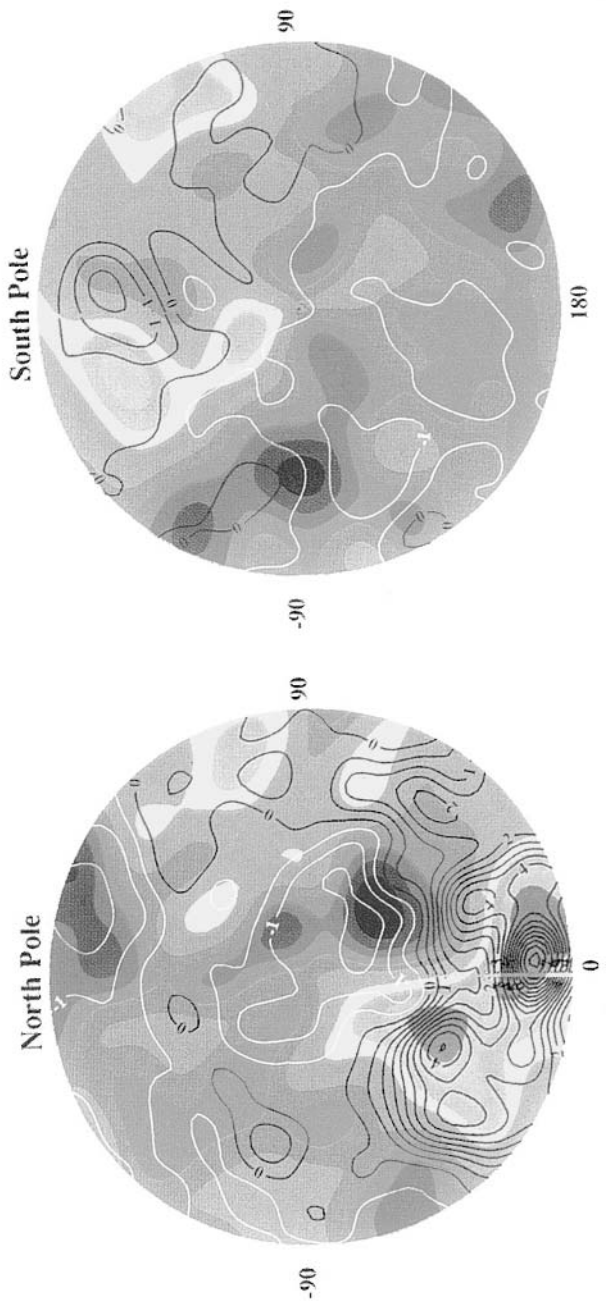


Fig. 2.32 (See also Plate IX) Gravity field of Venus' equatorial and polar segments, in milligals. From Nerem *et al.* (1993).

1992) is that dynamic support is required, i.e., mantle convection. Given the thin lithosphere, mantle convection would be expected to show a much more direct effect on the surface topography and geology than it does in the Earth, where the lithosphere is generally 100 km or more thick under the oceans and much thicker under the continents. Venus thus provides an unusually good planet on which to study the relationship between mantle convection (and mantle plume upwelling) and crustal features. This will be discussed further in Chapter 6, when we have considered the detailed topography of Venus obtained via *Magellan* radar images.

2.11 Summary

Space geodesy uses techniques of a precision and scope that would have seemed almost magical as recently as 1957, when the first artificial satellite was launched. Yet the problems it attacks are largely the same ones of “a world lit only by fire” in Manchester’s (1988) memorable phrase: the shape and size of the Earth; the origin of mountains; the cause of earthquakes. Parmenides, Eratosthenes, and John Harrison are looking over our shoulders as we track satellites and place retroreflectors on the Moon.

CHAPTER 3

Satellite studies of geomagnetism

3.1 Introduction

Geomagnetism is a complex but fascinating topic, one with great importance to the proverbial man in the street as well as to the scientist at the computer terminal or on the outcrop.

The Earth's magnetic field is, to begin, an important part of our shield against cosmic and solar particulate radiation, trapping much of it in the well-known Van Allen belts (Heirtzler, 1999). Magnetic storms, occurring when blasts of solar plasma ("coronal mass ejections") hit the ionosphere, can disrupt communications, confuse radar systems, produce spectacular auroral displays even at low latitudes, and knock out electric power grids. In 1989, such an event disabled the Quebec power grid for 9 hours, leaving some 6 million people in two countries shivering in the dark. Laptop computers carried on low-Earth-orbital Space Shuttle missions occasionally crash because of high-energy cosmic ray particles, especially in the South Atlantic Anomaly where the Van Allen belts are closest to the Earth. The magnetic field is known to reverse itself at intervals, about six times every million years (Lanzerotti *et al.*, 1993), during which its strength drops to a fraction of its present value as the magnetic poles meander around the planet (Jeanloz, 1983). Obviously, life itself survives these reversals, but the possible biological effects of a much-weakened magnetic field have begun to cause some concern. In geology, discoveries in geomagnetism – or to be precise, paleomagnetism – have had enormous effect, reviving the once-discarded theory of continental drift in a new incarnation as plate tectonics. Our ability to infer the orientation of the main magnetic field millions of years ago, though fraught with uncertainties, is finding application to a wide range of local geologic problems as well as global ones.

As we have seen, the main outlines of what is now called "space geodesy" had been anticipated before *Sputnik* and its successors. Developments in the study of geomagnetism from space, in contrast,

were somewhat unexpected, although they too began with the launch of the early satellites. The very first American satellite to reach orbit, *Explorer 1*, discovered the belts of geomagnetically-trapped radiation, soon named the Van Allen belts. Several successive satellites have carried magnetometers, and our knowledge of the Earth's magnetic fields is now far greater than it was before the Space Age. To fully appreciate the unique value of satellite magnetic field measurements, one must understand something of geomagnetism in general. Let us therefore review not only this subject, but a few key aspects of magnetism itself.

Magnetism is expressed as potential fields, which, like gravity fields, obey the inverse-square law. (Field *strength* decreases as the cube of the distance, being proportional to the derivative of the potential.) However, magnetism is fundamentally different from gravity in several important ways. It is in particular a much more dynamic phenomenon than gravity. A gravity field is produced simply by the presence of mass. A magnetic field, in contrast, is produced by a **changing electric field**, or **moving electric charges**. This phenomenon is expressed mathematically by one of Maxwell's equations, as lucidly explained by Pierce (1956). The most commonly encountered moving electric charges are an electric current, such as the flow of electrons in a wire. Electromagnets are familiar examples of this phenomenon, which may raise the question: What causes permanent magnetization? The answer is that, in a sense, *all* magnets are fundamentally electromagnets, generated by the orbital and spin motion of electrons. In ferromagnetism, the most familiar kind, the individual atoms have magnetic moments that interact strongly. A good intermediate-level discussion of this topic is provided by Butler (1992), who warns that a rigorous understanding of ferromagnetism requires "several years of mind-bending study."

This over-simplified explanation leads at once to the question of why all iron isn't magnetic. The answer is that the magnetism of an iron magnet arises from alignment of magnetic dipoles in "domains," small regions of the magnet with about 10^{18} molecules. Such alignment always exists, but can be altered by the influence of another magnetic field, i.e., by magnetic induction. In ferromagnetism, the induction path is not reversible, following a hysteresis curve. This means that when the magnetizing field is removed, the magnetization of the material does not return to zero, but retains a record of the applied field (Butler, 1992). The common analog tape recorder passes the gamma-iron oxide-bearing tape through a fluctuating magnetic field, producing corresponding fluctuations in the domains on the tape. Computer disks use the same basic phenom-

enon for digitized information, forming sequences of magnetization with opposite polarities.

Rocks in the Earth's crust may have magnetization impressed on them by the main field. There are two general classes of rock magnetism (Verhoogen, 1969): induced and remanent (or residual) magnetism. Induced magnetism is that produced instantaneously by an external field, and having the same orientation as that field even when the field is turned off. Remanent magnetism, as the term is used in geophysics, is the residual magnetism left in a rock when it crystallizes from a magma, or when it is recrystallized or cools in a magnetic field. The field referred to here is that of the Earth, but remanent magnetism has been found in lunar rocks (Hood *et al.*, 1981; Lin *et al.*, 1998), on Mars, and even in meteorites (Stacey, 1976). These surprising findings will be discussed later. Viscous remanent magnetism is that which increases during the time magnetism is applied, losing it at about the same rate when the impressed magnetic field is removed.

A few more elementary principles should be briefly reviewed, in particular the relation between electric currents and magnetism. Strange as it may seem, as late as 1800 a science text by Thomas Young could say that "there is no reason to imagine any immediate connection between magnetism and electricity" (Ratcliffe, 1951). But within a few years, the work of Oersted, Ampère, and Faraday showed that although electrostatic fields can exist without magnetism, electricity and magnetism are intimately interrelated. An authoritative review (Lanzerotti *et al.*, 1993) of the Earth's magnetic field in fact bears the title "Geoelectromagnetism".

Electric currents can be produced several ways, as in the chemical reactions of a battery or the discharge of a capacitor in an electronic flash. The mechanism that must be understood if one is to appreciate the nature of geomagnetism is *electromagnetic induction*, the production of electric currents by moving magnetic fields. Put most simply, an induced current is produced by movement of a magnetic field in relation to an electrical conductor, such as a wire. (It doesn't matter which is moving; that is, there is no such thing as absolute motion. This superficially obvious observation was in part the basis for Einstein's (1905) theory of special relativity.) In a transformer, magnetic lines of force from the primary coil move through the secondary coil as the current in the primary reverses, which incidentally is why transformers work only on alternating current. In a generator, wires in the rotating armature cut across magnetic lines of force of a stationary field. Things start getting complicated at this point, for the currents generated either way in turn generate magnetic fields themselves.

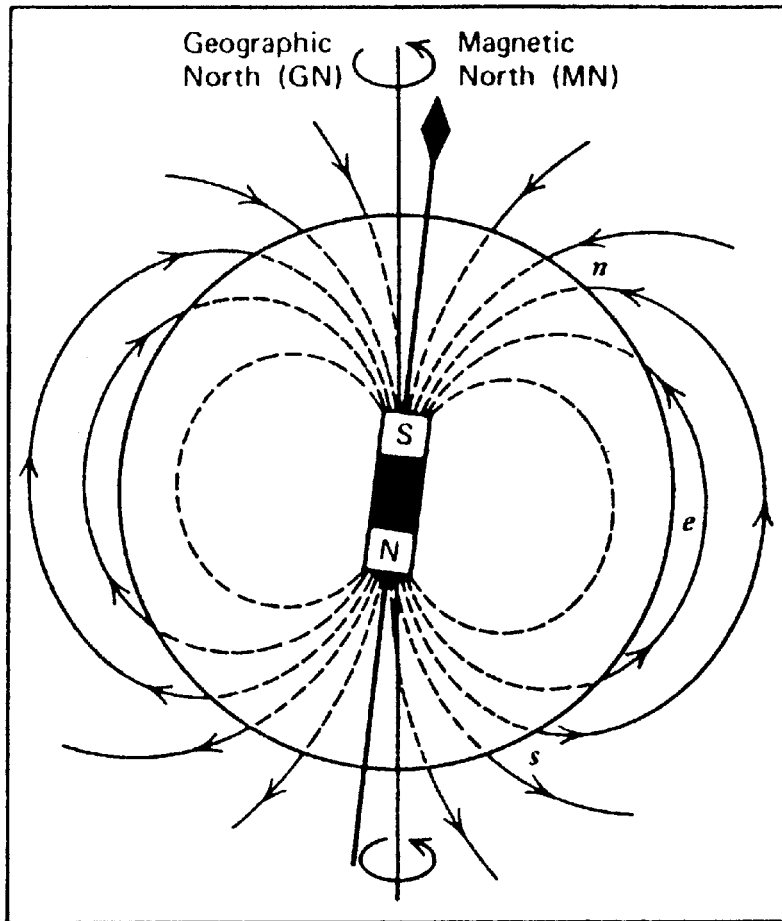


Fig. 3.1 Diagrammatic representation of the Earth's main field, which is analogous to that of a large bar magnet in the interior. Note orientation of field lines; roughly horizontal near magnetic equator and vertical near magnetic poles. From Wyllie (1976).

This elementary review may help the reader to appreciate the extraordinarily complex and dynamic nature of the Earth's magnetism. The general form of the main field, and the Earth's internal structure, are shown in Figs. 3.1 and 3.2. The magnetic field measured at any one point on or near the Earth's surface is the resultant of the main (core), crustal, and external magnetic fields (Cain, 1975; Langel, 1982, 1985, 1993). The external fields are those produced by currents outside the Earth, in the magnetosphere or ionosphere; useful reviews of this topic are those by Stern (1989), Van Allen (1991), and Russell (1991). The crustal fields detectable from orbit are those formed in magnetized materials (such as magnetite) in the

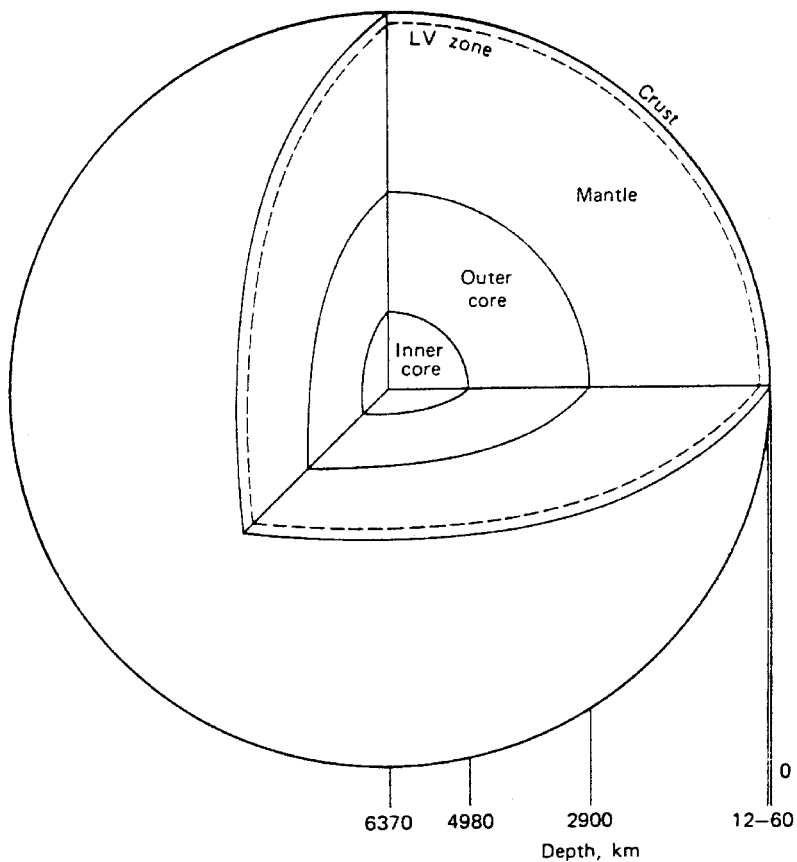


Fig. 3.2 Main division of Earth's internal structure. Outer core is deduced to be liquid from non-transmission of seismic shear waves. "LV" zone is a thin zone of low shear strength in upper mantle, found from low seismic velocities under ocean basins and tectonically-active continental areas. From Wyllie (1976).

crust roughly down to the Mohorovičić discontinuity. The Moho (crust–mantle boundary) appears to be a magnetic as well as a lithologic boundary (Wasilewski *et al.*, 1979) although it has been argued (Haggerty and Toft, 1985) that there are magnetic materials in the upper mantle as well. Both external and crustal fields are relatively weak, not more than a few thousand nanoteslas (nT) and generally much less. The main field is far stronger, typically 30,000–70,000 nT at the surface, depending on geomagnetic latitude.

The origin of the Earth's main field was called one of the great problems of physics by Einstein many years ago, although its general nature had been known since publication of Gilbert's *De Magnete* in 1600. The gross behaviour of the field, as summarized

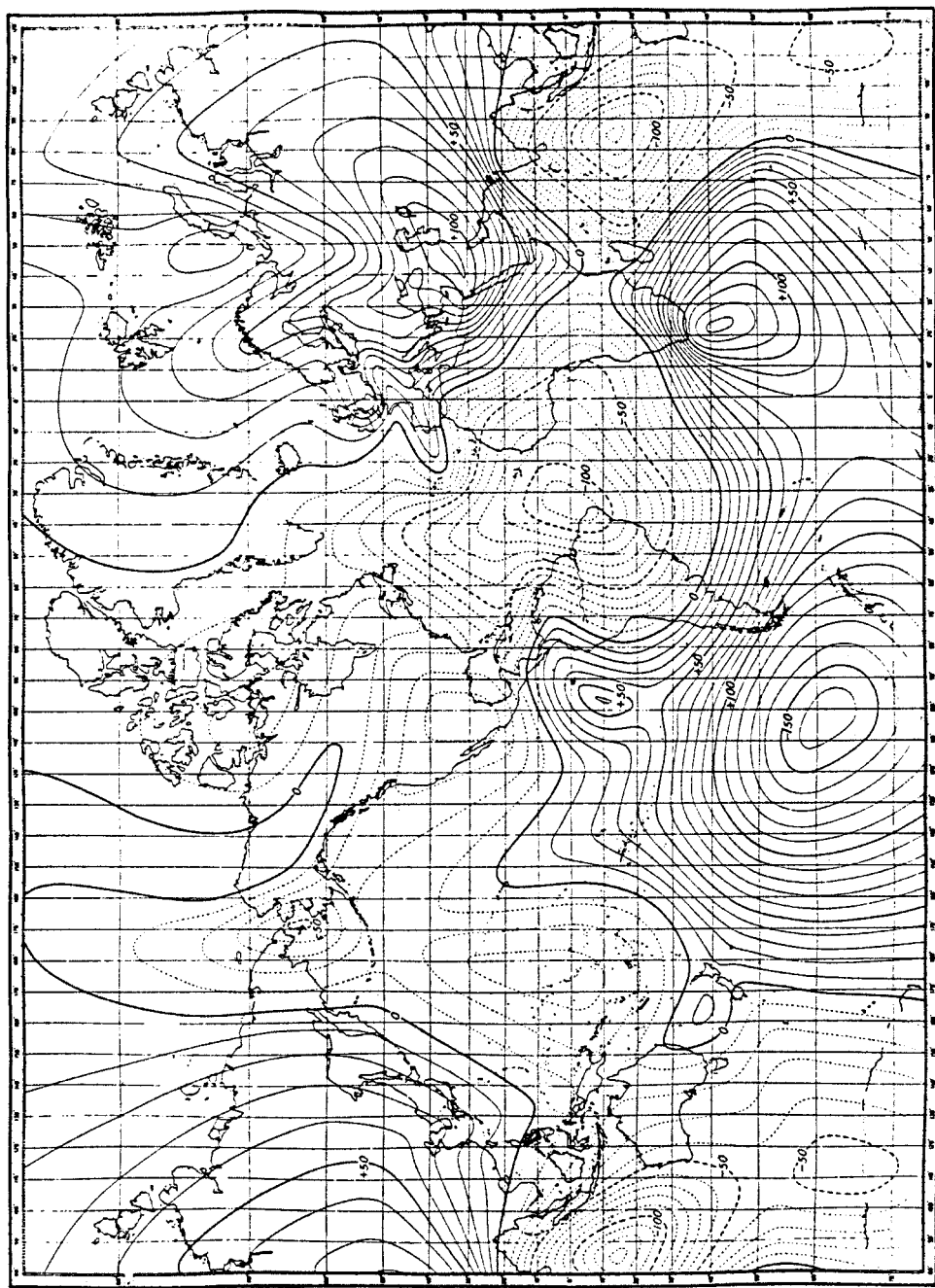


Fig. 3.3 Rate of change of the vertical component (Z) of the main field, in nT per year, for 1942. From Vestine *et al.* (1947).
Compare with Fig. 3.5.

by Bullard (1954), gives us some indication of where and how it is generated. The most important aspect of this behaviour is the field's secular variation, i.e., its changes in strength and orientation on a time-scale of months to centuries. The map in Fig. 3.3, from Vestine *et al.* (1947), shows these changes for only one year. As commented by Bullard (1954), such maps superficially resemble weather maps. Collectively, the main field's behaviour clearly points to an origin related in some way to fluid motion deep in the Earth. At this point, seismology comes to our aid, for the general structure of the deep interior has been inferred from the propagation of seismic waves. As shown in Fig. 3.2, the core of the Earth has a liquid outer part and a solid inner part. The bulk density of the Earth, and the cosmic abundance of elements, among other things, point convincingly to iron as the main constituent of the core, probably alloyed with nickel and containing an unknown fraction of lighter elements such as sulfur, oxygen, and potassium (Jacobs, 1992).

It was originally thought in the 17th century that the interior of the Earth might act as a giant permanent magnet, but temperatures in the core and mantle are far too high for that, to say nothing of the dynamic behaviour of the main field. The generally-accepted theory today for the origin of the main field stems from a concept proposed by Larmor in 1919 to explain the origin of the Sun's magnetic fields. As applied to the Earth by Elsasser and by Bullard, this can be termed the "self-exciting dynamo" theory. A good contemporary discussion of this theory has been published by Jacobs (1992); the reader may find it helpful to consult a text on elementary electricity such as that by Marcus (1968). The mechanism is roughly this.

The liquid iron of the outer core, cutting across a weak initial magnetic field – perhaps the interplanetary field – would generate electrical currents in the core. These electrical currents in turn produce a magnetic field which, being crossed by the molten iron, produces a still stronger current, and thus a stronger field, until a steady value is reached. This scheme, in which the field regenerates itself, may sound like perpetual motion, but thermal energy is generated in the system by some mechanism(s) – perhaps radioactivity and latent heat from solidification of the inner core – to keep the iron moving. This theory accounts in a general way for the dynamic behaviour of the main field discussed previously, such as the slow movement of the magnetic poles and the subsequent variation of magnetic declination from year to year.

It is well known that the Earth has a north and a south magnetic pole, and the main field is generally described as a dipole. However,

Table 3.1 *Magnetometer-carrying satellites and spacecraft in Earth orbit, 1958–1980. From Langel (1987).*

Satellite	Inclination	Altitude range (km)	Dates	Instrument	Approximate accuracy (nT)	Coverage
Sputnik 3	65°	226–1881	5/58–6/58	Fluxgates	100	USSR
Vanguard 3	33°	510–3750	9/59–12/59	Proton	10	Near ground station
1963–38C	Polar	1100	9/63–1/74	Fluxgate	30–55	Near ground station
Cosmos 26	49°	270–403	3/64	Proton	Unknown	Whole orbit
Cosmos 49	50°	261–488	10/64–11/64	Proton	22	Whole orbit
1964–83C	90°	1040–1089	12/64–6/65	Rubidium	22	Near ground station
OGO-2	87°	413–1510	10/65–9/67	Rubidium	6	Whole orbit
OGO-4	86°	412–908	7/67–11/69	Rubidium	6	Whole orbit
OGO-6	82°	397–1098	6/69–7/71	Rubidium	6	Whole orbit
Cosmos 321	72°	270–403	1/70–3/70	Cesium	Unknown	Whole orbit
Azur	103°	384–3145	11/69–6/70	Fluxgate (2-axis)	Unknown	Near ground station
Triad	Polar	750–832	9/72–present	Fluxgate	Unknown	Near ground station
S3-2	97°	230–900	10/72–present	Fluxgate	300λ (components)	Whole orbit
Magsat	97°	325–550	11/79–5/80	Fluxgate and Cesium	6 3	Whole orbit

this applies only to the field as it is measured at the surface, and is an approximation even there (Sugiura and Heppner, 1968). The field in the core itself is much more irregular (Jacobs, 1992), and the main field at the surface may not have been dipolar through geologic time.

3.2 Satellite investigations of the Earth's magnetic field

It will be apparent, from the above generalized discussion, that the Earth's magnetic "field" is actually a composite of many fields that are continually changing in magnitude and direction, changes that must be taken account of even on an hourly basis for geophysical surveys. When it became possible to put magnetometers in artificial satellites a new era in the study of geomagnetism began (Table 3.1). Orbital measurements made it possible to monitor the Earth's field globally, frequently, and with identical instruments at similar altitudes.

Systematic magnetic measurements began with *Vanguard 3* and *Sputnik 3*, which produced scalar (non-directional) data useful chiefly for the study of external fields. Later satellites, in particular *Cosmos 49*, the *Polar Orbiting Geophysical Observatories (POGO)*, and especially *Magsat* produced far better data on the main and external fields. A remarkable achievement (Zietz *et al.*, 1970; Regan *et al.*, 1975) was the extraction of extremely weak crustal anomalies from the main field, a feat analogous to photographing the stars by day. Further analyses (Langel, 1990a,b) produced more comprehensive and detailed maps from the *POGO 2, 4, and 6* data which, although obtained from high altitude, covered several years and all local times. One of these maps has already been presented in Fig. 1.6. The achievement of Regan and his colleagues led to development of *Magsat*, the first such satellite flown (in 1979) primarily for study of the main and crustal fields rather than the external ones.

Magsat was an unusually successful project in several aspects, including an on-time and within budget launch (Langel, 1982). Every proposal to NASA for a *Magsat* follow-on mission has to date been rejected. Fortunately, the European Space Agency's (ESA's) *Oersted* satellite has now picked up the torch, and has already produced an initial field model (Olsen *et al.*, 2000). *Magsat* results fill two dedicated issues of *Geophysics Research Letters* (9, No. 4, 1982) and the *Journal of Geophysical Research* (90, B3, 1985), which alone gives some idea of its success. The major achievements related to the solid earth are summarized in the following two sections.

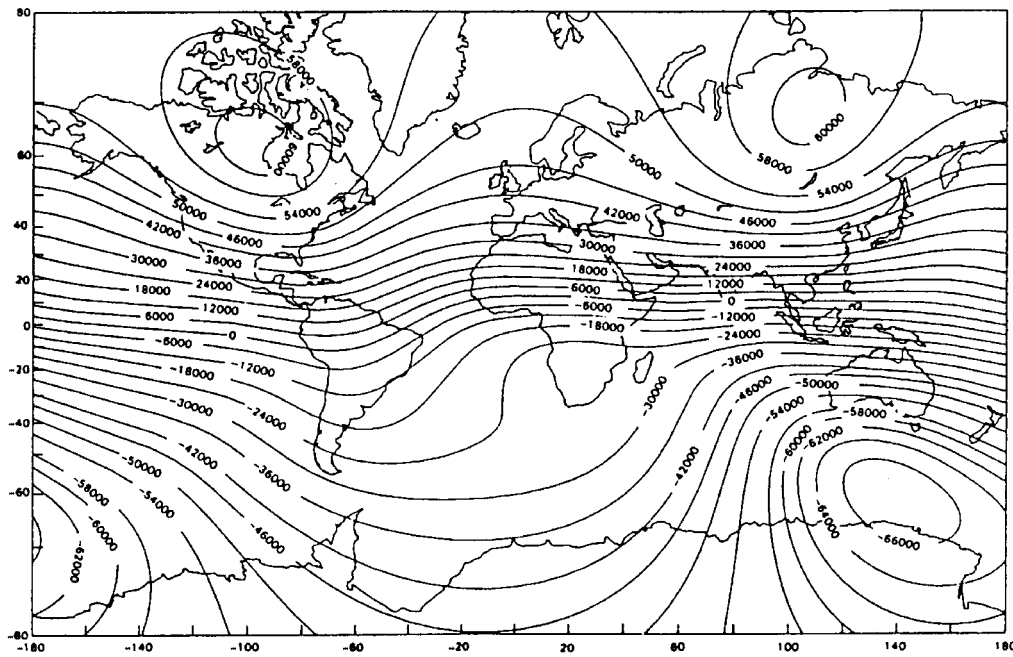


Fig. 3.4 World contour map, based on *Magsat* data, of the vertical component (Z) of the main field, in nT, for 1980. From Langel (1987). Note lack of relationship between crustal features (oceans, continents) and main field, because the latter's origin is in core.

3.3 The main field

Magsat carried both scalar and vector magnetometers (Langel *et al.*, 1982), thus permitting construction of the first global vector (as well as scalar) model (Fig. 3.4) of the core field, while accurately measuring the external fields as well. It shows that the main field has no relationship to crustal features, even to continents and ocean basins, because of its origin in the core. A comprehensive and accurate main-field model is vitally important for a variety of reasons. Aeromagnetic surveys for petroleum or mineral deposits must have a reference field to take out regional gradients, as well as a record of magnetic activity for a particular time. The review by Hood *et al.* (1985), though focussed on aeromagnetic maps, gives a good overview of how such maps are produced. Maps must have up-to-date corrections for changing declination; even with modern navigational methods, the magnetic compass is still a major navigational tool for ships, aircraft, and ground surveys. Scientific studies of the sort to be described below similarly require good reference fields. A World

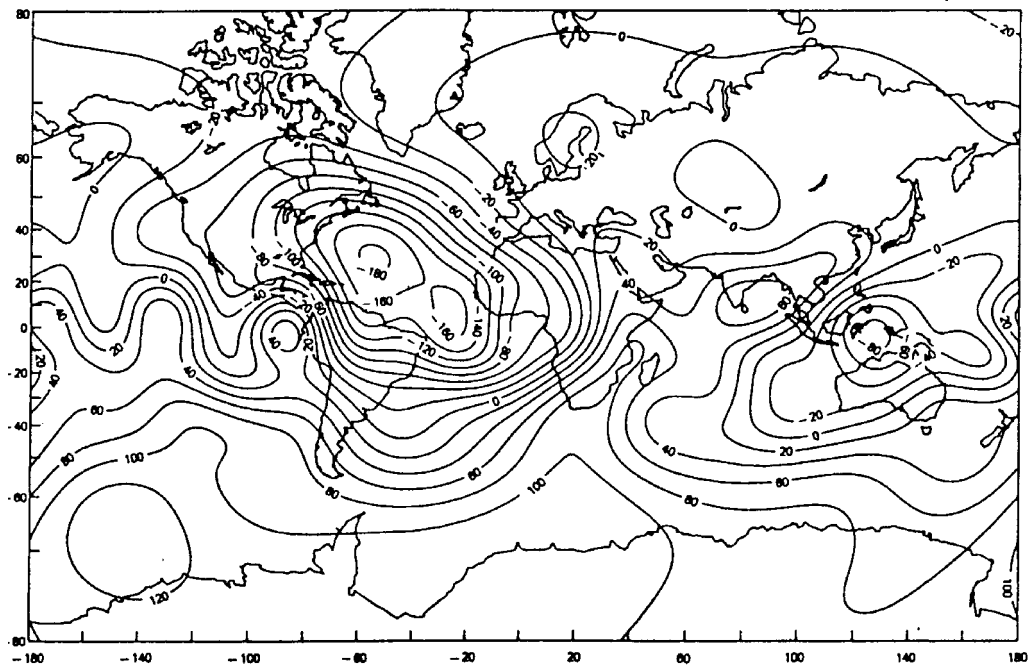


Fig. 3.5 World contour map, based on *Magsat* data, of the rate of change of the vertical component (Z) of the main field, in nT per year, for 1980. From Langel (1987). Compare with Figs. 3.3 and 3.4.

Magnetic Survey was proposed in 1954 by S. K. Runcorn (Langel, 1987) to the International Union of Geodesy and Geophysics to approach some of the needs for a reference field listed above.

An International Geomagnetic Reference Field (IGRF) for the 1955–1972 period was first adopted in 1968 (Langel, 1992). A second IGRF was adopted in 1975. However, it became increasingly outdated. The launch and operation for several months, in 1979–80, of *Magsat* permitted compilation of a third field, IGRF 1980, based mainly on data from *Magsat*. IGRF 1980 was a major improvement on previous fields, in accuracy and coverage, although even it was shortly improved.

Although *Magsat* operated for only seven months before re-entering the atmosphere, it permitted compilation of global maps showing not only the main-field components but also their rate of change in nT/year (Fig. 3.5).

New knowledge of the main field has been applied to a number of scientific problems. Voorhies and Benton (1982) used *Magsat* models to estimate the radius of the Earth's outer core, finding a

value agreeing within 2% of that determined from seismic data. They also confirmed that the core is an electrical conductor and the mantle, in general, an insulator, a customary but unverified assumption. Other studies used field models to study fluid motion in the outer core, structure at the core–mantle boundary (Bloxham and Jackson, 1992), and similar problems of core structure and behavior (Langel, 1985). The greatly improved model of crustal magnetism is useful for studies of the main field in that crustal anomalies are essentially noise in main-field measurements.

The importance of satellite data should not be exaggerated. The contributions of fixed ground observatories, of historical studies, and of surface surveys are still the backbone of geomagnetic research. Bloxham (1992), for example, used surface measurements made as far back as 1690 to study the secular variation of the main field, and to map flow at the core–mantle boundary. Nevertheless, even the few adequate orbital surveys made to date have provided a solid global background for other studies.

3.4 The crustal field

The crustal anomaly field has been studied locally with surface, aeromagnetic, and marine methods for many years. Development of modern magnetometers for submarine detection during World War II (Bates *et al.*, 1982) led to great progress in aeromagnetic surveys, which have been extensively used for mineral and hydrocarbon searches since then. One of the problems with using aeromagnetic surveys for regional or continental studies is the difficulty of tying together local surveys, often carried out years apart and at different altitudes. In addition, there are enormous areas of land and sea over which adequate conventional surveys are difficult or impossible. The contribution of satellite-derived crustal anomaly maps has been, first, to provide truly global coverage, and second, to provide coverage with similar altitudes and instruments. In addition, the speed of orbital surveys makes it possible to allow for time variations in the field. The main disadvantage of orbital magnetic data is their relatively coarse spatial resolution, generally several hundred kilometers. Since magnetic field strength follows an inverse cube law, magnetic anomalies decrease rapidly with altitude, and it was thus a major achievement simply to detect crustal anomalies from space. Most of the continental anomalies were thought to result largely from induced rather than remanent magnetism, although the marine anomalies may be dominantly remanent. The discovery of what are probably remanent magnetic anomalies on Mars, to be discussed in

Section 3.5, indicates that terrestrial anomalies are largely remanent (Purucker *et al.*, 2000), not induced – a striking example of comparative planetary geophysics.

Dozen of papers presenting and interpreting satellite magnetic maps have been published, the vast majority based on *Magsat* data because of its spatial resolution and the fact that these data are vector as well as scalar. *Magsat* and *POGO* data have been combined by Arkani-Hamed *et al.* (1994) to produce a new crustal anomaly map (Fig. 3.6). General reviews of satellite magnetic anomaly studies have been presented by Mayhew *et al.* (1985) and Schnetzler (1989). The definitive treatment of this subject is that of Langel and Hinze (1998).

The first feature to be identified in satellite magnetic data was the large east–west-trending anomaly over central Africa (Fig. 3.6), since termed the Bangui anomaly (Regan and Marsh, 1982). Apart from its historic significance, the investigation of the Bangui anomaly illustrates the peculiarities of satellite data, the methods of investigating them, and their geological interpretation. Accordingly, we shall discuss the work of Regan and Marsh in some detail.

The first satellite data studied were those from the *POGO* series, which produced measurements from various altitudes over many months cumulative time. The first step in extracting crustal anomalies from these measurements was selection of those acquired from low altitudes during magnetically quiet periods. An immediate problem faced by investigators working with low-latitude data is allowing for the equatorial electrojet; for a recent treatment of this phenomenon, see Cohen and Achache (1990). After intensive mathematical analysis, it was possible to delineate a broad east-trending magnetic low with a maximum amplitude of 12 nT (contrasted with the main-field strength in that area of 30,000 nT).

Previously acquired gravity surveys in the area showed a Bouguer anomaly partly coinciding with the magnetic anomaly, further confirming its reality and general outline. The geologic field reconnaissance carried out by Regan and Marsh, in combination with published geologic maps, showed that although magnetic iron formations occur in the area, they are insufficient to cause the satellite anomaly. They made the important observation that the anomaly is caused by a rock type not exposed on the surface (Fig. 3.7). This, and the broad extent of the anomaly, point clearly to an origin in the lower continental crust, probably a large dense mafic intrusion.

As first demonstrated by the Bangui investigation, the most general discoveries from continental anomalies concern the structure and

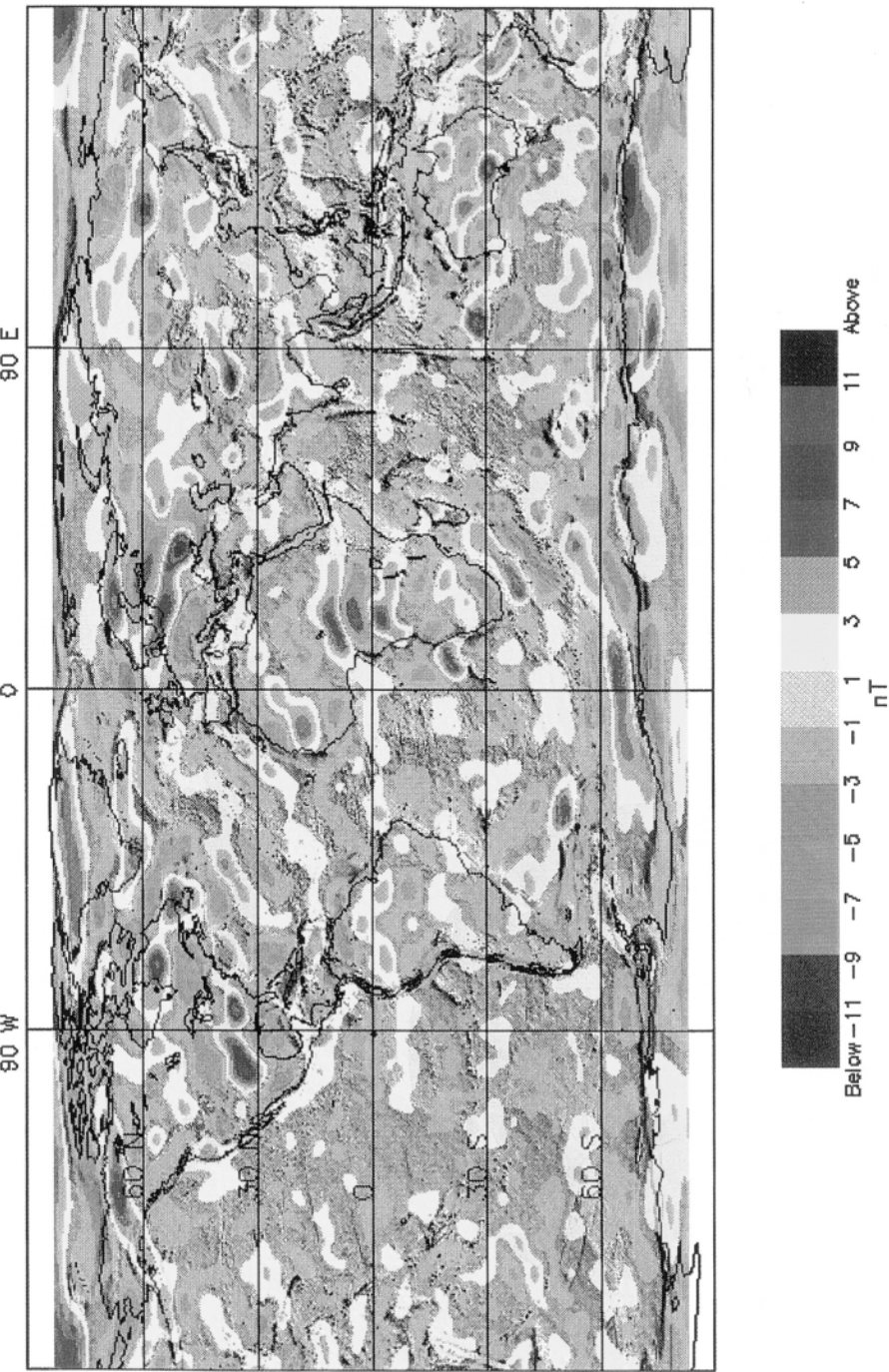


Fig. 3.6 (See also Plate X) World scalar map of crustal magnetic anomalies, from *MagSat* and *POGO* data. From Arkani-Hamed *et al.* (1994).

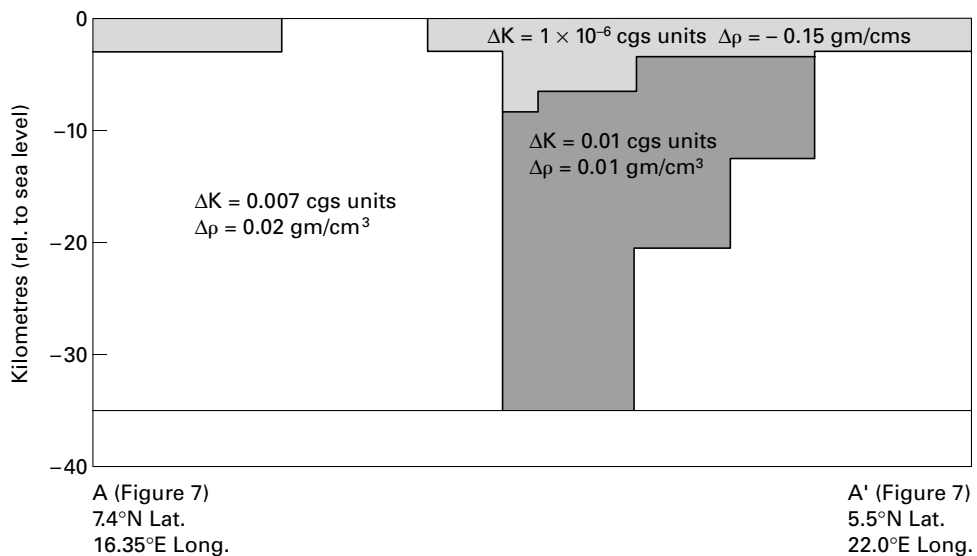


Fig. 3.7 Crustal model proposed by Regan and Marsh (1982) to account for magnetic and gravity anomalies shown in previous maps.

composition of the deep continental crust (Fig. 3.8) (Schnetzler, 1985). The lower crust, exposed in very few places, has until recently been poorly understood. Studies of crustal anomalies, coordinated with laboratory and field investigations of rock magnetism, have strongly supported the view that the lower continental crust is more mafic (iron- and magnesium-rich) and more highly metamorphosed (granulite grade) than the exposed upper crust (Wasilewski and Fountain, 1982; Coles, 1985; Schnetzler, 1985). Such interpretations, added to new knowledge of the lower continental crust from seismic reflection profiling and other sources, is rapidly opening up this important part of the lithosphere. This will be discussed further in Section 3.6.

A related finding from satellite magnetic data is that a number of large anomalies are the expression of intrusions of mafic rock possibly related to rifts, in the lower crust. Such interpretations have been made of anomalies over the Mississippi Embayment (Thomas, 1984), and Kentucky (Mayhew *et al.*, 1982). The significance of these findings is becoming more apparent in the light of recent studies of crustal evolution, indicating that much of the mantle differentiation since the Archean has involved separation of basalt from the mantle, with subsequent underplating of the continental crust. This will be discussed in Chapter 6. An interesting possibility suggested by Girdler *et al.* (1992) is that some *Magsat* anomalies, in particular the Bangui anomaly, may mark large Precambrian impact structures, or impact-triggered mafic intrusions.

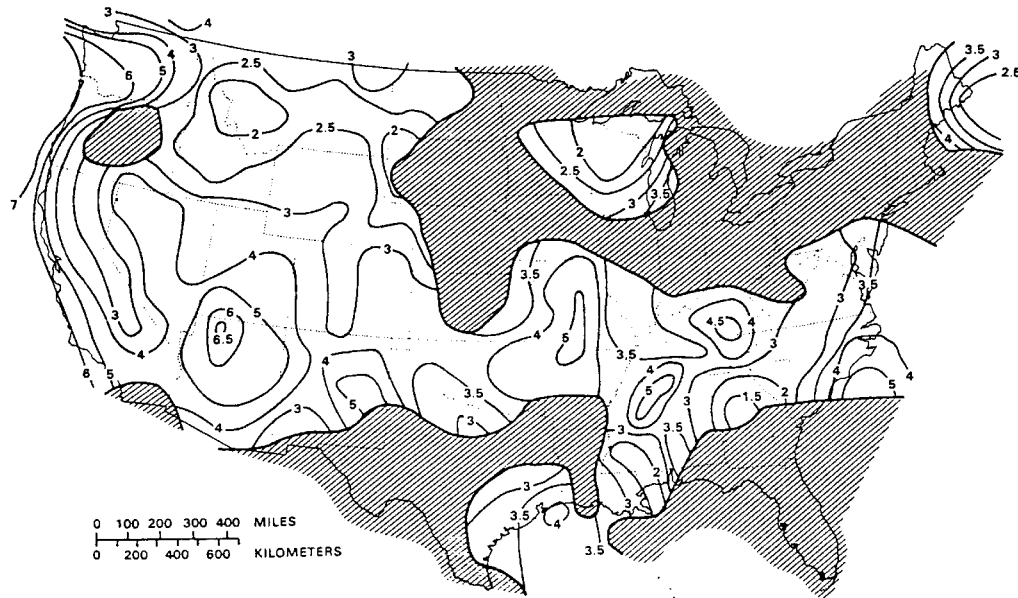


Fig. 3.8 Magnetization in the lower crust, as determined from seismic data, based on *Magsat*-derived anomaly field; units amperes per meter. Shaded areas are more than 225 km deep from measurement of either the Moho or Conrad discontinuities. From Schnetzler (1985).

The *Magsat* crustal anomaly maps have been compared with global and regional tectonic structure by several investigators. Mayhew and Galliher (1982) produced maps from *Magsat* data whose main features (Fig. 3.9) express the physiographic or tectonic provinces of the coterminous US surprisingly well. The Basin and Range Province, for example, is distinct from the Interior Plateaus. The Gulf of California, generally agreed to represent incipient ocean basin formation, also shows up distinctly. Frey (1982) found that many aulacogens (failed rifts) in central Asia had magnetic expression even on the scalar anomaly maps, as did several other major structures. Hinze *et al.* (1982) made similar interpretations for South America (Fig. 3.10). An interesting feature of the Hinze *et al.* map is that the continental margins show little expression in the scalar anomaly values at 350 km altitude. Given the great contrast in composition, one would expect this crustal boundary to be conspicuous. Newer studies (see Fig. 3.21) (Purucker *et al.*, 1998), incorporating crustal thickness and susceptibility values, have delineated the boundary.

Hall *et al.* (1985) studied *Magsat* data from several passes over the boundary between the Churchill and Superior Provinces of the

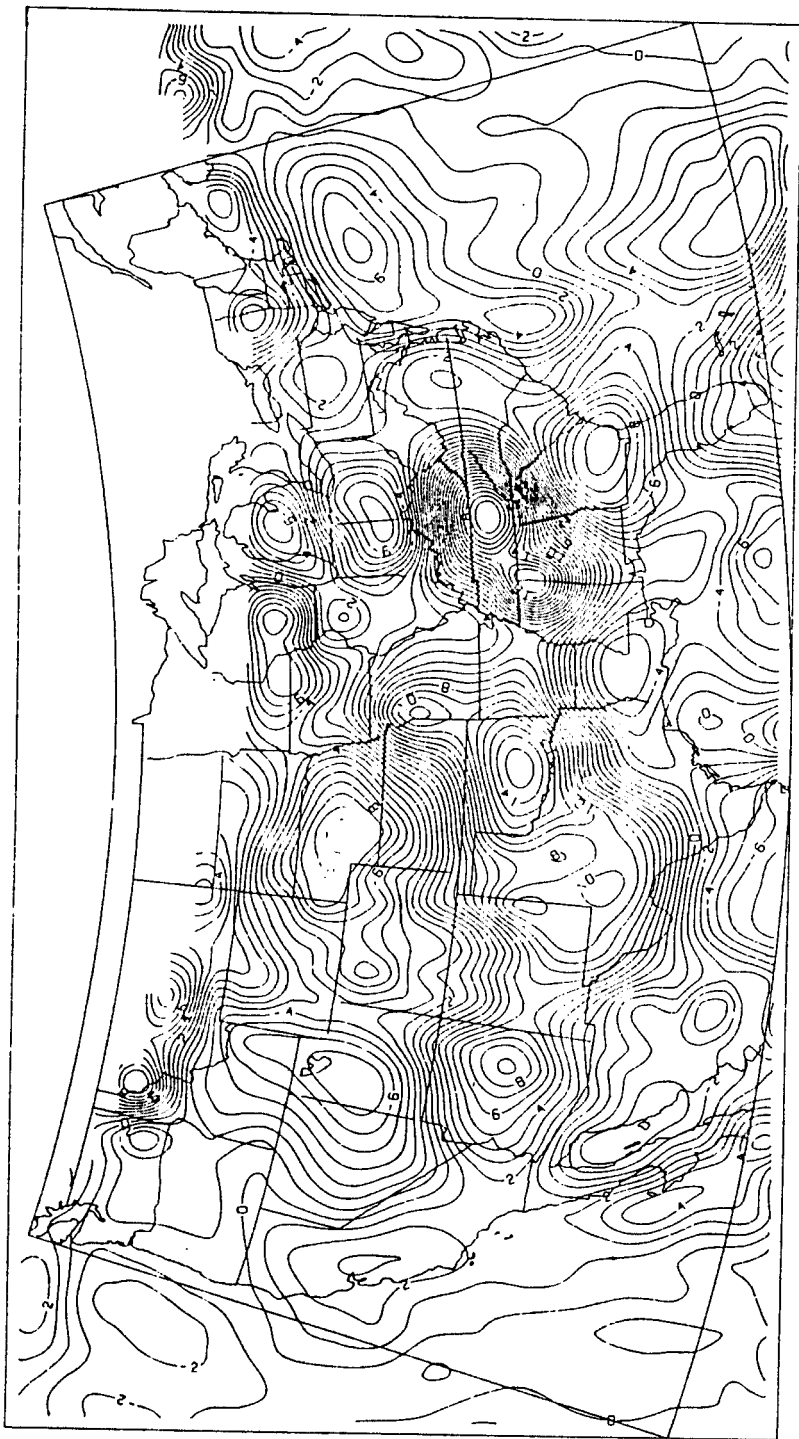
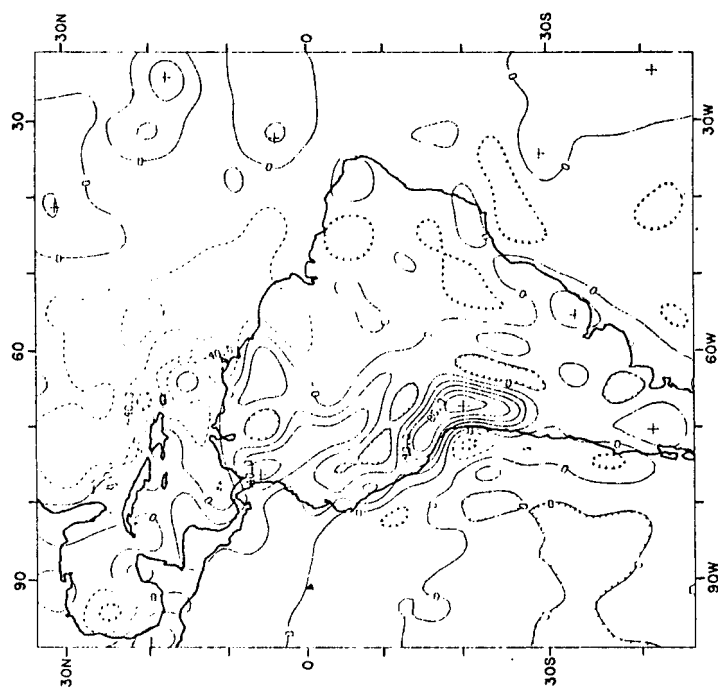
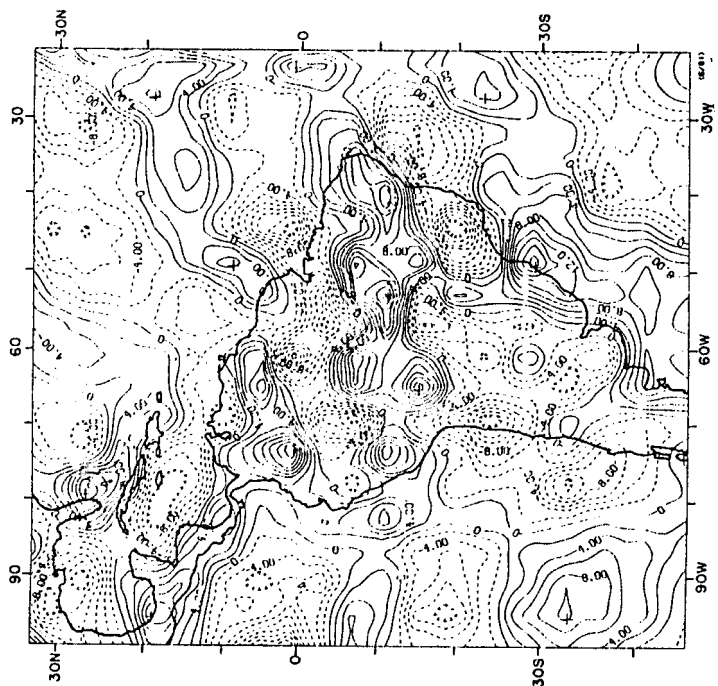


Fig. 3.9 Magnetic anomaly map based on *Magsat* data, showing field produced by magnetic dipoles spaced 136 km apart at 320 km altitude (equivalent source representation). Contour interval 1 nT. From Mayhew and Galliher (1982).

(b)



(a)



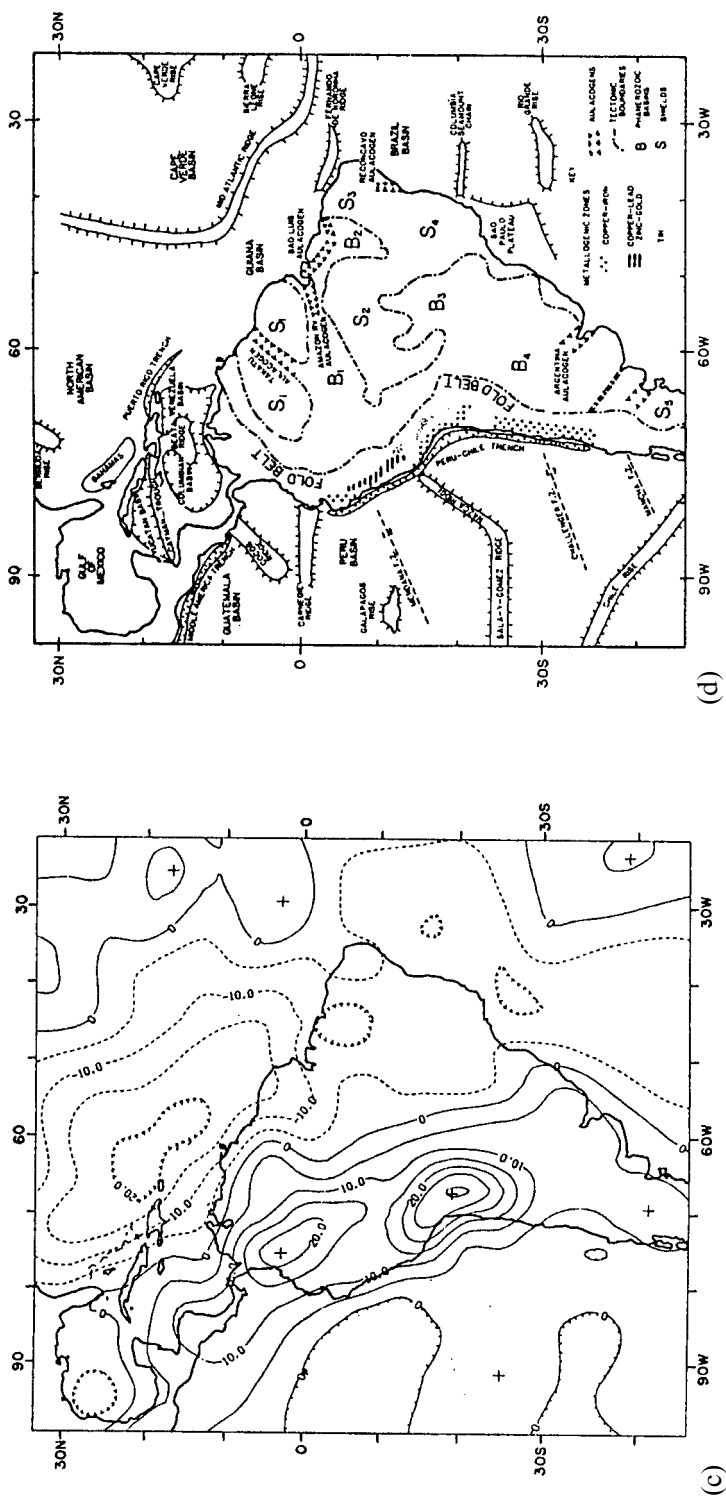


Fig. 3.10 (a) South American crustal anomaly field, based on *Magsat* data, showing equivalent point source scalar field at 350 km altitude. Contour interval 2 nT. (b) South American surface free-air gravity anomaly field, long-wavelength-pass filtered. Contour interval 20 milligals. (c) South American free-air gravity anomaly field, upward continued to *Magsat* altitude (350 km). Contour interval 5 milligals. (d) Generalized tectonic features. S1: Guiana Shield; S2: Central Brazilian Shield; S3: Sao Luiz Craton; S4: Sao Francisco Craton; B1: Patagonia Platform; B2: Amazon River Basin; B3: Parana Basin; B4: Chaco Basin. All from Hinze *et al.* 1115 (1982). Lambert conformal projection.

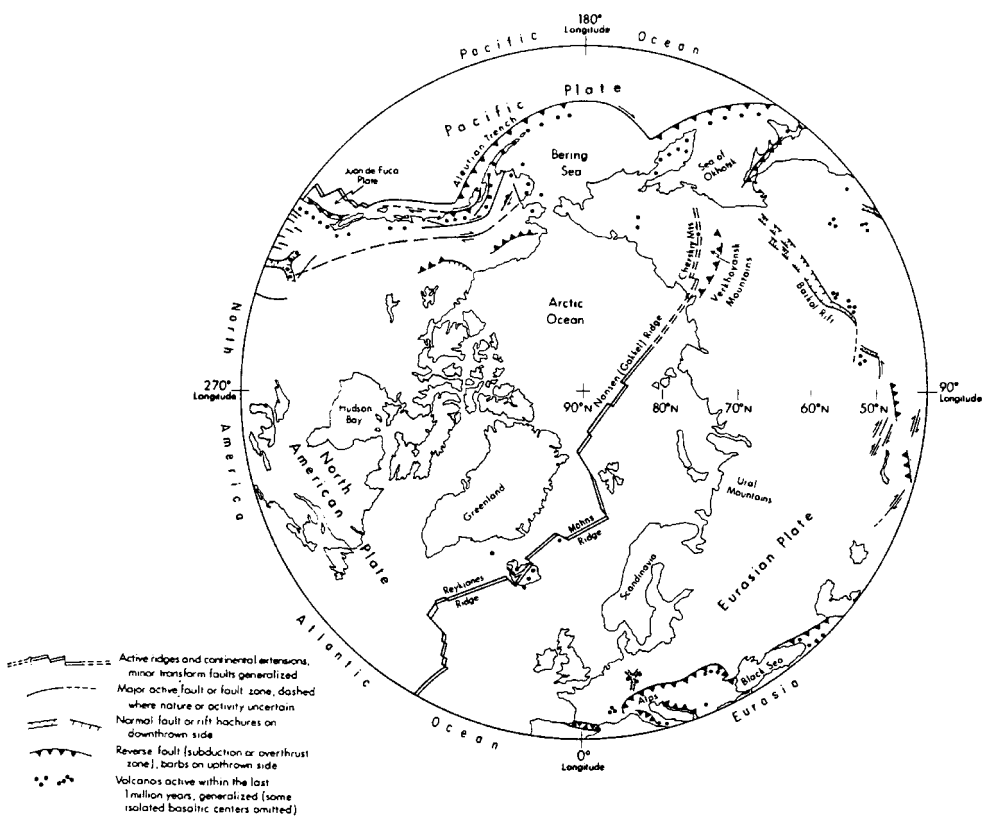


Fig. 3.11 Tectonically and volcanically active (within the last one million years) features of the Arctic Regions, north of 40th parallel. From Lowman (1984). Orthographic projection.

Canadian Shield, or Nelson Front, hypothesized to be a suture formed by terrane accretion (Gibb and Thomas, 1976). They found a definite magnetic signature over the boundary that was compatible with models derived from seismic data, thus providing an example possibly applicable to supposed sutures on other shields. Since terrane accretion is thought by many to be the major mechanism for formation of the continents, this local study is more significant than it might appear. (Field investigations along the Nelson Front later showed the suture concept to be incorrect, the magnetic anomaly noted by Gibb and Thomas resulting from interbedded serpentinites, not ophiolites (Lowman *et al.*, 1987).)

Improvements in analytical methods for *Magsat* in the decade after the satellite was launched are illustrated by the study by Ravat *et al.* (1993) who studied tectonic structures of Europe. They found a wide variety of features expressed in the *Magsat* data, including

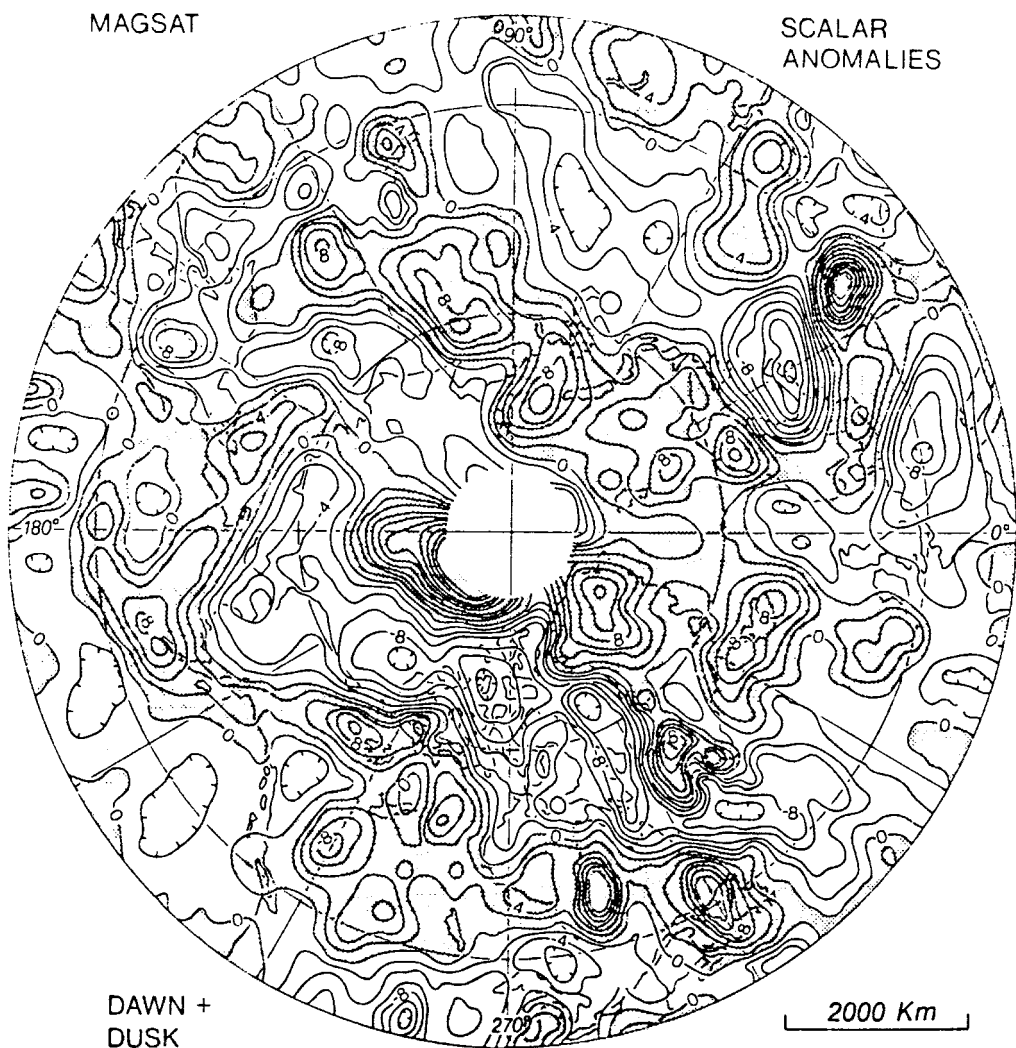


Fig. 3.12 Map of scalar magnetic anomalies, from *Magsat* data, of Arctic Regions. Average altitude 415 km; average of dawn and dusk passes. Contour interval 2 nT. From Coles (1985).

geologic provinces, regions of high heat flow and thin crust, the Kursk and Kiruna iron deposits, and others. The Ravat *et al.* study is a notable demonstration of the wide range of crustal features that can affect the magnetic field measured at satellite altitudes, and the great amount of information needed for a valid interpretation.

A comprehensive *Magsat* investigation of northern hemisphere high-latitude anomalies was carried out by Coles (1985) (Figs. 3.11, 3.12). On the one hand, these areas are inherently hard to study

magnetically because of the high intensity and rapid variability of the main field near the magnetic poles. On the other hand, the nature of the *Magsat* orbit helps compensate for these problems by crossing over any given area many more times than at low latitudes. As shown in Fig. 3.11, many of the scalar anomalies around the Arctic Ocean correspond to tectonically active features such as subduction zones and spreading centers. The large anomaly in Canada, just east of Hudson Bay, is a good example of the distinctive magnetic signatures of high-grade metamorphic terrains. This area is part of the Superior Province, in which lower-crust granulites are exposed over large regions.

An interesting study of a tectonically important area was carried out by Langel and Thorning (1982). The Nares Strait region, between Greenland and Ellesmere Island, Canada (Fig. 3.11), must be an area of major horizontal displacement if Greenland has drifted away from North America as the result of sea-floor spreading in Baffin Bay. However, a number of geologic markers appear not to be offset in the Strait (Kerr, 1982; Lowman, 1985). Langel and Thorning found that the magnetic contours from the *POGO* satellite data paralleled the Innuitian fold belt, and the Strait, suggesting that this feature is an extremely old and fundamental crustal boundary. This finding, supported by the map of Coles, neither proves nor disproves continental drift in the area, but suggests the application of satellite data to another fundamental problem.

Another category of new knowledge from the satellite data, namely the Earth's internal temperatures, has been demonstrated by the work of Mayhew (1985). It has been known since the time of Gilbert (1600) that magnetic materials become less magnetic with increasing temperatures, and totally non-magnetic above what is now called the Curie temperature in honor of Pierre Curie's 19th-century studies. For the lower crust, this temperature is generally estimated to be about 550 °C (823 K). The mantle is generally hotter than this, one reason it is considered non-magnetic. The temperature dependence of magnetic susceptibility (degree to which a substance can be magnetized) has been applied by Mayhew (1985) to a study of the depth of the subcontinental Curie isotherm. By comparing *Magsat* anomalies to heat-flow data for the western US, Mayhew showed that these anomalies often reflect the depth of the isotherm. This is not generally true for cratonic areas, but for tectonically and magmatically active areas this discovery points the way to a new method of studying the Earth's heat flow.

It is generally known that the "revolution in the earth sciences," or plate tectonics, was triggered largely by the discovery of system-

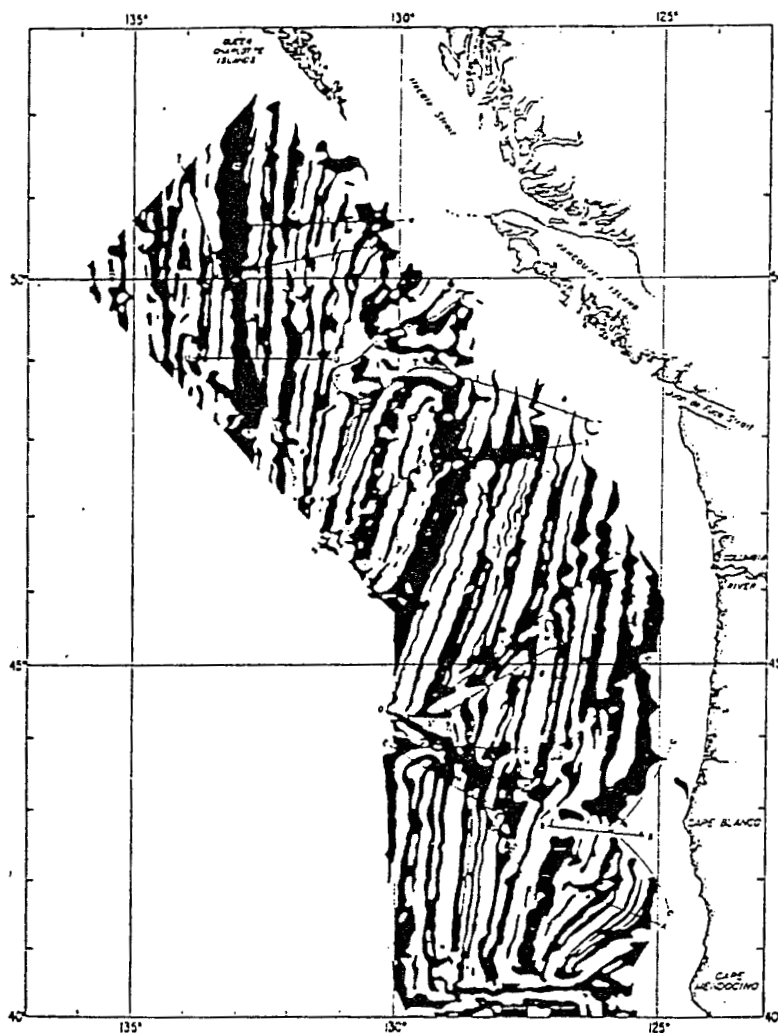


Fig. 3.13 Magnetic anomalies, total field, from marine surveys southwest of Vancouver Island, on Juan de Fuca Plate. Positive anomalies in black. From Raff and Mason (1961).

atic linear magnetic anomalies in the ocean basins. These were explained by Vine and Matthews (1963) (and independently, by Morley and Laroche, 1964) as having been formed by successive reversals of the main field, impressing thermal remanent magnetism bands of alternating polarity on the moving oceanic crust (Figs. 3.13, 3.14). Vine's description of the sea floor as "a conveyor belt and a tape recorder" is classic. It is natural to expect that satellite magnetometers would produce new information on the oceanic

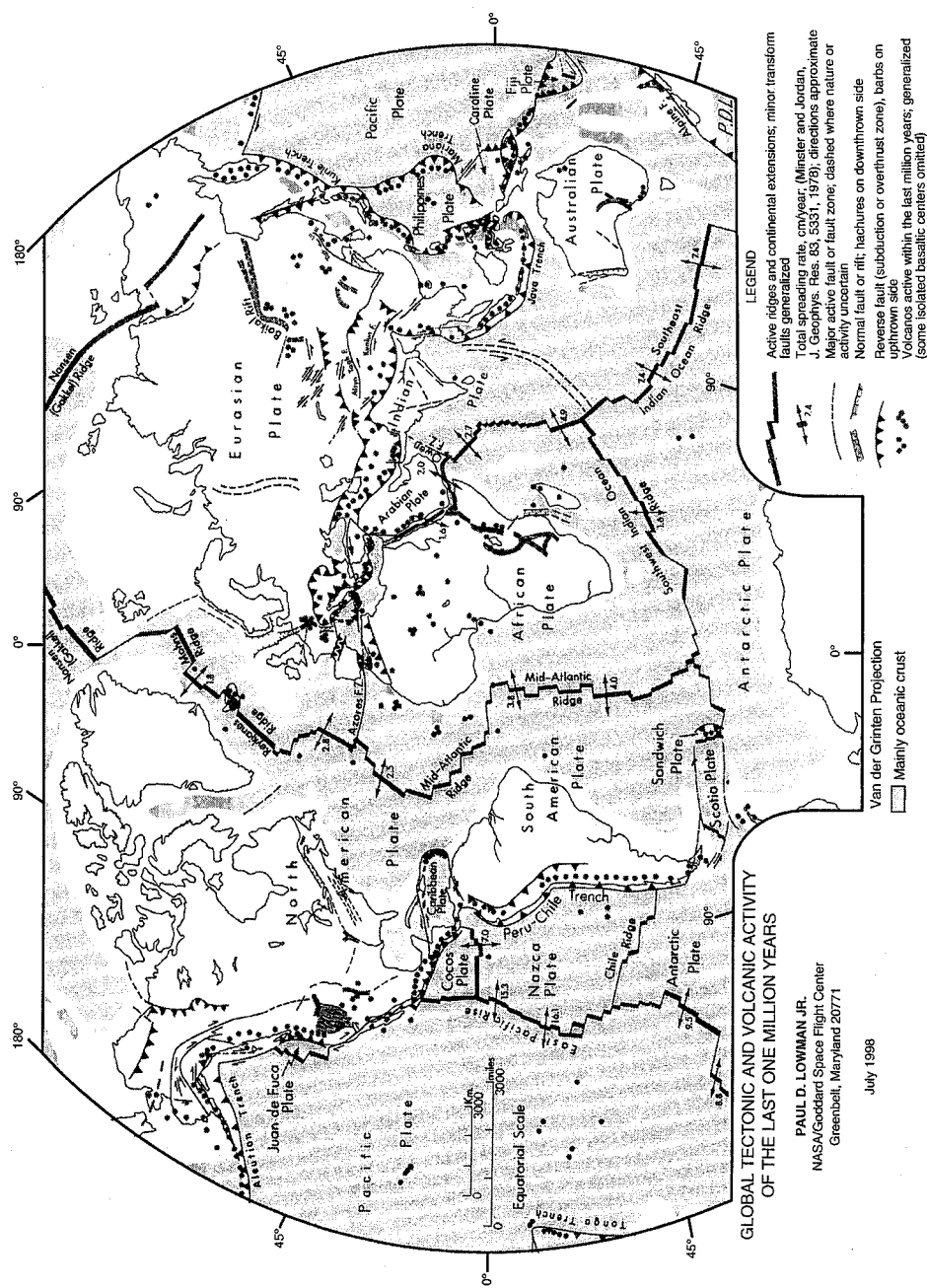


Fig. 3.14 Global tectonic and volcanic activity map for the last one million years, showing regional setting of Juan de Fuca Plate. From Lowman (1979).

“tape recorder.” However, there are very few distinct oceanic anomalies visible on the *Magsat* and *POGO* maps. The reason for this is the relatively low spatial resolution of the orbital data, on the order of 200 kilometers, and for some ocean areas the north–south inclination of the satellite orbits (Purucker and Dyment, 2000). The marine anomalies in most areas cancel out, resulting in the relatively featureless oceanic areas on the map (Thomas, 1987). Similarly, the continent–ocean boundaries, which should have magnetic expression, are not distinct (e.g., Taylor, 1991). One possible explanation suggested by Heirtzler (1985) is that, especially on active margins, the magnetic layer may be heated above the Curie temperature as it descends. Another explanation, by Meyer *et al.* (1985), is dominance of the main field over very-long-wavelength crustal anomalies. Development of the standard Earth magnetization model by Purucker *et al.* (1998, Chapter 1, Fig. 6) overcomes this problem by allowing for crustal thickness and susceptibility. Despite the difficulties, interpretations have been made of the magnetic properties of the ocean basins as seen from space.

Although the dominant linear anomalies found in most ocean areas are not resolved by the satellite data, some features expressing sea-floor spreading can be identified. LaBrecque and Raymond (1985) and Purucker *et al.* (1998) have shown (Figs. 3.15, 3.16), that the broad northeast-trending magnetic low in the Atlantic east of North America results from the Jurassic and Cretaceous “quiet zones.” These are broad belts of crust, roughly parallel to the spreading centers, formed during long periods of constant polarity of the main field and with consequent uniform crustal polarity. Similar features were identified in the North Pacific by LaBrecque *et al.* (1985) and Cohen and Achache (1990), and in the South Atlantic by Fullerton *et al.* (1989) and Purucker and Dyment (2000). They appear to be the only features on the satellite anomaly maps dominated by remanent rather than induced magnetism (Thomas, 1987).

Some tectonic features in the ocean basins can be readily identified on the satellite magnetic maps. The Aleutian Island subduction zone (see Fig. 3.14), a well-studied classic Benioff–Wadati zone of descending oceanic lithosphere, has been studied by Clark *et al.* (1985). They found that the *Magsat* anomaly along the Aleutian chain (see Fig. 3.6) could be interpreted in terms of magnetization contrast between the relatively cold down-going slab and the hotter (and thus non-magnetic) surrounding mantle. However, an additional slab of material from a former subduction zone was required to account for the anomaly north of the Aleutian chain in the Bering Sea, an interesting example of the tectonic value of *Magsat* data.

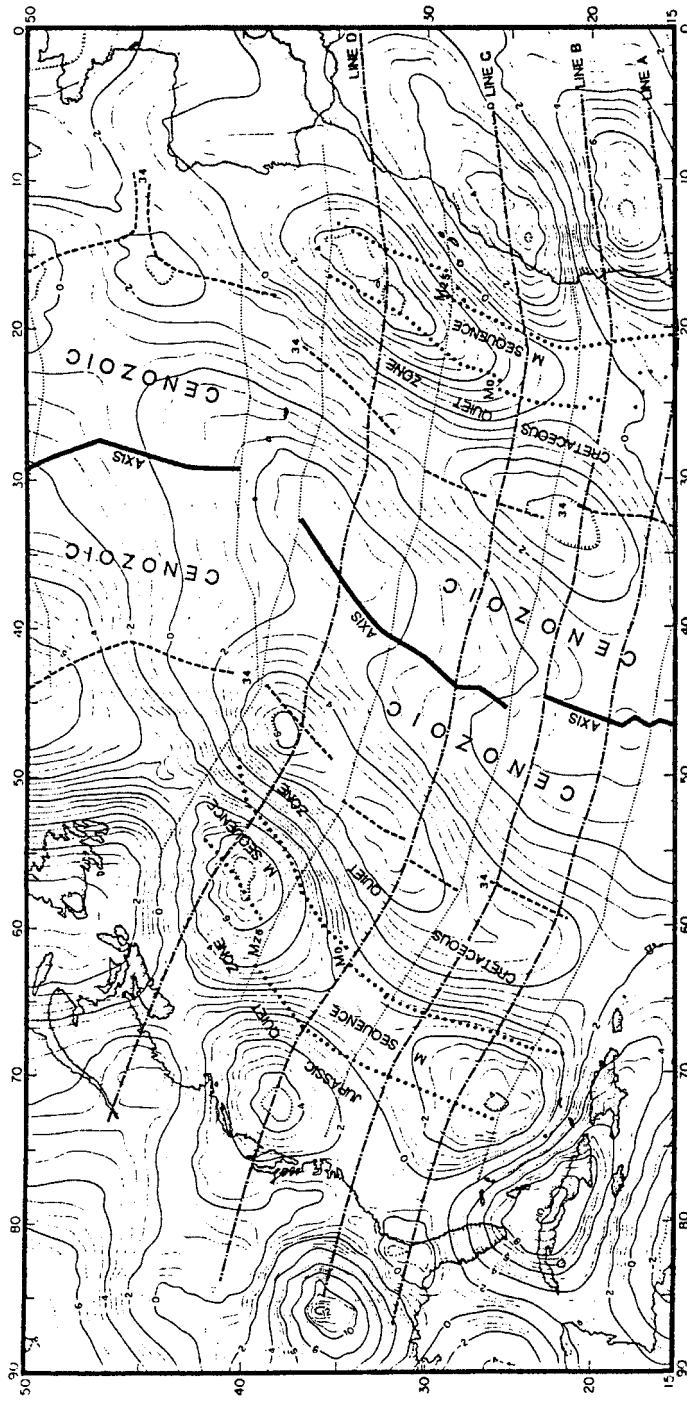


Fig. 3.15 Contour map of *Magmat* anomalies in the North Atlantic. Units nT. "AXIS" is Mid-Atlantic Ridge (Fig. 3.14), from which sea-floor spreading is thought to originate. Major isochrons derived from polarity reversal time-scale: AXIS, 0 Ma; 34, ca 84 Ma; M25, ca 150 Ma; ocean-continent boundary, 200 Ma. From LaBrecque and Raymond (1985).

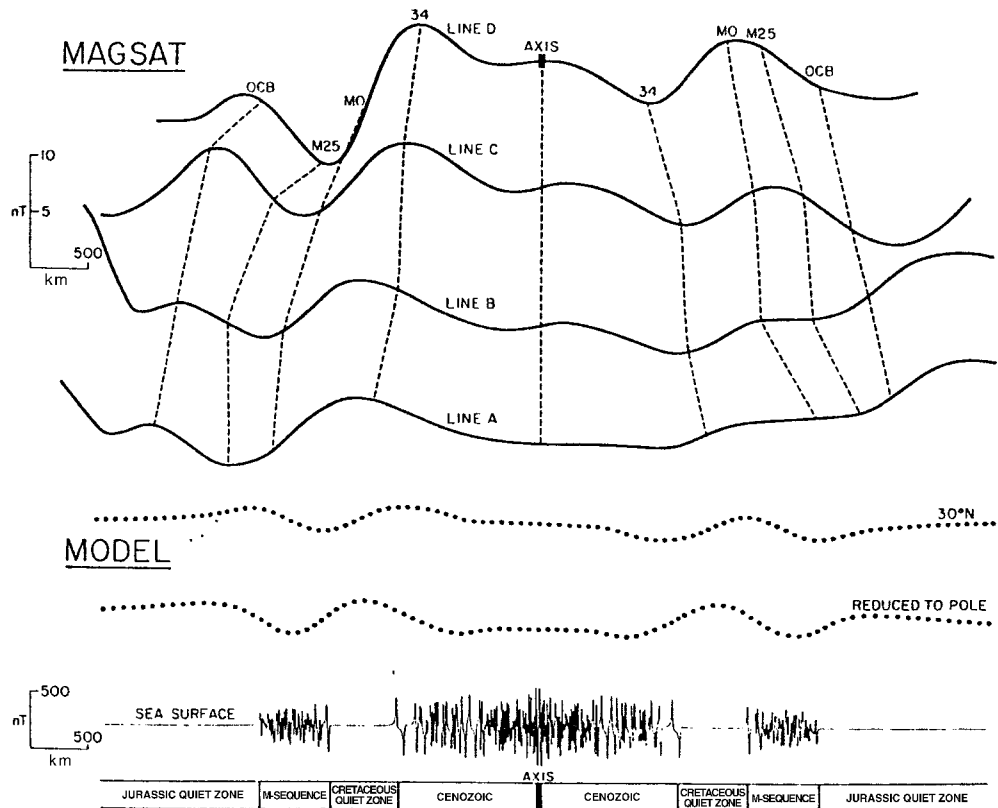


Fig. 3.16 Comparison of standard sea-floor spreading model with *Magsat* profiles A, B, C, and D on Fig. 3.15. Reading from bottom up, the profiles are: anomalies measured at sea surface; same anomalies extrapolated upward to satellite altitude and reduced to pole (i.e., corrected for magnetic latitude); and same anomalies at 30 deg. N, line C on Fig. 3.15 (top profile). From LaBrecque and Raymond (1985).

Another study of subduction zones as seen on *Magsat* data was carried out by Arkani-Hamed and Strangway (1987). On comparing the magnetic signatures of known subduction zones around the Pacific Ocean, they found that age of the subducted oceanic crust, as inferred from the magnetic time-scale, had strong influence on the magnetic anomalies. Older crust, such as that in the northwest Pacific, produced distinct anomalies, whereas younger (and warmer) crust, such as that of the Nazca Plate, produced none. A laboratory study of island arc xenoliths by Warner and Wasileski (1997) showed that mafic xenoliths might account for the magnetic anomalies detected over areas such as the Aleutians and Japanese islands.

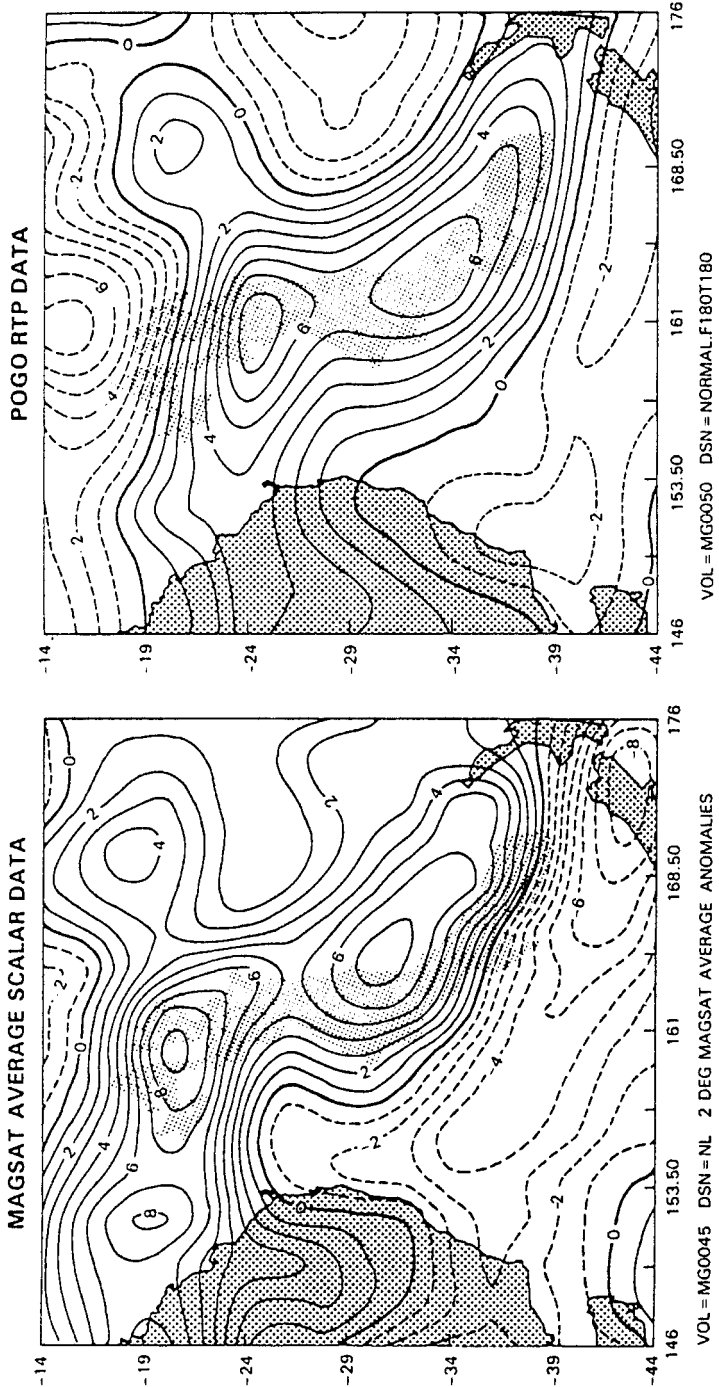


Fig. 3.17 *Magsat* and *POGO* magnetic anomalies over the Lord Howe Rise, between Australia (left) and New Zealand (lower right). Lord Howe Rise shaded, outlined by 2000 meter isobath. *POGO* anomalies reduced to pole. Contour interval 1 nT, scaled to constant 50,000 nT field throughout the map. From Frey (1985).

It has been proposed by several workers that, geophysically impossible as it may seem, continental crust can be converted to oceanic crust. A *Magsat/POGO* study (Fig. 3.17) by Frey (1985) showed what may be an actual example of such conversion, the Lord Howe Rise between Australia and New Zealand. This a deeply-submerged marine plateau whose lithology (e.g., ignimbrites) shows that it was at one time emergent; the fact that it is now at oceanic depths alone suggests that it is not normal continental crust. Frey showed that the magnetic susceptibility implied by the positive satellite magnetic anomaly indicates possible conversion of the lower crust to a more mafic rock type. Although further data would be needed to confirm this interpretation, its novelty suggests the value of the *Magsat/POGO* data for an extremely fundamental problem, the origin of ocean basins. The anomaly maps of Frey, like those of Hinze *et al.* (1982), show little expression of the continental margin, a problem to which we shall now turn.

The apparent failure of *Magsat* to delineate the continental/oceanic crust boundary, demonstrated in Indonesia by Taylor (1991), has been addressed by Purucker *et al.* (1998). They point out that the apparent lack of contrast at the boundary may be due to removal of these features by the spherical harmonic separation of the main field, or by the lack of spatial resolution in the satellite data. They therefore have developed an inverse technique to include a-priori information on crustal magnetization. The block diagram of this approach will be helpful (Fig. 3.18) in discussing it.

The technique, in brief, is an iterative one, starting with construction of a simple Earth magnetization model (SEMM) by assuming values of crustal susceptibility and thickness. The field such a crust (SEMM-0) would produce at 400 km altitude is then calculated, followed by other steps shown on the diagram until a new model field is produced. This field is then compared with observed anomalies. If it does not reproduce the anomalies, the procedure is repeated after dipole corrections, a new SEMM calculated, then its field constructed as before. Some idea of the number of geophysical parameters involved may be gained from Fig. 3.19. The result of this approach is a global magnetization model, SEMM-1 (Fig. 3.20) giving a much more understandable and realistic picture of the crustal anomaly field. Purucker *et al.* show how this model can be used to refine interpretations of crustal structure, composition, or heat flow in the Gulf of Mexico and over the Kentucky anomaly. Other factors are involved, such as the strength of the main field at different latitudes, which affects the induction process.

3 SATELLITE STUDIES OF GEOMAGNETISM

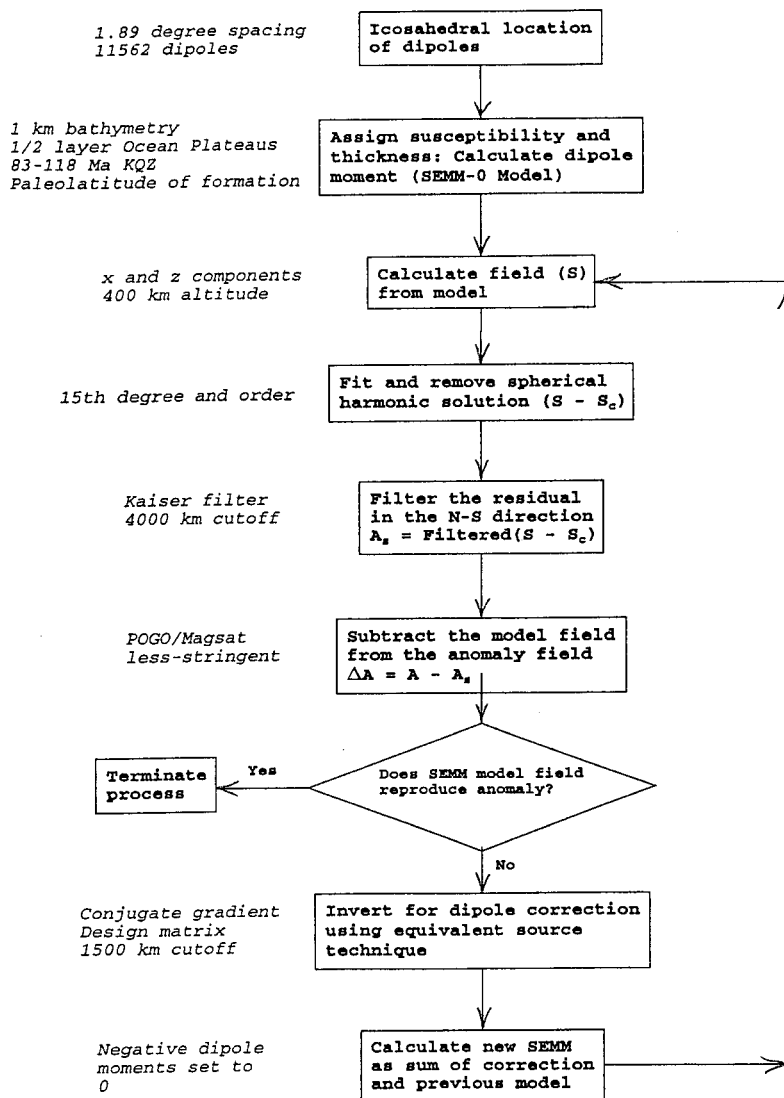


Fig. 3.18 Block diagram of the derivation of the global magnetic model.
From Purucker *et al.* (1998).

3.5 Extraterrestrial magnetic fields

As we have seen with gravity fields, we can gain a broader perspective from the magnetism of other planets (Ness, 1979; Dyal, 1992; Kivelson, 1995). Working outward from the Sun – which, being composed of intensely hot turbulent plasma, is strongly magnetic on all scales – we come first to Mercury. Given its resemblance to the Moon – an inactive and largely non-magnetic body – we might

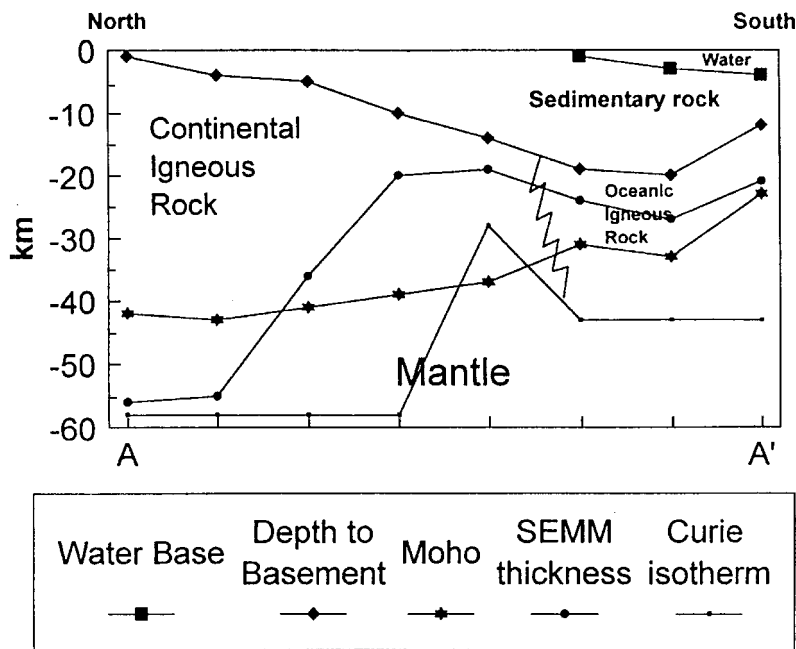


Fig. 3.19 North-south cross section through the crust of the Mississippi River embayment and adjacent Gulf of Mexico. From Purucker *et al.* (1998).

expect little or no main field, but it was found (Ness *et al.*, 1974) that Mercury has a surprisingly strong one, several hundred nanoteslas. Although only 1% of the Earth's field, this is much more than the interplanetary field, and has led to intensive study for an explanation. As summarized by Ness (1979), the consensus is that Mercury is differentiated into a liquid core and mantle, and has an active "dynamo" more or less analogous to that of the Earth. However, remanent magnetism may play a role, especially in view of the relatively large iron core.

Venus is in many ways similar to the Earth, and it might be expected to have a comparable magnetic field. Early Soviet and American missions failed to detect a planetary field. The magnetometer on *Pioneer Venus*, flown in 1978, did detect nightside fields of 20 to 30 nT (Russell *et al.*, 1979), but these were horizontally oriented and variable from one orbit to another. Generally consistent results were obtained by the *Galileo* mission, which went by Venus in 1991 as part of a gravity-assist maneuver (Kivelson, 1995). The ionosphere of Venus is electrically conducting, and thus interacts with the magnetic field of the solar wind ("moving electrical fields"). The weak fields detected were accordingly interpreted as resulting from interaction of the venusian ionosphere with the

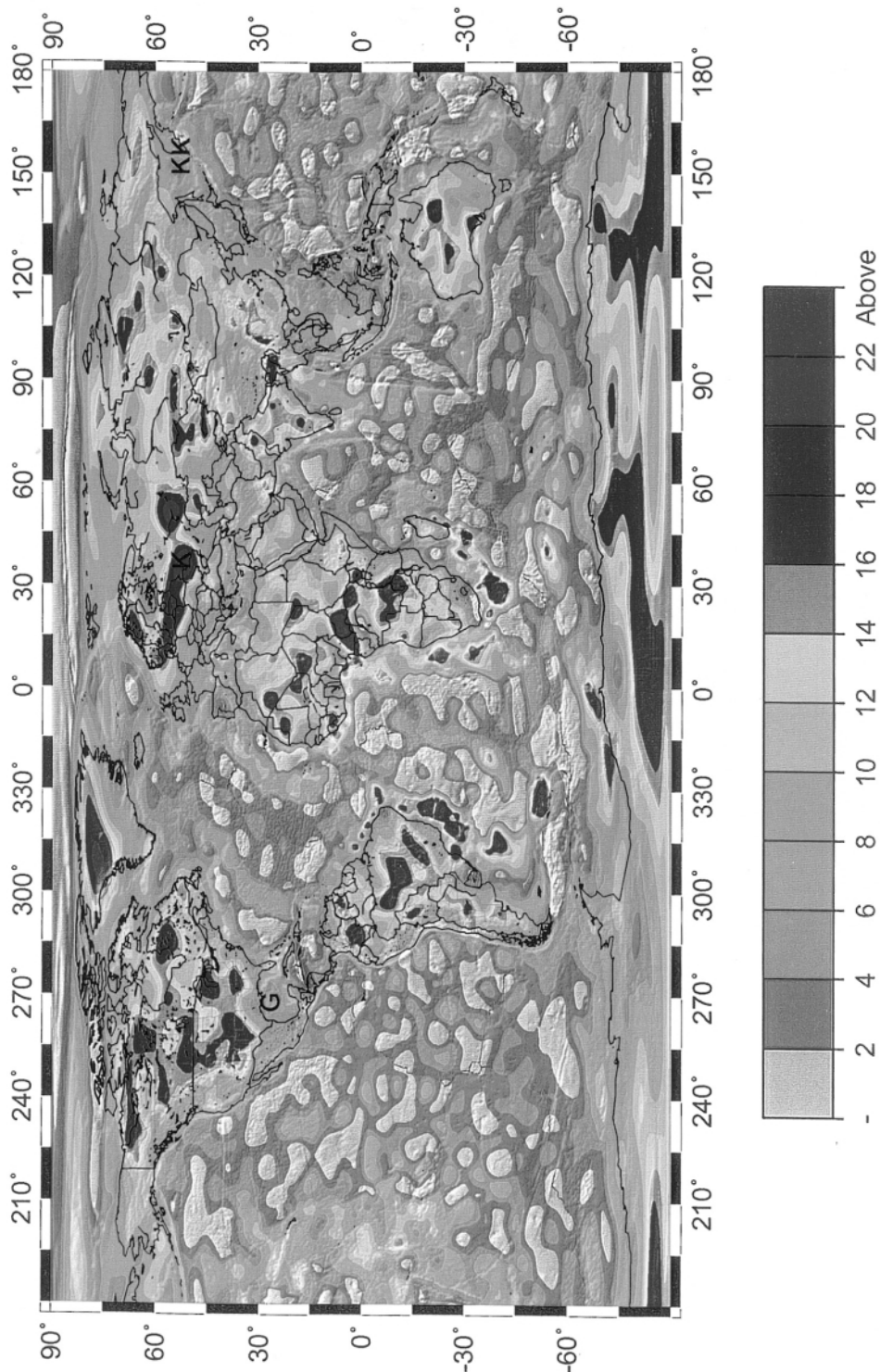


Fig. 3.20 (See also Plate XI) Global map of susceptibility times thickness (SI) times thickness times 10 of the SEMM-I model shaded by surface topography for correlation with major bathymetric and topographic features. Negative values in gray. Units are SI × km × 10. From Purucker *et al.* (1998).

solar wind, not from an internal dynamo. Venus must have a hot interior and a liquid core, but its very slow rotation rate (about 243 days) apparently inhibits generation of a core field (Russell and Luhmann, 1992).

The Moon has no bipolar main field (Ness, 1979), a discovery made by Soviet spacecraft in the early-1960s. However, more detailed investigations, notably those by subsatellites launched from the *Apollo* spacecraft, showed that there are local magnetic anomalies on the lunar surface (Figs. 3.21, 3.22) as strong as a few hundred nanoteslas (Hood *et al.*, 1981). Reiner Gamma (Fig. 3.23), the strongest of these, is particularly puzzling, having no visible relief, consisting apparently of high-albedo “swirls.” These anomalies in general have stimulated much theorizing. One explanation for their origin is that of Runcorn (1967), who suggested that the lunar anomalies are caused by remanent magnetism produced when the Moon had a strong main field, or was exposed to a strong field (that of the Earth or the Sun). Runcorn actually carried out paleomagnetic studies for the Moon. Another possible cause for the lunar anomalies is magnetization by impact, or shock remanent magnetization (Pilkington and Grieve, 1992). First suggested for terrestrial rocks by Pohl (1971) and Cisowski and Fuller (1978), the obvious importance of impact on the Moon suggested that this possibility be further investigated. Such investigation became possible with the *Lunar Prospector* mission (Lin *et al.*, 1998).

The *Lunar Prospector* (*LP*) spacecraft carried a magnetometer and electron reflectometer experiment in a near-polar low-altitude (ca. 100 km) orbit. Electron reflectometer magnetometry depends on the fact that magnetic fields will deflect or reflect charged particles (electrons), a technique only possible over airless bodies. The *LP* magnetic survey carried out confirmed previous findings, but permitted their application to almost the entire lunar surface. Perhaps the most interesting result of the *LP* magnetic survey was confirmation of the existence of strong magnetic anomalies antipodal to the large near-side impact basins, such as Mare Imbrium. Although the exact mechanism responsible for these anomalies is not understood, they are probably related to shock remanent magnetization, mentioned above. For reasons discussed by Lin *et al.* (1998), such remanent magnetization implies that when the mare basins were formed, around 3.9 to 3.6 billion years ago, the Moon had an internally-generated main field. This field has long since disappeared, presumably as the result of the Moon’s cooling and solidification to depths of several hundred kilometers, as discussed in later chapters of this book.

One of the most surprising discoveries related to extraterrestrial

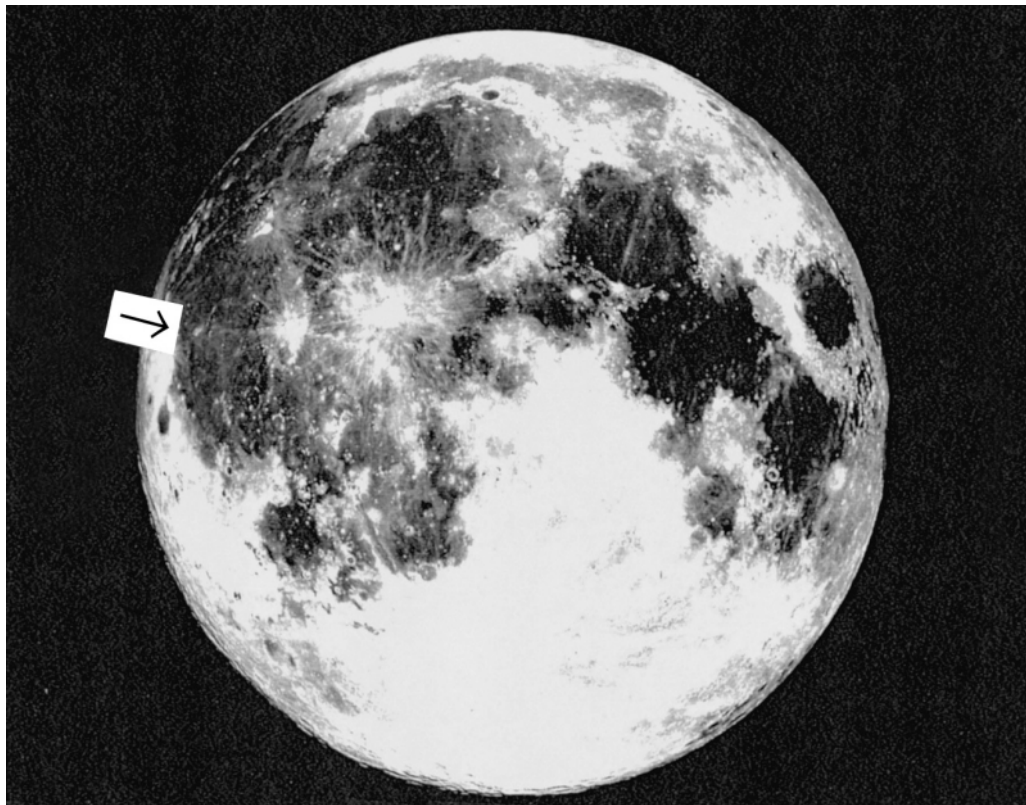


Fig. 3.21 Lick Observatory composite photograph of first and last quarter Moon. Reiner Gamma indicated with arrow: white, tadpole-shaped feature.

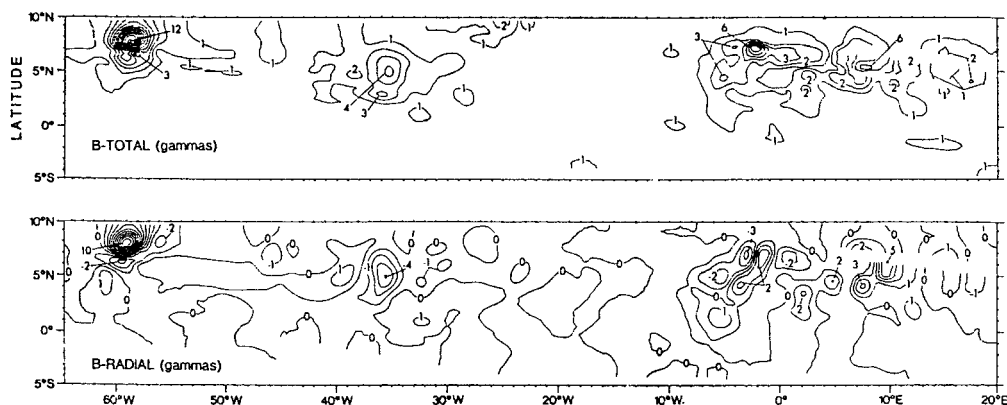


Fig. 3.22 Magnetic anomaly maps from *Apollo* subsatellite measurements: (top) total field intensity in nT ("gammas"); (bottom) vertical intensity. Reiner Gamma is anomaly at upper left. From Hood *et al.* (1981).

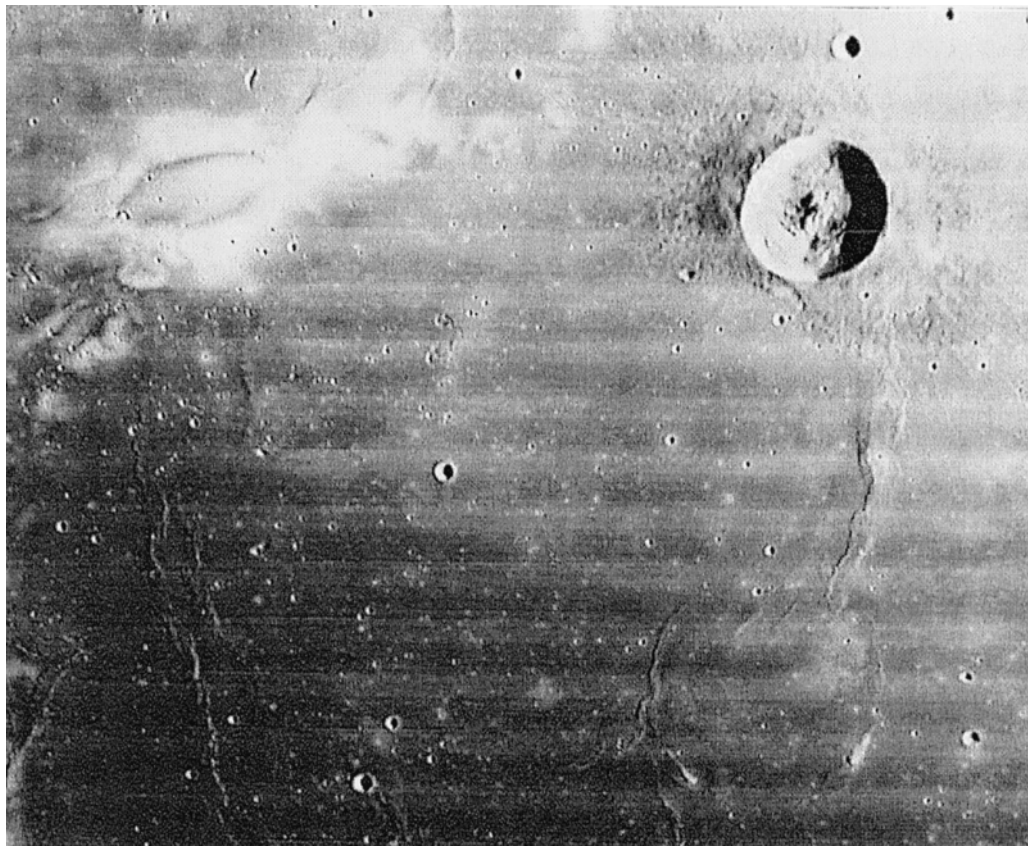


Fig. 3.23 *Lunar Orbiter IV* photograph 157H1 (north at top) showing crater Reiner at upper right, 30 km in diameter, and Reiner Gamma at upper left.

magnetic fields comes from Mars, specifically from the *Mars Global Surveyor (MGS)* (Acuña *et al.* 1998; Connerney *et al.*, 1999). It has been known for decades that Mars has little if any global magnetic field. But just as the Moon's lack of air and water makes it invaluable for comparative planetology, the absence of a global martian magnetic field has turned out to be extremely revealing. The *MGS* measurements have shown that there is no significant main field corresponding to that of the Earth. However, there are extremely strong linear magnetic anomalies detectable at altitudes of several hundred kilometers (Purucker and Clark, 2000; Purucker *et al.*, 2000) (Fig. 3.24). These are much stronger than comparable terrestrial anomalies (see Fig. 3.6). In the absence of a strong main field, the martian anomalies must be produced by some form of remanent magnetism (Kletetschka *et al.*, 2000). Connerney *et al.* (1999) interpreted the anomalies that they discovered as being essentially analogous to

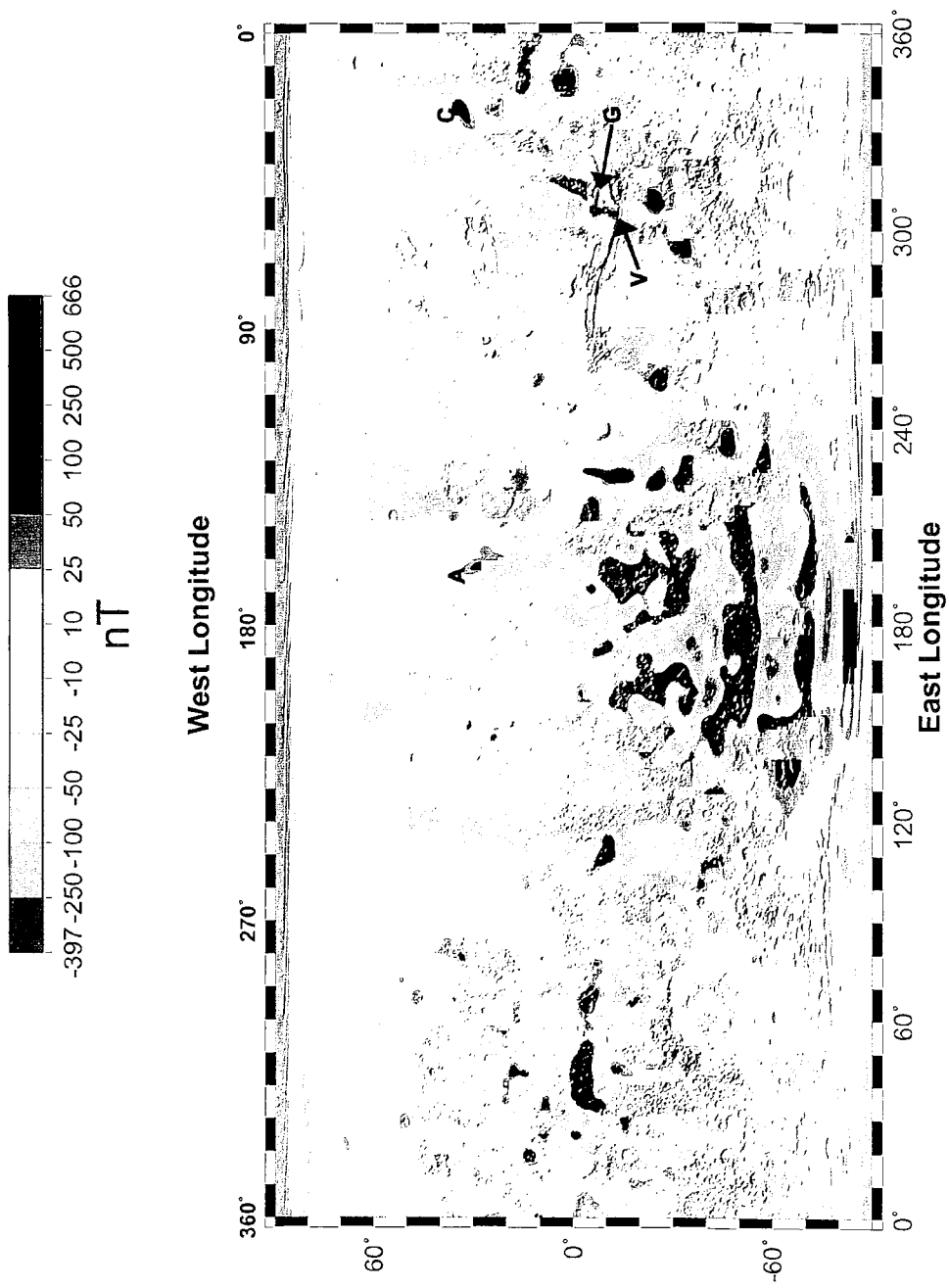


Fig. 3.24 (See also Plate XII) *Mars Global Surveyor* magnetic anomaly map of Mars. From Purucker *et al.* (2000).

those of the terrestrial oceanic crust and, like them, to have resulted from sea-floor spreading in the presence of a reversing primordial martian magnetic field. The *MGS* data then might imply that Mars, like the present Earth, has undergone a period of sea-floor spreading, the highland crust being the reworked “remnants” of an ancient oceanic crust.

Regardless of interpretation, the *MGS* discoveries and the interpretation by Connerney *et al.* are extraordinarily interesting, furnishing a striking example of the value of comparative planetary geophysics. The visible geology of Mars gives no support at all to the plate tectonic hypothesis, as in fact Connerney *et al.* note. More generally, Mars appears to be a planet that although still internally active never reached the stage of true plate tectonics. One specific implication of the *MGS* anomalies is the insight they may give to interpretation of terrestrial anomalies.

It has been uncertain whether the crustal anomalies detected from space are produced by induced or by remanent magnetism. The Earth’s main field is, as we have seen, very strong, quite strong enough to induce magnetic anomalies. However, Mars has no comparable field, nor does the Moon, at the present time. It thus seems likely that the anomalies detected on each body must be remanent, not induced, formed when there were strong inducing fields, of whatever origin.

The magnetic fields of the terrestrial (inner planet) bodies, in summary, appear to reflect several of their characteristics: rotational rate, size, and internal temperature. The Earth’s strong and relatively well-organized (dipolar) main field results from its unique combination of rapid rotation and a large, partly liquid, iron core.

The giant (outer) planets have all been visited, by *Pioneer*, *Voyager*, *Galileo*, or *Ulysses* spacecraft, and each has a magnetic field (Connerney, 1987; Kivelson, 1995). That of Jupiter is the strongest and most variable, as we might expect from Jupiter’s near-stellar composition and structure. The jovian magnetic field is thought to be produced by a dynamo mechanism, but one involving currents of liquid hydrogen (perhaps metallic) and comparably exotic conditions. An interesting complication in the jovian magnetosphere is the magnetic connection to its nearest large satellite, Io, through a torus of sulfur and oxygen ions produced by the erupting volcanos on Io. This connection is not a trivial effect, involving a million megawatts of power (Bagenal, 1998).

The years-long *Galileo* and *Ulysses* missions have produced a cornucopia of magnetic field results that can be summarized only briefly here; a good review has been published by Kivelson (1995).

The *Galileo* results are particularly relevant to the theme of this book.

Perhaps the most surprising *Galileo* findings, from the viewpoint of terrestrial geophysics, are that bodies that might be expected, from their size, composition, or temperature to be non-magnetic apparently do have significant magnetic fields. Ganymede and Callisto, both ice-covered satellites of Jupiter, have been found to perturb the solar wind, strongly implying that they both have magnetic fields. The most favored explanation (Kivelson *et al.*, 1998; Khurana *et al.*, 1998) is that both satellites have, under their icy crusts, oceans of salt water. Being a moving electrical conductor, such water could produce magnetic fields as they cut the lines of force of Jupiter's immense and strong field. The possible implications of this discovery for extraterrestrial life are extremely interesting, raising the possibility that at least simple life-forms may exist in these superficially hostile bodies.

The *Galileo* mission carried out a long and complex series of gravity-assist maneuvers. The spacecraft was diverted toward two asteroids, Gaspra and Ida (Kivelson, 1995), and found that even these small rocky bodies also perturbed the solar wind. Although the trajectory did not go close enough to detect magnetic fields directly, the existence of such fields can be inferred with some confidence.

Further discussion of other planetary magnetic fields would lead us too far astray, but it is worth noting that strange and unpredicted as they were, these phenomena have so far all proved understandable in terms of conventional electromagnetic theory. Quantum mechanics, quarks, and "strange" particles have not been invoked to explain them. Faraday, Oersted, and Maxwell would be able to follow discussions of magnetism in these unimaginably alien planets, indeed, to contribute to them.

3.6 Summary

How can we summarize the impact of space flight on studies of the Earth's magnetism? We should begin by pointing out that the first satellite dedicated to study of the global and crustal fields, *Magsat*, was only launched in 1978, and there was, until the 1999 launch of *Oersted*, no comparable successor. The situation is analogous to that of satellite meteorology if there had been no additional weather satellites launched after *Tiros 1*. NASA has been criticized by Dyson (1979) for its common practice of apparently considering a program completed with one successful mission. For *Magsat*, the criticism can not be easily dismissed.

What has been accomplished with the space data so far acquired? The most general and unarguable benefit is simply the broader perspective acquired from spacecraft that have already left the solar system after visiting every planet but Pluto. Geophysicists now have magnetic field data from all these planets to compare with that of the Earth. In addition, we now have a reasonably complete picture of the interaction of the Earth's magnetic field with the interplanetary field.

For the main field, the value of orbital data is obvious. This field is a dynamic and complex feature, affected by factors as diverse as shifting currents in the core and variations in the solar wind, changing on time-scales from millions of years to minutes. The first dedicated magnetic field satellite, *Magsat*, provided the primary data for the first adequate International Geomagnetic Reference Field. These data have provided the first synoptic vector data on the main field, giving the beginning of real understanding of the liquid core, starting with confirmation of its size and gross electrical properties.

The application of crustal anomaly orbital data can be summarized very generally as follows. First, the global nature of satellite orbits has provided a consistent picture of crustal magnetism in remote areas on land and sea that had been geomagnetically almost unexplored. A second result of satellite data has been a new and independent source of information on the lower continental crust, until very recently almost entirely unknown. Satellite magnetic measurements, revealing extremely broad and deep features, have thus proven a valuable complement to aeromagnetic and ground surveys that reveal much smaller and shallower features such as mafic dikes, banded iron formations, and greenstone belts. Many different structures and lithologies of the lower crust may be expressed in satellite data. However, interpretations of these data are beginning to converge with those from other lines of investigation, such as seismic reflection profiling. The lower crust in most areas appears to consist largely of high-grade metamorphic rocks, significantly more mafic than those of the exposed basement (Lowman, 1984; Rudnick, 1992). Several broad anomalies detected on satellite data have been interpreted as very large mafic intrusions, supporting petrologic and geophysical studies indicating that basaltic underplating, or intrusion, has been a major factor in evolution of the continental crust. We will return to this subject in Chapter 6. These developments typify the application of orbital magnetic data to geology. By themselves, they have produced few discrete discoveries, but combined with other lines of evidence they are contributing to a solid if still imprecise understanding of the structure, composition, and evolution of the continental crust.

3 SATELLITE STUDIES OF GEOMAGNETISM

The flood of global magnetic data from *POGO* and *Magsat* has had a stimulating effect on laboratory and field studies of what has been termed magnetic petrology, the study of magnetic materials in the crust. The importance of the satellite data in magnetic petrology stems from the nature of the anomalies these data reveal, arising largely from the deep and inaccessible crust. The magnetic properties of major rock types have been studied before, for interpretation of aeromagnetic and surface studies. But the satellite data have stimulated investigations of uncommon and poorly-exposed rocks, granulites in particular. Results of these studies are of course fed back into interpretations of satellite data, with mutual benefit.

An unexpected application of satellite magnetic data to geophysics has been in mapping the depth of the Curie isotherm, the surface below which the crust or mantle is too hot to be magnetic. Since the Curie isotherm reflects heat flow, the satellite data are giving us a new source of information on the Earth's thermal behavior. Because most tectonic activity in the Earth is fundamentally thermal in origin, this application of satellite magnetic field measurements has great potential value (no intentional pun).

Perhaps the most important long-term result of satellite magnetic field studies to date has been the discovery or at least the redefinition of geologic problems. For example, the Bangui anomaly has been suggested to be the possible expression of a major impact that triggered basaltic magmatism. This may stimulate study of the relations between terrestrial magmatism and impact, already a lively subject because of the flood of new data on such relations from the Moon, Mercury, Mars, and Venus. Another line of inquiry stimulated by satellite data concerns the distribution and origin of aulacogens, failed rifts that sometimes localize mafic igneous intrusions, expressed as satellite magnetic anomalies. Satellite data focus attention on the problem and may contribute to its solution.

CHAPTER 4

Remote sensing: the view from space

4.1 Introduction

Geophysics is sometimes distinguished from geology as being the study of the *inside* of the Earth, geology being the study of the *outside*: the surface of the Earth and structures expressed at the surface. These light-hearted definitions are actually a convenient introduction to what has become the most pervasive and important direct effect of space flight on geology: **remote sensing**.

This is a new term for an old technology, briefly defined as **the study of objects at a distance by means of electromagnetic radiation, reflected or emitted**. Vision obviously fits this definition, and in fact “remote sensing” can be thought of as the extension of human vision to far wider parts of the spectrum, and to far greater distances, than the unaided eye can reach. Astronomers have been doing “remote sensing” for centuries. However, as currently used, remote sensing refers to the acquisition, processing, and interpretation of images from satellites and aircraft (Sabins, 1998), images formed by electromagnetic radiation, as distinguished from potential fields (gravity and magnetic). This definition is to a degree artificial, in that electromagnetic radiation itself consists of transversely oriented electric and magnetic fields traveling through space at 300,000 km/s (in vacuum). Furthermore, as we will see, remote sensing and geophysics are increasingly used together, and many data-processing techniques and formats such as shaded relief maps are common to both.

The definition cited above, by Sabins, is notable for the priority given to “satellites.” Remote sensing from aircraft goes back to the first applied aerial photography in World War I, and for the first few years after the term was coined (in 1958, by Virginia Prewitt) it referred only to airborne sensors. Aerial methods continue to be widely used, but since the 1980s “remote sensing” has increasingly meant *orbital* sensing. For convenience, this usage will be followed here; unless specified otherwise, “orbital” is implied by “remote

sensing.” This chapter will cover only remote sensing of the Earth, with treatment of other planets reserved for Chapters 5 and 6.

It was suggested by Naisbitt (1984) that the achievement of orbital flight had been a major contributor to the emergence of the “information” or “post-industrial” society after World War II, the specific cause being development of communications satellites. Remote sensing from space has made a comparable and growing contribution to this “megatrend,” as discussed by Cary (1997). The field of remote sensing has consequently become an extremely large one, filling many library shelves, and this chapter does not pretend to cover the subject in general. The objective is to summarize the impact of remote sensing on geology. Accordingly, only the most important principles will be outlined, as well as the main events in the development of geologic remote sensing.

The electromagnetic spectrum is illustrated in Fig. 4.1, differing from diagrams in physics textbooks in the emphasis on atmospheric transmission as a function of wavelength. This aspect of the diagram can be thought of as window shades (black), pulled down over certain parts of the spectrum. It is extremely important in remote sensing as defined here, since orbital techniques as used around the Earth depend on radiation that must get through the entire thickness (actually a double thickness, if we include the Sun’s radiation) of the planet’s atmosphere. Another important aspect of the diagram may not be so obvious: the dependence of wavelength on size of the radiation’s source. Gamma rays come from the nucleus, X-rays from inner electron shells, visible light from the outer shells, thermal infrared from molecular motion, magnetron-generated microwaves from resonant cavities a few millimeters across, and broadcast band radio, with wavelengths of a few hundred meters, from large antennas on towers. The dependence of wavelength on antenna length is well known in radio engineering, and given by an equation that the reader will be spared. The more general dependence on radiation source, however, is fundamental to understanding the physics of remote sensing: **the longer the wavelength, the bigger the source.**

There are two general categories of remote sensing, depending on the source of the electromagnetic radiation: *passive* and *active*. Passive methods use only radiation reflected or emitted by the object being studied; the target is also the radiation source. Vision is the most obvious example of passive remote sensing, usually depending on visible light coming from the source. Active methods involve generation of electromagnetic radiation beamed at the object to be studied. Radar is the best-known active method, generally using

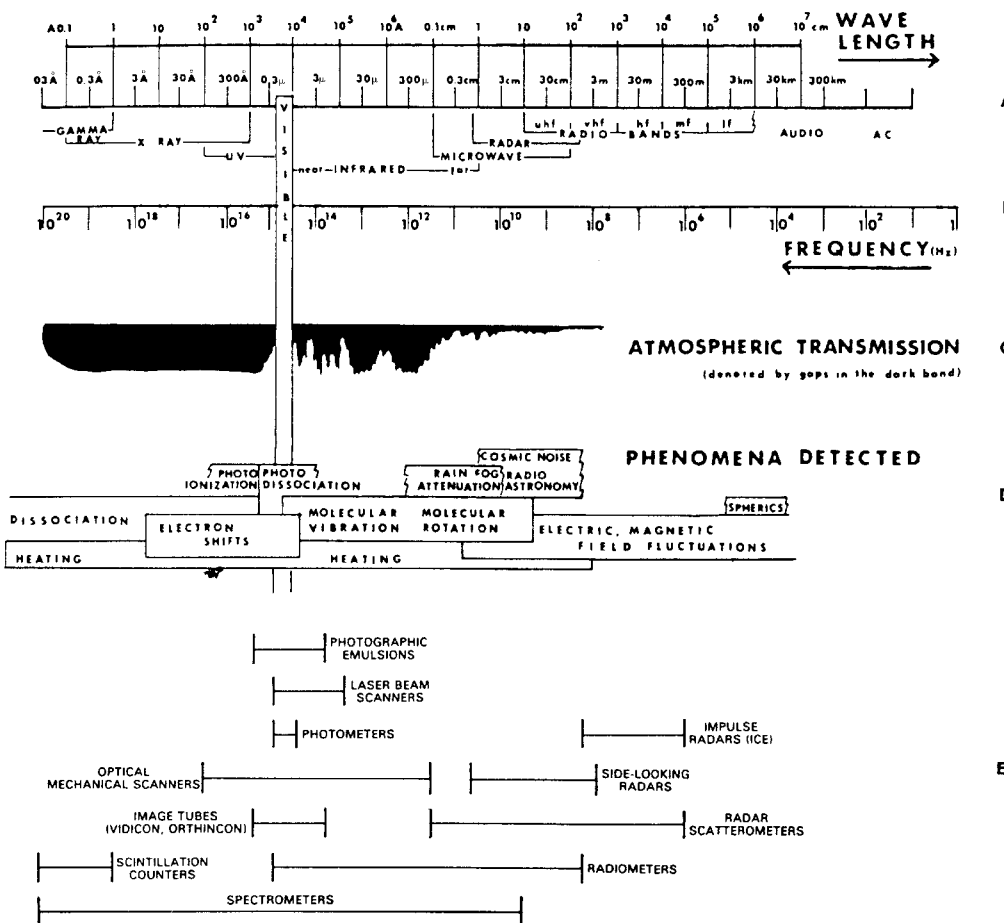


Fig. 4.1 Electromagnetic spectrum, atmospheric transmission, radiation sources, and instruments used.

microwave radiation reflected from the target. Optical radar, or lidar, using laser-generated visible or near-visible radiation, is coming into wide use. One category of active remote sensing has already been covered in Chapter 2, under space geodesy: radar and laser altimetry, techniques that are increasingly being included, correctly, in “remote sensing.” Altimetric data, showing marine or land topography, is fundamental to understanding of both satellite geophysical and geological methods.

The use of electromagnetic radiation in remote sensing involves a wide range of data-analysis techniques, most generally categorized as *analog* and *digital*. Analog methods, in this context, are illustrated by human vision, film photography, and older types of radar as

displayed on an air-traffic control screen. Digital methods, treated at length by Vincent (1997), are now by far the dominant method of data analysis used in remote sensing, depending not only on digital primary data but also on initially analog data such as photographic film that has been digitally scanned. A remarkable example of this latter approach is the spectacular collection of orbital photography by Apt *et al.* (1996), in which returned film images have been digitized and enhanced for publication. “Colorization” of old movies is a better-known example of digital reprocessing of originally analog data.

With this unavoidably brief sketch of the principles of remote sensing data acquisition and handling, let us turn to the application of remote sensing from space to geology. This chapter will be confined to orbital methods only, but the first space photographs used for geology were taken from sounding rockets, such as the *Viking* series, at altitudes of up to 200 km (Lowman, 1965). Many excellent photos were taken on lunar missions by American astronauts, as shown in the collection edited by Schick and Van Haften (1988).

4.2 Orbital remote sensing in geology: a brief history

The advantages of orbital remote sensing for meteorology were recognized well before artificial satellites were actually launched: global coverage, systematic repetition of coverage (or continual coverage from geosynchronous orbits), wide field of view, and capability for thermal measurements. The value of orbital images for topographic mapping and military reconnaissance was also realized at an early stage, but there was virtually no appreciation of the value of orbital methods for geology until the mid-1960s, after hundreds of satellites had been launched. The reasons for this are an interesting aspect of the history of space flight in general, and will therefore be discussed at some length; a detailed account has been given elsewhere (Lowman, 1999).

President Kennedy’s 1961 challenge to land a man on the Moon by the end of the decade led to a large and rapid increase in the civilian space program, i.e., NASA. Although focussed on the lunar landing, NASA planning in the early-1960s included several potential applications of our growing space capability. One of these was the use of manned space stations for earth-oriented remote sensing, primarily for earth resource studies, as distinguished from satellite meteorology. “Earth resources” of course included geology, and NASA studies in this field were managed by geologist Peter Badgley in cooperation with the US Geological Survey (USGS), the

Department of Agriculture, and the Office of Naval Research among others. These studies involved a wide range of airborne remote sensing experiments, carried out by the Manned Spacecraft Center (now the Lyndon B. Johnson Space Center) as well as by many other governmental and non-governmental organizations (Vincent, 1997). Many of the techniques developed were actually used successfully on the first American space station, *Skylab*, in 1973–4. However, geologic remote sensing was given a jump start, so to speak, by the *Mercury* and especially the *Gemini* programs.

Project *Mercury*, the first American manned space effort, began in 1958, with the first successful orbital flight by John Glenn in 1962. Beginning with the second flight, by Scott Carpenter, the *Mercury* pilots carried out terrain photography for geologic purposes, stimulated by the suggestion of Paul Merifield on the basis of his work with rocket photographs. The last *Mercury* flight, a 22-orbit one flown by Gordon Cooper, permitted acquisition of twenty-nine 70 mm color photographs, chiefly of southern Asia (O'Keefe *et al.*, 1963). In combination with Cooper's remarkable visual sightings, the *Mercury* terrain photographs generated the beginnings of wide appreciation of the geologic value of orbital photography (Lowman, 1965). They gave rise to a much more extensive photographic effort, the S005 Synoptic Terrain Photography Experiment, carried on the *Gemini* missions (Gill and Gerathewohl, 1964). By the time the 10 *Gemini* flights were over, some eleven hundred 70 mm color photographs suitable for geology, geography, or oceanography study had been acquired (Lowman, 1969). Published widely, these spectacular pictures generated world-wide interest among public and scientists alike (Merifield *et al.*, 1969). Their most important result for geology was the stimulus to the US Geological Survey's *Earth Resources Observation Satellite (EROS)* proposal of 1966, triggered primarily by the "demonstrated utility of the *Mercury* and *Gemini* photographs" (Pecora, 1969).

The *EROS* concept was based on use of a television system, proposed by the Radio Corporation of America (RCA), rather than returned film. The story becomes extremely complicated at this point, with *EROS* getting entangled in interagency conflicts. An authoritative account of these conflicts has been published by Mack (1990) and need not be recounted here. However, when the intrabeltway dust had settled, *EROS* had evolved into the *Earth Resources Technology Satellite (ERTS)*, a NASA program developed with the cooperation of the USGS, Department of Agriculture, and other government agencies. The first *ERTS* was launched in July 1972, and shortly thereafter re-named *Landsat*.

From a historical viewpoint, the most important aspect of *Landsat* was its derivation from the *Apollo* program. *Gemini* was solely technological preparation for a lunar landing; the remote sensing efforts sponsored by NASA Headquarters were explicitly part of the *Apollo* program; and the Manned Spacecraft Center was built for *Apollo*. *Landsat*, and the extensive remote sensing research that supported it, can thus be considered part of the *Apollo* legacy (Lowman, 1996, 1999).

The first *Landsat* was followed by two essentially identical satellites and then by the much more advanced "D" version, *Landsats 4* and *5*, carrying the Thematic Mapper (Salomonson and Stuart, 1989). However, the success of the first three, coupled with progress in remote sensing technology, led to development of remote sensing satellites by other countries, including France, the former Soviet Union, Japan, and India. Several countries also had been operating classified reconnaissance satellites since the early-1960s, but although their existence was common knowledge, they had little impact on non-military remote sensing. In 1995, the formerly-secret American *Corona* program was declassified (McDonald, 1995), and its thousands of photographs will no doubt find scientific application. By the mid-1990s, satellites for study of the Earth's surface, using reflected visible or near-infrared radiation, were in wide use. Leadership in orbital remote sensing has largely passed from the United States to other countries, notably France, Canada, Japan, and western Europe in general. Private industry is taking an increasingly greater role in the field.

Returned film orbital photography, which as we have seen was a major stimulus to *Landsat* and its cousins, has been carried out more or less continuously since the end of the *Apollo* program in 1975, by cosmonauts and, when the American Shuttle program began in 1981, again by astronauts. The Space Shuttle Earth Observation Program, SSEOP (Wood, 1989; Lulla *et al.*, 1993; Apt *et al.*, 1996) has produced thousands of high-quality color photographs, a valuable low-cost public domain supplement to *Landsat*, and one area in which the United States still leads. The quality of the photographs can be enhanced by digitization (Apt *et al.*, 1996), a technique applicable to older pictures as well. The ability of the astronauts to pick out specific features has made the SSEOP pictures valuable for studies of surface changes and transient phenomena (Lulla and Helfert, 1989; Strain and Engle, 1993). The journal *Geocarto International* has been the main outlet for SSEOP photography.

An important development in geologic remote sensing has been orbital imaging radar (Settle and Taranik, 1982). The first civilian

radar satellite, *Seasat*, demonstrated the geologic value of orbital radar in its short (3-month) lifetime in 1978 (Ford, 1980). Further imaging radar experiments were carried out in 1981 by the *Shuttle Imaging Radar-A* (SIR-A), followed by SIR-B and SIR-C in later years. The success of these short experimental missions stimulated the development of applied orbital radar by the European Space Agency, the Canada Centre for Remote Sensing, and the Japanese space agency NASDA (Singhroy, 1992a,b). The 1995 launch of Canada's *Radarsat-1* marked the beginning of operational radar from orbit (Mahmood *et al.*, 1998), producing by 1998 the first complete coverage of the entire land area (including the polar caps) of the Earth, in addition to many ocean areas.

Specific geologic applications of orbital radar will be presented later.

To summarize this brief historical section, remote sensing of the Earth's surface has evolved, from localized sounding rocket photography and the 70 mm pictures taken by *Mercury* and *Gemini* astronauts, into a major field of space applications, with global coverage of the Earth being returned regularly by dozens of satellites using passive and active methods. Geologists were initially slow to realize the advantages of orbital imagery, and the leaders in applications of such imagery have been physical geographers (Estes and Senger, 1974). However, this situation has finally changed, and remote sensing from space has begun to have fundamental impact on geologic research and geologic applications. Thousands of papers and reports on geologic remote sensing have been published, most primarily on technique development. This immense mass of material can be summarized only by covering the main areas of geology in which the data from space have been used. A basic reference for all types of geology is the compilation by Short and Blair (1986).

4.3 Tectonics and structural geology

4.3.1 Global tectonic activity map

The first and most important direct geologic application of orbital remote sensing has been in the study of crustal structure, both regional (tectonics) and local (structural geology). Taking the broad view first, one result of orbital remote sensing is the global tectonic activity map (GTAM) presented in previous chapters, but repeated here for convenience (Fig. 4.2). This is the first map to show global tectonic and volcanic activity of the geologic present, "present" being defined as the past one million years. It has been reproduced

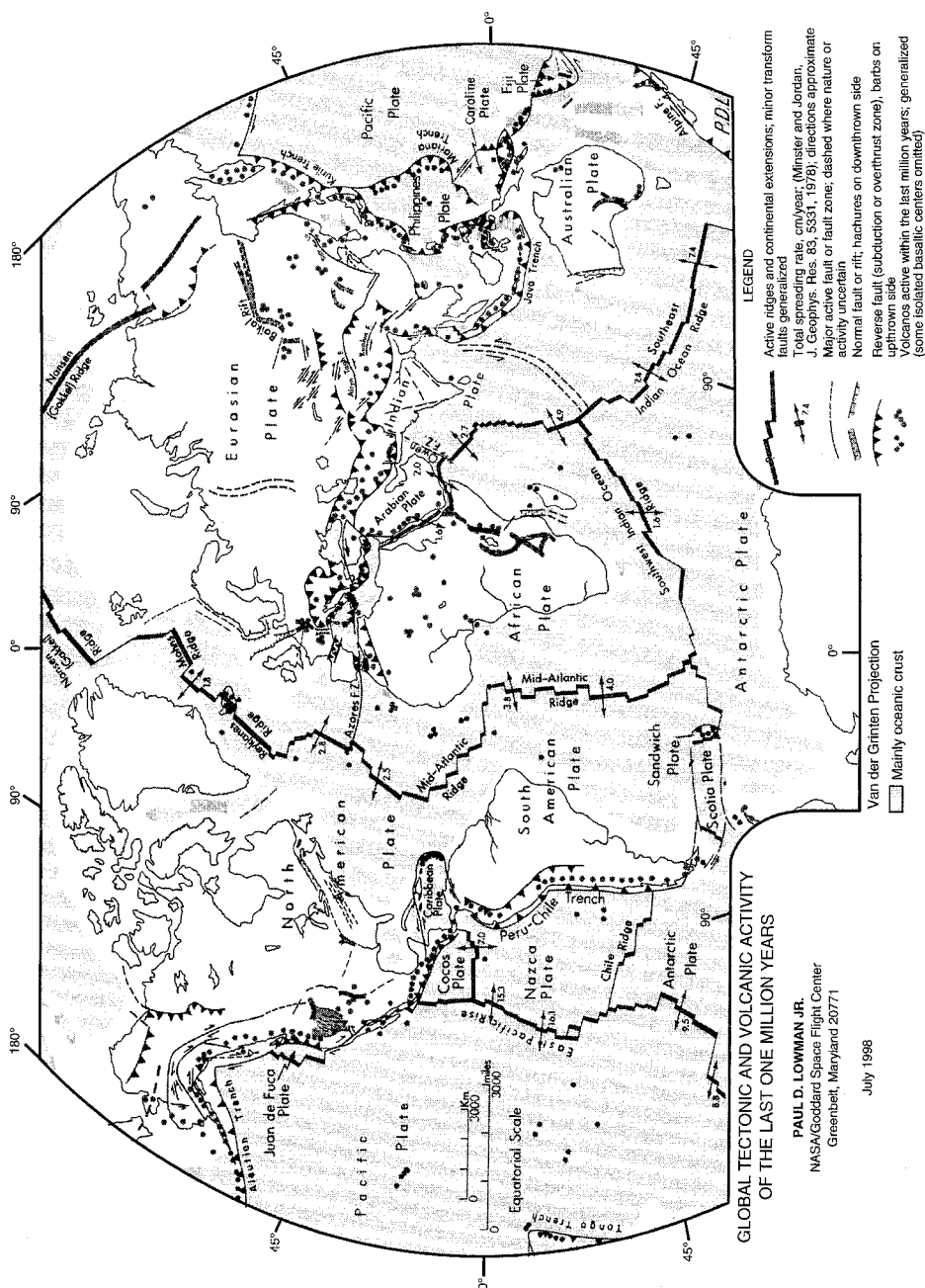


Fig. 4.2 Tectonic and volcanic activity of the last one million years.

in more than a dozen textbooks (e.g., Davis, 1984; Best, 1982; Peltier, 1989) and many scientific papers (e.g., Rubincam, 1982; McKelvey, 1986), and is currently available on the World Wide Web as discussed in Chapter 1. It was the hand-drawn precursor to the Digital Tectonic Activity Map presented in the first chapter, but has been updated in parallel with the compilation of the DTAM. The GTAM is based on remote sensing directly and indirectly: directly in that many tectonically active features were first mapped with *Landsat* imagery, in areas such as southern Asia, and indirectly in that a single compiler with a small travel budget could never have acquired enough knowledge of the planet's geology without the background provided by orbital photography, both film and digital. Data sources and compilation methods of this map have been described elsewhere (Lowman, 1981, 1982), and only the aspects relevant to remote sensing need be briefly summarized.

The primary value of remote sensing in compilation of the GTAM was the global coverage of large sparsely-settled areas such as North Africa, the Canadian Shield, and the Tibetan Plateau. For example, the Haruj al Aswad in Libya, a Quaternary volcanic field, is conspicuous from space (Fig. 4.3), but being historically inactive is not shown on maps of global volcanism. Once aware of its existence, the author was easily able to document the feature. Furthermore, its geomorphic freshness, apparent from orbital photographs, implied an age of the last activity of less than a million years. This example demonstrates the value of remote sensing for initial reconnaissance of an area, and subsequent focussing of attention on specific geologic features.

Like all global maps, the GTAM is a compilation from previously-published maps, many of which are themselves compilations. Remote sensing has been essential to the GTAM in that many of its source maps, especially in Asia, had been drawn from *Landsat*, *SPOT* (*Système Pour l'Observation de la Terre*), or other orbital imagery. The impact of remote sensing on tectonics can be illustrated first by studies of the structure of southern Asia with *Landsat* images.

4.3.2 Tectonics of southern Asia

It was the 70 mm photographs of Tibet by Gordon Cooper on the final *Mercury* mission in 1963 (O'Keefe *et al.*, 1963) that broke the ground, so to speak, for geology, but it was not until *Landsat* provided systematic vertical coverage of Asia that serious tectonic studies with orbital imagery were undertaken. Tibet and adjacent

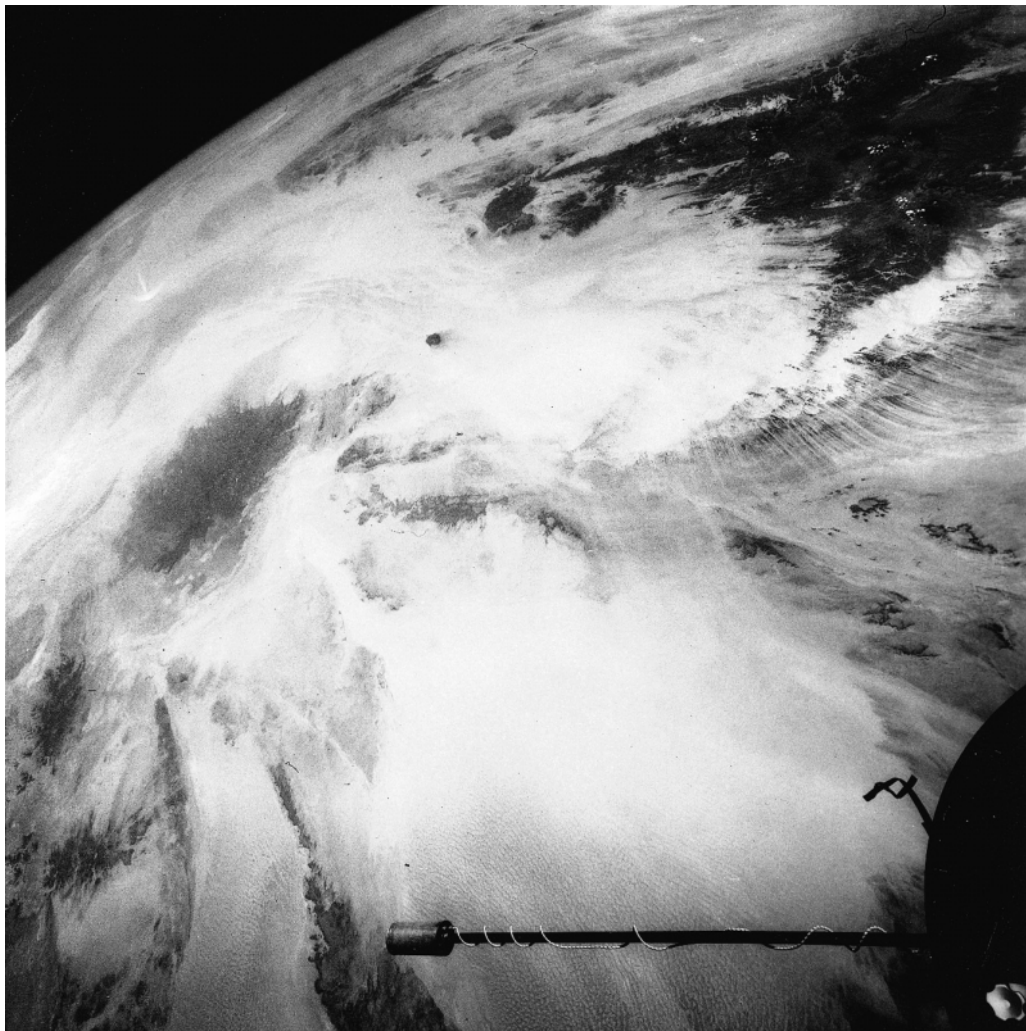


Fig. 4.3 *Gemini 11* photograph over North Africa, looking northeast. Tibesti Mountains at upper right; Marzuk sand sea bottom center, over *Agena* transponder antenna; Haruj al Aswad is largest dark area at left edge.

areas were for centuries isolated both physically and politically, and the regional geology was accordingly little known until the *Landsat* era. Molnar and Tapponnier (1975) acquired early *Landsat* MSS (MultiSpectral Scanner) imagery, whose quality is illustrated by Fig. 4.4. Similar work was done by Ni and York (1978), who compiled a monumental *Landsat* mosaic of all China and adjacent areas. Chinese geologists themselves began using *Landsat* images as soon as they became available, as demonstrated by maps in the volume

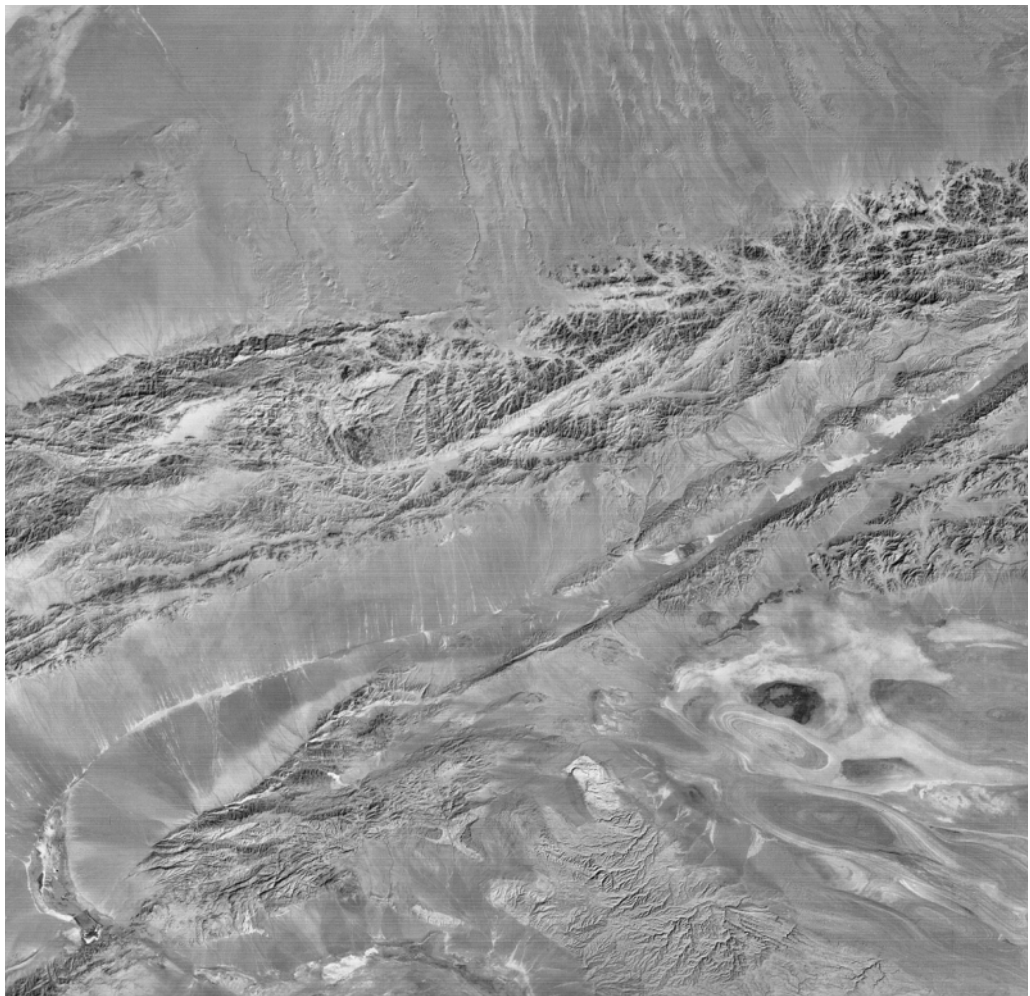


Fig. 4.4 *Landsat* picture of Altyn Tagh fault, western China, active left-lateral strike-slip fault with estimated 400 km offset. From Molnar and Tapponier (1975). *Landsat* scene 1449-04062, 15 October 1973. Width of view ~185 km.

Geotectonic Evolution of China (Huang, 1987). Dozens of papers have been based on the use of *Landsat* and more recently *SPOT*. An especially interesting use of *SPOT* images has been made by Zhang *et al.* (1995), who showed that the grabens of the Ordos Plateau (Fig. 4.5) and the faults just to the south could be explained by the extrusion models of Molnar and Tapponier.

The result of these efforts has been nothing less than a revolution in our knowledge of the tectonics and seismicity of southern Asia. Dozens of little-known active faults have been mapped and

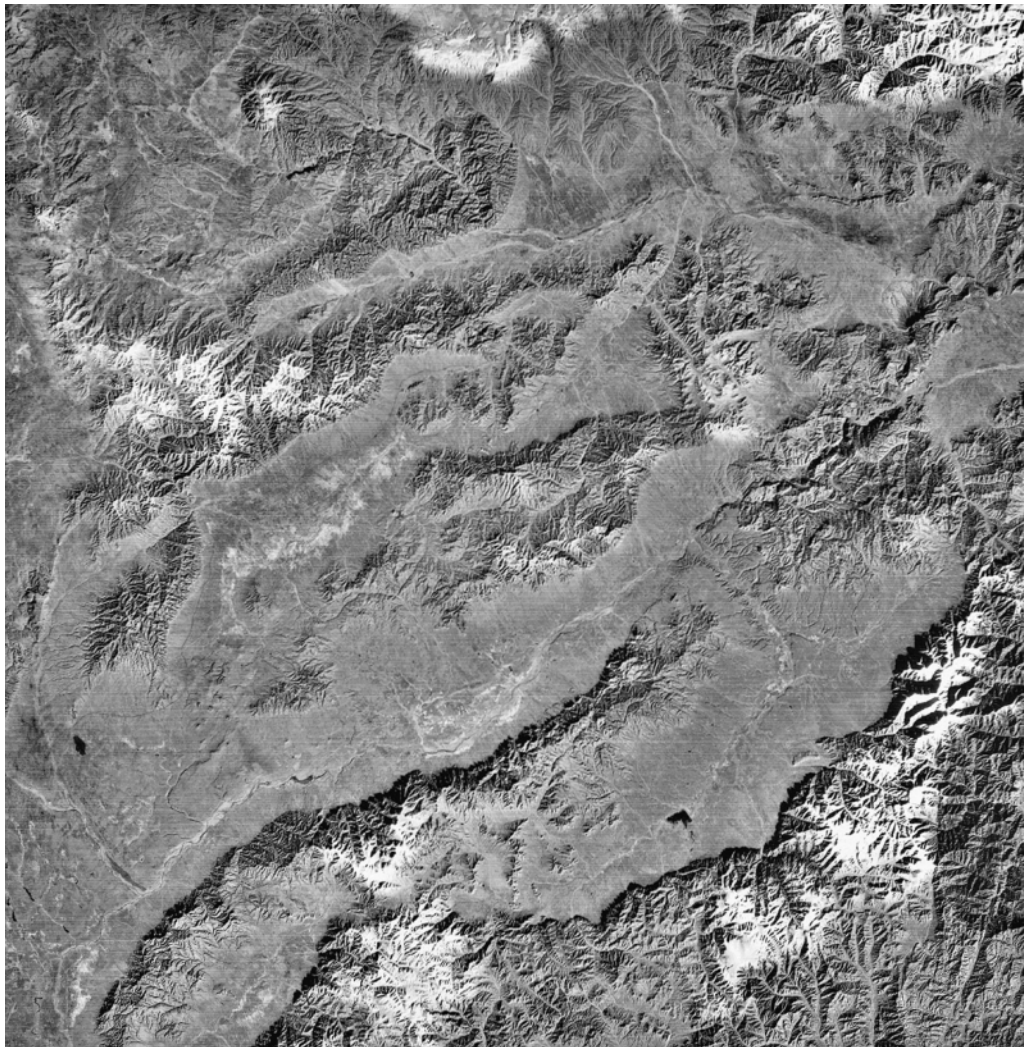


Fig. 4.5 *Landsat* picture of grabens in the Ordos Plateau, Inner Mongolia, about 500 km west of Beijing. Width of view 185 km.

their sense of motion determined, both from satellite imagery and from correlated seismic data. The main tectonic implications of the various studies are the following.

The validity of plate tectonic theory for southern Asia has been both confirmed and in a sense contradicted. Taking the contradictions first, the *Landsat* images and maps derived therefrom show that, contrary to early publications (e.g., Dewey and Bird, 1970), there is no definite plate boundary in southern Asia, in particular between the Eurasian and adjacent plates such as the Indian Plate

(see Fig. 4.2). A north-south region more than 2500 km wide, from the front of the Himalayas to Siberia, is actively deforming, as shown both by the distribution of seismic activity and the geomorphology of faults (see Figs. 4.4, 4.5). This area has been termed “intraplate” by York and co-workers in their *Landsat* study, and this term has been applied by many other authors to similar broad deformation zones elsewhere such as the Basin and Range Province (Fig. 4.2). However, if a “plate” is defined as a relatively rigid and inactive segment of lithosphere bounded by some combination of ridge, trench, or transform fault, the term is not at all valid for such areas. This contradiction gets to the very heart of modern tectonic theory: Can continental deformation be validly described in terms of plate interaction? It has been recognized for many years (e.g., McKenzie, 1968; Atwater, 1970; Burchfiel, 1980) that plate boundaries in continents tend to be diffuse ones. The tectonic studies of Asia with *Landsat* have shown clearly that simple application of plate tectonic concepts to such areas is unrealistic (Lowman *et al.*, 1999).

Taking a more positive view, the *Landsat* studies of Molnar and Tapponier, and the many subsequent ones, have shown that tectonic and seismic activity in southern Asia can be interpreted by a coherent model of rigid indentation (Molnar and Tapponier, 1975). The Indian subcontinent is treated as a rigid indenter, deforming a plastic medium, the resulting slip lines being expressed as faults. The resulting regional motion is one in which Tibet and western China are being extruded to the east. Similar interpretations have been applied to other continental areas. Whether these models are correct can not be discussed here at any length. For example, another *Landsat* study of western Tibet by Searle (1996) found that the Karakorum fault has apparently undergone only limited right-lateral offset, far less than the extrusion model requires. Searle thus argued that this fault was a relatively young feature, not related to the supposed early-Cenozoic of India with Asia. Allen *et al.* (1993) had previously used *Landsat* imagery of the Turfan Basin, far north but at roughly the same longitude as the Karakorum Fault, to infer thrusting, possibly along Paleozoic trends. The main point in the present context is that the use of remote sensing imagery of Asia has not only transformed our knowledge of this area, it has produced testable theories of the very nature of continental deformation.

The examples just discussed are from a large, remote, and until recently poorly-mapped region, and the advantages offered by satellite coverage were obvious immediately. However, it can be asked if remote sensing has much to show in areas already covered by modern, large-scale geologic maps. When *Landsat* imagery was first

acquired, L. W. Morley commented, referring to the Canadian Shield, that this imagery would have been useful 20 years earlier, but that the Shield had by 1973 already been mapped at a reconnaissance scale. Our next remote sensing example will therefore be taken from a nominally well-mapped area, southern California.

4.3.3 Elsinore Fault

Because of its low latitude, the part of California from Los Angeles south was covered by astronaut photographs beginning with the first *Gemini* mission (GT-3) in 1965. These photographs eventually produced an excellent example of remote sensing photointerpretation of easily accessible and well-mapped regions (Singhroy and Lowman, 1997).

The example begins with an early oblique 70 mm view of the Salton Sea (Fig. 4.6) and adjacent areas taken by astronauts Conrad and Cooper in 1965. Although notable for the conspicuous gyre in the Salton Sea (probably suspended sediment, circulated by the usually strong southerly winds from San Gorgonio Pass), this photograph also shows a number of conspicuous lineaments in the Peninsular Range, accentuated because they parallel the camera axis. It was noticed by the writer (Lowman, 1980) that several of these lineaments intersected the Elsinore Fault without horizontal offset. Since the Elsinore Fault is active, and parallels the other members of the horizontally-moving San Andreas fault family in southern California, this was a critical anomaly. Further orbital photography (Figs. 4.7, 4.8), this time from the *Apollo* 9 mission flown by astronauts McDivitt, Scott, and Schweikart, produced systematic multispectral coverage as part of the S065 experiment (Lowman, 1969), essentially a returned film simulation of *Landsat*. The Peninsular Range photograph was used to make a much more detailed map, and showed the most crucial areas for field checking and low-altitude reconnaissance flights (Figs. 4.9, 4.10).

This field checking showed that a bedrock ridge, the extension of a lineament visible on the original GT-5 photograph, was cut by the Elsinore Fault, but with no horizontal offset. Close-range examination of the fault plane on the ridge showed slickensides (Fig. 4.11) indicating pure dip slip, at least for the last movement. It was concluded that, contrary to all previous interpretations, the Elsinore Fault in this area is a dip-slip fault, not a strike-slip one (Lowman, 1980). Independent field mapping by others (Todd and Hoggatt, 1989), and an orbital radar study by Schultejann (1985) confirmed this interpretation.

The sequence of events in this example is worth summarizing to



Fig. 4.6 (See also Plate XIII) *Gemini 5* photograph over Salton Sea, looking northeast. Note linear valleys at lower left, crossing Elsinore Fault without offset. Gyre in Salton Sea is formed by winds through San Gorgonio Pass (left). Width of view ~150 km at center of photograph.

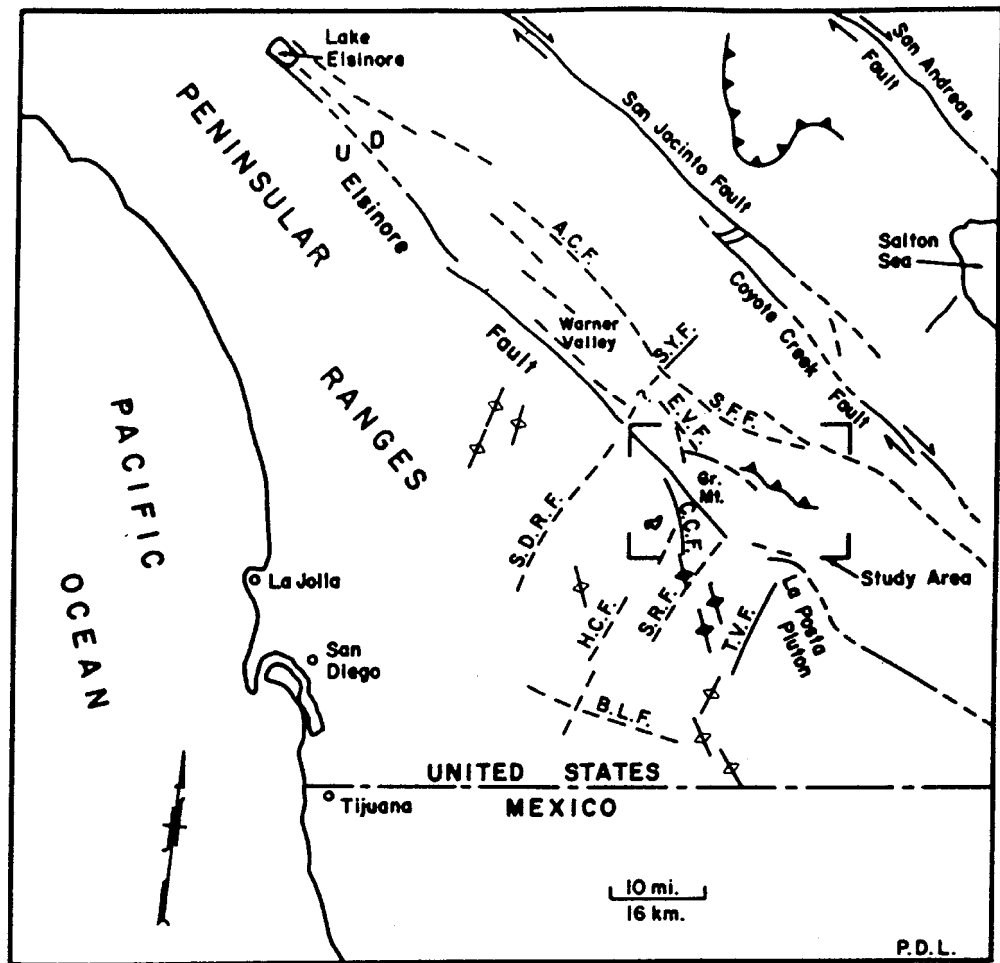
illustrate the geologic use of remote sensing even for well-mapped areas. The first photographs, from GT-5, revealed an apparent anomaly: bedrock features cut by an active supposed strike-slip fault but without horizontal offset. Subsequent photographs, from *Apollo 9*, revealed critical areas on which field work should be focussed, guided by standard air photos and low-altitude reconnaissance obliques. This field work confirmed the photogeologic interpretation, one directly contradicting all previous views. Furthermore, the field work occupied less than three weeks total outcrop time, and was done by an eastern geologist initially unfamiliar with the area. The



Fig. 4.7 *Apollo 9* view of Peninsular Ranges, California. The original (one of a four-frame series) was a false color infrared image. See Fig. 4.8 for interpretation of features.

point of this example is not the cleverness of the interpretation, which could have been done – given the photographs, and having the problem defined – by a third-year geology student with strong legs. Rather, the Elsinore Fault study is presented as a typical example of the methodology permitted by remote sensing, starting with the most crucial part of any scientific research: recognition of the problem (Singhroy and Lowman, 1997).

A much more advanced remote sensing investigation of southern California structure has been carried out by Ford *et al.* (1990), using *Landsat Thematic Mapper* (TM) imagery to map faults in the Mojave Desert. This example is notable in that Ford *et al.* used

LEGENDMajor fault:

- A.C.F. Aqua Caliente
- B.L.F. Barrett Lake
- C.C.F. Chariot Canyon
- E.V.F. Earthquake Valley
- H.C.F. Horse-thief Canyon
- S.F.F. San Felipe
- S.D.R.F. San Diego River
- S.R.F. Sawtooth Range
- T.V.F. Thing Valley

Thrust fault; barbs on upper block

Generalized foliation in steeply dipping metamorphic (↔) or igneous (↙) rocks

Fig. 4.8 Sketch map of Fig. 4.7. From Lowman (1980).

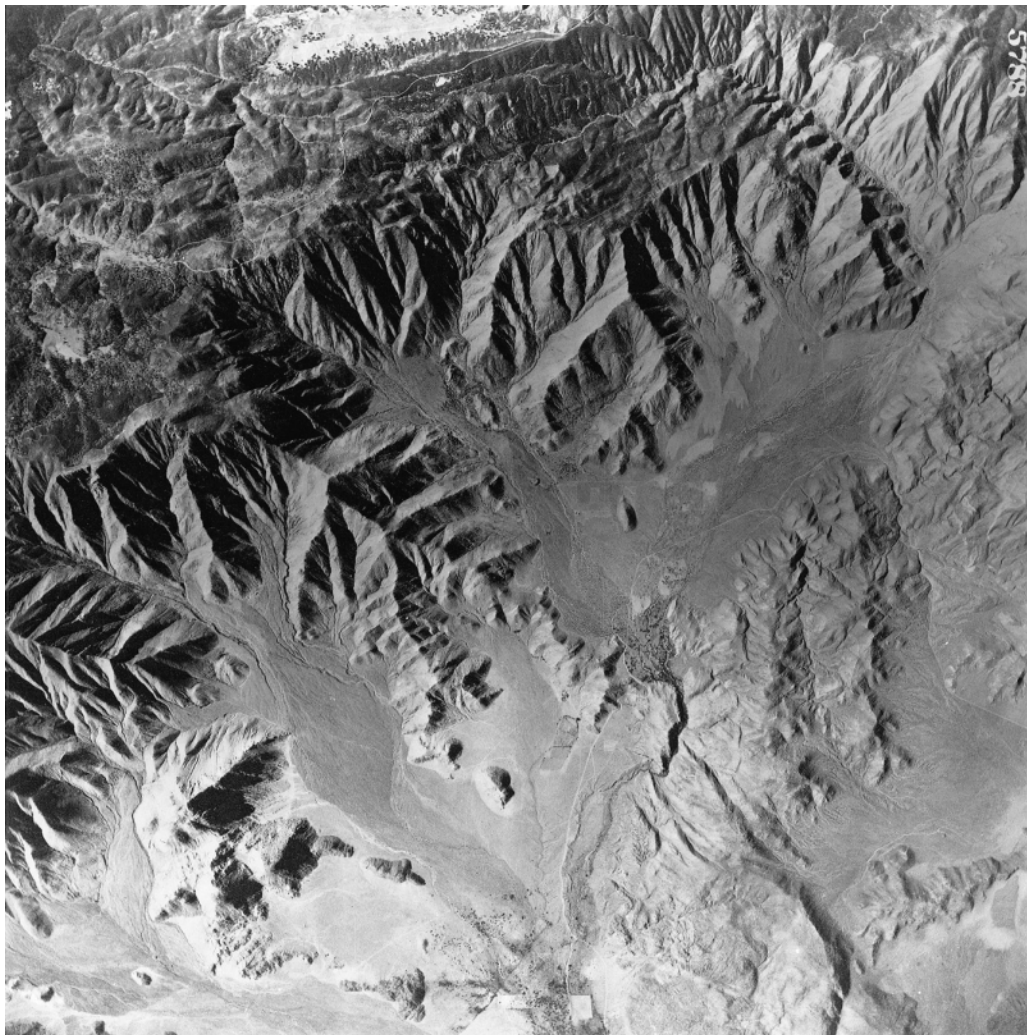


Fig. 4.9 High-altitude aerial photograph of east edge of Peninsular Ranges; note angular ridge at center (Sawtooth Range). Width of view 10 km.

lithologic discrimination based on TM infrared bands, rather than simple photogeology based on landforms. The example also demonstrates again the value of remote sensing in an accessible and supposedly well-mapped area, in this case just 2 hours drive from Los Angeles.

Radar interferometry, to be discussed in Subsection 4.5.1 on volcanism, has produced an entirely new type of tectonic activity map of the Mojave Desert (Massonet *et al.*, 1993a). This technique permits continuous mapping of crustal displacement as small as a few centimeters over hundreds of square kilometers.



Fig. 4.10 Low-altitude oblique photograph from 2000 feet above ground, looking to northeast, over Sawtooth Range. From Lowman (1980). Elsinore Fault crosses ridge where highway makes a U-curve; exposed in road cut at Campbell Grade. Photograph taken 1970, by author. Width of view ~5 km at center of photograph.

4.3.4 Lineament tectonics

It has been known for many years that the continental crust in stable areas, i.e., cratons, is pervaded by a network of lineaments: straight or nearly straight topographic features of regional extent that express some sort of bedrock structure, commonly fractures (Fig. 4.12). It was proposed by Hobbs (1911) that these features form a relatively simple pattern of roughly orthogonal fractures, global or nearly so in extent (Hodgson, 1976). Aerial photographs were used to map these features for many years, but the sudden availability of global coverage from *Landsat*, beginning in 1972, triggered a surge of interest in what became known as “basement tectonics”



Fig. 4.11 Outcrop view of fault plane of Elsinore Fault, showing slickensides indicating dip slip for last movement. Pen gives scale.

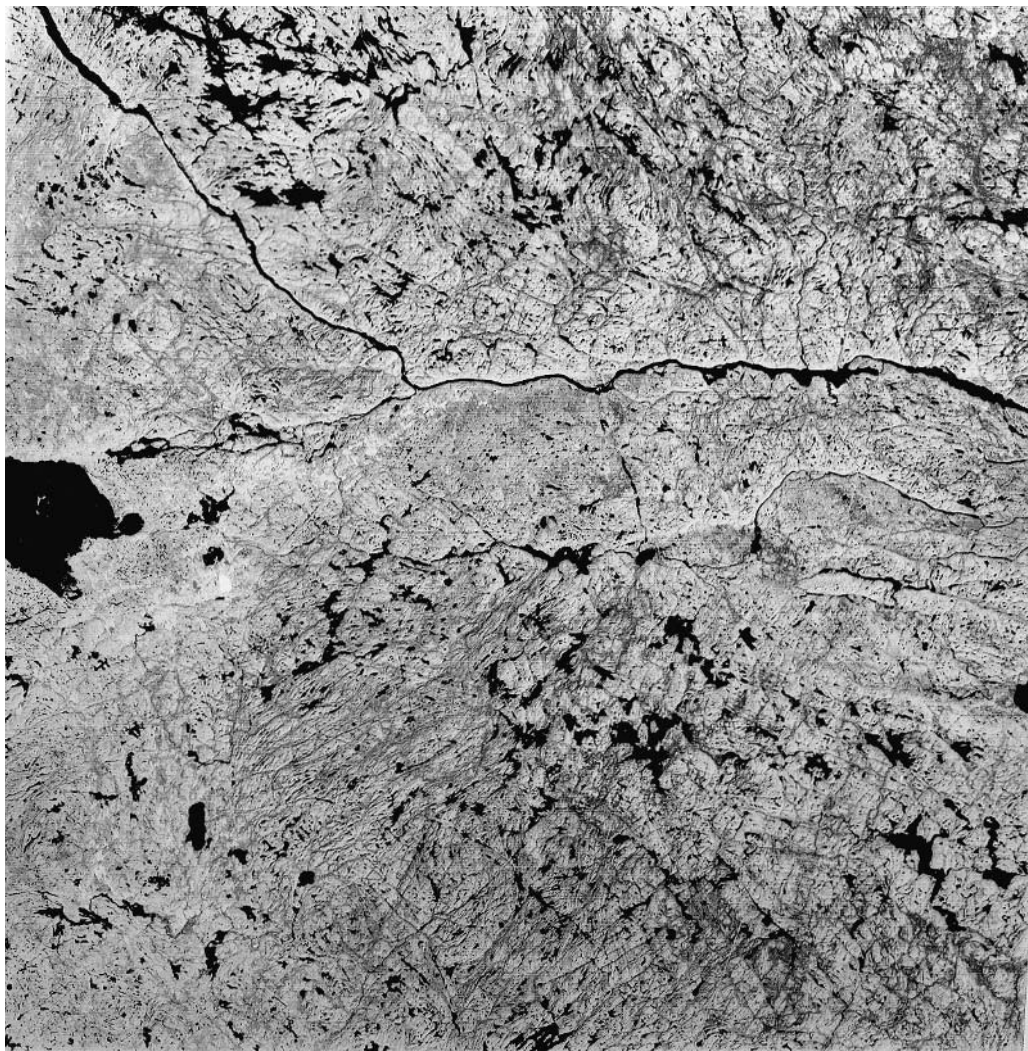


Fig. 4.12 *Landsat* picture of Ottawa River in Ontario; Lake Nipissing and North Bay at extreme left. Scene acquired October 1973; accentuates topography and fracture systems. Valley considered part of Ottawa–Bonnechere graben system, suggested by Kumarapelli and Saull (1966) to be a branch of the world rift system through the St. Lawrence River. Width of view 185 km.

(Nickelsen, 1975; Hodgson *et al.*, 1976). Several symposia with that title were held, and scores of papers on lineaments were published in other places. However, the topic remains controversial, with little agreement on the nature, origin, and to some extent even the existence of lineaments. As used here, “lineament” will refer to well-defined, relatively narrow linear topographic features, although

the term is sometimes applied to broad zones of faults, dikes, igneous intrusions, and volcanic features. The term will also exclude lines expressing the strike of sedimentary strata, igneous flow structure, or volcanic layering. This exclusion, following conventional photogeologic techniques, is necessary to prevent lineament maps from becoming simply pen-and-ink sketches of the aerial or space photographs.

The reality of lineaments, as the term is used here, is actually unarguable for many areas such as the Canadian Shield (Fig. 4.12). Furthermore, they are generally agreed to express brittle fractures of some sort, either faults or joints, or dikes intruding such fractures. Lineaments are of far more than scientific interest, being known in many areas to localize mineral deposits (Kutina and Hildenbrand, 1987), oil or gas reservoirs, or ground water. In addition, as basement fractures, they may represent local geologic hazards, such as mine roof falls or slope failure in road cuts, and may localize seismic activity (Mollard, 1988). Kusaka *et al.* (1997) have applied orbital radar and optical imagery to lineament mapping in Japan, finding the orbital data a valuable aid in estimating landslide risk. Remote sensing has thus found immediate and wide application in lineament tectonics. Geophysical studies, aeromagnetic and gravity field in particular, have also been applied to lineament problems (Quersh and Hinze, 1989).

The primary questions about lineaments are, first, whether they do in fact form a global unified network of more or less orthogonal fractures, and, second, whether they are tensile or compressional (i.e., vertical shear) fractures. Given the purpose of this chapter – to review the impact of space remote sensing on geology – treatment will be restricted to a few examples of how remotely-sensed data are being applied to lineament tectonics, with some of the conclusions reached.

The Canadian Shield is an ideal area in which to study lineaments by remote sensing. It has been tectonically quiet for at least one billion years, providing ample time for differential erosion to etch out lineaments. By definition, the basement, i.e., the Precambrian crystalline rock, is generally well exposed. Finally, the Shield lies in two countries with close scientific ties and strong remote sensing capabilities. For these reasons, a major study of lineaments on the Shield was undertaken by the writer and his colleagues (Lowman *et al.*, 1992), with the general objective of testing the theory that lineaments form a unified global or at least continental network, or “regmatic shear pattern” (Sonder, 1947). Standard

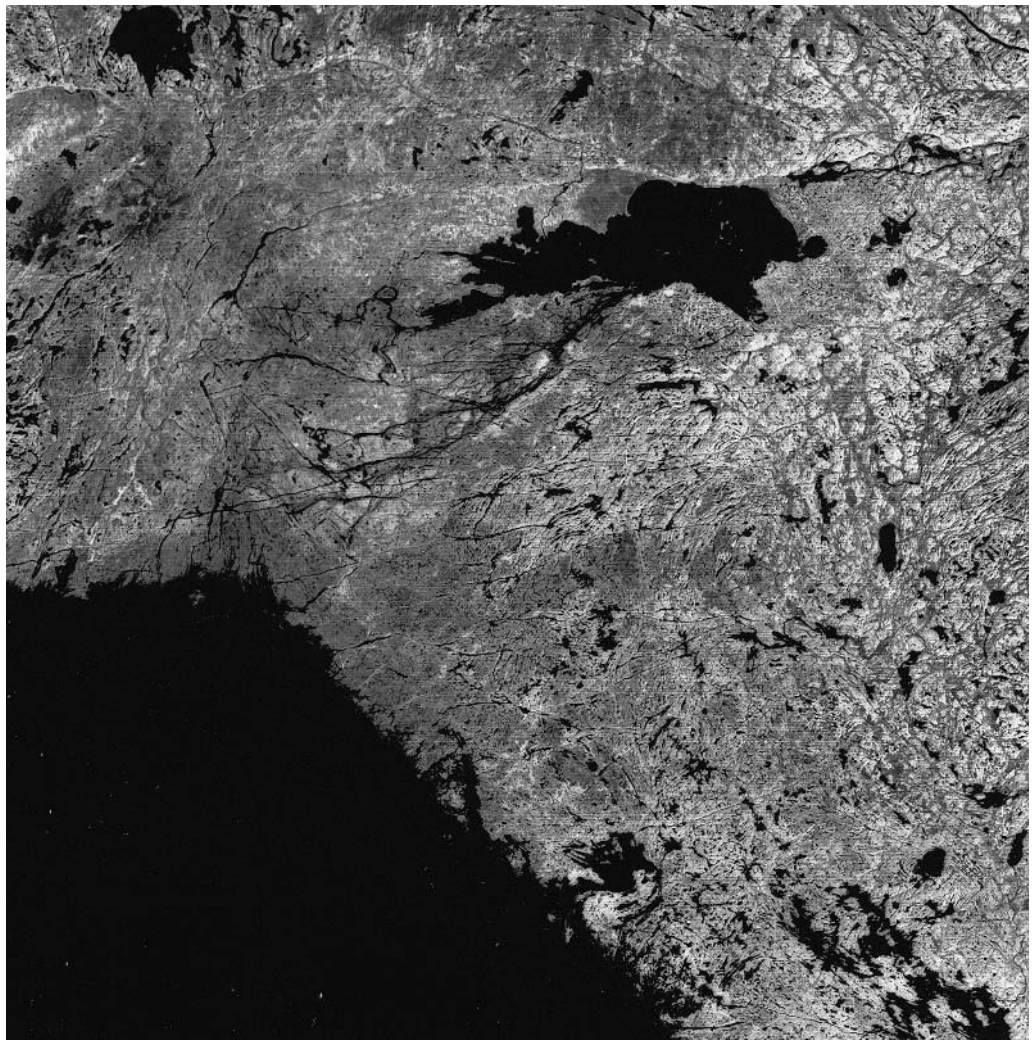
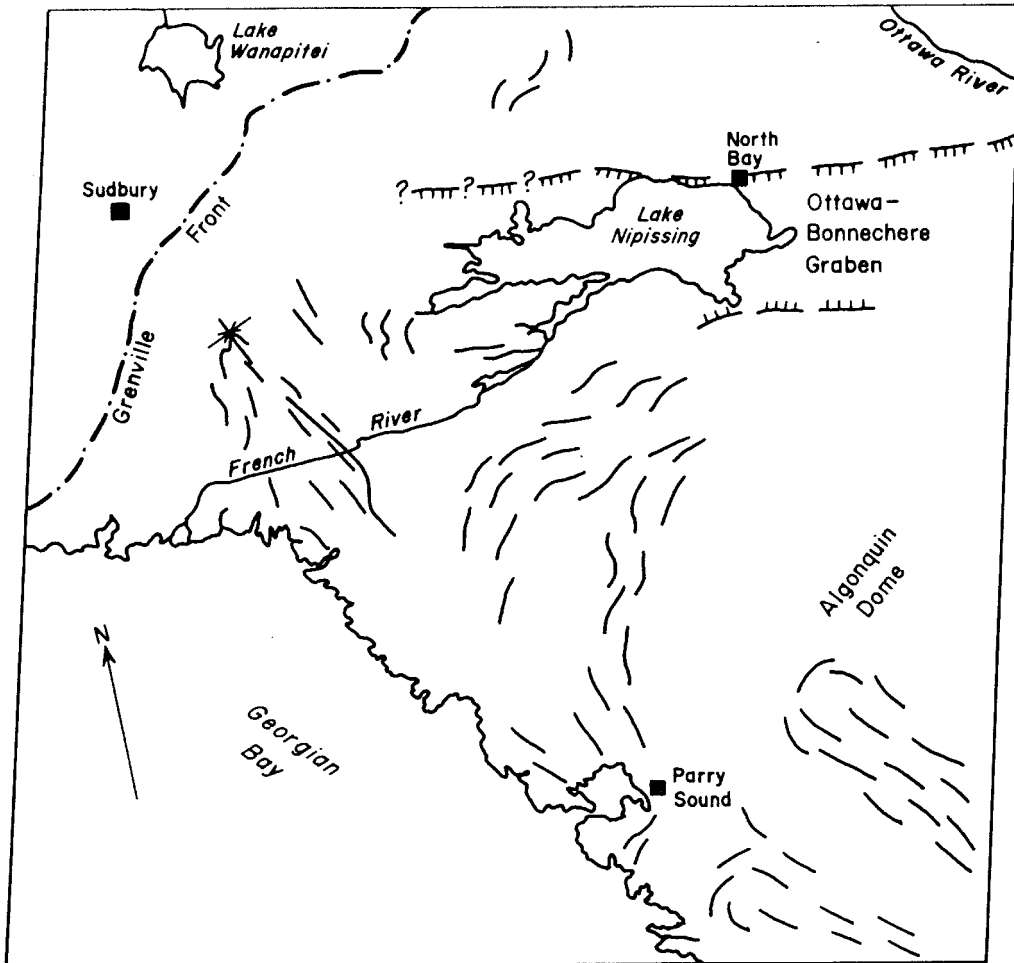


Fig. 4.13 *Landsat* picture of Georgian Bay, Ontario, and adjacent Grenville Province. North Bay at top center. From Lowman *et al.* (1992). Width of view 185 km.

photogeologic methods were applied to 60 low-Sun-angle *Landsat* scenes covering parts of all structural provinces of the Shield (e.g. Fig. 4.13). The resulting lineament maps (Fig. 4.14 (a–c)) were digitized and rose diagrams (azimuth-frequency plots) drawn by computer. Some field checking was done, although the enormous area covered by 60 *Landsat* scenes obviously made anything like thorough field work impossible. Orbital radar imagery was available for



GEOLOGIC SKETCH MAP

Landsat 2 MSS Scene, 2620-15192-7
Scene Center N45°54', W80°10'; Width 185 km.

LEGEND

- ||— Strike of foliation, lithologic contacts, or flow structure
- Normal fault; teeth on down-thrown side
- Trace of Grenville Front

P.D. Lowman

Fig. 4.14(a) Sketch map of Fig. 4.13.

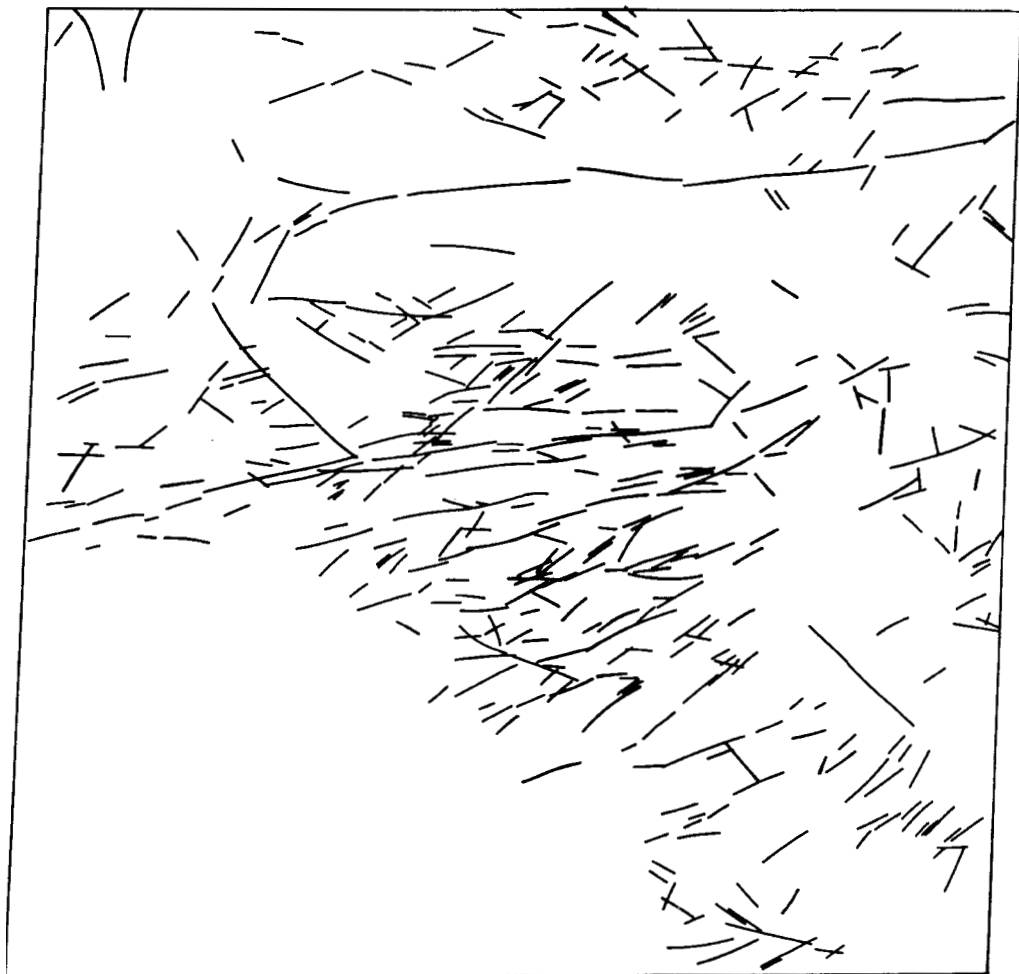


Fig. 4.14(b) Lineaments drawn from Fig. 4.13.

some areas (e.g. Fig. 4.15), providing an interesting comparison with *Landsat*. Radar has proven unusually valuable for structure mapping and lineament mapping in general (Singhroy *et al.*, 1992; Lowman, 1994; Kusky *et al.*, 1993), one reason being its sensitivity to look direction. Structures nearly perpendicular to the illumination are strongly highlighted, as Fig. 4.15 shows, bringing out subtle features not obvious on standard visual images.

Several conclusions were reached, some contradicting majority opinion on the nature of lineaments. The most general conclusion

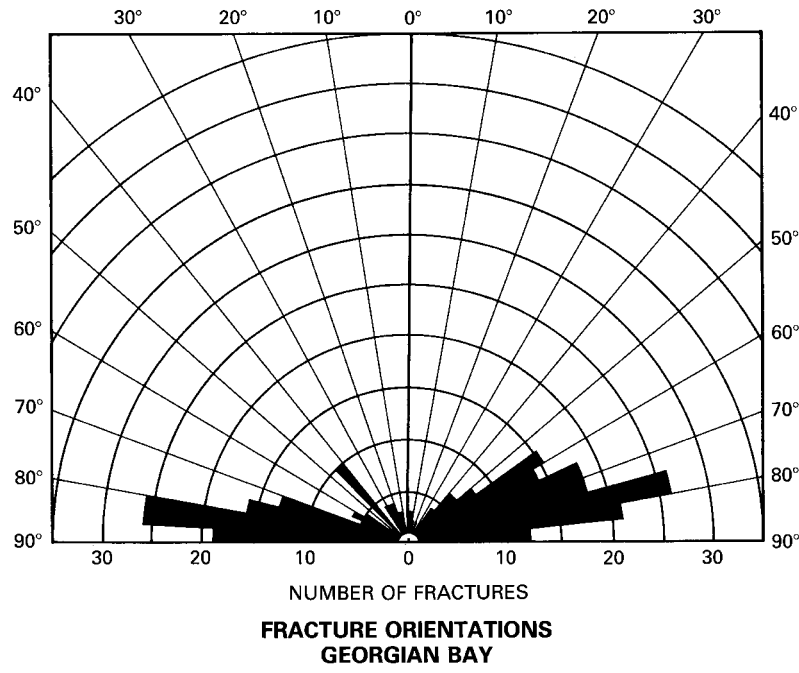


Fig. 4.14(c) Rose diagram of lineaments in Fig. 4.14(b).

was that if there is such a thing as a unified network of orthogonal fractures, it is not visible on *Landsat* images. The reality of the mapped lineaments is unquestionable, thanks to field checking and available geologic maps, and many of them turned out to be basaltic dikes of known dike swarms, or empty fractures parallel to such dikes (Fig. 4.16). The unfilled lineaments checked in the field proved to be extensional, either normal faults or joints, not shear fractures. A similar conclusion had been reached by Nur (1982) on the basis of *Landsat* images of Israel, where the desert climate has etched out lineaments.

An important conclusion reached by many lineament investigators is that lineaments in relatively young rock may be re-activated fractures of much greater age. The term “recurrent tectonics” has been applied by Onasch and Kahle (1991) to the Bowling Green fault in Ohio, which appears to represent movement along the one billion year old Grenville Front, whose southwest extension continues under the Paleozoic sediments of the mid-continent region. The Ottawa–Bonnechere graben, shown in Fig. 4.12, localizes low-level seismic activity, even though it is Paleozoic or older in age. The extent of such fracture re-activation is an important problem, since



Fig. 4.15 ERS-1 radar image of Sudbury area, northern Ontario. Linear contrast stretch applied at Goddard Space Flight Center. Image acquired July 1992. Illumination from right. Width of view ~100 km.

“neotectonic,” i.e., newly-formed joints should parallel the principal horizontal stress direction (Engelder, 1982; Hancock, 1991) thus providing a good indication of regional stress fields.

One very interesting aspect of the Canadian Shield *Landsat* study was that the mapped lineaments were found to be fractal, i.e., scale-

CUMULATIVE FRACTURE ORIENTATIONS CANADIAN SHIELD

province boundary
 shield boundary
 Base: Tectonic Map of North America, P.B. King, 1969
 Bipolar oblique conic conformal projection

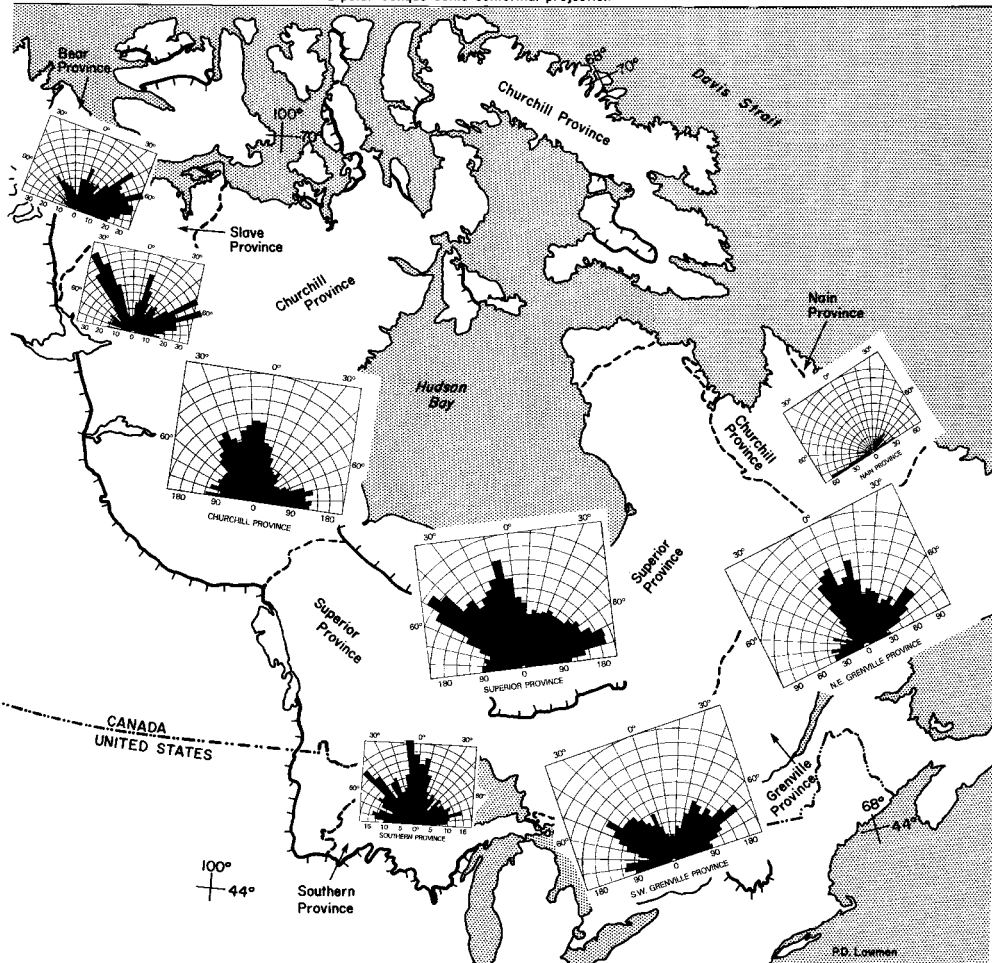


Fig. 4.16 Cumulative rose diagrams for provinces of Canadian Shield, drawn from 60 low-Sun-angle *Landsat* scenes. From Lowman *et al.* (1992 1994).

invariant. Those mapped along the Ottawa–Bonnechere graben in Ontario, for example, were found to be similar in orientation and origin to joints visible in outcrop (Figs. 4.17, 4.18). The Ottawa–Bonnechere graben has been shown by Kumarapeli and Saull (1966) to be possibly related to the world rift system through



Fig. 4.17 View to west from Highway 69 bridge over French River, Ontario; see Fig. 4.14(a) for location. Valley occupies site of a now-eroded diabase dike, part of the Grenville Swarm (Fahrig and West, 1986), controlled by Ottawa–Bonnechere graben.

the demonstrably tectonic St. Lawrence valley. If this interpretation is correct, it shows how tectonic features of global scale can be traced down to the outcrop – a striking example of the fractal concept.

The fractal concept has been familiar to structural geologists for a century, though not under that name, in that small structures such as joints often mirror regional joint networks. Small folds similarly parallel much larger ones. The fractal nature of geologic structures in general is important for the use of remote sensing data, by showing that structures visible from space may be repeated at increasingly smaller sizes. The fractal dimension of *Landsat*-mapped lineaments on the northern Great Plains was applied to tectonic interpretation by Shurr *et al.* (1994).

This summary has only touched on the now-enormous literature on lineament tectonics. The subject will be revisited below in relation to other geologic fields, such as mineral deposits and petroleum exploration. At this point, it can only be noted that despite the flood of remote sensing imagery, and the large number of studies using it, lineaments are in general still a controversial and poorly-understood feature of the Earth's crust.



Fig. 4.18 Joints in outcrop on south side of French River (left in Fig. 4.17). Joints parallel French River and other lineaments; main joint by Brunton compass strikes due west. Compass is 8 cm square.

4.4 Exploration geology

Exploration for oil, gas, and minerals has traditionally been the chief field of applied geology, and it is understandable that remote sensing has had perhaps its greatest geologic impact in these areas (Rowan, 1975; Goetz *et al.*, 1983). Potential oil traps in the then poorly-mapped Tibetan Plateau were found on the very earliest orbital photography, taken by Gordon Cooper on the MA-9 mission (O'Keefe *et al.*, 1963), one of the factors that, as mentioned previously, stimulated interest in remote sensing for earth resources. In the decades since, exploration geology has applied a wide range of remote sensing techniques, and orbital data have long since become an operational tool, not simply an experimental one. The following subsections and examples are intended to summarize this now-enormous field, and to guide interested readers to further information sources.

4.4.1 Petroleum exploration

The search for oil and gas, lumped hereafter for convenience as "petroleum," has for many years been one of the most fertile fields for application of new discoveries in geophysics and geology, and this is now true for remote sensing. As pointed out by Vincent (1997), the petroleum industry was initially sceptical about remote sensing because the resources it seeks are generally far below the surface. The easily-found on-shore reservoirs, i.e., those visible from above, have already been found, although Halbouty (1976) showed that many giant oil fields could have been located with *Landsat* had it been available earlier. However, remote sensing has turned out to be so valuable for petroleum exploration, directly and indirectly, that it is now a standard tool for discovery and development of new fields and a shining example of the ultimate value of space technology.

A brief review of the principles of petroleum exploration will be helpful. Most exploration techniques are not intended to find oil or gas directly; they are instead focussed on locating traps where hydrocarbons have accumulated. These traps may be structural, such as anticlines, or stratigraphic (concordant hydrocarbon-bearing strata sealed from the surface), or they may occur around salt domes or igneous bodies. However, the first oil fields were located by seeps, and even today seeps are useful targets, especially for offshore exploration where they may be visible from space, especially with radar (Estes *et al.*, 1985) as slicks. An increasingly useful indicator for petroleum has been developed primarily from *Landsat* (Donovan *et*

al., 1974) and other remote sensing methods: subtle discoloration of bedrock, soil, or vegetation caused by chemical reactions with escaping hydrocarbon gases.

Petroleum exploration has become an extremely complex process, generally involving a wide range of geophysical, field geology, and now remote sensing techniques, and it is only rarely that a successful exploration well is drilled on the basis of a survey with one technique. The most effective use of remote sensing data, such as *Landsat* imagery, is generally as a means of focussing surface and subsurface surveys. Seismic prospecting, for example, can be far more efficient if survey lines can be laid out on the basis of structure mapping with remote sensing techniques. At least one company has made *Landsat* reconnaissance a requirement before seismic surveys are begun in a new area (Sabins, 1998).

The obvious question to be answered sooner or later is: Has any oil or gas actually been discovered by remote sensing from space? A simple answer is not possible. One might as well ask: Did radar win World War II? The answer to both questions is essentially yes, BUT only in combination with many other technologies and as part of broad strategic approaches. Remote sensing has played a vital role in several petroleum discoveries, described by Sabins (1998), Vincent (1997), and many other authors. The use of remote sensing can best be summarized with two examples, from the work of Sabins (1998) of data from areas now in production.

The first of these examples, from Sabins (1997) is focussed on northwestern Colorado (Figs. 4.19, 4.20) shown on a *Landsat* MSS image that brings out the structure unusually well. The area shown includes several producing oil and gas fields, all localized by anticlines so well-expressed they are locally termed "sheep-herder structures." These fields long pre-date *Landsat*, but they illustrate the potential value of *Landsat* and similar imagery for regional reconnaissance of less-known areas.

The second example, from Sabins (1998), is in Saudi Arabia. It is an extremely useful one in that *Landsat* TM images were used to detect a structural trap more than 2 kilometers down. The area is on the Central Arabian Arch, a regional eastward-dipping homoclinal flanking the Precambrian Arabian Highlands, as shown first on a *Landsat* mosaic (Fig. 4.21) and then on a single *Landsat* frame (Fig. 4.22). As related by Sabins, the Saudi government directed Aramco to carry out petroleum exploration outside the already producing areas flanking the Persian Gulf. Using *Landsat* Thematic Mapper images (Figs. 4.23, 4.24), Sabins and his colleagues identified a geomorphic feature, the Raghbir anomaly, a topographic depression

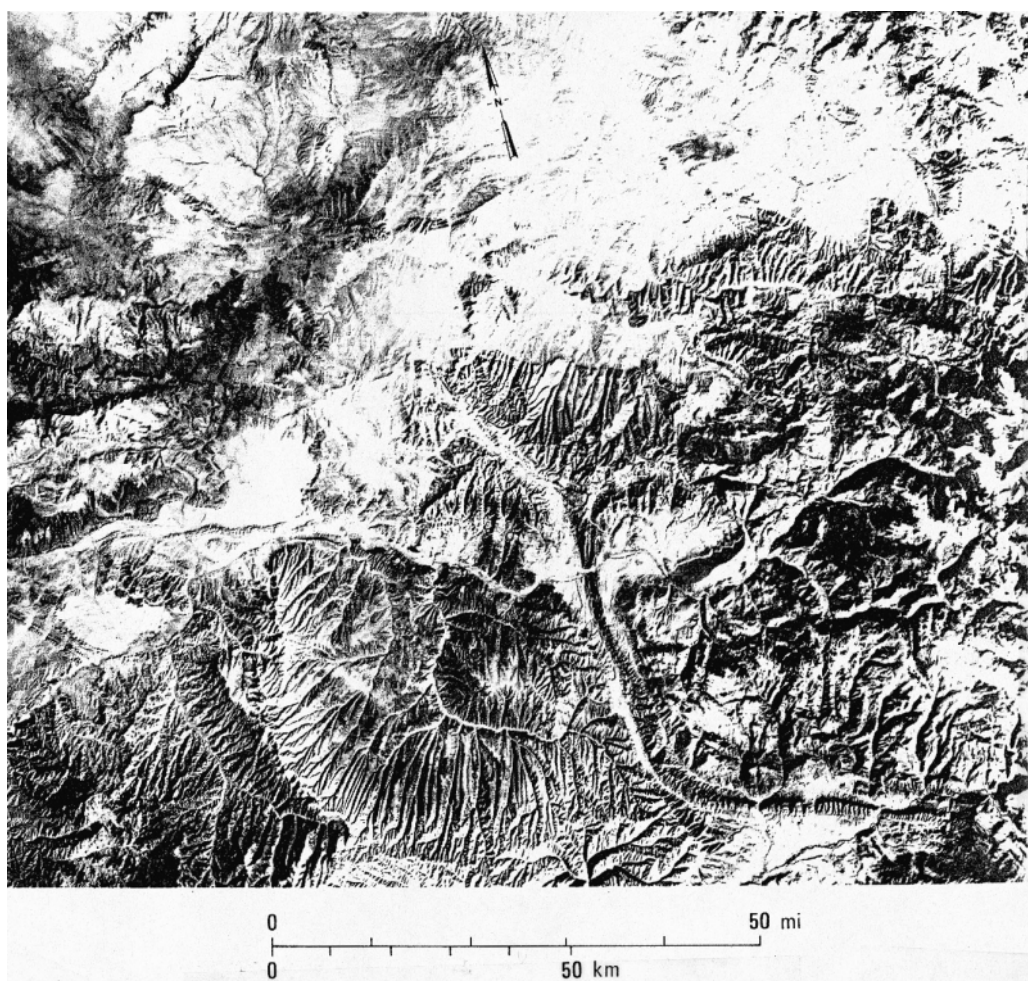


Fig. 4.19 *Landsat* picture of White River uplift, northwest Colorado. From Sabins (1997).

expressing a flattening of the regional dip caused, in turn, by an anticline in the Paleozoic strata about 2.5 km down. This anticline was formed by movement on steeply-dipping faults in the Precambrian basement, an incidental example of the importance of basement tectonics even though there are no visible lineaments in this area. Guided by the *Landsat* interpretations, seismic surveys and field checking were carried out. The Raghib anomaly was drilled in 1989, with commercial amounts of oil and gas found.

The Raghib case history should be a classic example of the use of remote sensing for petroleum exploration “to generate exploration targets” in the apt phrase of Agar and Villanueva (1997). In

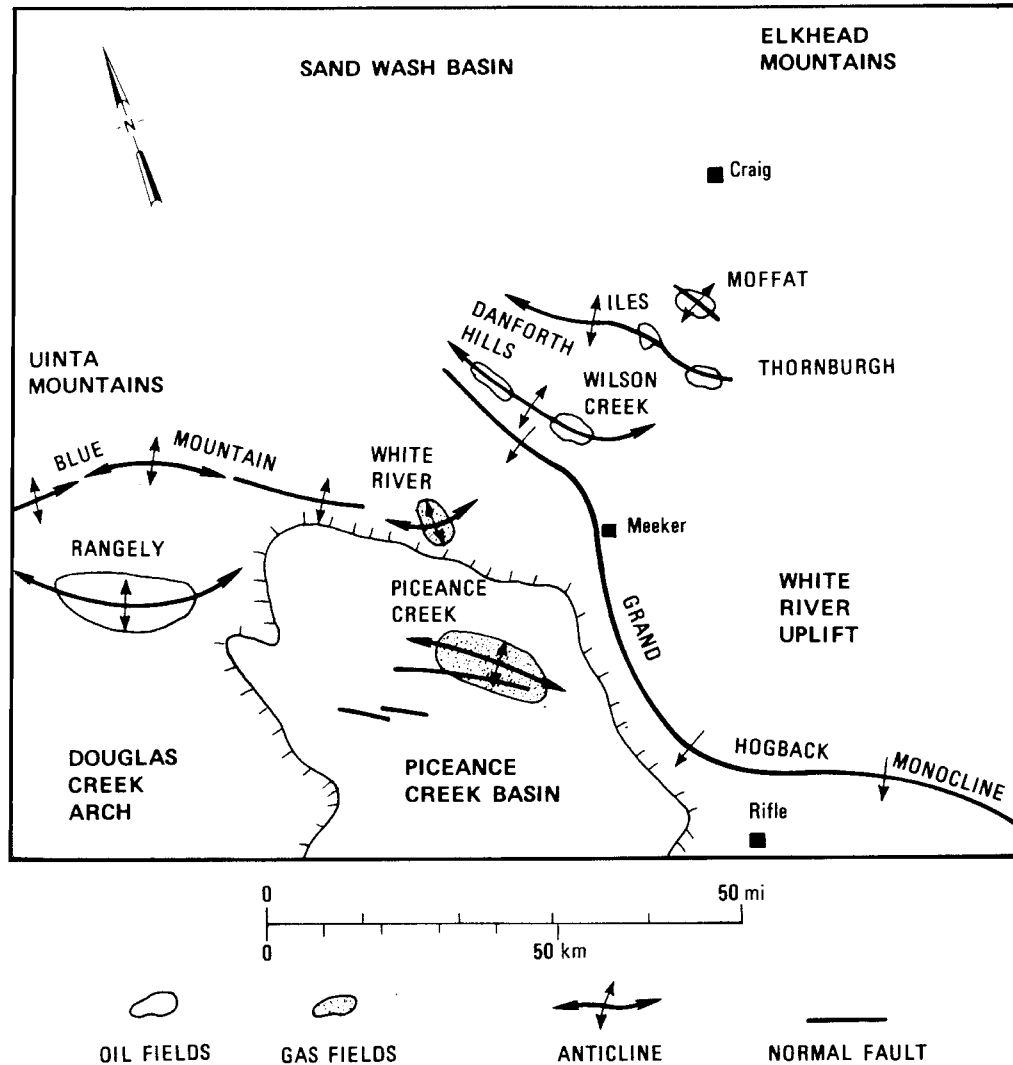


Fig. 4.20 Map of Fig. 4.19. From Sabins (1997).

some ways it parallels the Elsinore Fault study previously discussed, in that orbital imagery permitted recognition of a structural anomaly, and focussed subsequent field work on crucial areas. Furthermore, like the Elsinore Fault, the Raghib anomaly was found in an area that was already covered by excellent geologic maps. Finally, this example demonstrates the need for supplementing remote sensing data with conventional surface and subsurface methods, methods that can be used far more efficiently when they are combined with orbital imagery.



Fig. 4.21 (See also Plate XIV) *Landsat MSS mosaic of Red Sea area.*

Before leaving the subject of petroleum exploration, another application of remote sensing should be mentioned, one concerned with the final stage of petroleum production: minimizing the environmental impact *after* oil fields have been established. Groth and Rivera (1997) have presented an example of this from Ecuador,



Q_s Sand Dunes
 Q_p Piedmont Gravel
 Q_w Wadi Deposits
 K_a Anuma Limestone
 K_w Westi Sandstone
 K_b Biyadh Formation
 (Sandstone & shale)
 K_{bu} Buwa Limestone
 K_s Sulary Limestone
 J_a Arab Formation
 (Anhydrite)
 J_j Jubaila Limestone
 J_n Hanifa Limestone
 J_{tm} Turfa Mtn. Limestone
 J_d Dhurma Limestone
 J_m Minjur Sandstone
 J_{kj} Jilh Formation
 (Sandstone & Shale)

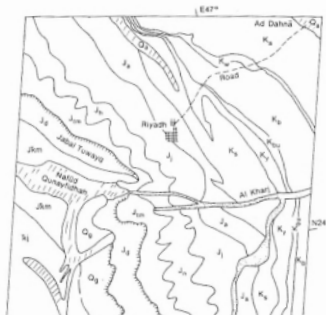


Fig. 4.22 (See also Plate XV) *Landsat* picture of Riyadh area, Saudi Arabia. From Short and Blair (1986). Area of scenes shown in Figs. 4.23 and 4.24 is at extreme lower right corner. Black circles (see higher-magnification view in Fig. 4.23) are irrigator patterns.



Fig. 4.23 Partial *Landsat* TM picture of Raghib anomaly area. From Sabins (1998).

where oil production from the Amazon basin rain forest, has begun. It was found that petroleum exploration inadvertently promoted settlement, with subsequent deforestation, of the region's rain forest, in that seismic profiling provided access to previously uninhabited areas. Using old and new *Landsat* imagery, Groth and Rivera were able to assess the patterns of such settlement. The Ecuadorian government subsequently imposed controls, such as check-points on former exploration trails, as a means of controlling destruction of

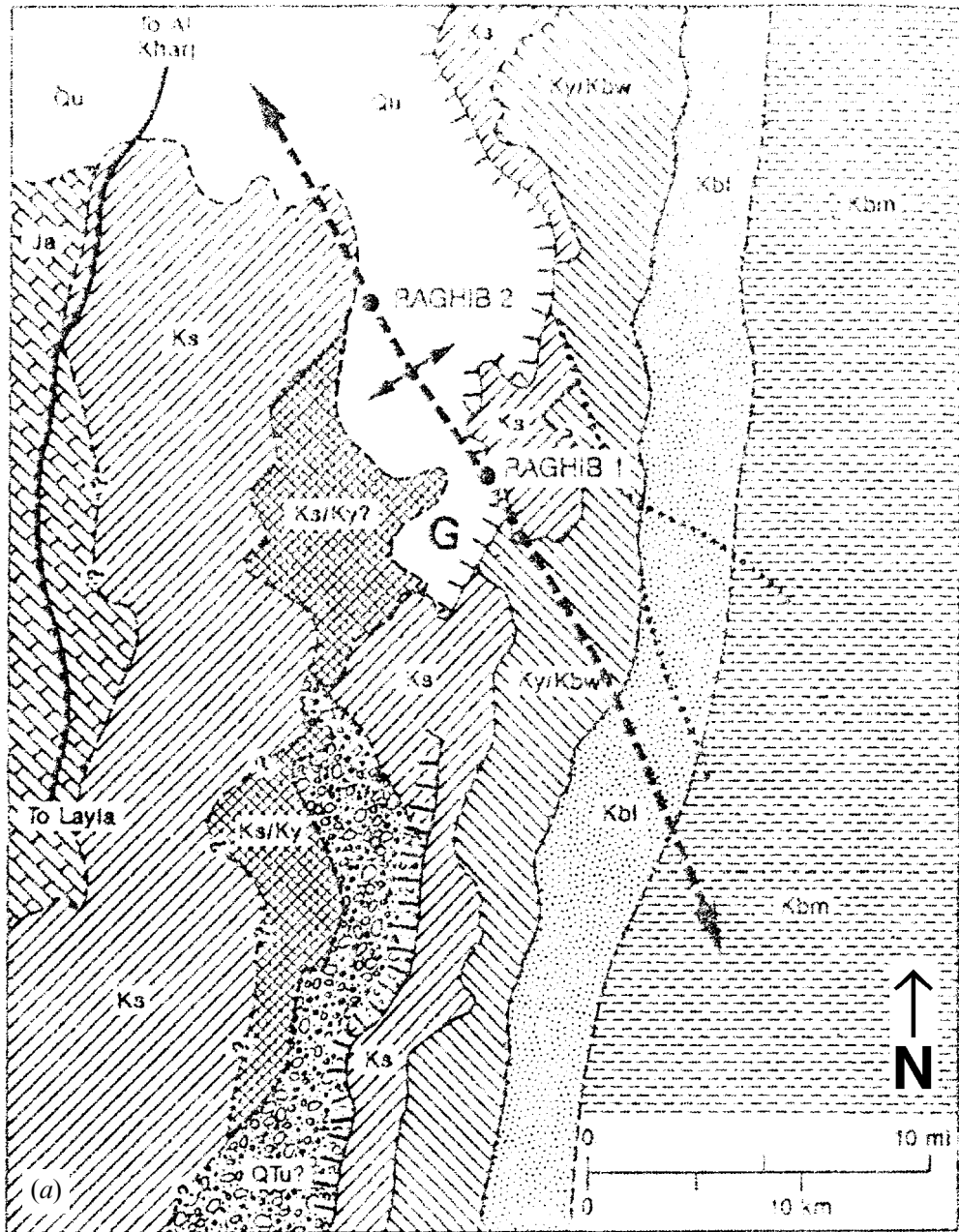
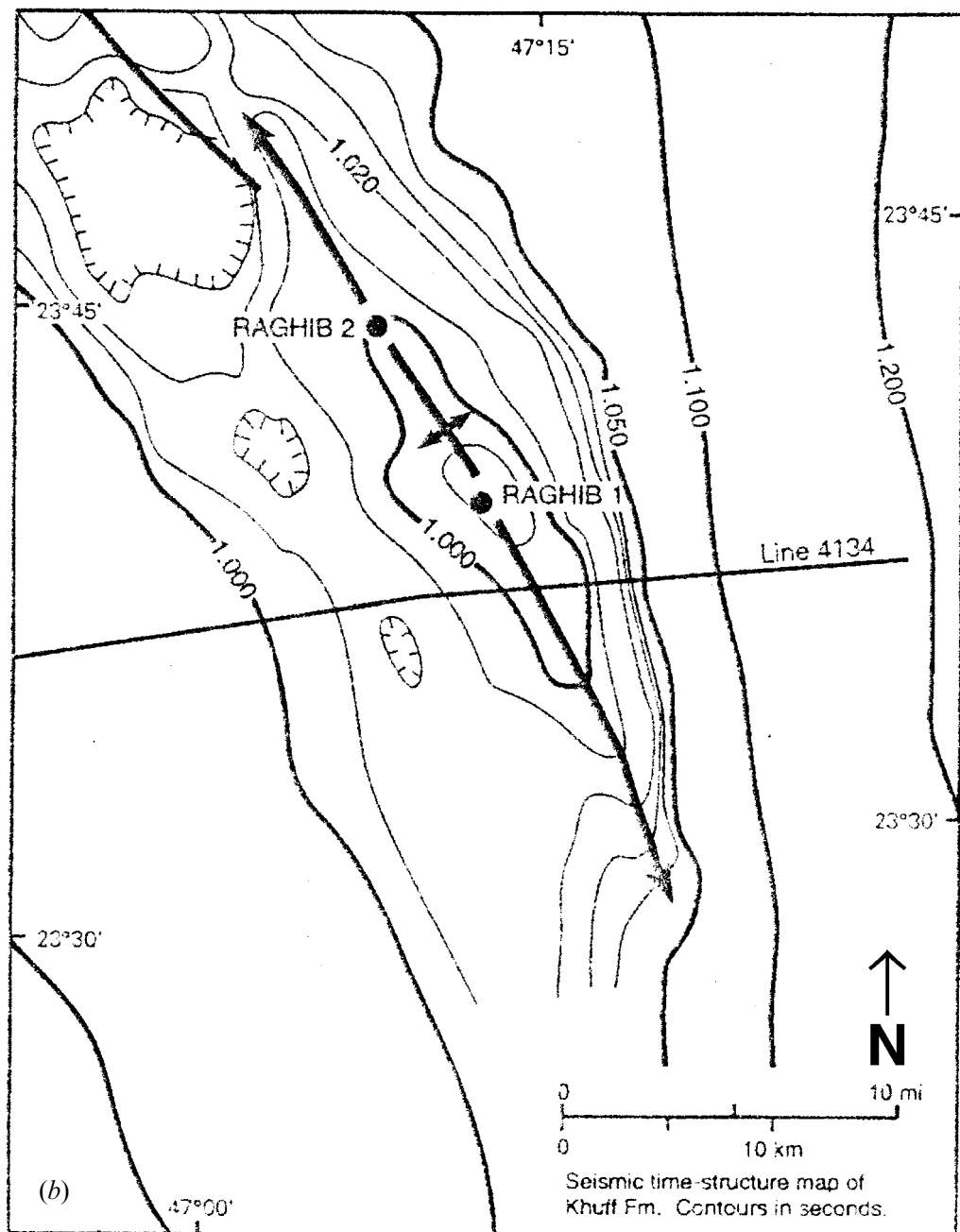


Fig. 4.24 (a) Sketch map of Fig. 4.23. (b) Structure map of Raghib anomaly. Both from Sabins (1998).



the rain forest. Remote sensing can thus contribute not only to discovery and extraction of earth resources, but to protection of the environment after these resources have been extracted.

4.4.2. Mineral exploration

The term “mineral” as used in economic geology is a broad one, including not only ore deposits of metals such as iron, copper, and uranium, but minerals themselves, such as diamonds, and natural fuels such as coal (an organic rock, not a true mineral). In addition, a wide range of common materials such as sand, gravel, and limestone are generally categorized as “industrial minerals.” Society has been dependent on minerals since the Bronze Age, and mineral exploration is thus a field dating back millennia. However, remote sensing has become an increasingly important tool for mineral exploration. Some helpful general references are those by Goetz *et al.* (1983) (and papers in the special issue introduced by this paper), Vincent (1997), and Sabins (1998). The *Proceedings of the Twelfth International Conference on Applied Geologic Remote Sensing* included a wide range of papers on mineral exploration.

Two general approaches have emerged for the use of remote sensing in mineral exploration, based primarily on *structural* or *compositional* methods although obviously the two aspects of geology are inseparable. These categories are a useful framework for discussion of the subject in general.

The “structural” approach is well illustrated by the study of mineral deposits in Nevada by Rowan and Wetlaufer (1979), using a *Landsat* mosaic. The example can be introduced by an aerial view of western Nevada (Fig. 4.25), showing the high relief and scarce vegetation of this huge desert, factors making Nevada an ideal test site for remote sensing research. The Basin and Range Province, as shown in Fig. 4.25, is a unique and still poorly-understood tectonic feature, best illustrated by a *Landsat* mosaic (Fig. 4.26). The area has since the 19th century been a rich source of gold, silver, copper, and other metals, to say nothing of non-metallic resources such as evaporites and even pumice (the “feather-rock” popular with landscapers).

Rowan and Wetlaufer carried out an extensive lineament mapping program on the *Landsat* imagery. Most of the lineaments proved to be previously-mapped faults, frequently the bedrock/alluvium contacts prominent in Fig. 4.25. However, the broad view provided by the *Landsat* mosaic also showed a group of much larger regional lineaments. One of these, the Walker Lane, goes through



Fig. 4.25 (See also Plate XVI) Aerial view from 37,000 feet, looking northeast in western Nevada near Lake Tahoe, showing typical Basin and Range topography. Photo taken July 1998, by author.

the area shown on the aerial photograph, but the restricted coverage even from 37,000 feet makes it impossible to see the unified nature of this lineament. Rowan and Wetlaufer showed (Fig. 4.27) that most metal production from Nevada had come from deposits localized by the lineaments visible on the *Landsat* mosaic, still another example of the importance of lineament tectonics.

The “compositional” approach to mineral exploration depends on a wide variety of remote sensing techniques to determine the lithology, mineralogy, or chemical make-up of the area under investigation. It will be obvious that composition mapping, especially from space, encounters major difficulties not faced in the “structural” approach (which depends largely on gross topography). Much of the Earth’s land area is covered by vegetation, and even in apparently barren areas, such as the Canadian Arctic, outcrops will be found at close range to be coated with lichens. In extremely dry deserts, such as the Arabian Peninsula, the well-exposed bedrock will often have a weathered crust, and obviously large parts of most deserts are covered with wind-blown sand or dust, alluvium, or



Fig. 4.26 *Landsat* mosaic of Nevada.

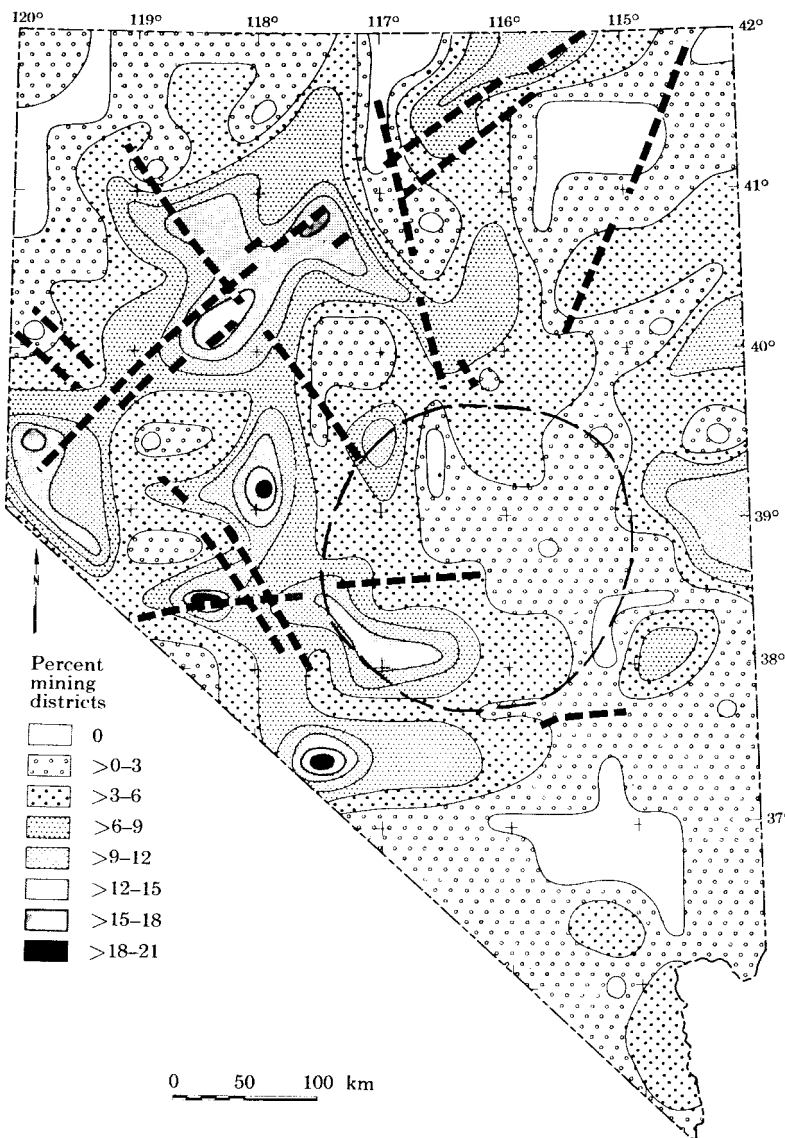


Fig. 4.27 Mineral deposits and lineaments in Nevada. From Rowan and Wetlaufer (1979).

evaporite deposits, as shown in Fig. 4.25. The compositional approach to mineral exploration is thus a large and extremely complex topic. A now-classic investigation by Abrams *et al.* (1977) of the Cuprite area in Nevada and the detailed discussion of the Cuprite study by Vincent (1997) are highly recommended.

A Canadian example from Nova Scotia, by Harris *et al.* (1990)

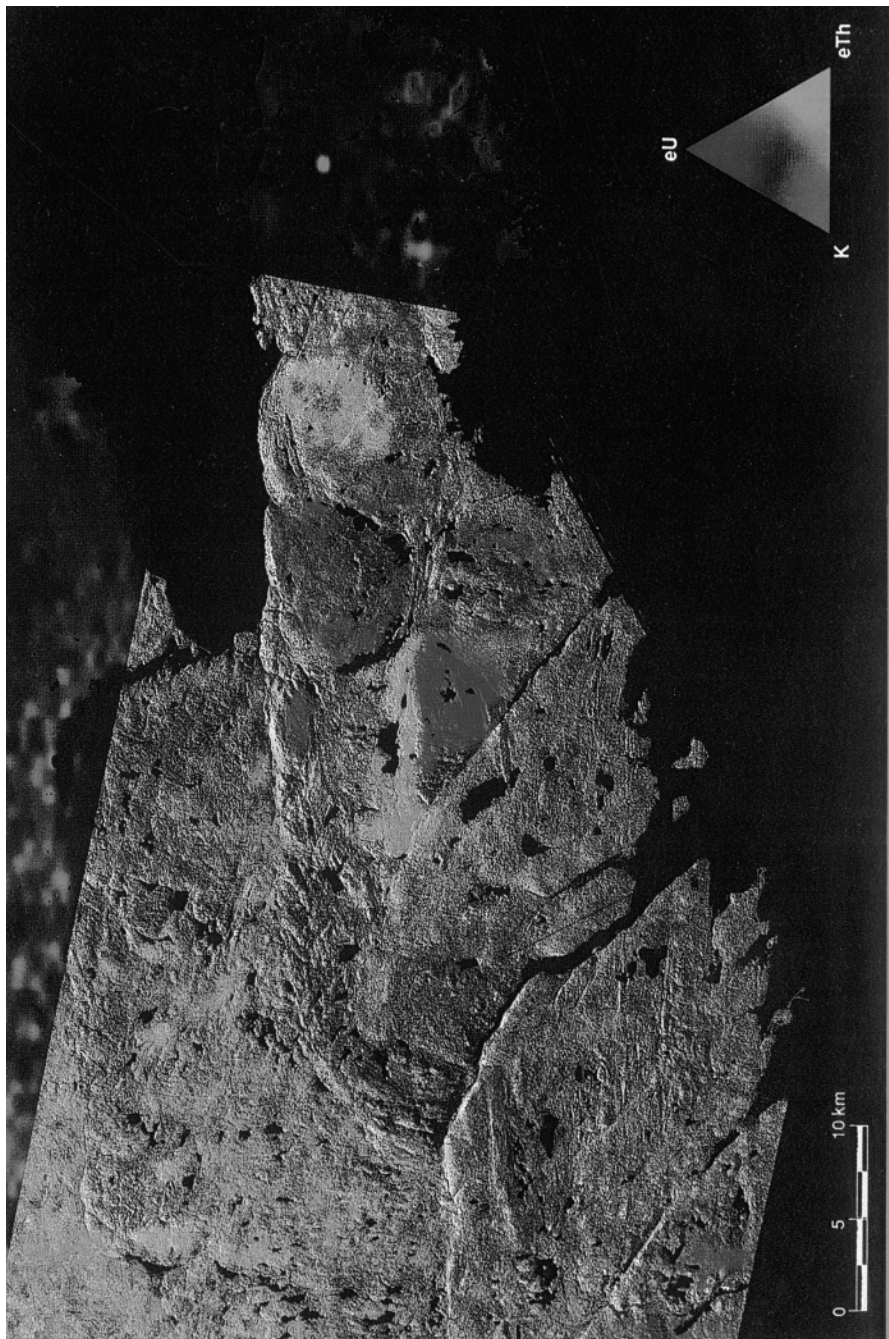


Fig. 4.28 (See also Plate XVII) IHS transform-modulated radar image of Nova Scotia, with proportions of potassium, uranium, and thorium used for IHS (see text). From Harris *et al.* (1990).

illustrates the use of radar imagery, in this case airborne, in combination with gamma-ray data, to delineate gold-associated structures and rock types (Figs. 4.28, 4.29, 4.30). The “IHS transform” refers to a technique in which different remote sensing data types are used, digitally, to modulate the intensity, hue, and saturation of another type of data, in this case the radar imagery.

4.5 Environmental geology

Environmental geology is a new term for several long-established geologic specialties. An authoritative definition (Bates and Jackson, 1980) describes it as essentially the application of geologic knowledge and principles to problems of the physical environment, in particular those caused by man's occupancy of that environment. The Bates and Jackson definition is a broad one, including engineering geology, hydrogeology, topography, and economic geology. As used here, the term will be somewhat more restricted, concentrating on fields not already covered above and on those usefully approached by orbital remote sensing methods. The order of presentation will roughly reflect the degree to which remote sensing has had an impact on various fields of environmental geology.

4.5.1 Active volcanism

Millions of tourists have seen “active volcanism” in reasonably safe locations, such as Yellowstone National Park or Kileauea. But, like the caged and well-fed tigers in a zoo, volcanos can be deadly perils in other circumstances. Remote sensing from space has now become a well-established means to mitigate these perils in a wide variety of ways.

Volcanic hazards take several forms. Lava flows are the most obvious, but paradoxically are among the less hazardous. Molten silicates, i.e., lava, generally move slowly, slowly enough in occasional sad examples to permit homeowners to remove their furniture and photograph lava creeping across their lawns. Ash flows, on the other hand, erupt suddenly and move rapidly, as the 40,000 fatalities in St. Pierre from the 1902 eruption of Mt. Pelee demonstrate. Volcanic mud flows (lahars) triggered by volcanic eruptions, recently those of Mt. St. Helens and Mt. Pinatubo, can be equally dangerous (Mouginis-Mark *et al.*, 1993). Several large American cities, such as Seattle and Tacoma, are built on material deposited by lahars. Turning from geology to meteorology, we see that volcanic eruptions have produced phenomena such as the “year without a summer” in

LEGEND

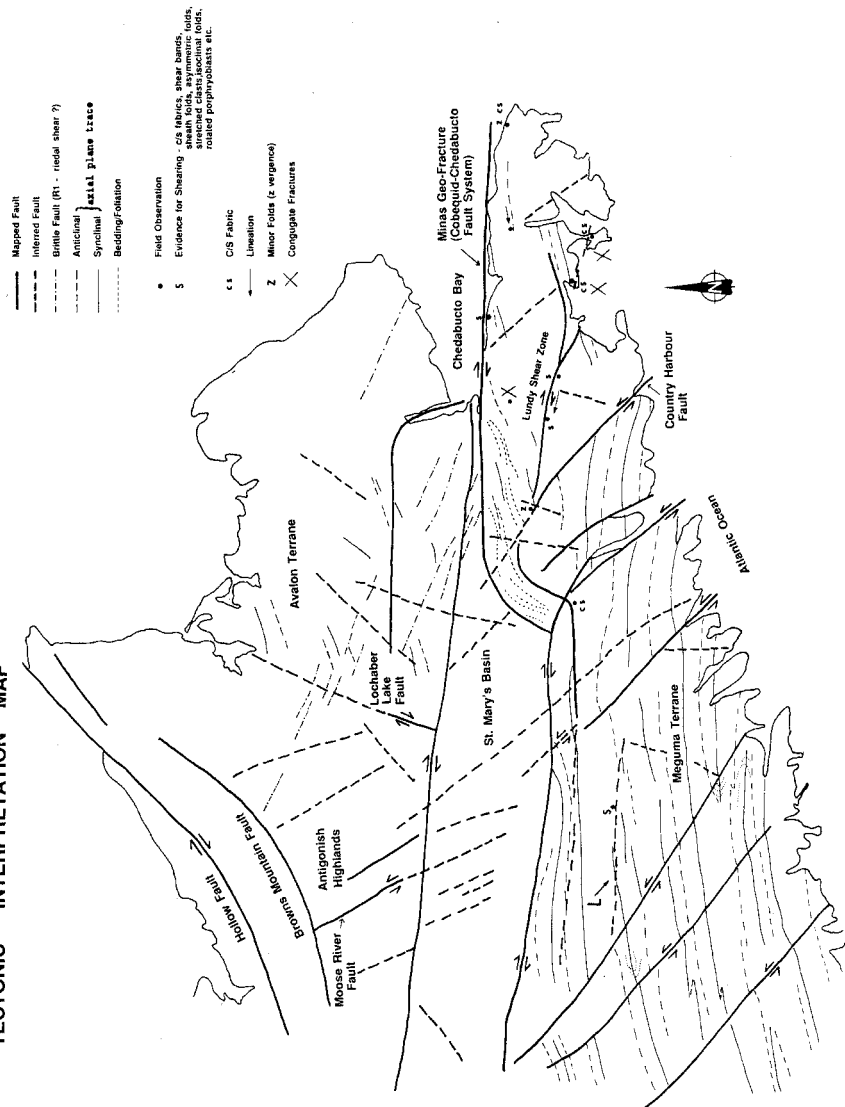


Fig. 4.29 Structure of area shown in Fig. 4.28. From Harris *et al.* (1990).

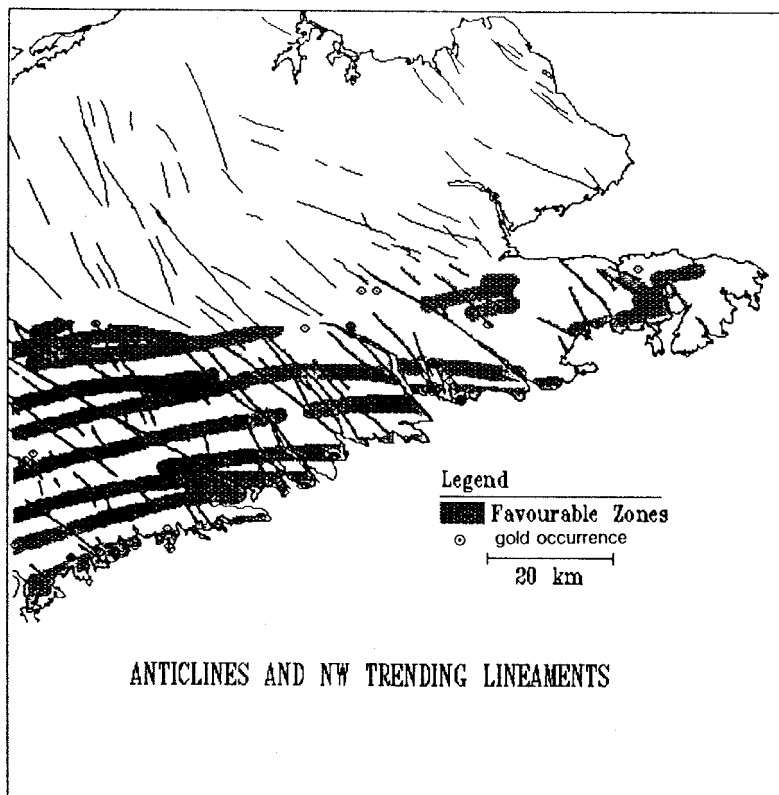


Fig. 4.30 Gold potential map of area shown in Fig. 4.28. From Harris *et al.* (1990).

1815, caused by the eruption of Tambora in Indonesia. Volcanic ash driven into the stratosphere has caused millions of dollars worth of damage to jet airliners, an important problem well suited to monitoring from space, as will be shown.

Remote sensing is now well established as a defense measure against active volcanism and its accompanying phenomena. Only a few of the most important techniques can be illustrated; a more comprehensive summary has been compiled by Mouginitis-Mark *et al.* (2000), from which the following examples have been taken. The global tectonic activity map will be referred to again (see Fig. 4.2) for background as showing the long-term distribution of active volcanism around the world.

The most obvious thing to know about volcanic hazards is where the volcanoes are, especially the young and potentially active ones. The International Decade for Hazard Reduction listed global mapping of all active or potentially active volcanoes as a specific goal



Fig. 4.31 *Landsat* picture of volcanos in Andes of Chile (left) and Argentina at latitude 24 deg. S. Volcanos chiefly stratocones. White area at right is Salar de Arizaro, large salt playa in Argentina. *Landsat* scene 2221-13474, 31 August 1975. From De Silva and Francis (1991).

(Francis, 1989). The value of remote sensing for such a goal was demonstrated by some of the first space photographs acquired for geologic purposes (Lowman *et al.*, 1966), when those taken by astronauts McDivitt and White revealed a large unmapped volcanic field only 100 km west of El Paso. Although not an obvious hazard, judging from the eroded condition of the volcanos (Lowman and Tiedemann, 1971), this finding provided an interesting preview of later discoveries.

The active volcanoes of the Andes are well known and demonstrably dangerous, but orbital imagery (Fig. 4.31) has been used by De Silva and Francis (1991) to identify more than 60 major volcanoes as potentially active, in comparison to the 16 previously catalogued. The reason for this surprising ignorance of Andean volcanoes lies in the sparse population, remoteness, and the fact that the Andes lie in several countries. However, history shows that many volcanoes thought to be extinct, such as El Chichon, are only dormant. For example, Mt. Lamington, in Papua New Guinea, was not even recognized as a volcano until it erupted. The tectonic activity map is an attempt to give a more realistic picture of global volcanism by showing not just the last 10,000 years of volcanic activity, but that of the last one million years.

Prediction of volcanic eruptions is another obvious measure to reduce volcanic hazards. Very few volcanoes erupt with no warning at all, eruptions being generally presaged by earthquakes, steam venting, and other phenomena. The eruption of Mount St. Helens in 1980 had been approximately predicted several years earlier on the basis of geologic mapping and morphology, and warnings of the actual eruption were issued weeks in advance on the basis of seismicity and steam venting. However, these examples are in a densely-populated and highly-developed country. For the rest of the world, satellite methods are proving valuable in reducing the casualties from volcanic eruptions.

The simplest (in principle) satellite approach is monitoring thermal anomalies over volcanoes, to detect the increasing activity before an actual eruption (Rothery *et al.*, 1988; Francis, 1989). An early example of the use of remote sensing, described by Mouginis-Mark *et al.* (1993) was for the volcano Lascar, where a thermal anomaly was discovered accidentally in 1985 on *Landsat* TM infrared imagery. Temperatures were estimated at 800–1000 °C, clearly indicating magmatic activity. The volcano erupted in 1986, but because of its remoteness, the first evidence of the eruption was ash fall 300 km away, in Argentina.

Volcanoes frequently swell up before erupting, because of the rise of magma below them. Ground measurements of such swelling, or deformation, have been useful in predicting eruptions. However, it is hardly practical to monitor the 600 or so volcanoes active worldwide with ground-based methods. Orbital remote sensing has here found dramatic application, for monitoring pre-eruption swelling, and for tracking the products of eruptions after they happen.

Pre-eruptive deformation has been monitored by means of radar interferometry, a relatively new technique (Zebker and Goldstein,

1986; Massonet *et al.*, 1993b). Useful reviews of this technique as applied to volcano deformation have been presented by Zebker *et al.* (2000) and Massonet and Sigmundsson (2000), which can be described, with extreme simplification, as follows.

Radar is basically a ranging technique, most commonly using pulsed microwaves with wavelengths on the order of 5–30 centimeters. If two pulses are transmitted, at different times, from a single antenna to a stationary target with unchanged back-scatter properties, the return pulses will be in phase. However, if the target has moved, or been deformed, between pulses, the return pulses will interfere, being out of phase. Radar images produced this way will show interference fringes, generally reproduced as colored interferograms. If the antenna moves between pulses, the interferogram can express topography, roughly analogous to stereographic aerial photography. This is however a major topic by itself that will not be covered here.

As applied with orbital radar, interferometry of volcano deformation is carried out from satellites such as *ERS-1* with repeated orbits, supplying the equivalent of a “single antenna.” If the target – in this application, the surface of the ground – moves between successive passes, as in an inflating volcano, the ground movement, or deformation, will appear as interference fringes or colors in an image constructed from this repeated coverage. An important advantage of interferometry is that, depending on phase differences, it can detect movements of the same order as the wavelength involved, for radar a few centimeters. This is far better than the spatial resolution, generally tens of meters in range and azimuth, of the same radars. These principles were applied by Massonet *et al.* (1993b) to monitor pre-eruption deformation of Mount Etna. The technique has since been applied to many other volcanos; two examples will be presented here.

For instructional purposes, the study of Fernandina volcano, in the Galápagos, by Zebker *et al.* (2000) is most useful. As shown in Fig. 4.32, radar coverage from *ERS-1* and 2 spanning a five-year period revealed not only the broad deformation of the volcano before the eruption of 1995, but the location of a major dike feeding the eruption. The value of this technique for study of individual volcanos is obvious.

A second example has implications not only for volcanology but for understanding of global tectonic activity. Iceland has been intensively studied for many years, both for its continual volcanic activity and because it is one of the few places (see Fig. 4.2) where a major sea-floor spreading center, the Mid-Atlantic Ridge, is exposed on

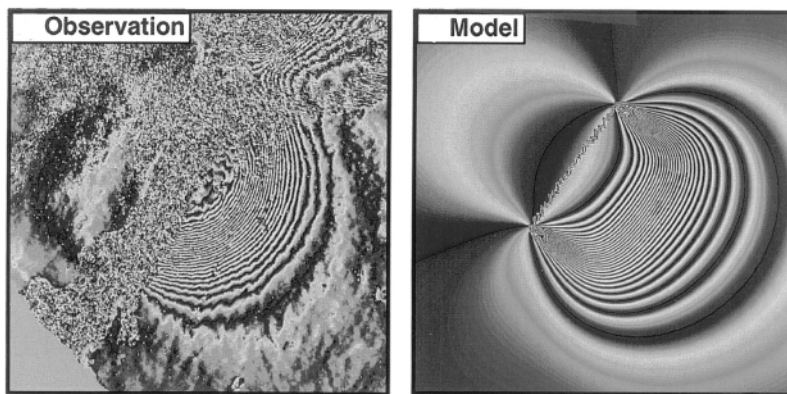
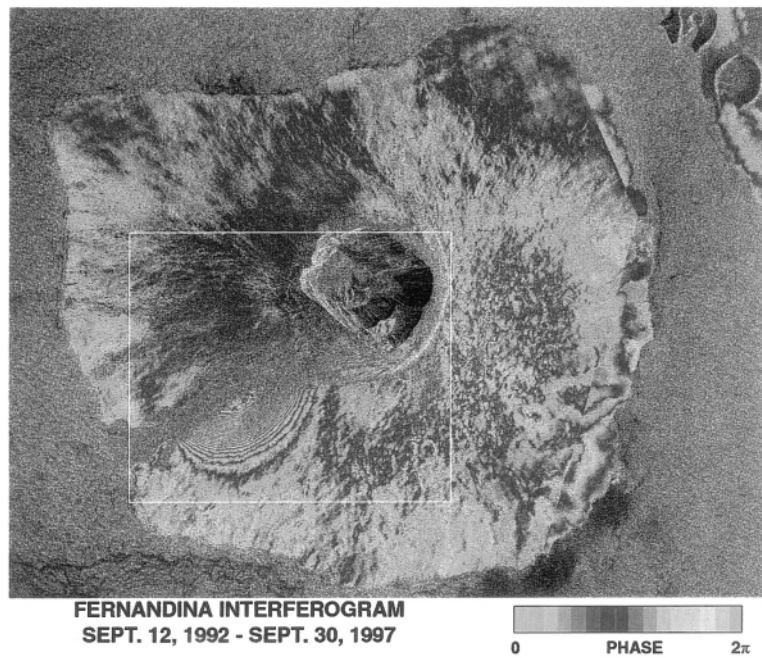


Fig. 4.32 (See also Plate XVIII) *Top:* Differential interferogram of Isla Fernandina, Galápagos Islands, Ecuador. Island is roughly 60 km east to west. Interferogram shows deformation during five-year period, including a flank eruption in 1995. *Bottom left:* Observed interferogram fringes over Fernandina flank. *Bottom right:* Best-fit model from interferogram, indicating a lava source dike striking N 47° E, dipping 33° to SE. From Zebker *et al.* (2000).

land. Satellite radar interferometry of this area thus has fundamental implications. The Reykjanes Peninsula has been studied with radar interferometry by Vadon and Sigmundsson (1997) using data from *ERS-1*. As shown in Fig. 4.33, they were able to detect not only localized subsidence over the Reykjanes volcanic field, but oblique movement along the central rift, i.e. the landward expression of the Mid-Atlantic Ridge. This study thus demonstrates that not only volcanic phenomena but the actual motion of plates can, in principle, be monitored with satellite radar interferometry.

Remote sensing has become an operational method for tracking the products of volcanic eruptions, specifically ash clouds. Volcanic ash is produced in immense clouds by andesitic volcanoes, such as those overlying subduction zones around the Pacific Ocean. Ash flows, the volcanic equivalent of turbidity currents, have long been known as potential catastrophes; the 40,000 deaths at St. Pierre in 1902 were caused not by ash fall but by ash flows. However, the volcanic ash injected into the stratosphere has in recent years become a major hazard because of its effect on high-flying jet aircraft (Casadevall, 1994; Schneider *et al.*, 2000). The problem can be summarized, in brief, as follows.

The volcanic ash clouds from andesitic eruptions are conspicuous (Fig. 4.34), and no pilot would intentionally fly through one. However, it has been found from satellite monitoring (Krueger *et al.*, 2000) that such clouds retain their identity for days or weeks, and after traveling many thousands of kilometers. Such clouds are not visually obvious at altitudes of 20–40 thousand feet, where most commercial air traffic flies. Jet aircraft, whose engines function by ingesting large volumes of unfiltered air, are especially susceptible to volcanic ash. As documented by Casadevall (1994), damage from undetected volcanic ash at high altitudes had, even in the early-1990s, caused damage estimated at tens of millions of dollars, though fortunately no fatalities at this writing.

The potential danger of volcanic ash presents a striking example of the synergism among geology, meteorology, and aeronautics. The most specific demonstration of this synergism is in the North Pacific Ocean. All commercial air routes between North America and northeast Asia (including Japan) are great circles. These great circles are downwind from, and parallel to, the volcanically active island arcs of the Aleutians and the Kamchatka Peninsula (see Fig. 4.2), and several nearly-catastrophic flame-outs have resulted from this coincidence of air routes with volcanically active areas. Individual volcanoes such as Mt. Etna (Fig. 4.34) can similarly be dangerous in heavily-traveled areas.

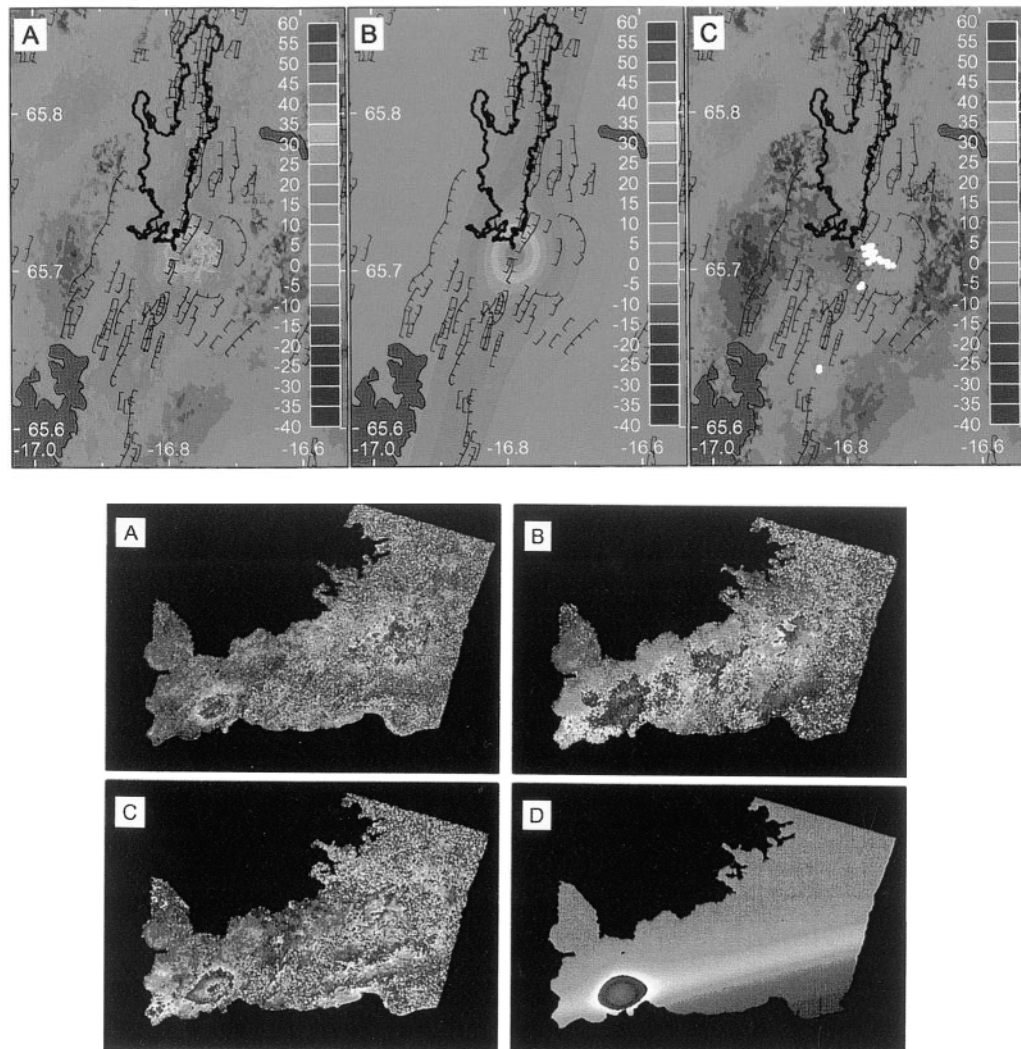


Fig. 4.33 (See also Plate XIX) *Top:* Radar interferogram of Krafla, Iceland, showing (A) range changes in mm over a one-year interval dominated by a 40-mm-deep subsidence bowl over a magma chamber. (B) is best-fit model allowing for pressure decrease in magma chamber. (C) is residuals from the model. Interferogram shows that the subsidence bowl is superimposed on 14 mm subsidence along the Krafla rift axis.

Bottom: Radar interferogram of 50 × 25 km area of Reykjanes Peninsula in southwest Iceland. (A) covers 0.83 years; (B) 2.29 years; (C) 3.12 years; (D) is model interferogram showing best-fit 2.29 year deformation. Figure shows subsidence caused by geothermal energy fluid withdrawal, superimposed on along-axis range increase showing plate separation. From Massonet and Sigmundsson (2000).



Fig. 4.34 (See also Plate XX) *Landsat* picture of volcanic plume coming from Mount Etna, Sicily, during eruption in 1983. Processed by Telespazio, Italy. Acquired 23 April 1983.

The most obvious application of satellite remote sensing to this problem is simply the detection of eruptions in remote areas, a major contribution in itself. The use of satellite thermal instruments for monitoring volcanic hot spots, as described by Harris *et al.* (2000) and Flynn *et al.* (2000) has become an invaluable operational technique. Geosynchronous weather satellites provide routine coverage of nearly entire hemispheres, and can permit Internet posting of eruption alerts within an hour of the event. Non-geosynchronous satellite instruments such as the Advanced Very High Resolution Radiometer (AVHRR) provide information on hot spots due to lava flows, fumaroles, and geothermally-heated lakes.

Satellite investigations originally undertaken to study atmospheric composition and circulation have proven unusually valuable for mitigation of volcanic hazards to air travel, as demonstrated by Krueger *et al.* (2000). The ozone content and distribution are first-order problems themselves, and it was found that orbital observations could effectively monitor ozone. However, it soon developed that ultraviolet observations from space could be applied to the

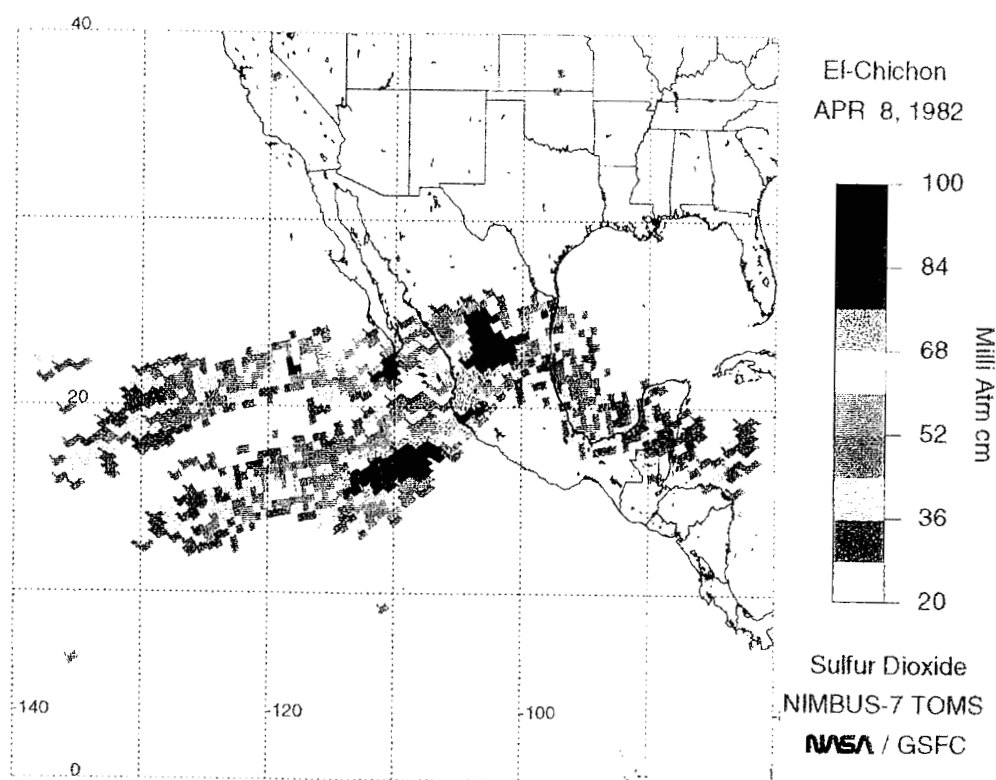


Fig. 4.35 (See also Plate XXI) Sulfur dioxide cloud from the 4–5 April 1982 eruption of El Chichon, Mexico, after drifting southwest for 4 days at 25 km altitude, as tracked by Total Ozone Mapping Spectrometer (TOMS) on Nimbus 7. From Krueger *et al.* (2000).

monitoring of ash clouds from volcanoes. The Total Ozone Mapping Spectrometer (TOMS) (Krueger *et al.*, 2000) proved effective in mapping the distribution of sulfur dioxide, which in turn showed the location and density of volcanic ash clouds (Fig. 4.35). The result of this and other unexpected discoveries is that satellite observations have become an operational and international method to warn airline pilots of potentially dangerous eruptions. The eruption of Mount Spurr, in Alaska (Fig. 4.36), was tracked by its sulfur dioxide all the way to the Atlantic Ocean, and was still dense enough over Toronto to require diversion of commercial flights from Europe.

The print and electronic news media in the United States almost invariably preface reports of new satellites or other space projects with the cost. For example, the readers were informed in the sixth line of a half-page article that the *Terra* satellite (launched in 1999)

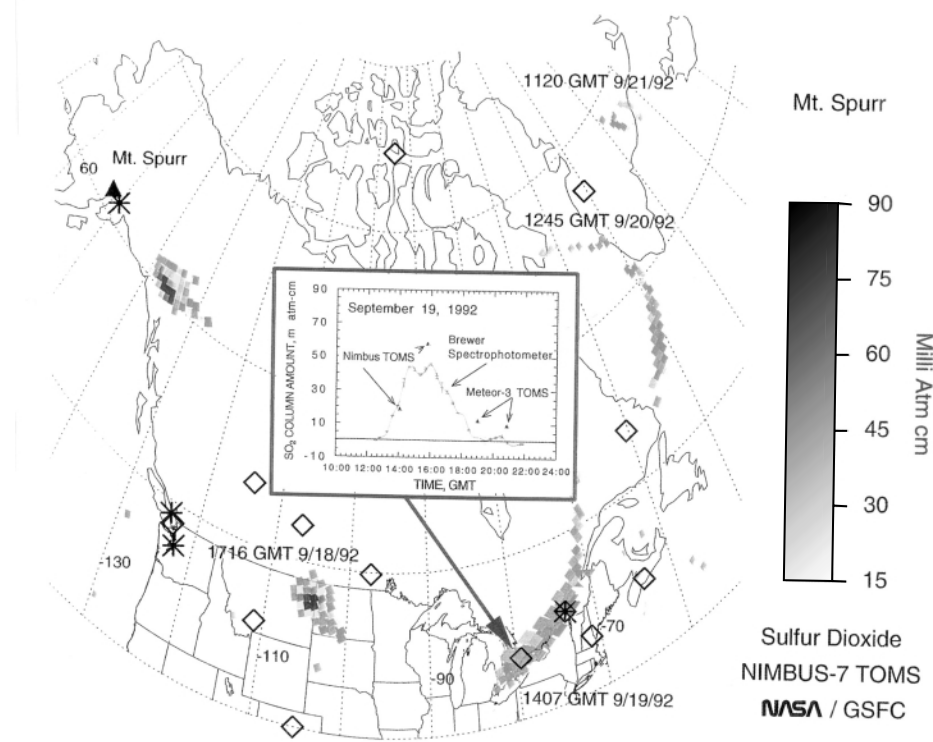


Fig. 4.36 (See also Plate XXII) Composite image of the 17 September 1992 Mount Spurr eruption sulfur dioxide cloud, showing path to southeast across North America. Inset shows sulfur dioxide measured by ground-based instruments as the cloud passed over Toronto. From Krueger *et al.* (2000).

had cost \$1.3 billion (Supplee, 2000). Just one of the many *Terra* instruments is already in use for volcano monitoring. A wide-body jet generally carries 200–400 people; roughly 200–400 such jets fly great-circle Pacific routes downwind of andesitic volcanoes (Casadevall, 1994). If loss of even one such airplane could be prevented by satellite remote sensing, it would go a long way toward satisfying the taxpayers that their money is being well spent.

4.5.2 Glacial geology

The normal climate of the Earth for the last several hundred million years has been warm from pole to pole; some 60 million years ago, alligators, turtles, and palm trees could be found on Ellesmere

Island, Canada, at 80 degrees north latitude. However, from time to time, ice ages have occurred – “snow-ball earths” in the most extreme case (Hoffman *et al.*, 1998) – driven primarily by a combination of astronomical parameters. The most recent of these ice ages, in the Pleistocene, began about three million years ago, and has not yet ended. A whole continent (Antarctica), the world’s largest island (Greenland), and parts of the Canadian Arctic are still covered with remnants of the Pleistocene ice sheets. In addition, there are innumerable valley glaciers in various mountainous regions, even at the equator, but these have been produced primarily by local conditions permitting seasonal accumulation of snow. Finally, the terrain in large areas of North America and western Europe is dominated by glacial or periglacial landforms and deposits related to Pleistocene ice sheets. Glacial geology is thus an extremely important part of environmental geology, even though most inhabitants of the planet have never actually seen a glacier.

Glacial geologists were among the first to make extensive and systematic use of orbital remote sensing data, which provided them with global repetitive coverage utterly impossible with airborne methods. Our coverage of environmental geology thus continues with examples of the application of remote sensing to “glaciers and glacial landforms.” This useful phrase is from the chapter by R. S. Williams (1986) in *Geomorphology from Space* (Short and Blair, 1986), recommended to the reader as an excellent introduction to glacial geology as well as an example of remote sensing applications in the field. Following previous practice, this large subject will be selectively sampled, with a few of the best examples.

Mountain (or valley) glaciers are the most familiar to the average reader, and the first orbital picture (Fig. 4.37), from *Landsat*, shows a section of southern Alaska unusually well suited for showing how glaciers form and evolve. The high latitude, coastal location, and high relief collectively produce heavy year-round precipitation, generating the snow fields conspicuous here. As pointed out by Williams (1986), the snow can be considered a sedimentary rock which, with enough pressure, is transformed into glacial ice, the equivalent of a metamorphic rock. The ice flows plastically (as in metamorphic deformation) down the valleys. Variations in flow, in particular glacial surges, can be inferred from the visibly crumpled ends of glaciers, formed by pressure from the upstream active segments. Although not obvious from simple inspection of the *Landsat* photograph, the glaciers in this area have been receding during the 20th century. Hall *et al.* (1995) used *Landsat* imagery of the Glacier Bay area, just south of here, to show that the Muir Glacier receded

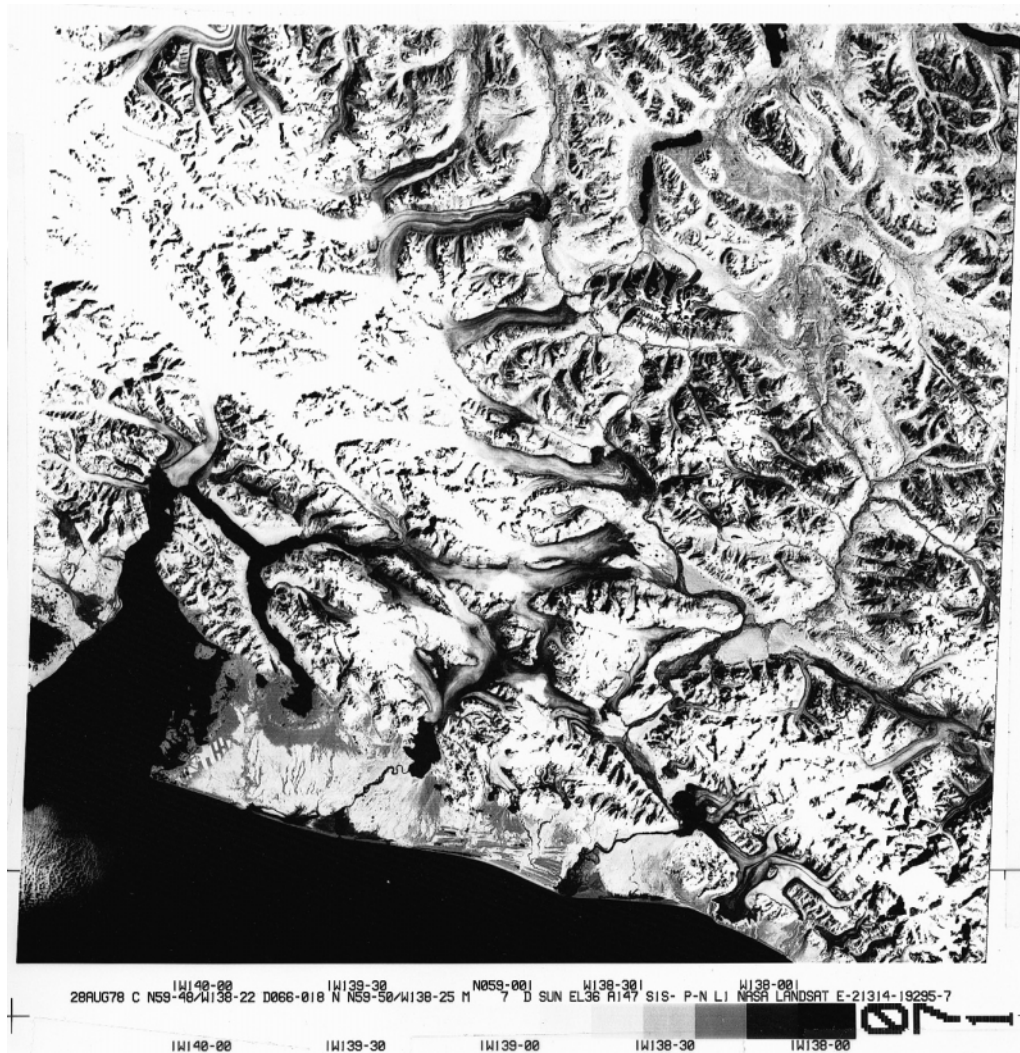


Fig. 4.37 *Landsat* picture of southern Alaska and British Columbia, Canada, showing Yakutat Bay area and glaciers.

7.3 km between 1973 and 1992, an excellent example of the value of remote sensing in glacial geology. Hall *et al.* noted that local influences and positive feedback effects have probably influenced this rate. Similar applications of *Landsat* images to glacial regime studies have been made in Austria by Bayr *et al.* (1994), and several other regions cited by Williams *et al.* (1997). Long-term or global temperature changes can not be inferred from any one area, because of the effects of local conditions. However, collectively, satellite-based glacial studies will be an essential contribution to the question of



Fig. 4.38 (See also Plate XXIII) *Landsat* multispectral composite picture of Vatnajokull, Iceland. From Williams (1986). *Landsat* scene 1372–12080, 30 July 1973.

whether global warming is happening and, if so, what man's contribution to it is.

A different type of glacier is shown in our next example (Fig. 4.38), from Williams (1986). Williams *et al.* (1997) have used *Landsat* images (Fig. 4.39) to measure the Vatnajokull ice cap on Iceland. Vatnajokull is a classic area, the most-studied ice cap on Earth. Its

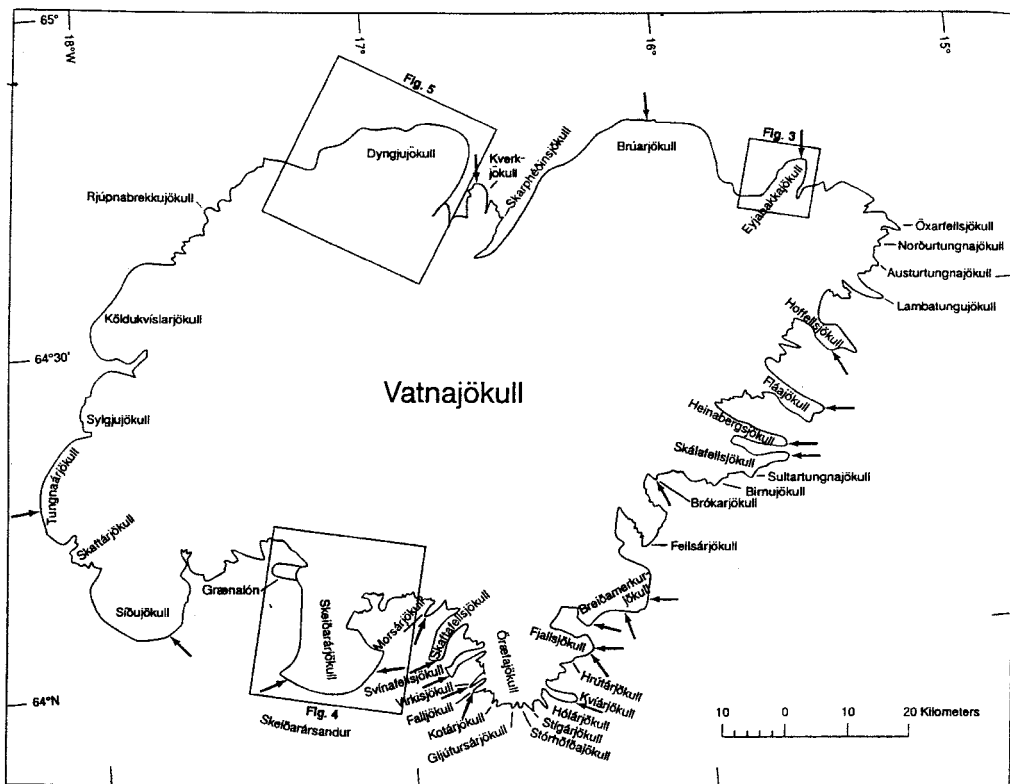


Fig. 4.39 Map of area of Fig. 4.38, from Williams *et al.* (1997).

location is unique, straddling the Mid-Atlantic Ridge (Fig. 4.2), an area of active sea-floor spreading and continuous volcanic activity. Like southern Alaska, Iceland has the ideal combination of latitude and precipitation to produce “jokulls” (Icelandic for ice cap). However, these ice caps are unusual because of their tectonic location, with large active volcanoes underneath, with consequences to be discussed. Because Vatnajökull has been studied scientifically for almost two centuries by the Icelanders, it provides an invaluable baseline for studies using remote sensing. Williams *et al.* (1997) have used *Landsat* to measure recession rates for some of the outlet glaciers from Vatnajökull. However, a much more rapid and locally catastrophic glacial phenomenon has also been studied by satellite techniques, in this case orbital imaging radar.

The eruption of volcanoes under an ice sheet can produce huge floods, first recognized on Iceland and termed jokulhlaups. Such a flood occurred in 1996, from Vatnajökull, causing \$15,000,000 in damage to the Icelandic road system. As shown by Garvin *et al.* (1998), the extent of this jokulhlaup was monitored by repetitive

coverage with *Radarsat* imagery (Fig. 4.40). Guided by this imagery, Garvin *et al.* carried out airborne laser altimetry surveys over the “sandur,” the alluvial plains formed by the jokulhlaup. These surveys showed that the net result of this flood was substantial deposition, despite the obvious erosion. Apart from the obvious importance for glacial geology studies, the surveys of the 1997 jokulhlaup illustrate the importance of catastrophic events in geomorphology, another demonstration that “uniformitarianism” must include what was once called “catastrophism.”

This brief review of the use of remote sensing in glacial geology would be incomplete without a now-classic *Landsat* view (Fig. 4.41) of the Channeled Scablands of Washington state. This deranged topography, visible in its entirety only from space, was produced by the sudden release of glacier-dammed water from the Columbia River in the Pleistocene. This explanation, originally proposed by J. Harlan Bretz in the 1920s, was for decades rejected by geologists of the day, wedded to “uniformitarianism” in the classic sense. It was eventually realized that Bretz was right, in time to award him the Penrose Medal in his 90s. Had synoptic views of the Scablands been available to him, the award might have come much sooner.

4.5.3 Aeolian geology and desertification

The term “aeolian geology” is intended to cover the study of wind-dependent processes and the deposits and landforms produced by wind. It is roughly equivalent to desert geology, for obvious reasons, but it should be pointed out that there are large areas of aeolian features that are not, or are no longer, deserts. Much of Nebraska, for example, is covered by stabilized sand dunes (the Sand Hills), dating from the late-Pleistocene, when winds from the continental ice sheets deposited them.

Many of the world’s great deserts lie at low latitudes, and accordingly have been well covered by orbital photography and other types of remote sensing beginning in the early-1960s. Many of the desert photographs taken by *Gemini* and *Apollo* astronauts are unsurpassed even today, possibly because the Earth’s atmosphere has become less clear as a result of man-made air pollution. A *Gemini 5* photograph (Fig. 4.42) demonstrates the potential value of such imagery for study of “sand seas.” The Namib Sand Sea has in fact been studied with *Landsat* imagery by White *et al.* (1997), who were able to map the iron oxide content of these dune sands. The study of global sand seas has been revolutionized by remote sensing, as shown by the massive compilation of sand-sea investigations edited

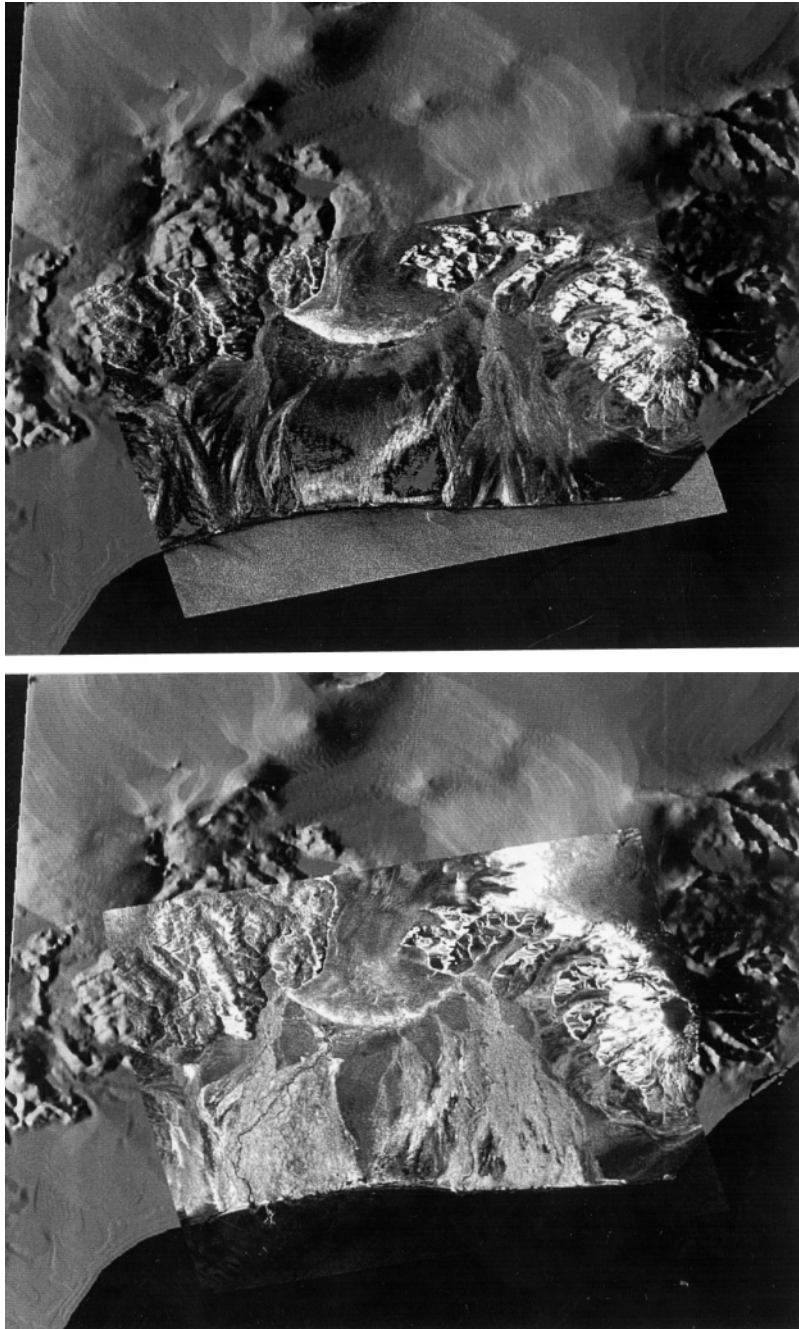


Fig. 4.40 *Radarsat* standard beam images of Skeidararsandur, Iceland, acquired 5 October 1996 (top) and 9 November 1996 (bottom), pre- and post-jokulhlaup respectively, with 30 deg. incidence angle. Bright areas on 9 November image show flood deposits. *Radarsat* is operated by the Canadian Space Agency. Image courtesy of Dr. James B. Garvin.

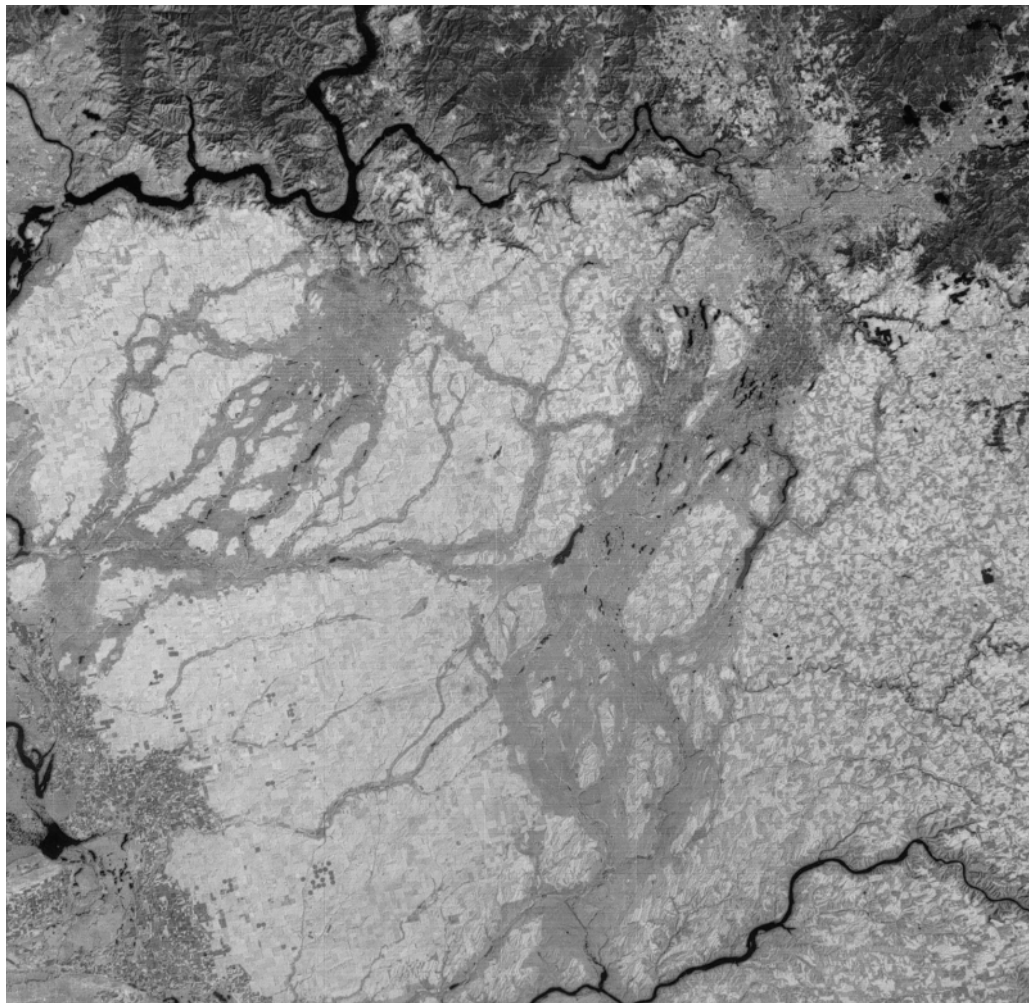


Fig. 4.41 (See also Plate XXIV) *Landsat* picture of Channeled Scablands, Washington; Spokane at upper right, Columbia River at upper left. Light gray and black patterns show valleys carved out by catastrophic glacial floods. *Landsat* scene 1039-18143, 31 August 1972.

by McKee (1979). A comparable compilation of aeolian landforms has been published by Walker (1986), including images of sand seas on Mars.

An environmental geology topic closely related to aeolian geology is desertification, essentially the destruction of arid or semi-arid environments by human activity, aggravated in some areas by natural conditions. It has been estimated by the UN that 35% of the Earth's land area is in danger of desertification (Zhenda and Yimou,



Fig. 4.42 (See also Plate XXV) *Gemini 5* 70 mm photograph of Walvis Bay area, Namibia, showing sand dunes of Namib Desert. Northward transport of dunes is stopped by the Kuiseb River. NASA photograph S-65-45579, 1965. Width of view ~100 km.

1991), and most of this is in developing countries such as India and China, least able to withstand the process. Both countries have developed strong orbital remote sensing capabilities (Kasturirangan, 1985). The Indian Remote Sensing (*IRS*) satellites have proven useful in a wide range of environmental geology applications. China has to date largely used other countries' satellite data, but very effectively. A comprehensive collection of reports on remote sensing approaches to environmental change in Asia was edited by Murai (1991).

Remote sensing was recognized as a valuable tool in monitoring desertification even with the earliest *Landsat* images (Otterman *et al.*, 1976), as demonstrated by Fig. 4.43, showing overgrazed native preserves in Zimbabwe. Even in highly-developed but semi-arid countries, such as those around the Mediterranean, satellite images are being used to monitor desertification and related conditions, such as deforestation and soil erosion (Hill *et al.*, 1995).

Several anthropogenic processes contribute to desertification, including deforestation, overgrazing, sand dune migration, and salinization. The term "wastelands" used by Nagaraja *et al.* (1991) for India encompasses several of these processes. Satellite remote sensing, by *IRS*, has been shown by these authors to be an effective means of monitoring the status of wastelands.

Perhaps the broadest view of desertification, a global one, has been provided for some decades by various meteorological satellites, monitoring radiation in the microwave region. This technique, not previously discussed here, uses passive remote sensing in the centimeter range to map physical characteristics of the Earth's surface, in particular the vegetation distribution (Townshend *et al.*, 1993). Dense vegetative cover is obviously the inverse of desertification. However, passive microwave methods have been directly applied to desertification by Choudhury (1993). The technique, in brief, depends on the difference in detected intensity between horizontally- and vertically-polarized 8-mm wavelength radiation, the greatest difference indicating the most barren terrain. The images produced this way give a good global view of the distribution of vegetation. More localized views, confined to a single continent, show seasonal vegetation changes. Further discussion would be beyond the scope of this review, but it is clear that desertification can be monitored by several different orbital remote sensing techniques.

Our final example of remote sensing as used in environmental geology is from the *Terra* satellite, that is, the \$1.3 billion *Terra* satellite, launched in 2000. Among the instruments carried was the MODerate Resolution Imaging Spectroradiometer (MODIS), which

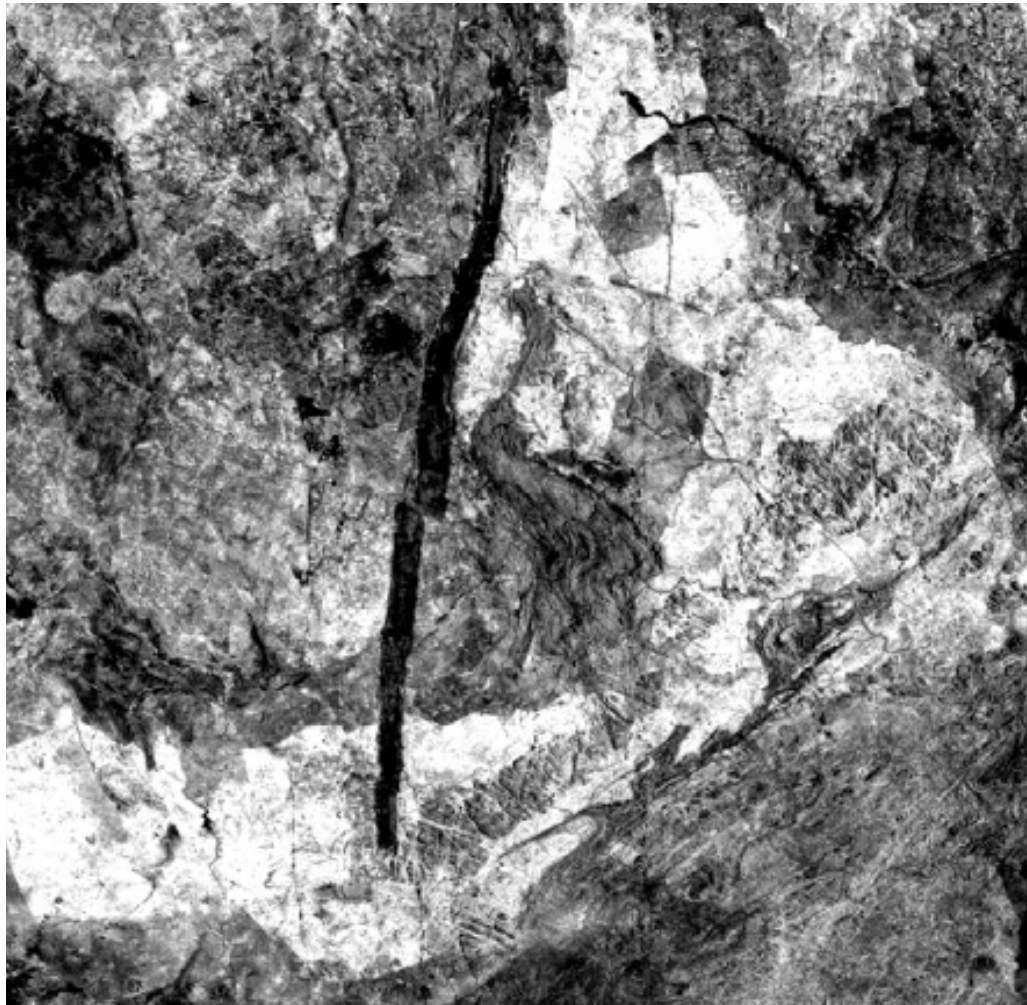


Fig. 4.43 *Landsat* picture of Zimbabwe. Feature in center is Great Dike. Light and dark patterns represent areas of overgrazing. Bedrock is granite-greenstone terrain; note large elliptical batholith left (west) of Great Dike. *Landsat* scene 1103-07285, 3 November 1972.

produces multispectral images with extremely wide swaths (Fig. 4.44). This scene was acquired March 6, and covers the United States and southern Canada from the Mississippi River to the Atlantic Ocean. The photograph was taken near the time of maximum seasonal change in vegetation, i.e., mid-spring. Apart from giving an outstanding view of regional geology, it also provides an unprecedented picture of deforestation on a subcontinental scale. When the scene was acquired, on a single pass, crops were not yet up



Fig. 4.44 (See also Plate XXVI) MODIS image of eastern United States and southern Canada, acquired 6 March 2000. Natural color.

except in the deep south, and bare fields show up on the picture as light areas in contrast to forests. This is most obvious in the Ridge and Valley Province of Pennsylvania, where the valleys are farms (now fallow) and the ridges are forest. In parts of the Coastal Plain, southern Ontario, Michigan, and Wisconsin, areas of forest cover similarly show up dark. The MODIS scene thus provides, by a lucky combination of season, clear weather, little snow cover, and swath

width, an almost frightening view of the enormous amount of forest cover removed since the continent was settled. Environmental problems such as soil erosion and sediment pollution are much more easily grasped with this graphic example.

4.6 Summary

A summary of the impact of orbital remote sensing on geology must begin on a slightly apologetic note: the impact has only begun to be felt by geologists (as distinguished from specialists in remote sensing as such). It should be admitted at once that remote sensing has had nothing like the fundamental effect on geology that, for example, the Deep Sea Drilling program had. In applied geology, the situation is quite different, with orbital data in routine use for petroleum and mineral exploration, and increasingly for environmental geology (especially for monitoring volcanic hazards). However, geology is becoming increasingly an applied science, with basic research being de-emphasized by government funding sources. Geology is even losing its identity to some degree, being merged with “earth sciences,” “environmental studies,” and other fields to form “earth system science.” These trends, whether good or bad, will almost certainly lead to increasing use of remote sensing in “geology.”

The future for remote sensing in basic geologic research is less clear. The apparent success of plate tectonic theory has produced a generation of geologists that considers the big problems of geology to have been solved, at least in principle, by this master plan. Continents are now assumed to be formed by accretion of terranes, mountain belts by continental collisions. “Opening of the Atlantic” is referred to as confidently as if the event had happened during the 1969 Geological Society of America meeting in Atlantic City. This unhealthy situation may be remedied by the stimulus of new discoveries from seismic reflection profiling, the *World Stress Map* project, and planetary exploration. Furthermore, remote sensing may come to its own rescue, so to speak, in that the continuing stream of new imagery from satellites can hardly fail to excite interest in geologic problems among students. The *International Space Station* may make it possible for more professional geologists to see the Earth from orbit; at this writing, only two (Drs. Kathryn Sullivan and Harrison Schmitt) have had this privilege.

On balance, it can be said that orbital remote sensing has now taken its place firmly as a useful geologic tool. The new century will show if it will be more than this.

INDEX

This index includes terms from the body of the text only; captions are not included

- active volcanism, 167–78
- admittance, 25
- Advanced Very High Resolution Radiometer, 176
- aeolian geology, 183–7
- Aegean Sea, 56
- Alaska, 58, 61, 179, 180
- Altyn Tagh fault, 133
- AM-2 model, 53
- Ames structure, 212, 213
- Andes, 38, 170, 171, 235
- andesite, origin of, 270
- andesitic crust, 209, 270, 280
- angular momentum, 67
- Anatolian block, 56–7
- Apollo*
 - laser retroreflectors, 21, 23, 71
 - missions, 71
 - earth terrain photography, 137, 138, 183
 - program, 224, 256
 - subsatellite, 117
- Bangui anomaly, 12, 95, 97, 220
- basaltic magmatism, 122, 220, 254, 265, 267, 271, 279, 285, 286
- Basin and Range Province, 162, 163
- biogenic theory, 278–280
- Bouguer anomaly, 72, 78, 95
- Callisto, 120
- Canadian Shield, 137, 144–50, 203, 251, 252, 255, 258, 260
- Channeled Scablands, 183, 185
- Chicxulub Crater, 211, 212, 222, 224
- China, 9, 55, 132–5
- Clairaut's Theorem, 35, 76
- Clementine* mission, 71–3
- coesite, 195, 196, 204
- comparative planetology, 227–71
 - compensation
 - Airy, 38, 73
 - Pratt, 38
 - continental crust, origin, 227–71
 - continental drift, 14, 45, 50–6, 285
 - continental nuclei, 208
 - continuum tectonics, 56–7
 - Copernicus, 192
 - Corona* program, 128
 - cube corner reflectors, 19–23
 - Crustal Dynamics Project, 46, 47, 51
 - crustal magnetism, 10, 11,
 - Curie isotherm, 104, 122
 - Curie temperature, 104, 107
- Deccan Traps, 223
- deforestation, 187, 188
- deformation lamellae (planar deformation features), 195, 196, 218
- desertification, 185, 187
- dike swarms, 251, 252, 258, 265, 285
- domains, 84
- Doppler tracking, 18, 79
- DORIS, 18
- Earth Gravitational Model 1996, 26
- Earth
 - core, 89, 91–4, 227, 278, 279
 - expansion, 67, 68
 - flattening, 34, 35

- geoid, 34, 35, 39, 40, 43, 44
gravity anomalies, 17, 37–39
gravity field, 16, 22, 26,
gravitational model 1996, 26
life on, 272–81
magnetic field, 83, 86–94, 119
mantle, 87, 89, 105, 122, 278, 279
ocean basins, 209, 210, 279
origin, 244
petrologic evolution of, 269–71
rotation, 67–70
shape, 33–7
tectonic evolution of, 278–281
- Earth Resources Observation Satellite*, 127
Earth Resources Technology Satellite, 127
East African Rift Valleys, 39
East Pacific Rise, 2
El Chichon, 177
electromagnetic induction, 85
electromagnetic spectrum, 125
Ellesmere Island, 10
Elsinore Fault, 136–41, 142, 157
environmental geology, 167–90
equipotential surface
Eros (asteroid 433), 242
eugeosyncline, 238
European Remote Sensing Satellite-1, 149, 172, 174
expansion tectonics, 67–8
exploration geology, 153–67
Explorer 1 mission, 84
extraterrestrial intelligence, 225
- feedback, 273, 275, 276, 286
ferromagnetism, 84
first differentiation, 245–53, 261–5, 270
Flannan Reflector, 55
fractal concept, 149, 151
free-air gravity anomalies, 26–30, 38, 79
fullerenes, 222
- Gaia, 272–6, 278, 286
Galapágos Islands, 172–3
Galileo mission, 113, 119, 120
Ganymede, 120
Gaspra, 120
Gemini missions, 9, 127–32, 136–7, 183, 186
geodesy
 geophysical, 16
 geometrical, 16, 17
geoid, 26, 34, 35, 39, 40, 43
geomagnetism, 83–122
Geopotential Research Mission, 33
glacial geology, 178–183
Global Positioning System, 7, 33, 56–68
GLONASS system, 24
granite, 238, 240, 276
granulite, 257, 261
gravimetric geoid, 26, 31
gravity anomalies, 33–9, 72, 78, 79
Great Dike, 188
greenstone belts, 220, 237–9, 251, 256, 286
Grenville Front, 148, 232,
Grenville Orogeny, 234, 240, 241
- harmonics, 35–8
Haruj al Aswad, 132
homeostasis, 273
hot-spot trails, 14, 40, 42
hypervelocity impact, 192–5
hysteresis curve, 84
- Iceland, 172, 174–5, 181–4
Ida, 120
IHS transform, 166, 167
imaging radar, 128, 129
impact cratering, 191–226
impact melt, 195, 201, 219
Indian Remote Sensing Satellite-1, 187
induced magnetism, 85
International Decade for Hazard
 Reduction, 169
International Geomagnetic Reference
 Field, 93, 121
International Latitude Service, 45
International Space Station, 190
Io, 119, 197, 261, 263
isostatic compensation, 25, 73, 79
isotopic evidence, 259, 266
Isua Supracrustal Sequence, 240
- jokulhaup, 182–4
Jupiter, 119, 196, 221, 227, 261
- Kenai Peninsula, 58, 61
Kenoran Orogeny, 240
KREEP, 243, 261
- LAGEOS*, 19–21, 47, 48, 55, 57,
Landsat, 7, 9, 10, 65, 66, 128, 131–6, 141,
 145–8, 150, 151, 153–9, 162–4, 170,
 171, 176, 179–83, 185–8

INDEX

- length of day 67–70
 lineaments, 141–52, 165, 169
LITHOPROBE, 219, 232, 234, 239, 240,
 256
Loma Prieta earthquake, 62–4
lopolith, 217, 218
Lord Howe Rise, 110–11
 lunar laser ranging, 21, 23
Lunar Orbiter missions, 71–3, 117
Lunar Prospector mission, 71–6, 115
Lunokhod, 21
 magma ocean, 209, 243
 magnetic equator, 12
 magnetic field, 10, 11
 magnetic poles, 10
 magnetism, 84, 85
 magnetosphere, 86
Magellan mission, 79–82, 230
Magsat, 10, 11, 91–112, 120–2
 Makran Range, 9
 mantle convection, 39, 44, 82
 mantle plumes, 40, 42, 82, 261
 marine geoid, 25, 26, 39–44
Mariner 9 mission, 245–7
 Mars
 andesite, 211, 271, 275, 283
 crust, 79, 245, 271
 first differentiation, 247, 271
 gravity field, 76–9
 life on, 275, 276
 magnetism, 117–19
 plains, 267
 plate tectonics, 254
 sea-floor spreading, 119, 254
 second differentiation, 265
Mars Global Surveyor mission, 76–8,
 117–19, 210, 246, 270
 Mars Observer (Orbiter) Laser Altimeter,
 78
 mascons, 72–5, 78
 mass extinctions, 221–3
 Mercury
 core, 113, 245
 first differentiation, 245
 impact basins, 208
 magnetic field, 112–13
 mantle, 113
 plains, 254, 267
 second differentiation, 269
Mercury project, 9, 127, 129, 131, 153
 Meteor Crater (Barringer Crater), 192,
 196, 203, 204, 214
 microplates, 14, 56, 57
 Mid-Atlantic Ridge, 2
 mineral exploration, 161–7
 Minitrack system, 19
 Moderate Resolution Imaging
 Spectroradiometer, 187–90
 Mohorovičić discontinuity (Moho), 87
 Moon
 craters, 197–203, 206
 crust, 243
 first differentiation, 245
 second differentiation, 265
 gravity field, 71–6
 magma ocean, 209, 243
 magnetic field, 115–17
 maria, 74
 shape, 71
 origin, 76, 206, 244, 264, 283, 285
 “Moonwatch” program, 18
 Mount Etna, 174, 177
 Mount Spurr, 177, 178
 multi-ring basins, 73, 196, 201, 202
 Namib Sand Sea, 183
 Namibia, 186
NAVSTAR (Naval Space Surveillance
 system), 24
 Nares Strait, 105
Near-Earth Asteroid Rendezvous mission,
 230
 Nelson Front, 102
 neodymium isotopes, 259
 New Madrid seismic zone, 51
 nuclear explosion craters, 203
 nucleosynthesis, 244
 NUVEL-1 model, 7, 46, 48, 50, 52, 53,
 68, 285
 Ordos Plateau, 133, 134
 Orientale Basin, 202
Oersted mission, 120
 optical satellite tracking, 18
 Ottawa–Bonnechere graben, 148–51
PAGEOS, 16
Pathfinder mission, 210, 246, 270, 271
 pear-shaped Earth, 35–7
 Penokean Orogeny, 240
 petroleum exploration, 153–161

- Pioneer* mission, 119
Pioneer Venus Orbiter, 79
planar deformation features, 196, 218, 222
plate motion, 7, 45–50
plate tectonic theory, 2, 13–15, 282, 284, 285
Polar Orbiting Geophysical Observatory, 11, 91, 95, 107, 110, 111, 111, 111
prokaryotic life, 280, 286
pseudotachylite, 195
Puerto Rico Trench, 25
radar interferometry, 140, 171–5
radar tracking, 19
Radarsat, 129, 183, 184
radio telescope interferometry, 33
radio tracking, 18–19
Red Sea, 157
redifferentiation, 266, 269, 277
Reiner Gamma, 115–17
regional metamorphism, 195, 198, 277, 286
remanent magnetism, 85
remote sensing, 123–90
retroreflector-bearing satellites, 20, 21
Rhine Graben, 51
ridge push, 14, 271, 285, 286
satellite laser ranging, 7, 19, 20, 21
satellite tracking methods, 17–33
San Andreas fault, 49, 62–6, 136, 284
Salton Sea, 136, 137
Saudi Arabia, 154
sea-floor spreading, 2, 14, 265, 277, 279, 280
seamounts, 40–2
Seasat, 129
sea-surface satellite altimetry, 5, 24–7, 31
second differentiation, 253, 254, 261, 262, 265, 269, 271
shape of the Earth, 33–7
shatter cones, 197, 217
shock metamorphism, 192, 195, 196, 198, 204, 213, 218, 277
shock remanent magnetism, 115
shock waves, 194, 195
Shoemaker-Levy-9, 195, 221
Shuttle Imaging Radar, 129
Sierra Madera, 210–12
silane, 227
snow-ball earth, 179, 286
Sojourner, 246
South Atlantic Anomaly, 83
South Pole-Aitken Basin, 206, 207
Southern Province, 236
space geodesy, 16–82, 284–6
Space Shuttle, 83, 128, 129
Space Shuttle Earth Observation Program, 128
Spaceguard Survey, 226
special relativity, 85
Sputnik, 33–5, 91
Starlette, 19
stishovite, 195, 196, 204
Strait of Hormuz, 9
subduction (subduction zones) 2, 45, 49, 50, 55, 107, 109, 175, 260, 263, 264, 269, 271, 279, 287
Sudbury Igneous Complex, 209
Sudbury Structure, 193, 195, 239, 277, 279, 280, 287
Supernova 1987A, 244
surge tectonics, 55, 267, 284, 286
sutures, 102, 232–7
Systeme Pour l'Observation de la Terre (*SPOT*), 131, 133, 284
taphrogeosynclines, 239
tektites, 214–16
Terra satellite, 177–8, 187
terrane accretion, 102, 231–7, 239, 241, 259, 280, 282
terranes, 233, 234
thetomorphic crystals, 195
Tibetan Plateau, 9
Total Ozone Mapping Spectrometer 177, 178
Tiros 1, 120
Tracking and Data Relay System Satellites, 18
transform faults, 13, 284
Transit system, 23
Tunguska, 200
Tycho, 198, 200–3
Ultralong Baseline Interferometry, 26
Ulysses mission, 119
Vanguard missions, 35, 36, 91
Van Allen belts, 83
Vatnajokull, 181–2

INDEX

- Venus
atmosphere, 79
basalts, 265, 283
crust, 248–51, 263, 283, 285
first differentiation, 253
gravity field, 79–82
isostatic compensation, 79
lithosphere, 79, 82
magnetic field, 113, 115
mantle convection, 82
plate tectonics, 264, 283
second differentiation, 269
topography, 79, 249
very long baseline interferometry, 7, 26–30
Viking missions, 76, 192, 245
volcanic ash clouds, 174, 177
Voyager mission, 119
water, geologic role, 276–81, 286
Whittier Narrows earthquake, 62
World Stress Map, 53–5, 190, 267, 268, 285, 286
Zagros Mountains, 9